

**SYNTHESIS, ANALYSIS AND THERMOLYSIS OF
COPOLYMERS OF METHYL METHACRYLATE
WITH ALKALI METAL METHACRYLATES.**

by

ABDELHAMID HAMOUDI

A thesis submitted in partial fulfilment of the
requirements for the degree of PHILOSOPHIAE DOCTOR
in the Faculty of Science at the University of
Glasgow, Scotland.

NOVEMBER, 1975

SUPERVISOR : DR. I.C. McNEILL

ProQuest Number: 13803962

All rights reserved

INFORMATION TO ALL USERS

The quality of this reproduction is dependent upon the quality of the copy submitted.

In the unlikely event that the author did not send a complete manuscript and there are missing pages, these will be noted. Also, if material had to be removed, a note will indicate the deletion.



ProQuest 13803962

Published by ProQuest LLC (2018). Copyright of the Dissertation is held by the Author.

All rights reserved.

This work is protected against unauthorized copying under Title 17, United States Code
Microform Edition © ProQuest LLC.

ProQuest LLC.
789 East Eisenhower Parkway
P.O. Box 1346
Ann Arbor, MI 48106 – 1346

FOREWORD

The work described was carried out between October, 1972 and October, 1975 in the Physical Chemistry department, which is under the general supervision of Professor G.A. SIM, and was supported during this period by a grant award to the author by the government of the Democratic and Popular Republic of Algeria.

ACKNOWLEDGEMENTS

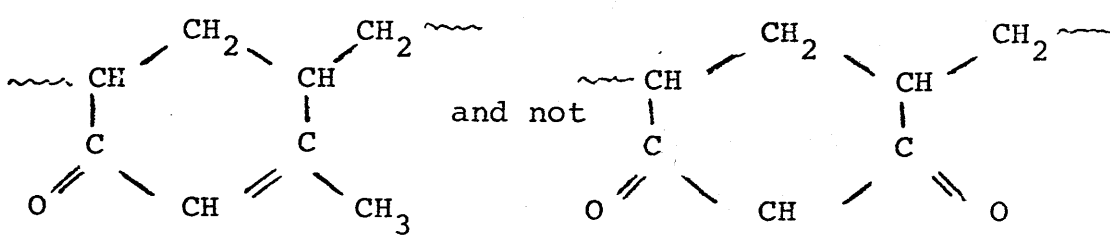
The author wishes to express his appreciation to Doctor I.C. McNEILL both for the suggestion of this topic and also for his guidance and constant encouragement throughout this work.

The author is also indebted to members of staff and all members of the polymer group for their helpful discussions and good humour, and also acknowledges the technical assistance provided by Mr. J. Gorman, Mr. R. Ferrie and Mr. G. McCulloch.

Thanks are finally due to the grant awarding authority for the financial support.

THE AUTHOR

- ERRATA -

<u>Page</u>	<u>Line</u>	
18	8	"and" and not "an"
20	(B)	
		
21	7	"pyrolysis" and not "pyrolisis"
21	11	"a β hydrogen atom".
33	17	"reactions" and not "reacitons".
41	3	"Hg" and not "HG".
42	15	"Trap 1" and not "trap A".
70	7	"radical M_1 " and not "radical M_1 "
71	10	" M_1 " and not " M_2 ".
111	25	"and" redundant.
120	12	$K^+ < Na^+ < Li^+$
144	11	"for" and not "to".
147	12	"80°C" and not "150°C".
147	23	"70°C" and not "120°C".
163	1	"if" redundant.
182		Vertical axis: "mole %" and not "number %".
190	1	"ethylenic" and not "ethylemic".

SUMMARY

This work deals with random copolymers of methyl methacrylate with the lithium, sodium and potassium salts of methacrylic acid.

The three series of copolymers together with the related homopolymers, have been prepared in a homogeneous solvent medium under vacuum.

The characterization and analysis of the copolymers have been carried out and ultimately, the reactivity ratios for the three systems were obtained. These showed that, during copolymerization, the reactivity of the alkali metal methacrylate radical towards MMA addition, increased with the decrease of the size of the metal ion. This has been explained in terms of variation of the electrostatic forces along the chain (due to cation binding character) with the size of the metal ion.

In a second major part, the work deals with the thermal degradation in vacuo of these copolymers.

The basic experimental technique used was thermal volatilization analysis with differential condensation of the products, coupled with thermogravimetric analysis. Differential thermal analysis was also used to some extent.

The analysis of the degradation products was carried out using mainly infra red spectroscopy and gas liquid chromatography.

In general, the copolymers show degradation products similar to those obtained from the corresponding homopolymers, but additional products arise by interaction between dissimilar monomer units along the chains, and this effect also leads to an increase in the overall thermal stability compared with PMMA depolymerization.

Two main breakdown stages are discerned during the programmed thermal decomposition of the copolymers:

(a) Firstly, depolymerization of MMA segments along the chains occurs in competition with production of methanol presumably originating from the decomposition of pendant ester groups. Methanol production is favoured by the formation of anhydride rings between unlike monomer units after elimination of alkali metal methoxide. At this stage of the reaction, the anhydride structures are also decomposing to yield carbon dioxide, carbon monoxide and isolated methacrylic acid units in the chain which will escape, at a later stage, to the cold ring together with other isolated MMA units.

(b) At higher temperatures, the remaining alkali metal methacrylate units, which are more stable, decompose independently in a more or less similar manner

to that of their parent homopolymers (production of alkali metal methacrylate and metal isobutyrate by depolymerization, carbon dioxide, carbon monoxide, methane, alkenes, carbonyl containing compounds and a residue consisting mainly of charcoal and metal carbonate).

The major degradation products (i.e., methyl methacrylate, methanol, carbon dioxide, metal carbonate, alkali metal methacrylate and alkali metal isobutyrate) were assayed and the results are summarised below:

(i) At any particular copolymer composition, the production of methanol and carbon dioxide increases as the size of the metal ion increases, whereas, in this same order, the evolution of MMA monomer decreases significantly.

(ii) The depolymerization of the alkali metal methacrylate parts of the copolymers were found to:

- increase as the size of the metal ion decreases in the composition region ranging between 0 and 50% MMA in the copolymers;

- increase as the size of the metal ion increases in the rest of the composition region of the copolymers.

These results are discussed in detail in chapter V and VI.

To determine the origin of methanol, additional

experiments were needed:

(1) Thermal degradation of PMMA/alkali metal methoxide blends.

(2) Considerations on the sequence distribution of the two types of monomer units along the chains.

(3) Assay of methanol and methyl methacrylate production under isothermal conditions.

In short, copolymerization of methyl methacrylate with alkali metal methacrylates, stabilizes PMMA decomposition and concurrently reduces the MMA monomer yield. This inhibition of depolymerization is believed to result from a direct blockage of the "unzipping" process by the presence along the chains of anhydride rings, formed by interaction between dissimilar monomer units. Because of this blockage phenomenon, chain scission preceding monomer release needs to be re-initiated more often along the chains and this results in an increase in the activation energy for MMA production, an effect which will allow scission to occur, not only along the chains, but also on pendant ester groups, thus allowing methanol formation in significant amounts.

CONTENTS

	<u>PAGE</u>
<u>CHAPTER I</u> <u>INTRODUCTION</u>	1
AIM OF THIS WORK	1
COPOLYMERIZATION	2
POLYELECTROLYTES	3
CONTRASTS BETWEEN POLYELECTROLYTES & NON IONIC POLYMERS	5
POLYMER DEGRADATION	9
THERMAL DEGRADATION OF VINYL POLYMERS	11
- CHAIN SCISSION REACTIONS	13
- EFFECT OF POLYMER STRUCTURE UPON DEPOLYMERIZATION	14
- SUBSTITUENT REACTIONS	17
 <u>CHAPTER II</u> <u>EXPERIMENTAL PROCEDURE AND</u> <u>TECHNIQUES OF THERMAL ANALYSIS</u>	 22
THERMAL VOLATILIZATION ANALYSIS	22
PRINCIPLE OF TVA	22
DIFFERENTIAL CONDENSATION TVA	25
PRODUCT ANALYSIS OF TVA FRACTIONS	27
CALIBRATION OF THE OVEN THERMOCOUPLE	29
SAMPLE HEATING RATE	30
THE DISADVANTAGES OF TVA	30
ADVANTAGES OF TVA	32
THERMOGRAVIMETRIC ANALYSIS	33
DIFFERENTIAL THERMAL ANALYSIS	34
INFRA RED SPECTROSCOPY	35
GAS CHROMATOGRAPHY	35
MASS SPECTROMETRY	37

	<u>PAGE</u>
QUALITATIVE DISTILLATION OF CONDENSABLE PRODUCTS	37
QUANTITATIVE ANALYSIS OF CARBON DIOXIDE	40
PRODUCT COLLECTION UNDER ISOTHERMAL CONDITIONS	42
<u>CHAPTER III</u> <u>MONOMER AND POLYMER PREPARATION</u>	44
INTRODUCTION	44
PREPARATION AND PURIFICATION OF MONOMERS	47
DISTILLATION OF METHACRYLIC ACID	47
PREPARATION OF THE ALKALI METAL SALTS OF MAA	48
CHARACTERIZATION OF Li, Na AND K METHACRYLATES	49
SOLUBILITY OF METHACRYLATE METAL SALTS	52
STABILITY OF METHACRYLATE METAL SALTS	53
PURIFICATION OF METHYL METHACRYLATE	55
PURIFICATION OF INITIATOR	55
POLYMERIZATION	55
POLYMER ISOLATION AND PURIFICATION	58
PROOF OF COPOLYMERIZATION	59
INFRA RED ANALYSIS	59
ANALYSIS OF THE COPOLYMERS	60
EFFECT OF THE WATER ABSORBED ON THE CHEMICAL STRUCTURE OF THE POLYMERS	62
SOLUBILITY OF THE COPOLYMERS	67
<u>CHAPTER IV</u> <u>MONOMER REACTIVITY RATIOS</u>	68
THE COPOLYMERIZATION EQUATION	68

	<u>PAGE</u>
MONOMER REACTIVITY RATIOS	69
METHODS FOR DETERMINING r_1 AND r_2 VALUES	70
A-) THE CURVE FITTING METHOD	71
B-) THE INTERSECTION METHOD	71
C-) THE LINEARIZATION METHOD	72
D-) THE NEW METHOD	73
EXPERIMENTAL ERRORS	75
ANALYSIS OF DATA	76
REACTIVITY RATIOS	79
FIRST OBSERVATIONS	89
A-) LiMA/MMA COPOLYMER	89
B-) NaMA/MMA COPOLYMER	93
C-) KMA/MMA COPOLYMER	93
PREVIOUS WORK	94
DISCUSSION OF THE PRESENT RESULTS	96
CONCLUSION	98

CHAPTER V THE THERMAL DEGRADATION OF COPOLYMERS
OF METHYL METHACRYLATE WITH ALKALI
METAL METHACRYLATES. I : PRODUCTS AND
GENERAL CHARACTERISTICS OF THE REACTION 100

INTRODUCTION	100
THERMAL DECOMPOSITION OF PMMA	100
THERMAL DECOMPOSITION OF POLY(ALKALI METAL METHACRYLATES)	101
THERMAL DECOMPOSITION OF METHACRYLIC ACID/METHYL METHACRYLATE COPOLYMER	111
THERMAL VOLATILIZATION ANALYSIS	113
THERMAL VOLATILIZATION ANALYSIS OF PMMA	114

	<u>PAGE</u>
THERMAL VOLATILIZATION ANALYSIS OF POLY(ALKALI METAL METHACRYLATES)	116
THERMAL VOLATILIZATION ANALYSIS OF THE COPOLYMERS	122
THERMAL VOLATILIZATION ANALYSIS OF LiMA/MMA COPOLYMERS	122
THERMAL VOLATILIZATION ANALYSIS OF NaMA/MMA COPOLYMERS	131
THERMAL VOLATILIZATION ANALYSIS OF KMA/MMA COPOLYMERS	138
THERMOGRAVIMETRIC ANALYSIS OF THE COPOLYMERS	145
DIFFERENTIAL THERMAL ANALYSIS	147
VOLATILES ANALYSIS	149
INFRA RED ANALYSIS OF THE TOTAL VOLATILES	149
LIQUID PRODUCTS ANALYSIS BY GAS LIQUID CHROMATOGRAPHY	152
COLD RING FRACTION (CRF) ANALYSIS	156
RESIDUE ANALYSIS	159
STRUCTURAL CHANGES DURING DEGRADATION	159
QUANTITATIVE ANALYSIS FOR METHANOL AND MMA	165
QUANTITATIVE ANALYSIS FOR CARBON DIOXIDE	171
QUANTITATIVE ESTIMATION OF METAL CARBONATE IN THE RESIDUE	174
QUANTITATIVE ESTIMATION OF METAL METHACRYLATE MONOMER AND METAL ISOBUTYRATE IN THE CRF	180
QUANTITATIVE ANALYSIS FOR SOME CARBONYL CONTAINING PRODUCTS BY GLC	185
CONCLUSIONS	189

CHAPTER VI

THE THERMAL DEGRADATION OF COPOLYMERS OF METHYL METHACRYLATE WITH ALKALI METAL METHACRYLATES. II : ORIGIN OF METHANOL AND DISCUSSION

193

	<u>PAGE</u>
THERMAL DEGRADATION OF PMMA/SODIUM METHOXIDE BLEND	193
THE STATISTICS OF CYCLIZATION REACTIONS IN VINYL HOMOPOLYMERS	195
THE STATISTICS OF CYCLIZATION REACTIONS IN VINYL COPOLYMERS	197
THEORETICAL RESULTS FOR THE FRACTION OF CYCLIZABLE ELECTROLYTE UNITS IN COPOLYMERS	201
RESULTS COMPARED WITH METHANOL PRODUCTION	202
ISOTHERMAL DEGRADATION OF KMA/MMA COPOLYMERS	212
A-) METHANOL PRODUCTION UNDER ISOTHERMAL CONDITIONS	213
B-) ORIGIN OF METHANOL	218
C-) MMA PRODUCTION UNDER ISOTHERMAL CONDITIONS	219
JUSTIFICATION FOR ALKALI METAL METHOXIDE FORMATION	230
FATE OF ALKALI METAL METHOXIDE	232
<u>CHAPTER VII</u> <u>GENERAL CONCLUSIONS</u>	234
DISCUSSION	235
SUGGESTIONS FOR FUTURE WORK	241
<u>APPENDIX 1</u> <u>THE FORTRAN PROGRAMME USED FOR CALCULATING THE REACTIVITY RATIOS OF A COPOLYMER SYSTEM, BEING GIVEN AN INITIAL ESTIMATE OF r_1 AND r_2 AND THE COMPOSITION ANALYSIS DATA</u>	242
<u>APPENDIX 2</u> <u>PREPARATION OF SODIUM METHOXIDE</u>	245
<u>APPENDIX 3</u> <u>ACTIVATION ENERGY ESTIMATION FOR MMA PRODUCTION FROM COPOLYMERS</u>	246
<u>REFERENCES</u>	247

LIST OF FIGURES

<u>CHAPTER I</u>		<u>PAGE</u>
I-1	Reduced viscosity of poly(4-vinyl-n- butyl- pyridinium bromide) ^(27,28)	6
I-2	Reduced viscosity of PMAA in pure water, neutralized to various extents by tetra-n- propylammonium hydroxide ⁽²⁹⁾	8
 <u>CHAPTER II</u>		
II-1	Basic TVA apparatus	24
II-2	Sample heating assembly	24
II-3	Differential condensation TVA apparatus	26
II-4	The oven thermocouple calibration	31
II-5	The products distillation system	38
II-6	The qualitative distillation of 50% LiMA/MMA copolymer	38
II-7	Assembly for product collection under isothermal conditions	43
 <u>CHAPTER III</u>		
III-1	TG curves for alkali metal methacrylates	54
III-2	Infra Red analysis of (A) PMMA; (B) 40% KMA/MMA copolymer; (C) PKMA	61
III-3	TG curves for poly(alkali metal methacrylates), showing the amount of water taken up from the atmosphere within four days	63
III-4	TG curves for three NaMA/MMA copolymers, showing the amount of water taken up from the atmosphere within four days	63
III-5	Effect of water on the chemical structure of the 40% KMA/MMA copolymer	65
 <u>CHAPTER IV</u>		
IV-1	Mayo & Lewis diagram for the copolymerization of MMA (1) and LiMA (2)	80

	<u>PAGE</u>
IV-2 Fineman & Ross diagram for the copolymerization of MMA (1) and LiMA (2)	81
IV-3 Mayo & Lewis diagram for the copolymerization of MMA (1) and NaMA (2)	82
IV-4 Fineman & Ross diagram for the copolymerization of MMA (1) and NaMA (2)	83
IV-5 Mayo & Lewis diagram for the copolymerization of MMA (1) and KMA (2)	84
IV-6 Fineman & Ross diagram for the copolymerization of MMA (1) and KMA (2)	85
IV-7 Curve fitting for the copolymerization of LiMA and MMA	90
IV-8 Curve fitting for the copolymerization of NaMA and MMA	91
IV-9 Curve fitting for the copolymerization of KMA and MMA	92
IV-10 Variation of the reactivity of the alkali metal methacrylate radical (towards MMA addition during copolymerization) with the size of the metal ion	95

CHAPTER V

V-1 TG/TVA for poly(methyl methacrylate)	115
V-2 TG/TVA for poly(lithium methacrylate)	117
V-3 TG/TVA for poly(sodium methacrylate)	118
V-4 TG/TVA for poly(potassium methacrylate)	119
V-5 TG/TVA for 4% LiMA/MMA copolymer	123
V-6 TG/TVA for 20% LiMA/MMA copolymer	124
V-7 TG/TVA for 38% LiMA/MMA copolymer	125
V-8 TG/TVA for 52% LiMA/MMA copolymer	126
V-9 TG/TVA for 91% LiMA/MMA copolymer	127
V-10 TG/TVA for 5% NaMA/MMA copolymer	132
V-11 TG/TVA for 9% NaMA/MMA copolymer	133
V-12 TG/TVA for 37% NaMA/MMA copolymer	134

	<u>PAGE</u>
V-13 TG/TVA for 61% NaMA/MMA copolymer	135
V-14 TG/TVA for 90% NaMA/MMA copolymer	136
V-15 TG/TVA for 9% KMA/MMA copolymer	139
V-16 TG/TVA for 21% KMA/MMA copolymer	140
V-17 TG/TVA for 50% KMA/MMA copolymer	141
V-18 TG/TVA for 75% KMA/MMA copolymer	142
V-19 TG/TVA for 92% KMA/MMA copolymer	143
V-20 DTA curves for PMMA, PKMA and 50% KMA/MMA copolymer	148
V-21 Comparison between IR spectra in the gas phase of the total condensable (at -196°C) products from programmed degradation to 500°C of: (A) PLiMA, (B) 41% LiMA/MMA copolymer	150
V-22 GLC analysis of the liquid degradation products from 70% LiMA/MMA copolymer	154
V-23 Infra red spectra in KBr discs of : (A) lithium isobutyrate, (B): CRF from degradation of 25% LiMA/MMA copolymer, (C): lithium methacrylate monomer	157
V-24 Infra red spectra for fraction of CRF soluble in CCl_4 , from degradation of : (A) 25% LiMA/MMA copolymer; (B) 25% KMA/MMA copolymer	158
V-25 Infra red spectra of : (A) Black residue from programmed degradation to 500°C of LiMA/MMA copolymers, (B) Analar lithium carbonate	160
V-26 IR solid state spectra for 38% KMA/MMA copolymers heated isothermally at 300°C for different lengths of time	161
V-27 GLC calibration plots for : (A) methanol (B) MMA, using n-butanol as internal standard	166
V-28 Methanol production for the three series of copolymers	168
V-29 MMA production from the three series of copolymers	169
V-30 Carbon dioxide production from the three series of copolymers	172

	<u>PAGE</u>
V-31	Residue data for LiMA/MMA copolymers 176
V-32	Residue data for NaMA/MMA copolymers 177
V-33	Residue data for KMA/MMA copolymers 178
V-34	Quantitative estimation of salt units (in the form of metal methacrylate or metal isobutyrate) in the CRF, from the three series of copolymers 182

CHAPTER VI

VI-1	Methanol production in LiMA/MMA copolymer: (A) found experimentally, (B) predicted from sequence distribution 207
VI-2	Methanol production in NaMA/MMA copolymer; (A) found experimentally, (B) predicted from sequence distribution 208
VI-3	Methanol production in KMA/MMA copolymers: (A) found experimentally, (B) predicted from sequence distribution 209
VI-4	Methanol evolution under isothermal conditions for 5% KMA/MMA copolymer 214
VI-5	Methanol evolution under isothermal conditions for 20% KMA/MMA copolymer 215
VI-6	Methanol evolution under isothermal conditions for 50% KMA/MMA copolymer 216
VI-7	Methanol evolution under isothermal conditions for 75% KMA/MMA copolymer 217
VI-8	Weight loss for PMMA under isothermal conditions 220
VI-9	Arrhenius plot for MMA evolution in PMMA (see fig. VI-8) 221
VI-10	MMA evolution under isothermal conditions for 5% KMA/MMA copolymer 223
VI-11	MMA evolution under isothermal conditions for 20% KMA/MMA copolymer 224
VI-12	MMA evolution under isothermal conditions for 50% KMA/MMA copolymer 225
VI-13	MMA evolution under isothermal conditions for 75% KMA/MMA copolymer 226
VI-14	Arrhenius plots for MMA evolution in 4 KMA/MMA copolymers (see figs. VI-10,11,12 and 13) 227

LIST OF TABLES

<u>CHAPTER III</u>		<u>PAGE</u>
III-1	Analytical results for the monomeric salts	50
III-2	C=O and C=C frequencies of absorption for the monomeric salts in comparison with those of methacrylic acid	52
III-3	Approximate solubilities of the monomeric salts in anhydrous Analar methanol at ambient temperature	53
 <u>CHAPTER IV</u>		
IV-1	Analytical results from copolymerization of MMA (1) and LiMA (2) in methanol	77
IV-2	Analytical results from copolymerization of MMA (1) and NaMA (2) in methanol	77
IV-3	Analytical results from copolymerization of MMA (1) and KMA (2) in methanol	78
IV-4	Reactivity ratios for the three systems studied, found by the intersection method	79
IV-5	Reactivity ratios for the three systems studied, found by the Fineman & Ross method	86
IV-6	Results obtained by the new method on each iteration for the system LiMA (2) - MMA (1)	87
IV-7	Results obtained by the new method on each iteration for the system NaMA (2) - MMA (1)	87
IV-8	Results obtained by the new method on each iteration for the system KMA (2) - MMA (1)	88
IV-9	Final reactivity ratios of monomers in copolymerization of MMA with MetMA (Met = Li, Na and K)	88
IV-10	Reactivity ratios "predicted" using the empirical Q and e scheme	99

<u>CHAPTER V</u>	<u>PAGE</u>
V-1 TG/TVA data for poly(alkali metal methacrylates)	121
V-2 TVA data for LiMA/MMA copolymers	129
V-3 TVA data for NaMA/MMA copolymers	131
V-4 TVA data for KMA/MMA copolymers	138
V-5 Weight % of residues from degradation of copolymers of MMA with alkali metal methacrylates	146
V-6 Assignment of IR peaks from degradation of PLiMA	151
V-7 Assignment of liquid products from the GLC trace shown in fig. V-22	155
V-8 Methanol and MMA production from LiMA/MMA copolymer on programmed degradation to 500°C	167
V-9 Methanol and MMA production from NaMA/MMA copolymer on programmed degradation to 500°C	170
V-10 Methanol and MMA production from KMA/MMA copolymer on programmed degradation to 500°C	170
V-11 Carbon dioxide production from copolymers of MMA with alkali metal methacrylates	173
V-12 Data of residue analysis for LiMA/MMA copolymer at 500°C	175
V-13 Data of residue analysis for NaMA/MMA copolymer at 500°C	175
V-14 Data of residue analysis for KMA/MMA copolymer at 500°C	179
V-15 Estimation of salt content (in the form of metal methacrylate or metal isobutyrate) in the CRF from programmed degradation of copolymers of MMA with alkali metal methacrylates	183
V-16 Ketone formation from two LiMA/MMA copolymers	186
V-17 Ketone formation from two NaMA/MMA copolymers	187

<u>CHAPTER VI</u>		<u>PAGE</u>
VI-1	Theoretical determination of $f_c(B)$ for LiMA/MMA copolymers	203
VI-2	Theoretical determination of $f_c(B)$ for NaMA/MMA copolymers	204
VI-3	Theoretical determination of $f_c(B)$ for KMA/MMA copolymers	205
VI-4	Methanol production in LiMA/MMA copolymers. Comparison between experimental and theoretical yields (predicted from sequence distribution data)	206
VI-5	Methanol production in NaMA/MMA copolymers. Comparison between experimental and theoretical yields (predicted from sequence distribution data)	206
VI-6	Methanol production in KMA/MMA copolymers. Comparison between experimental and theoretical yields (predicted from sequence distribution data)	210
VI-7	Activation energies (E_A 's) associated with MMA production from four KMA/MMA copolymers and from PMMA homopolymer	222
VI-8	Mode of breakdown of the MMA parts of the LiMA/MMA copolymer chains (mole%)	229
VI-9	Mode of breakdown of the MMA parts of the NaMA/MMA copolymer chains (mole %)	229
VI-10	Mode of breakdown of the MMA parts of the KMA/MMA copolymer chains (mole %)	230

CHAPTER VII

VII-1	Quantitative summation of the products from programmed degradation (to 500°C) of LiMA/MMA copolymers ; weight %	238
VII-2	Quantitative summation of the products from programmed degradation (to 500°C) of NaMA/MMA copolymers ; weight %	239
VII-3	Quantitative summation of the products from programmed degradation (to 500°C) of KMA/MMA copolymers ; weight %	246

CHAPTER I

INTRODUCTION

AIM OF THIS WORK

This work deals with the synthesis, analysis and thermolysis of copolymers of methyl methacrylate (MMA) with the salts of methacrylic acid (MAA). These copolymers are prepared from monomers which when polymerized separately lead to materials having markedly different physical and chemical properties and commercial applications.

Poly(methyl methacrylate) (PMMA) is a familiar polymer in everyday use with very good physical properties and is still of great interest to the research polymer chemist as will be seen subsequently.

As polyelectrolytes, the polymers of the salts of MAA have also a large variety of commercial applications because of their unique properties in aqueous solutions⁽¹⁾; they also show high thermal stability.

From these considerations, the study of materials resulting from the copolymerization of these two types of monomer has obvious interest. The importance and the commercial uses of copolymers made out of two monomers, one neutral, the other ionic, have already been appreciated. For example, the copolymers of acrylic acid, methacrylic acid and their salts, respectively, with acrylamide are

intensively used as drilling and mud additives,⁽²⁾ flocculating agents⁽³⁾ and in papermaking.^(3,4) But if a lot of work has been published on the commercial uses of these copolymers hardly any systematic study has been made of the mechanisms of polymerization or decomposition of these materials.

Consequently, it is appropriate to discuss briefly in an introduction to this work, both the general aspects of copolymerization and the marked contrasts in the chemical behaviour of polyelectrolytes and non-ionic polymers.

COPOLYMERIZATION

Scientific, commercial and industrial interests in the macromolecules field is shifting increasingly from polymerization to copolymerization. Synthetic copolymers are now found everywhere, in the clothes we wear, in the cars we drive, throughout our homes, and in a growing number of industrial and agricultural applications.

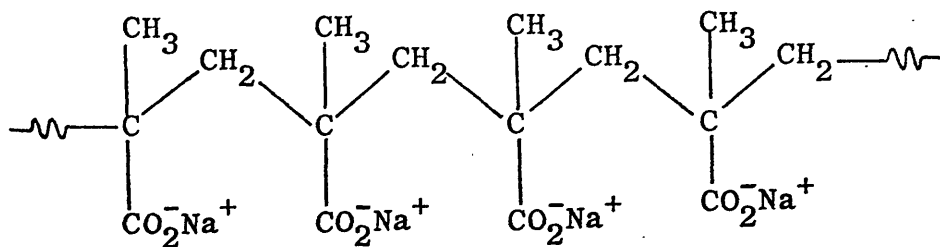
From a historical point of view the first copolymerization reactions were purposely carried out around 1910 in the course of the systematic polymerization studies of diolefins.⁽⁵⁾ Since then, an increasing number of publications and patents shows how copolymerization can improve the physical properties

of the corresponding homopolymers. (6-13)

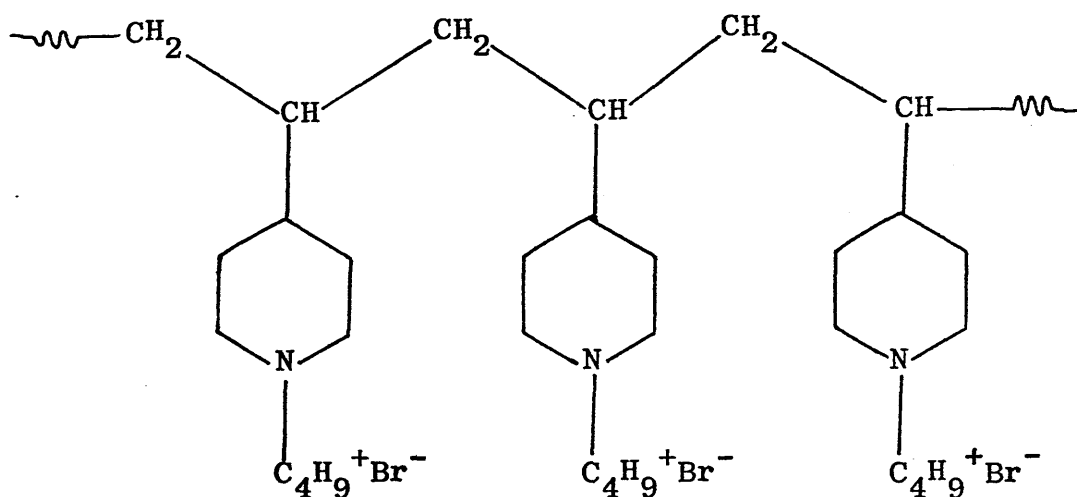
It was established, in the early 1930's that copolymers of vinyl chloride with vinyl acetate and acrylic esters lead to very interesting plastics⁽¹⁴⁾ while copolymers of butadiene with styrene and acrylonitrile lead to valuable elastomers.⁽¹⁵⁾ During these years and for many years after, the emphasis of the work was placed mostly on the preparation and development of useful products. It was not until the 1940's that the first systematic attempts were made by Staudinger & Schneider,⁽¹⁶⁾ Norrish & Brookman,^(17,18) Wall⁽¹⁹⁾ and Marvel,⁽²⁰⁾ to elucidate the mechanism of copolymerization itself. This period, distinguished by rapidly increasing development and production activity in the fields of copolymerization, was followed in the 1950's by new and important contributions to copolymerization theory with the elucidation of incompletely understood phenomena and in particular applications to the broad new field of stereoregular polymerization. These contributions in the last twenty years added greatly to our overall understanding.

POLYELECTROLYTES^(1,21-25)

A polyelectrolyte is defined as any polymeric substance in which the monomeric units of its constituents possess ionizable groups.⁽²⁶⁾ Examples of polyelectrolytes are poly(sodium methacrylate) (PNaMA), the salt of polymethacrylic acid:



and poly(4-vinyl-N-butylpyridinium bromide), a cationic polyelectrolyte:



They undergo ionic dissociation in aqueous solutions, and this leads to large repulsive forces among the charged groups in the chain. These forces produce important conformational expansions and this gives rise to very large intrinsic viscosities, as well as abnormalities in other thermodynamic properties.

At concentrations above 1% the macromolecules in a polyelectrolyte are in close enough contact to overlap partially and are not appreciably expanded; the

specific viscosity is approximately normal. As the solution is diluted the molecules no longer fill all the space and some of the mobile ions leave the regions of the chain which develop net charges and expand to a maximum. The specific viscosity may actually rise with increasing dilution. At the same time the reduced osmotic pressure π/c may rise as the ions are released to act as separate osmotic units. Related effects are observed in other physical properties such as light scattering and conductance.

CONTRASTS BETWEEN POLYELECTROLYTES & NON IONIC POLYMERS

The first marked difference that one may put forward is perhaps the solubility criterion: of the common solvents, strongly ionizing polyelectrolytes are soluble only in water, and, to a lesser extent in the lower alcohols.

It is also appropriate and instructive to compare the concentration dependence of the reduced viscosity

$\eta_{sp}/c, c$ in g/100ml) of poly (4 - vinyl - N - butyl - pyridinium bromide), a strong polyelectrolyte, with that of its non-ionic parent polymer poly(vinyl pyridine) with the same chain length. The neutral polymer diluted in 90% alcohol gives as a result a linear decrease in the reduced viscosity in agreement with the well known Huggins equation:

$$\eta_{sp}/c = [\eta] + k'[\eta]^2 c$$

The effect of dilution on η_{sp}/c for the related polyelectrolyte is remarkably different^(27,28) as shown in Fig I-I.

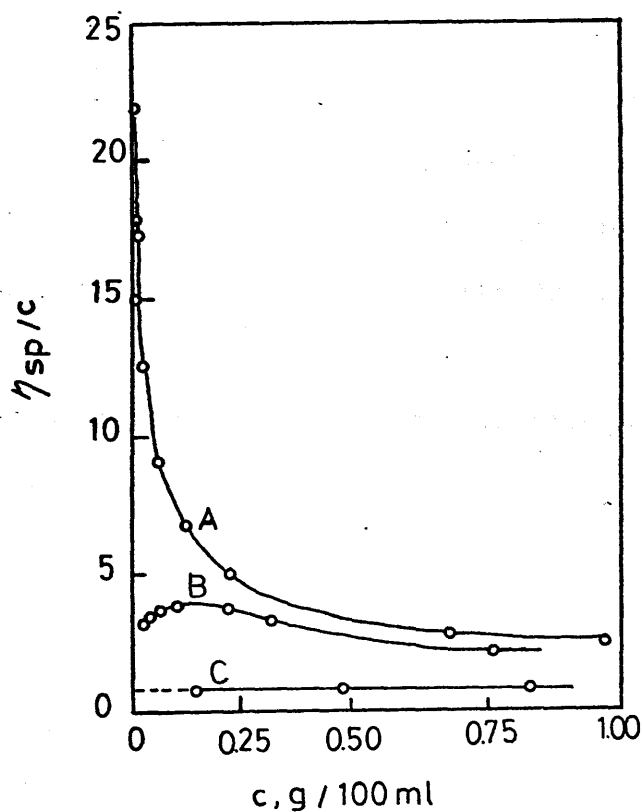


Fig I-I

Reduced viscosity of poly (4 - vinyl - N - Butyl - pyridinium bromide) solutions. Key: Curve A, water as solvent; curve B, 0.001N KBr as solvent; curve C, 0.034N KBr as solvent; Data of Fuoss and Strauss.^(27,28)

In this case (curve A) the reduced viscosity increases sharply with dilution and at high dilution η_{sp}/c approaches the ordinate almost asymptotically. The fundamental observation here is that at low concentrations the viscosities of the two solutions depend upon the solute concentrations in strikingly different ways: one increases linearly with c , whereas in the same range of concentrations the other decreases with c very markedly.

Furthermore, the properties of solutions containing macroions are extremely sensitive to the presence of added simple electrolyte. Curves (B) and (C) in Fig I-I show how addition of KBr suppresses the loss of mobile ions and bring back the viscosity to a more normal behaviour.

Another major manifestation of the pronounced dependance of the reduced viscosity upon polyelectrolyte concentration is given by Gregor, Gold and Frederick⁽²⁹⁾ (Fig I-2). For a weak polyelectrolyte such as poly (methacrylic acid) (PMAA) the observed reduced viscosity at any given concentration of polyion changes drastically with the degree of neutralization.

At very low α_n , PMAA has a viscosity characteristic of non ionic polymer solution. Upon addition of base however, the viscosity increases slowly at first then sharply. The value attained at complete neutralization is an order of magnitude greater than the value observed at low α_n .

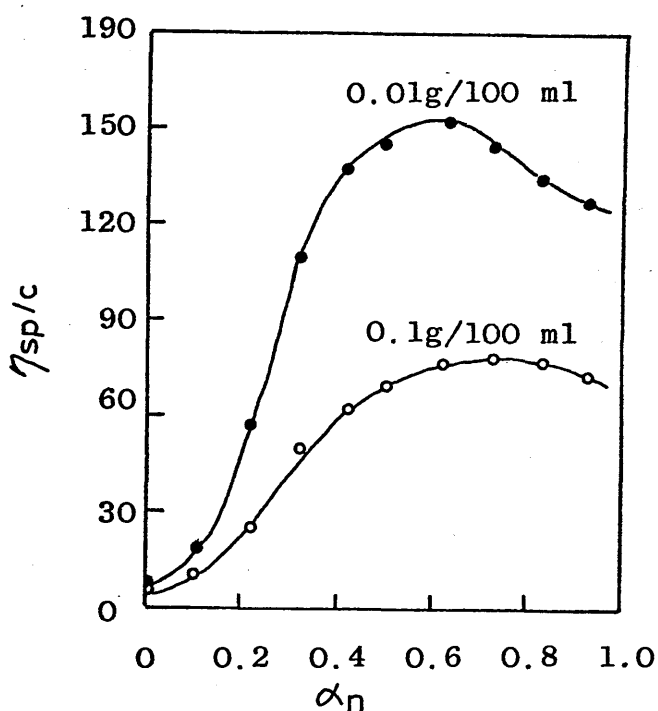


Fig I-2

Reduced viscosity of PMAA in pure water, neutralized to various extents by tetra - n - propylammonium hydroxide. Upper curve: $c = 0.01$ g/100ml; lower curve: $c = 0.1$ g/100ml. Adapted from Gregor, Gold & Frederick. (29)

This increase in η_{sp}/c is much more spectacular for the more diluted solution of PMAA (Fig I-2 upper curve).

In short, assuming that the reduced viscosity at high dilution is a direct measure of macromolecular

extension in solution, one may draw the following conclusions from the experimental data observed:

I - The dimensions of a polyion in salt free aqueous solution are strongly dependent on the concentration of the polyion.

2 - At very low concentrations macroions appear to be highly extended and in the limit of infinite dilution probably adopt rodlike configurations.

3 - The addition of simple electrolyte results in a pronounced contraction of the polyion; in the presence of large excess of simple electrolyte the macroion is probably coiled in a manner which resembles the configuration of non ionic polymers in organic solvents.

4 - Weak polyelectrolytes appear to uncoil and expand dramatically upon neutralization.

In conclusion, the viscometric evidence presented indicates that a realistic model of polyelectrolyte solution differs drastically from a model of neutral polymer solution in the sense that it must provide for changes in polyion dimension with at least three variables: polyion concentration, concentration of added salt and degree of neutralization.

POLYMER DEGRADATION

The increasing needs and commercial uses of polymers in every day life have brought in the last decade or so substantial developments in most of the important

aspects of polymer degradation including that induced by light, heat, high energy radiation, oxygen, mechanical stresses, chemical attack and bacteria. The reason for this is that polymers were found to be subject to a number of modifying influences depending on the particular environment and application of the substance. Accounts in some of these polymer degradation aspects have been given at various times in reviews of the current position. (30-33) Development and progress in all these directions has been intensified by the analytical techniques which have become available in the form of commercial instruments in the past twelve years, or which are currently being developed. (34-37) Thermal analysis techniques in the form of TGA, DTA, DSC and TVA, spectroscopic techniques in the form of n.m.r. and e.s.r., and G.L.C., and G.P.C., have been particularly effective. These have allowed a very much closer analysis of the changes in polymer structure which occur during degradation, and of the volatile products, the detection and analysis of which are often of immense significance in getting towards a clearer understanding of reaction mechanism.

The term "degradation" from the chemical point of view means a breaking down of chemical structure. In polymer chemistry this would imply a decrease in

molecular weight. By the usage of this term, however, this meaning is not always valid and today "polymer degradation" involves any deterioration of those properties which make the product useful commercially as plastic, rubber or fibre. Certain polymers, for example, change their colour under the effect of light or heat. This phenomenon is referred to as degradation, although in most cases the chemical reaction causing it makes no change or may even result in an increase of molecular weight. In order to give the widest scope possible for discussion, the term "degradation" will therefore be used to cover all reactions of polymers.

There has always been great preoccupation during the period under review to produce more and more highly stable polymers. To this end, it was often found advantageous to improve the stability of homopolymers by copolymerizing their corresponding monomers with other ones, and retaining at the same time that degree of flexibility necessary to make the material useful practically. As a general principle, more highly stable polymers were obtained by building cyclic structures in the polymer chain backbone. This is exemplified in the vast existing literature relating to the synthesis of these materials and the assessment of their general stability, usually by thermal analysis techniques. (30,38-40)

THERMAL DEGRADATION OF VINYL POLYMERS

The chemical structure of the repeating unit is clearly

of importance in determining the thermal stability and mode of decomposition of any polymer. Quantitative data from comparative studies of the decomposition of model compounds is not always sufficient in itself to allow the breakdown of polymers to be defined. Often polymeric materials prove to be less stable than one might predict⁽⁴¹⁾ from the behaviour of smaller models. PVC would be expected by comparison with simple chloroparaffins to give during decomposition hydrogen chloride and an olefinic residue; the polymer does indeed decompose thermally in these ways, but at temperatures as much as 200°C lower than the corresponding model.

All thermal degradation reactions are conveniently classified into two broad categories:

- (A) CHAIN SCISSION REACTIONS OR DEPOLYMERIZATION REACTIONS.
- (B) SUBSTITUENT OR NON CHAIN SCISSION REACTIONS.

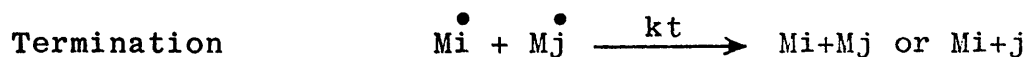
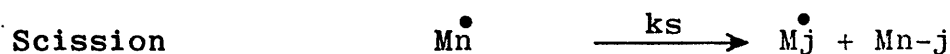
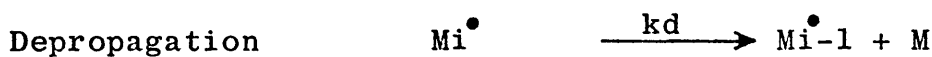
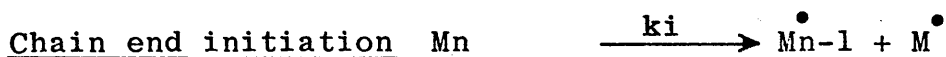
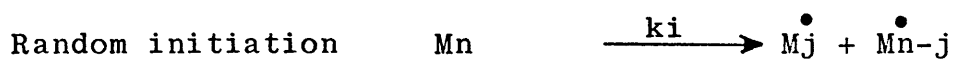
Chain scission reactions are characterized by the breaking of the main polymer chain backbone. The products at any intermediate stage of the reaction are similar to the parent material. In other terms the monomer units are still distinguishable in the chains.

Substituent reactions, on the other hand, result in the elimination of small molecules from the chain leaving a chemically different residue. These small molecules can be anything but monomer. Examples of both types of decomposition reaction are available in this work and it is therefore appropriate to examine briefly their main features.

CHAIN SCISSION REACTIONS

These proceed by a free radical chain process. Many addition polymers depolymerize thermally within the meaning of that term as it has been defined. Chain scission is the predominant process occurring during the decomposition of PMMA, polypropylene (PP) and polyethylene (PE) and takes place to various extents in a number of other addition polymers. When these reactions were studied in detail it was found however, that whereas decomposition of PMMA⁽⁴²⁾ leads to quantitative monomer formation, both PP and PE give little monomer, the products being mainly longer chain olefinic fragments.⁽⁴²⁻⁴⁵⁾

Simha, Wall and Blatz⁽⁴⁶⁻⁴⁹⁾ showed that these two extremes of behaviour may be interpreted in terms of a single free radical chain reaction mechanism which may be represented as follows:



where n is the chain length of the starting material

and \dot{M}_i , \dot{M}_j etc., and \ddot{M}_i , \ddot{M}_j etc., represent respectively "dead" polymer molecules and long chain radicals, i , j , etc., monomer units in length.

It has been shown by Grassie and Melville⁽⁵⁰⁾ that during the thermal degradation of PMMA, initiation occurs initially at unsaturated chain ends, then the radicals depropagate to monomer in the complete absence of transfer reaction. On the other hand, when intermolecular transfer is the predominant reaction in a degradation, the overall process approximates the situation in which the polymer chains are being randomly broken; the rate of volatilization passes through a maximum and the outcome will be a rapid decrease in molecular weight; thus, there is present at all stages of the reaction a continuous spectrum of products of various chain lengths, the smaller fragments being volatile at the reaction temperature. The yield of monomer is very low. It was found that whereas linear PE shows behaviour characteristic of intermolecular transfer during thermal decomposition, branched PE appears to undergo intramolecular transfer.^(51,52)

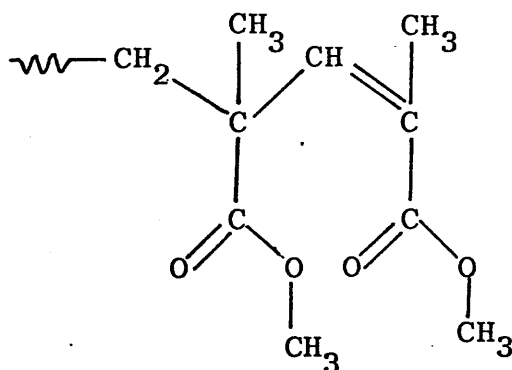
EFFECT OF POLYMER STRUCTURE UPON DEPOLYMERIZATION

The products and overall rate characteristics of the depolymerization of a variety of polymers have been examined by Wall, Madorsky and their co-workers. Observation of the results showed that the relative importance of transfer and depropagation depends

basically on two factors:

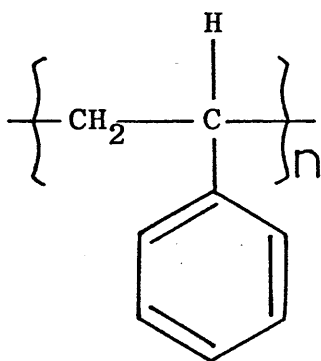
- (i) the availability of reactive atoms (usually hydrogen) in the polymer chain;
- (ii) the reactivity of the degrading polymer radical.

Both factors are dependant upon polymer structure. The importance of labile structures within the polymer molecule upon depolymerization is typically exemplified by the degradation of PMMA. The concentration of these structures is dependant upon the polymerization conditions employed.⁽⁵³⁾ Thus where termination of free radical propagation occurs by disproportionation reaction, the unsaturated chain end so formed is unstable compared with the remainder of the macromolecule. The chain end is illustrated below:

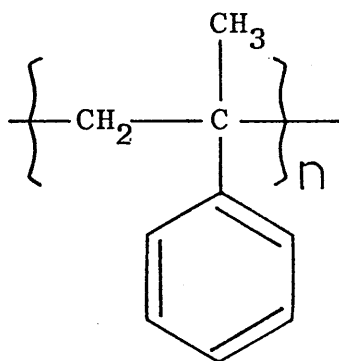


The strength of bond in the conjugated position with respect to the unsaturation is reduced by the resonance energy of the allylic radical formed by its scission. Such a radical shielded by bulky substituents will depropagate rather than abstract neighbouring hydrogen atoms which are relatively unreactive and sterically hindered. The rate of

depolymerization of PMMA will be therefore dependant upon chain end concentration and hence inversely proportional to molecular weight. From this fact one sees that the increasing of the substitution in a polymer chain reduces generally the potential number of transfer sites by shielding the chain from radical attack. This behaviour is again exemplified by comparison of the degradations of polystyrene (PS)(a) and poly(α methyl styrene) (P α MS)(b):



(a)



(b)

Chain transfer reactions are reduced by replacement of the tertiary hydrogen in PS by a methyl group leading to an increased result in monomer yield from about 40% in PS at 300°C - 400°C to almost 100% in P α MS.

In general conclusion, highly substituted radicals are more stable electronically and therefore less likely to attack C-H bonds. Steric hindrance to the approach between radical and polymer chain will also increase with both substitution and the size of the substituent. Therefore tertiary radicals may be

expected to be least active and hence will tend to reduce the "unzipping" to monomer.

SUBSTITUENT REACTIONS.

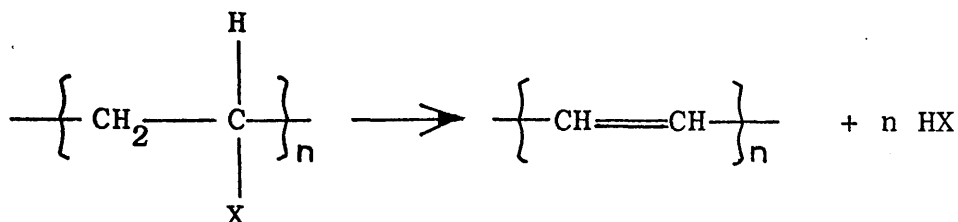
Substituent reactions will only take place when they can be initiated at temperatures lower than those at which chain scission occurs. Even the most structurally favoured chain scission processes seldom take place below 200°C and often substituent reactions, if they can occur at all, are well advanced at this temperature.

Substituent reactions differ from chain scission reactions mainly in that the basic mechanism of decomposition depends predominantly upon the chemical nature of the pendant functional groups. Free radical, molecular or ionic processes may take place. Substituent reactions may be classified in three main categories:

- (a) elimination reactions.
- (b) cyclization reactions.
- (c) ester decompositions.

- Elimination reactions.

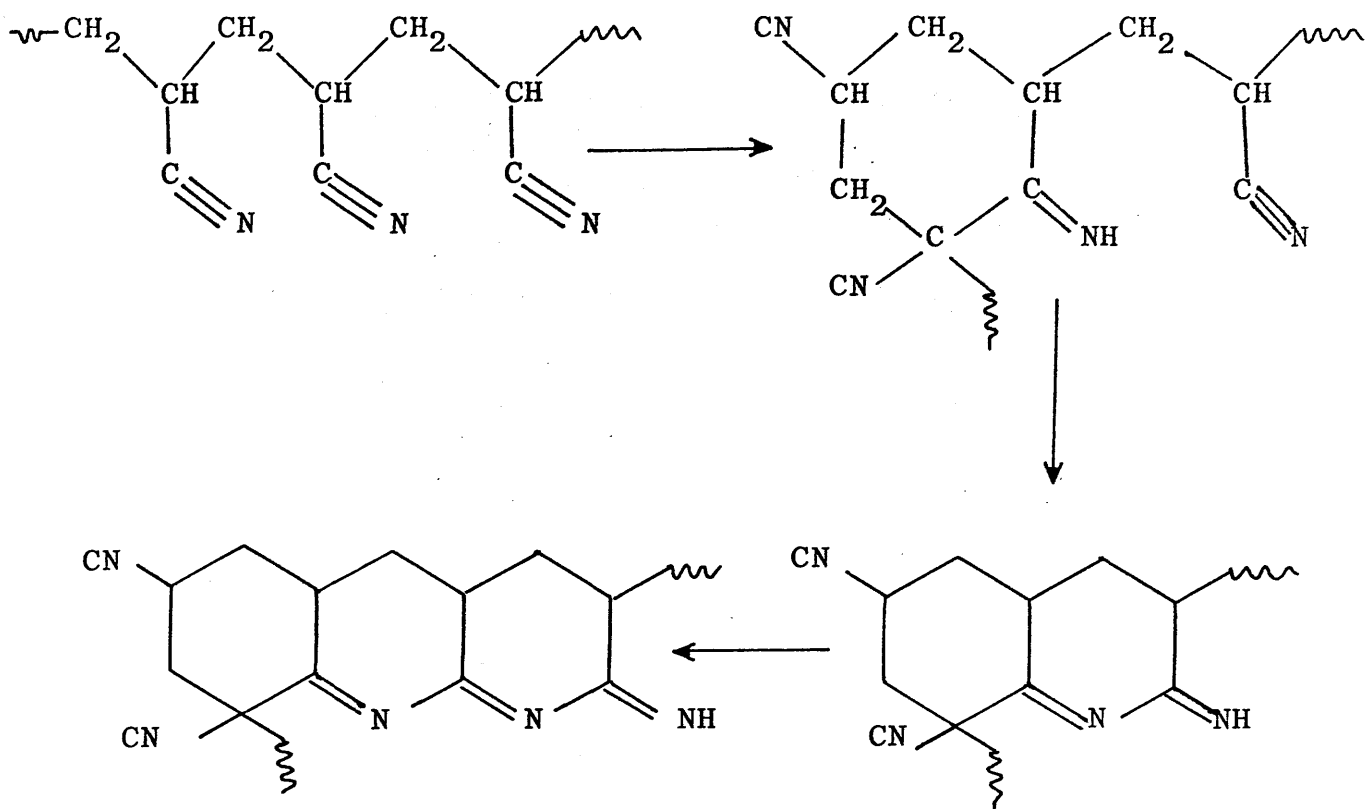
Type (a) is best illustrated by PVC⁽⁵⁴⁾



This kind of elimination was also found to take place in the case where $X = \text{OH}$, Br or $\text{O}-\text{C}-\text{CH}_3$ respectively.⁽⁵⁵⁾ Most detailed work $\begin{array}{c} \text{O} \\ \parallel \\ \text{O}-\text{C}-\text{CH}_3 \end{array}$ towards the understanding of this type of reaction, has been concerned with PVC degradation and yet the mechanism is still very much in doubt. It has been suggested on various occasions that the elimination is radical, molecular or ionic with evidence to support each case.^(54,56) Most workers appear to favour the radical mechanism and yet neither autocatalysis by HCl ⁽⁵⁷⁾ nor the interaction of stabilizers can be explained in a satisfactory manner by this mechanism.

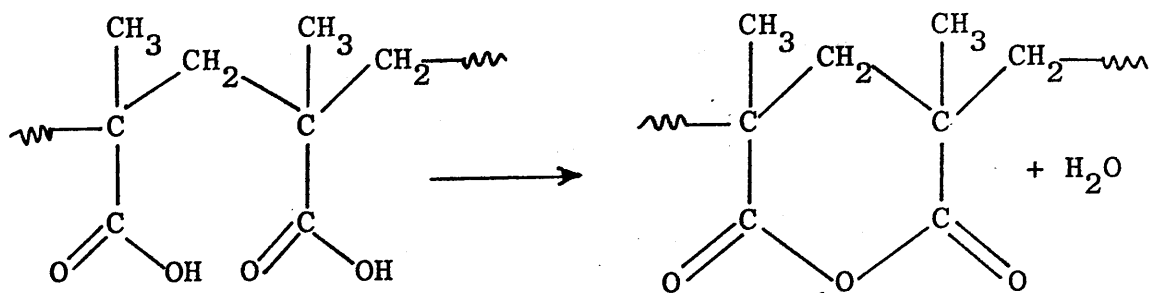
- Cyclization reactions.

The neighbouring functional groups or atoms, between which reaction takes place, may be vicinal or separated by three or more carbon atoms. In the latter case, the interaction results in the formation of cyclic structures in the polymer chain which in some cases are ladder-like in character with several pairs of substituents being involved successively along the particular segments of the polymer chain. A common example of this is the thermal colouration of poly(acrylonitrile) (PAN).^(58,59)



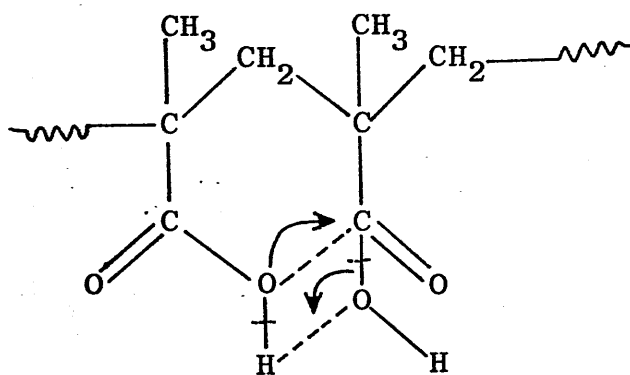
As in the previous example of elimination reactions, this too results in a conjugated structure, chemically different from the initial polymer with the difference that evolution of small molecules does not occur.

In certain cases the two types of reactions may take place simultaneously. Examples are found in both PMAA decomposition (A) and that of poly (methyl - vinyl - ketone) (PMVK) (B) where water is the eliminated product, (60,61)

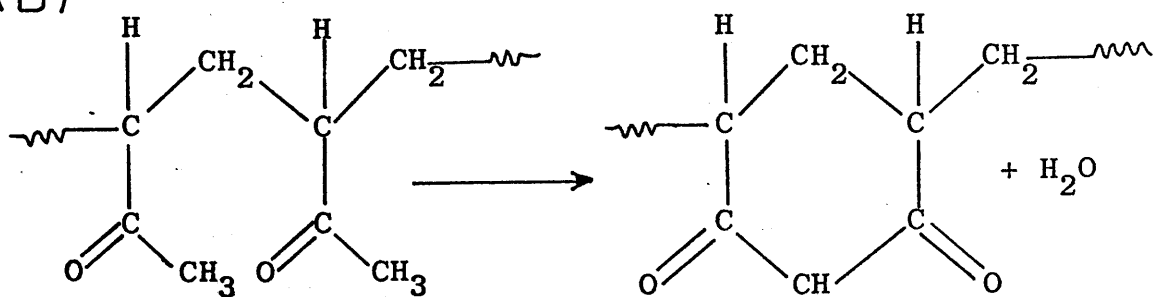


(A)

the reaction passing through the transition state

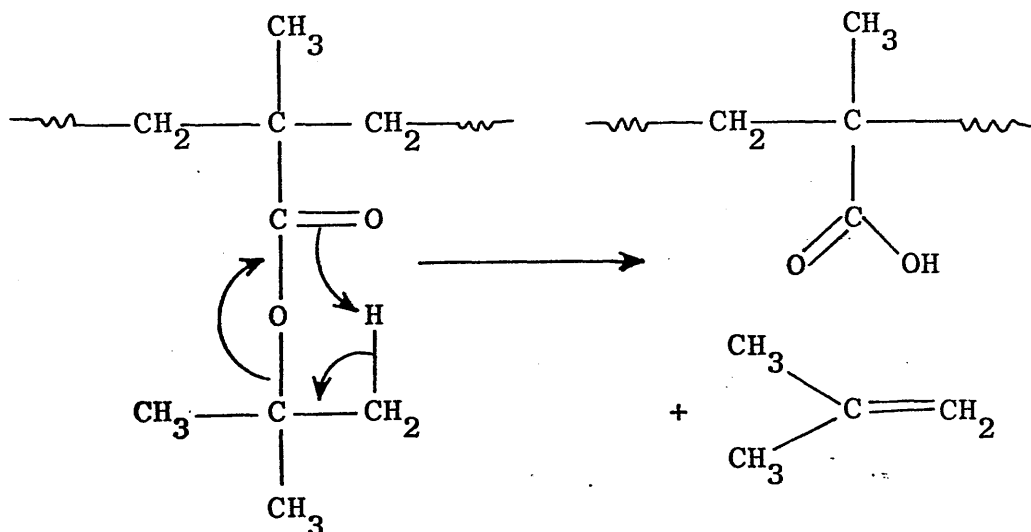


(B)



Ester decomposition reactions.

These involve generally the release of parent acid together with an olefin and were found to take place in certain (but by no means all) ester polymers as in short chain ester pyrolysis. A typical example of the process is given by the pyrolysis of poly (tert - butyl - methacrylate) (PtBMA) which involves the formation of PMAA in the residue with the evolution of isobutene. (60)



Ester decomposition is characteristic of other polymethacrylates containing a hydrogen atom in the alcohol residue. This reaction is also found to take place during the course of the polymerization of n - butyl - methacrylate effectively producing copolymers containing small amounts of methacrylic acid. (62)

CHAPTER II

EXPERIMENTAL PROCEDURE AND TECHNIQUES OF THERMAL ANALYSIS

The experimental techniques and apparatus used in this work are briefly described in this chapter. The preparation, purification and characterization of monomers and polymers dealt with in this work will be considered in detail in the next chapter.

THERMAL VOLATILIZATION ANALYSIS (TVA)

As TVA was intensively used throughout this work it is appropriate to give a full description of the apparatus, operation, advantages and limitations. TVA and its applications to polymer chemistry has recently given rise to an increasing number of publications⁽⁶³⁻⁷³⁾ and now is a well established technique of thermal analysis.

PRINCIPLE OF TVA

The TVA technique and its applications have been developed by McNeill.^(65,68) It is essentially a "physical" technique involving continuous measurement of the pressure exerted by the volatile products as

they are released from the heated sample, the whole system being continuously under high vacuum. The volatiles, products of degradation, are continuously pumped out from the polymer sample past a Pirani gauge to a cold trap. The response of the Pirani gauge is continuously recorded as a function of oven temperature and gives a measure of the rate of volatilization of the sample. Discrete reactions which produce volatiles from the polymer sample give rise to "peaks" on the TVA thermogram.

A schematic picture of the general experimental layout is shown in fig. II-1, while details of the sample heating assembly are given in fig. II-2.

The polymer sample, usually in the form of a fine powder or as a film cast from a suitable solvent, is heated on the base of a glass tube, 20 cm long and 4.5 cm diameter, constructed from a pyrex SRB 40 socket. The top of the degradation tube is cooled by a water jacket ("cold ring") during the experiment. The tube is heated using a Perkin Elmer F11 precision oven connected to a linear temperature programmer which enables the sample to be heated isothermally or linearly from room temperature up to 500°C at different heating rates that can be selected from 1 to 40°C/min. The oven temperature is recorded using a chromel-alumel thermocouple located just below the base of the TVA tube inside the oven.

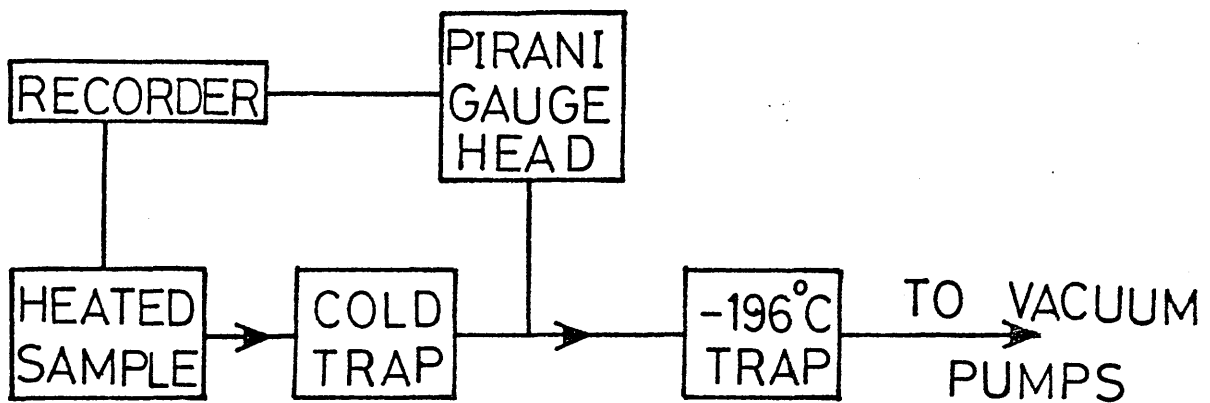
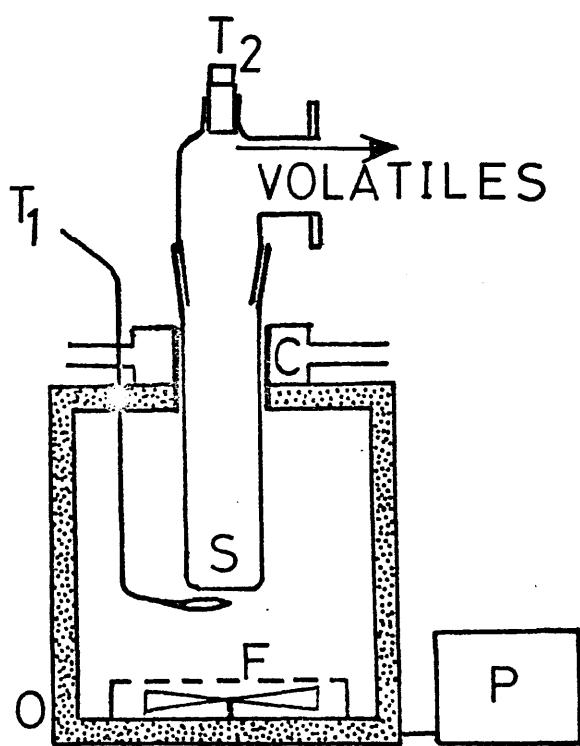


Fig. II-1

BASIC TVA APPARATUS



C: Cold ring

F: Fan

O: Oven

P: Temperature programmer

S: Sample tube

T₁: Oven thermocouple

T₂: Port for calibration thermocouple

Fig. II-2

SAMPLE HEATING ASSEMBLY

Sample temperatures are determined by a calibration procedure which involves continuous measurement of the temperature differential across the base of the tube as the temperature is raised. This will be discussed subsequently.

DIFFERENTIAL CONDENSATION TVA (67,68)

This approach is basically similar to TVA, but here the volatiles are pumped along four geometrically equivalent routes to a common "back up" trap at liquid nitrogen temperature (see fig. II-3). The four routes contain traps of different temperatures. In this laboratory, the four standard temperatures of the traps are respectively 0°C , -45°C , -75°C and -100°C . Each trap, including the common -196°C trap, is followed by a Pirani gauge and outputs from these five gauges are transmitted to a twelve channel recorder via a multihead switch unit. In the differential condensation TVA thermogram the five Pirani pressures are recorded continuously as the oven temperature is increased. Products condensable at liquid nitrogen temperature can be collected for analysis at the points indicated in fig. II-3.

It can be shown empirically that the same amount of volatiles passes into each of the four routes, but when a trap is reached, one or more of the components

P: Pirani gauge head
S: Sample collection point
●: Vacuum tap

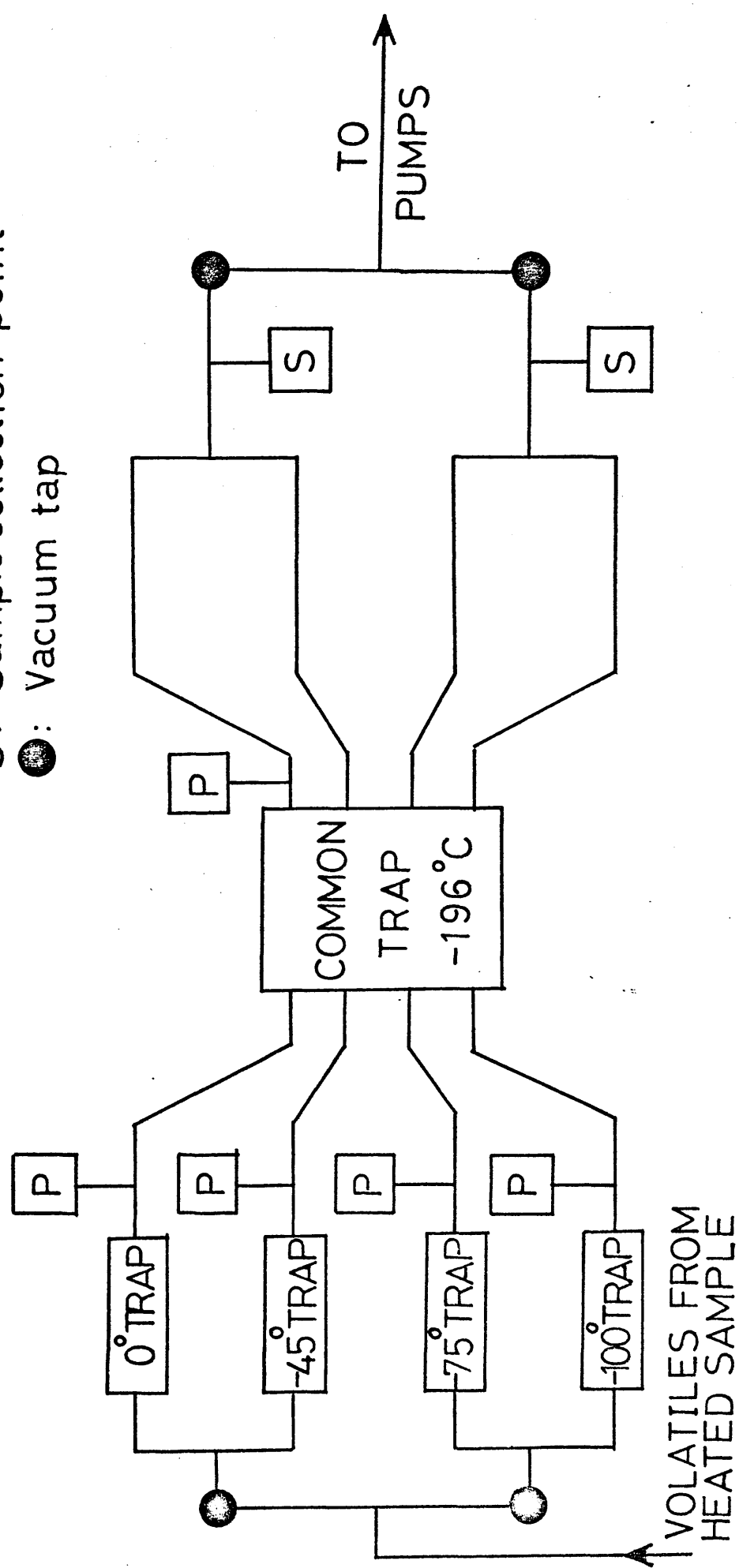


Fig.II-3. DIFFERENTIAL CONDENSATION TVA APPARATUS

may be condensed out, so that for a mixture of volatiles, the Pirani traces are often non-coincident. As a result, the volatiles from the heated sample may be fractionated according to their condensability at each of the five temperatures of the traps, and a differential condensation TVA thermogram is obtained.

By means of spectroscopic analysis of the products and a prior knowledge of the behaviour of various substances in the different traps, it is often possible to obtain useful qualitative information on the degradation pattern at various temperatures. For example, when a product shows "limiting rate" effect in one of the traps, this often facilitates its identification. The limiting rate behaviour occurs when a product condenses in one of the initial traps, and then slowly starts to distil over into the -196°C trap; the Pirani response thus generated is often seen on the thermogram as a "plateau" (see curves for PMMA in chapter V) and the displacement of this (in millivolts) from the baseline is often characteristic for a particular material.

PRODUCT ANALYSIS OF TVA FRACTIONS

The products of degradation from a polymer sample in the TVA apparatus can be classified into two main categories:

- (i) THE INVOLATILE RESIDUE;
- (ii) THE VOLATILE PRODUCTS, which can be further subdivided into three classes:
 - (a) The cold ring fraction (CRF) which contains those products volatile at the degradation temperature, but involatile at ambient temperature;
 - (b) the condensable products which are substances volatile at both degradation and ambient temperatures, but involatile at liquid nitrogen temperature;
 - (c) and finally the non-condensable products which are substances such as hydrogen, methane and carbon monoxide, volatile even at liquid nitrogen temperature.

The nature of the functional groups present in the involatile residue, remaining in the tube base, have been identified by infra-red spectroscopy.

Products forming in the CRF which were found to collect on the upper portion of the degradation tube in the area cooled by the water jacket (fig II-2), can be extracted for subsequent analysis by wiping this region of the tube with a tissue impregnated with a suitable solvent. Solvent extraction will then lead to solutions of sufficient concentrations to permit an infra-red (IR) spectrum to be run. In this work, analysis of the CRF was also carried out in the solid form. Using a spatula, small samples were removed and finely ground with potassium bromide to form a disc for IR analysis.

The condensable products can be distilled over from the common trap into a receiver and characterized by various techniques such as IR spectroscopy, mass spectrometry or gas chromatography.

The non condensables were identified using an alternative closed system, the details of which have been described by McNeill and Neil.⁽⁷³⁾ This consists mainly of an IR gas cell and cold trap to condense the less volatile substances.

CALIBRATION OF THE OVEN THERMOCOUPLE

The oven thermocouple, since it is situated outwith the relatively large glass degradation tube which has a correspondingly large thermal capacity, records always a higher temperature at any particular time during the degradation, than the true temperature of the polymer sample. The difference ΔT between the recorded temperature and the true sample temperature will, therefore be particularly dependent upon the mass of the degradation tube and the heating rate employed. The temperature of the tube is always lower than that of the oven.

The internal tube base temperature can be obtained by calibration using a second chromel-alumel thermocouple the junction of which is surrounded at the point of contact with the glass base of the tube by a small bead of Apiezon L grease to improve thermal

contact and to simulate molten polymer.⁽⁶³⁾ The calibration plot for a tube of 150g weight and a heating rate of 10°C/min is shown in fig. II-4. McNeill⁽⁶³⁾ found that at a particular heating rate the temperature lag was reproducible, and that it increased with increasing rate of heating. It can be seen on fig. II-4 that the correction required decreases with increasing temperature.

In using this calibration it is assumed that the polymer sample temperature is equal to that of the base of the tube, which is reasonable considering the large mass of the tube and the small mass of polymer, which is thinly distributed over the tube base.

SAMPLE HEATING RATE

Unless otherwise stated, all TVA data in the present work, including Tmax values (i.e. temperatures at which peak maxima occur) refer to a programmed heating rate of 10°C/min which is the standard rate used in this laboratory.

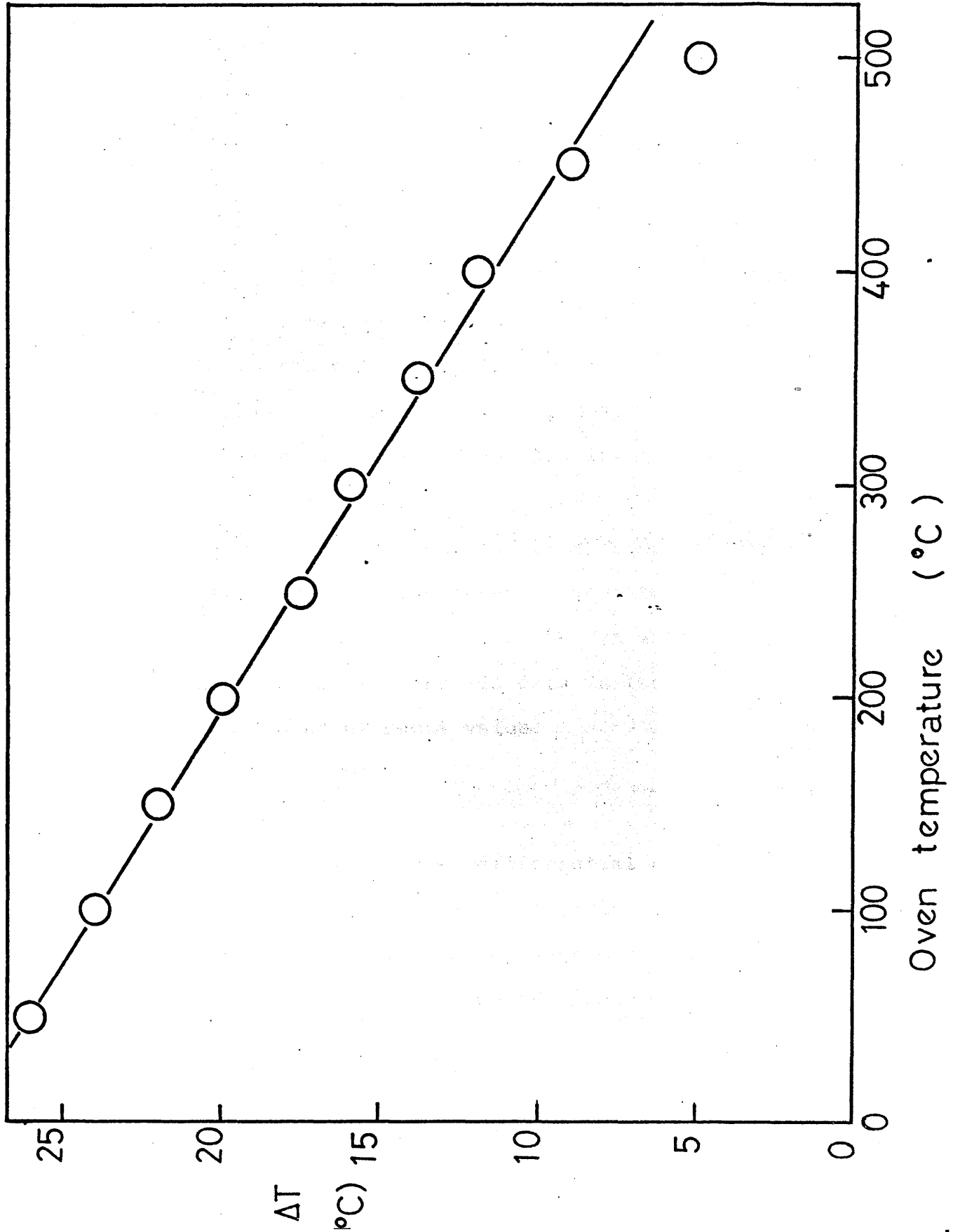
THE DISADVANTAGES OF TVA

The main limitation of TVA is that, unless detailed calibration experiments are carried out for each volatile substance, it can only be used as a semi-quantitative technique of thermal analysis, since the Pirani response is only linear with the rate of volatilization for

Fig. II- 4

TVA OVEN THERMOCOUPLE CALIBRATION

(heating rate: 10°C /min)



signals lower than one millivolt. At higher flow rates, the Pirani response becomes progressively less sensitive, although calibration is possible using a flow-meter.

It was also found that Pirani response per unit mole is dependent on the substance distilling, so that a direct comparison of amounts of different volatile materials, even at low Pirani responses, is not possible.

In addition, the peaks on a TVA thermogram often merge and this may obscure discrete reactions occurring in the polymer during degradation.

And finally, it is only those products which are sufficiently volatile to reach the Pirani filament that give a response on the recorder. This means that not all processes detected by thermogravimetry can be detected by TVA. However a micro-balance system can be incorporated with the TVA system and the combination of TVA and TGA data in the same experiment can be of great value.

ADVANTAGES OF TVA

Despite its limitations, differential condensation TVA provides a lot of useful qualitative information for polymer characterization or degradation studies.

By simple inspection of the TVA traces corresponding to traps at various temperatures, it is often possible

to make useful deductions about the volatile products which are contributing to each peak, assuming that no more than one shows the same condensability characteristics. Limiting rate effects can be of great help in the identification of specific products of degradation.

Since in TVA the sample is heated either in the form of a very thinly distributed powder or as a film, the temperature gradients within the sample are minimized, and the sample temperature can be accurately measured because of the massive degradation tube.

Furthermore, the large area available for the sample, and the continuous and efficient removal of the volatiles from the sample, are factors which tend to reduce the chance of diffusion controlled processes and secondary reactions between products or between products and sample, occurring during decomposition.

THERMOGRAVIMETRIC ANALYSIS (TGA)

For experiments carried out under vacuum a CAHN micro-balance built into a differential condensation TVA system was used. A thermogram obtained from such an experiment will be subsequently referred to as a TG/TVA trace.

A circular platinum pan (2cm diameter) was used

and samples of no more than 25mg were used. These were carefully spread as a thin layer of powder on the pan before each thermogravimetric experiment.

TGA experiments were also carried out under a dynamic nitrogen atmosphere using a Du Pont 950 Thermogravimetric Analyser. With this instrument, a boat shaped platinum sample holder (dimensions 1 x 0.5 x 0.25cm) was used. The temperature measuring thermocouple was placed at 0.1cm above the sample holder. The rate of nitrogen flow was 80cm³/min., and the sample sizes used were from 5 to 10mg. Programmed degradation was carried out at the rate of 10°C/min from room temperature up to 500°C. Isothermal conditions were also used in some experiments.

The observations obtained from TGA under vacuum were in agreement with the qualitative data obtained from TVA as will be seen in each of the TG/TVA thermograms in chapter V.

DIFFERENTIAL THERMAL ANALYSIS

A Du Pont 900 unit was used for this purpose. 10mg polymer samples in powder form were packed into a small glass tube 2.5cm long by 4mm diameter; a chromel-alumel thermocouple was forced down so that the junction pierced the polymer mass. The reference junction was in an identical tube containing the same weight of small

glass beads. Sample and reference tubes were fitted into a heater block contained in a glass dome through which nitrogen gas passed at a flow rate of $80\text{cm}^3/\text{min}$. Again here, the experiments were carried out at the heating rate of $10^\circ\text{C}/\text{min}$ from ambient temperature up to 500°C .

INFRA-RED SPECTROSCOPY

A Perkin Elmer 257 Grating Spectrophotometer was used for all infra-red (IR) experiments.

Polymer samples, degradation residues and cold ring fractions were examined in KBr discs, each time 2mg approximately were finely ground with 300mg of especially pure KBr (Analar grade) and the mixture was pressed for three minutes ($8\text{tons}/\text{in}^2$) under vacuum. This gave small and clear discs from which IR spectra were run. The part of the CRF which was soluble in carbon tetrachloride or chloroform was also examined in a solution cell.

The volatile products from degradation of polymer samples were examined in the gaseous phase.

GAS CHROMATOGRAPHY

For the most part, G.L.C data were obtained using a Perkin Elmer F11 gas chromatograph equipped with a hot wire detector. The liquid degradation products from copolymers dealt with in this work, had boiling points

ranging from 50°C to 160°C. This caused problems of collection. The TVA apparatus, because of its large surface area proved to be inefficient for the distillation of the high boiling point ketones into the receiver. A simpler arrangement with a minimum surface area was used to this end (fig. II-5).

Two columns were used for the identification and quantitative estimation of the liquid products:

(A) A six foot long, $\frac{1}{8}$ inch diameter, 10% PEG 400 on Chromosorb P, 80 - 100 mesh column was used both for ketones and methyl methacrylate under isothermal conditions between 50°C and 70°C;

(B) A six foot long, $\frac{1}{8}$ inch diameter, 13 $\frac{1}{2}$ % BMEA + 6 $\frac{1}{2}$ % bi - 2 - ethyl - hexyl sebacate on chromosorb P, 80 - 100 mesh column which was used isothermally:

(i) at 50°C for aldehydes, methanol, methyl methacrylate and low boiling point ketones;

(ii) at 70°C for high boiling point ketones.

Quantitative measurements on the liquid volatiles were made by adding a known weight of a suitable material as internal standard (n - butyl - alcohol was used throughout this work) to a weighed quantity of liquid products. Several mixtures were made up with known amounts of the internal standard. Measurements of the peak areas on G.L.C traces were mainly carried out by planimetry since the peak area for one particular substance is proportional to the weight present.

An Infotronic integrator was also used for the quantitative estimation of ketones. If the sensitivity factor, k , for any product X is defined as the ratio of the peak areas of standard to product when equal weights of both are considered, then the percentage by weight of X in G grams of sample is given by:

$$\% X = k \cdot \left(\frac{\text{peak area of } X}{\text{peak area of standard}} \right) \cdot \left(\frac{100}{G/\text{weight of standard}} \right)$$

and the number of moles of product X in the sample will simply be:

$$N = k \cdot \left(\frac{\text{peak area of } X}{\text{peak area of standard}} \right) \cdot \left(\frac{\text{weight of standard}}{\text{weight of 1 mole of } X} \right)$$

MASS SPECTROMETRY

This was carried out on volatile products using an AEI MS12 Mass Spectrometer. Products collected from TVA experiments were either directly expanded into the spectrometer or fractioned using a liquid nitrogen trap to separate condensable and non-condensable products.

QUALITATIVE DISTILLATION OF CONDENSABLE PRODUCTS^(74,75)

The total condensable products were trapped at liquid nitrogen temperature in trap A, fig. II-5. On completion of degradation, pumping was carried on for a further ten minutes to ensure that all the products had been removed

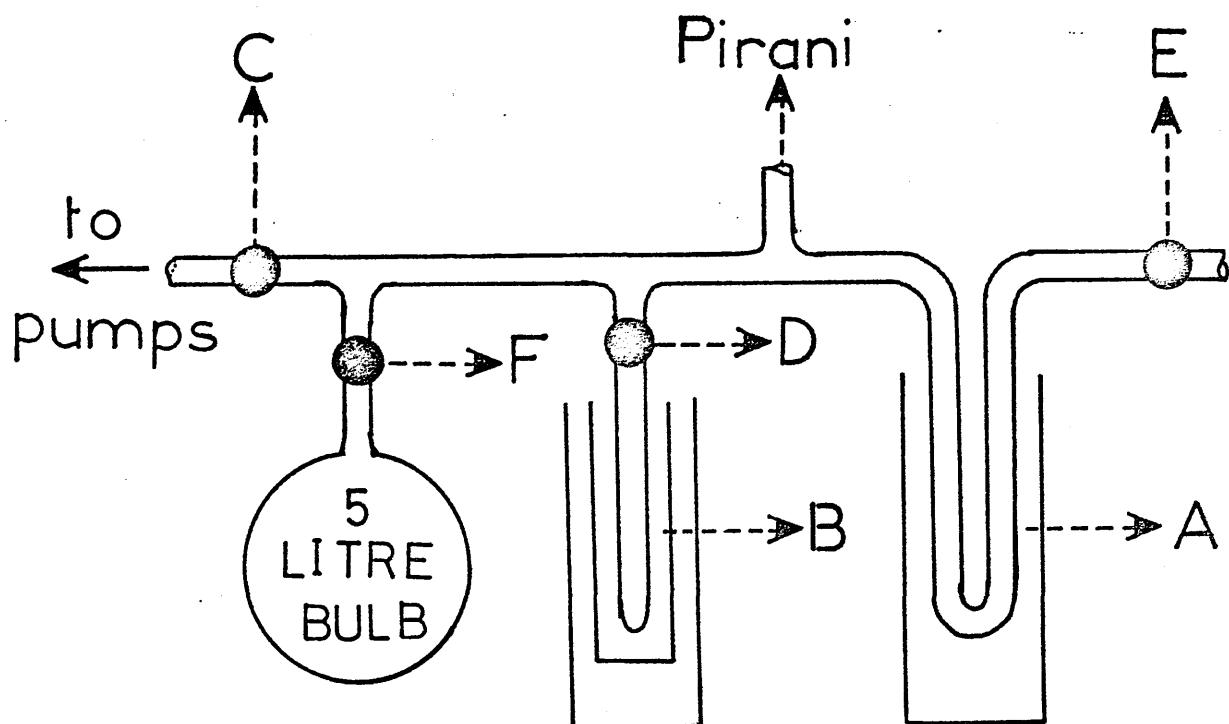


Fig.II-5. THE PRODUCTS DISTILLATION SYSTEM

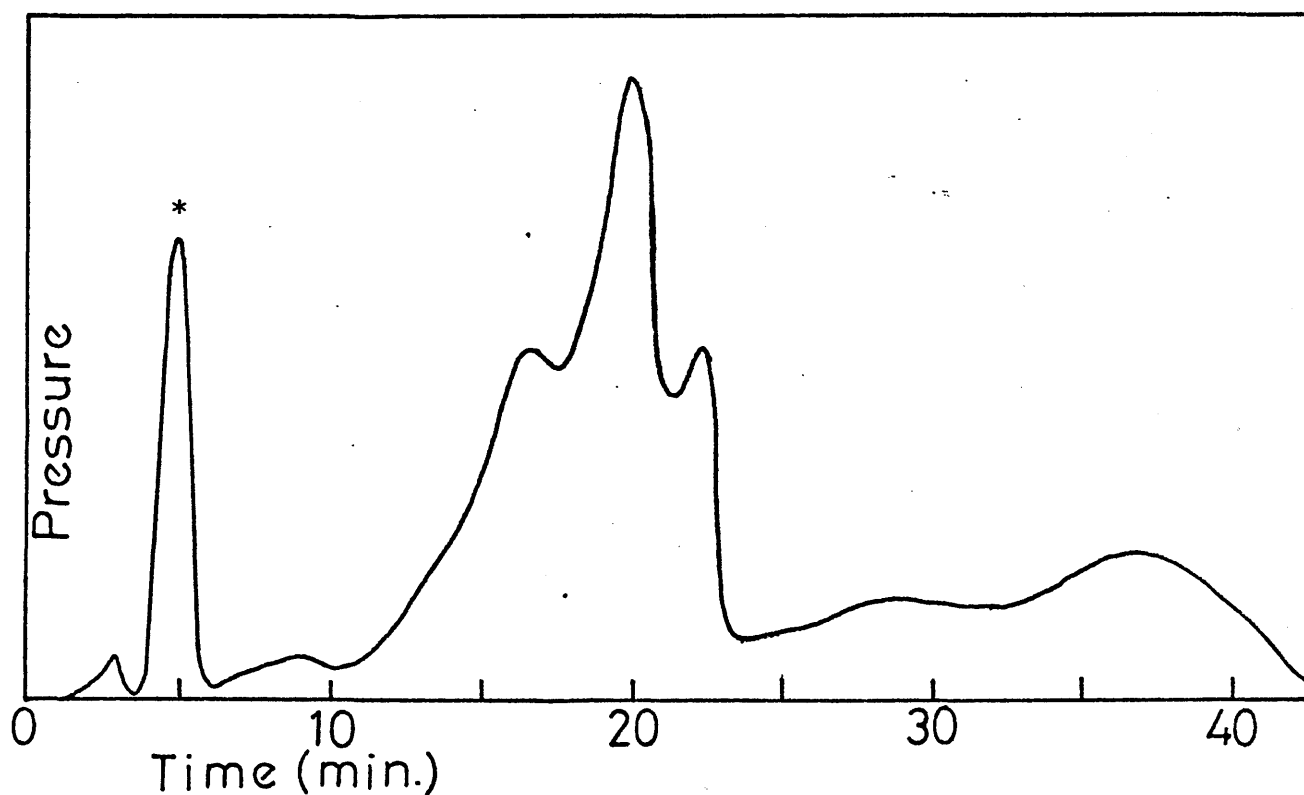


Fig.II-6. THE QUALITATIVE DISTILLATION CURVE OF THE PRODUCTS
ON DEGRADATION OF 50% LiMA/MMA COPOLYMER.

from the polymer sample. Stopcocks C, E and F were then closed and the products rapidly distilled over into cold trap B. The inner tube around this trap contained benzene, and the outer Dewar contained liquid nitrogen. Trap A was re-cooled to liquid nitrogen temperature and the liquid nitrogen Dewar around trap B removed. The products distilled over into trap A and a Pirani gauge connected to a recorder was used to plot the pressure changes as the distillation went on. A typical distillation curve of the degradation products from a 1:1 molar ratio copolymer of lithium methacrylate and methyl methacrylate is shown on fig. II-6.

Ideally, if all degradation products had appreciably different boiling points, each peak would correspond to one particular compound and the separation between one product and the next would be neatly discernable. This would lead to a succession of peaks reaching a maximum pressure and returning to a pressure of better than 10^{-5} mm. Hg. (baseline) when distillation of the corresponding compound is completed.

Unfortunately, such a separation is far from being achieved in this manner under the experimental conditions employed. In the case of the products dealt with in this work, the complex nature of the volatiles gave an ideal separation for only one product: carbon dioxide marked with an asterisk on fig. II-6.

However the qualitative distillation of the products coupled with IR analysis of mixtures of products corresponding to each peak was of great assistance in identification of the different volatile products.

QUANTITATIVE ANALYSIS OF CARBON DIOXIDE

The qualitative distillation technique just described can be adapted for quantitative measurements^(74,75) provided the product dealt with is ideally separated from the others by it. This was carried out as follows: Vacuum taps C and E remained closed while D was closed immediately after complete distillation of carbon dioxide alone, anything distilling before it having been evacuated firstly. The end of the distillation of the product is indicated by the Pirani gauge returning to a pressure of 10^{-5} mm Hg. Trap B was re-cooled while the liquid nitrogen Dewar round trap A was removed and carbon dioxide was allowed to evaporate and expand into the closed system. The final pressure was noted when the system was at ambient temperature. Qualitative distillations were most sensitive when the volume of the system was small while for quantitative distillations a larger volume was required if the Pirani was not to be used in the region where it was less sensitive. This requirement was satisfied by opening vacuum tap F to a five litre flask when trap A was warmed up to room temperature during the experiment.

Polymer samples of no more than 10mg were used for this purpose. The Pirani gauge had to be previously calibrated in its most accurate region (0 to 0.1mm HG), with a MacLeod gauge. The volume V of the system between C and E, including the five litre flask, was calculated as follows:

The line was completely evacuated, then a receiver of a known volume V_1 containing carbon dioxide at atmospheric pressure, was attached to the system on D and stopcock D was then opened. Vacuum taps C and E were closed at a pressure P_1 given by the Pirani. Then trap D was closed again and the system was re-evacuated. When the Pirani gauge showed no reading on the pressure scale, taps C and E were closed again and tap D re-opened to the system. The Pirani gauge gave another pressure reading $P_2 < P_1$.

At this stage one can calculate the volume V of the system from the following expression:

$$P_1 V_1 = P_2 \cdot (V_1 + V)$$

If the pressure corresponding to the amount of carbon dioxide expanded in the system of volume V is known, the number of moles of carbon dioxide in the degradation products will simply be given by the expression:

$$n = PV/RT$$

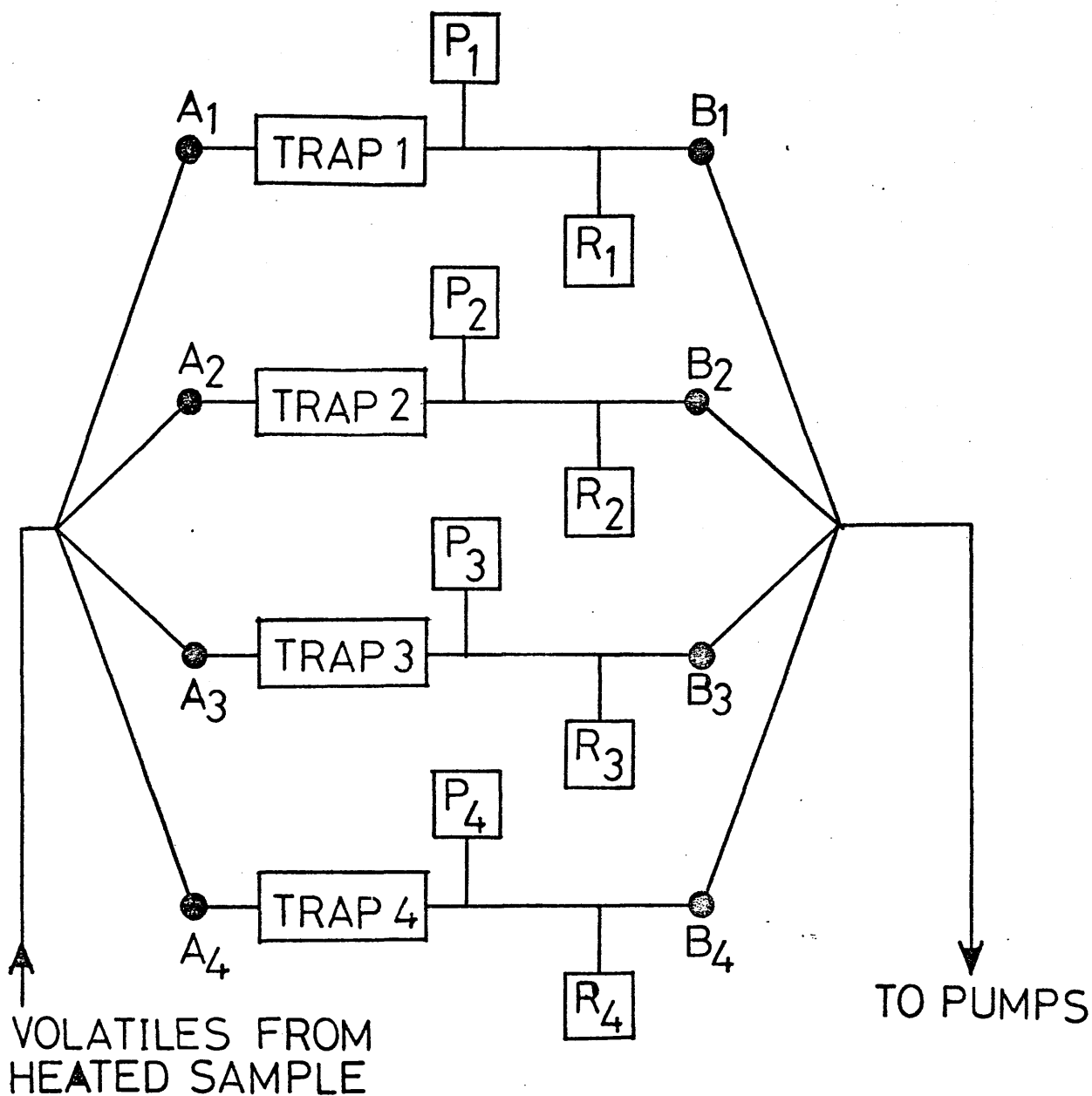
The method gave results that were reproducible to within 5% and results for particular copolymer systems are shown in the appropriate chapters.

PRODUCT COLLECTION UNDER ISOTHERMAL CONDITIONS

Quantitative analysis of major condensable liquid products under isothermal conditions was carried out by gas chromatography. This usually requires the availability of appreciable amounts of polymer samples since for each length of degradation time a fresh sample has to be used. Since only limited amounts of polymer samples were available a simple assembly for product collection was constructed in order to use the same polymer sample for several collections (see fig. II-7). A 100mg sample was degraded isothermally at a temperature T and the first collection was made in trap 1, the second in trap 2 after closing vacuum taps A_1 and B_1 , the third collection in trap 3 closing A_2 and B_2 , etc. Trap A can again be used for a fifth collection after the distillation of the first one into receiver 1 and evacuation.

The Pirani gauges show when the distillation of a complete fraction is finished.

The system was found highly efficient and convenient from both time and sample saving point of view.



P_i Pirani gauge heads
 R_i Products receivers
 ● Vacuum taps

Fig. II-7

ASSEMBLY FOR PRODUCT COLLECTION
UNDER ISOTHERMAL CONDITIONS

CHAPTER III

MONOMER AND POLYMER PREPARATION

Since none of the salts of methacrylic acid was commercially available preparation and characterization of lithium, sodium and potassium methacrylates had to be carried out. In this chapter, preparation, purification and characterization of both monomers and polymers are described.

INTRODUCTION

Most research on methacrylic monomers has been centred on the nitrile and ester derivatives and to a lesser extent on the amide. A smaller amount of attention has been devoted to the salts of methacrylic acid.

Several workers⁽⁷⁶⁻⁷⁹⁾ have studied the solid state polymerization of alkali and alkaline earth metal salts of methacrylic acid. Although solid state polymerization is now recognised to be possible for a wide variety of monomers, there is still little fundamental understanding of the process or even of the relative importance of the chemical and physical

parameters involved. In fact most of the investigations undertaken on solid state polymerization were carried out to determine whether or not a crystalline polymer was formed.

Many workers⁽⁸⁰⁻⁸⁵⁾ have studied the kinetics of methacrylic acid aqueous polymerization and they all agree on one fact: the dependance of the rate of polymerization on the pH of the medium.

Alkali metal salts of methacrylic acid were prepared by Kikuchi et al⁽⁸⁶⁾ who also studied the kinetics of aqueous polymerization of potassium methacrylate. They found that KMA can easily be polymerized in aqueous solution using ammonium persulphate as initiator at pH 8.2 and showed that in the initial stage, the rate of polymerization was proportional to the first power of the monomer concentration and also to the first power of the initiator concentration. However, they did not characterize the polymer so obtained.

If not much attention has been given to the characterization of the polymers of salts of methacrylic acid, even less work has been devoted to their copolymers.

Wojnarowski and co-workers⁽⁸⁷⁻⁹¹⁾ prepared in aqueous media a series of copolymers of salts of methacrylic acid and acrylic acid with styrene

and acrylamide. They showed that in the case of the aqueous polymerization of acrylamide with alkali metal acrylates⁽⁸⁹⁾ and methacrylates,⁽⁸⁷⁾ the monomer reactivity ratios, the overall rate of copolymerization and some electrochemical properties of the copolymers depend closely upon the nature of the cation in the corresponding acrylate or methacrylate salt. The r_1 values (reactivity ratios for monomer 1:acrylamide) increase in the order $\text{Li}^+ < \text{Na}^+ < \text{K}^+$ in the case of copolymerization with salts of both acrylic acid and methacrylic acid, whereas the r_2 values decrease. This effect of the nature of the cation upon reactivity of monomer appears to be mainly due to the electrostatic nature of the salt. These effects are related to cation binding by polyacid, which is equivalent to incomplete dissociation of polysalt even in aqueous solution.

As far as copolymers of alkali metal salts are concerned only one case is known: the heterogeneous copolymerization of sodium methacrylate with methyl methacrylate has been carried out by various workers^(92,93) in a stirred aqueous medium using a persulphate as initiator. A general picture of the kinetics of the copolymerization is given, but so far nothing has been published about the characterization or the reactivity ratios of such copolymer systems.

In the present work the alkali metal salts of

methacrylic acid were all synthesised and copolymerised with methyl methacrylate in a homogeneous non-aqueous medium. The respective homopolymers poly(lithium methacrylate), poly(sodium methacrylate) and poly(potassium methacrylate), subsequently denoted PLiMA, PNaMA, PKMA respectively, were also prepared under the same conditions for comparison, although the details of their polymerization, characterization and thermal degradation have recently been investigated in this laboratory by McNeill and Zulfiqar.⁽⁹⁴⁾

PREPARATION AND PURIFICATION OF MONOMERS

Several relatively simple processes may be employed to make the alkali metal salts. Neutralization of methacrylic acid with the hydroxide or the carbonate of the corresponding metal is the most direct method and was the one used throughout this work.

The literature shows also that saponification of methyl methacrylate was sometimes found to be a convenient route.

DISTILLATION OF METHACRYLIC ACID

Methacrylic acid (Koch Light) contains 0.1% of hydroquinone to stabilize it. It was purified and freed from inhibitor by distillation at low pressure.⁽⁹⁵⁾ Even at low pressure and in presence of inhibitor, the

distillation was difficult because polymer forms readily. Many precautions had to be taken in order to avoid polymerization and the conditions used in this work were as follows. Distillation was carried out at a pressure of 0.8 mm Hg and 0.1% of cuprous chloride (CuCl) was added to the stillpot to act as an inhibitor. The column and the condenser were packed with copper helices and the fraction boiling at $38-39^{\circ}\text{C}$ was used for preparation of the methacrylate salts. The methacrylic acid thus obtained, was stored in the dark at -10°C .

PREPARATION OF THE ALKALI-METAL SALTS OF MAA

The lithium, sodium and potassium salts were prepared as follows:

The corresponding hydroxide was dissolved in a minimum of methanol (Analar grade). The alkali solution was neutralized by addition (drop by drop) of freshly prepared methacrylic acid using phenol-phthalein as indicator. The whole reaction was carried out at 0°C and the solution was kept under constant stirring. These two precautions are very important since the bulk addition of methacrylic acid to the alkali solution might produce sufficient heat of neutralization to result in the polymerization of the unsaturated acid. The neutralized solution was then filtered and the methacrylate salt was precipitated out into a large

excess of anhydrous diethyl ether (Analar grade) under vigorous stirring. The white precipitate was filtered, washed several times with diethyl ether and Analar acetone, dried under vacuum, re-dissolved in methanol, re-precipitated in Analar anhydrous diethyl ether, filtered, washed again with acetone and finally dried overnight at 60°C under vacuum. The white crystalline solid was ground into a very fine powder which was then passed through a sieve (mesh number 150) and re-dried for a further forty-eight hours at 70°C in a vacuum oven before further analysis or polymerization.

CHARACTERIZATION OF Li, Na and K METHACRYLATES

In comparison with conventional salts, these materials display a pattern of chemical behaviour analogous to such related salts as the propionates or acetates. They all give alkaline solutions in water. The sharp contrast in chemical behaviour between these salts and those of the isobutyrate class is accounted for by the presence of the double bond in the methacrylate metal salts.

Characterization of the monomers was carried out by three different routes:

- (a) carbon and hydrogen analysis
- (b) estimation of metal content
- (c) infra red spectroscopic investigation for

carbonyl and double bond absorptions.

(a) C, H analysis

Several microanalyses were performed and the average of the results is stated for each salt in table III-1.

Table III-1

Analytical results for the monomeric salts

	<u>C, H analysis</u>				<u>Metal content</u>	
	<u>Theoretical</u>		<u>Experimental</u>		(%)	
	C %	H %	C %	H %	<u>Theoretical</u>	<u>Experimental</u>
<u>MetMA</u>						
LiMA	52.20	5.48	52.55	6.07	7.54	7.3
NaMA	44.45	4.66	44.18	5.20	21.24	21.9
KMA	38.68	4.06	38.39	4.9	31.48	31.0

(b) Metal contents

sodium and potassium methacrylates were analysed by flame photometry and lithium methacrylate by atomic absorption spectroscopy. The flame photometer and the atomic absorption spectrophotometer were calibrated using standard solutions of the corresponding metal chloride in each case.

(c) Infra red spectrometry of monomers

The IR spectra were obtained by the KBr disc technique using 1 to 2 mg of monomer and 300 mg of KBr (see chapter II). The >C=O and >C=C< stretching frequencies of methacrylic acid are at 1700cm^{-1} and 1645cm^{-1} respectively, but in the case of the monomeric salts the >C=O frequency is moved downwards by approximately 150cm^{-1} with almost unchanged >C=C< frequencies. The >C=O and >C=C< frequencies of the three salts are summarized in table III-2

Table III-2

C=O and C=C frequencies of absorption for the monomeric salts in comparison with those of methacrylic acid.

MetMA	C=O (cm^{-1})	C=C (cm^{-1})
LiMA	1560	1645
NaMA	1555	1640
KMA	1550	1640
MAA	1700	1640

SOLUBILITY OF METHACRYLATE METAL SALTS

Apart from water the monomers were found to dissolve in methanol and very slightly in absolute ethanol. The polymerization reactions were carried out in methanol and the approximate solubilities of the salts at ambient temperature are given in table III-3.

Table III-3

Approximate solubilities of the monomeric salts in anhydrous Analar methanol at ambient temperature.

MetMA	Solubility in g/litre
LiMA	190
NaMA	95
KMA	100

STABILITY OF METHACRYLATE METAL SALTS

None of the monomeric salts showed a melting point and thermogravimetric curves (fig. III-1) confirm a very high stability to temperature. No weight loss was observed up to 325°C.

Thermogravimetric analysis curves and analysis of the products of thermal degradation showed similarity with the degradation pattern of the corresponding homopolymers.⁽⁹⁴⁾ Isothermal heating at 300°C for fifteen minutes under vacuum resulted in a more or less complete polymerization of the monomeric salts in the solid state.

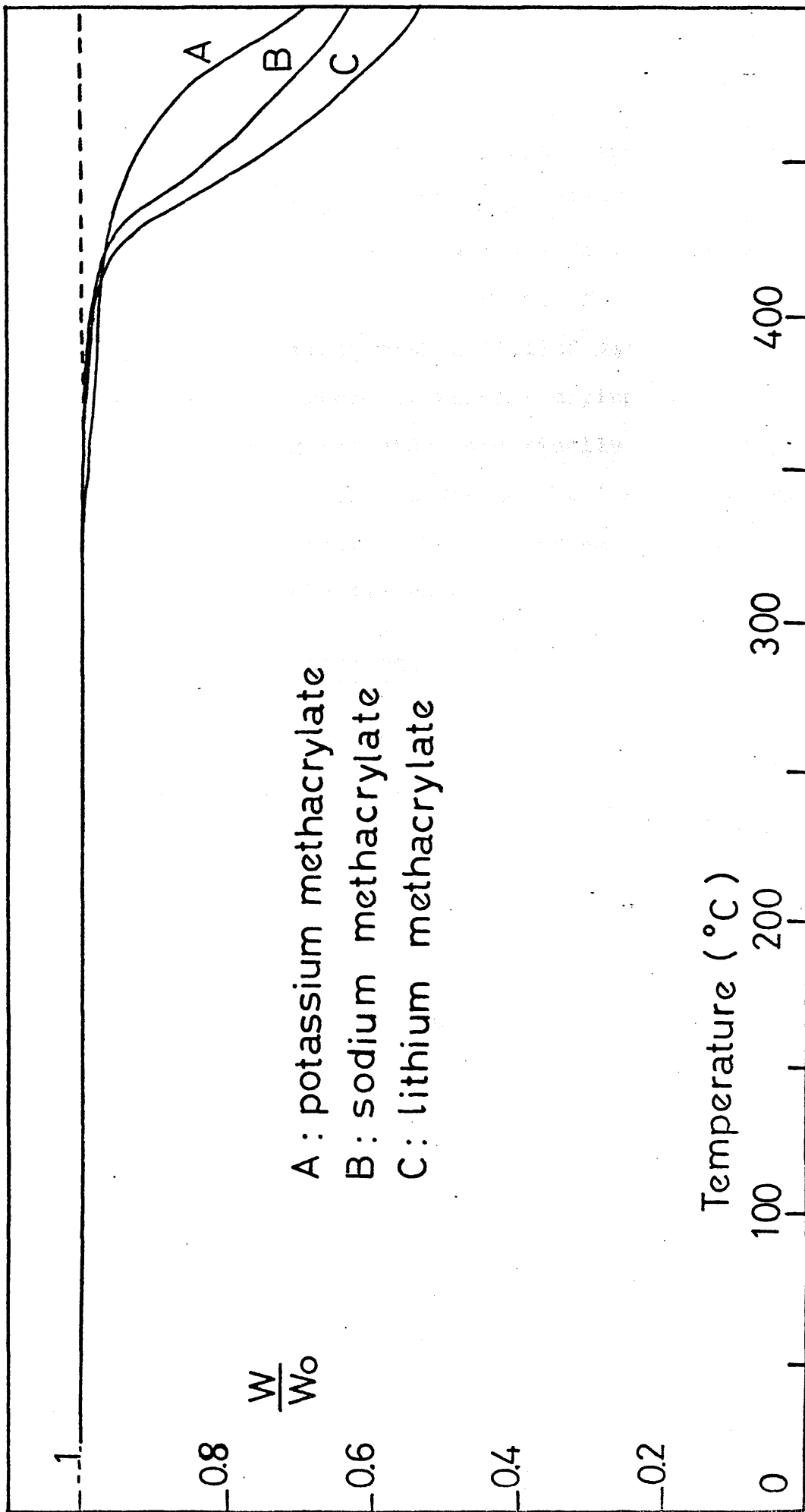


FIG.III-1: TG CURVES FOR ALKALI METAL METHACRYLATES. (HEATING RATE: $10^{\circ}\text{C}/\text{MINUTE}$).

PURIFICATION OF METHYL METHACRYLATE

Methyl methacrylate (I.C.I. Ltd.) was purified by standard techniques. These involved vigorous washing several times with 0.1 N sodium hydroxide until the washings were colourless, followed by washing several times with distilled water to remove residual traces of alkali, drying over anhydrous calcium chloride, and finally distilling under high vacuum, the first and the last 10% being eliminated; thereafter the monomer was stored in the dark at -10°C until used.

PURIFICATION OF INITIATOR

The copolymerization initiator 2,2' - azobisisobutyronitrile (Eastman Kodak) (AIBN) was purified by recrystallising twice from absolute ethanol, the solution being filtered hot to remove insoluble products of decomposition of the initiator. (96) The crystals were filtered off, dried under vacuum and kept in the dark at 0°C .

POLYMERIZATION

All polymers and copolymers were prepared in methanol solution. Apart from water Analar methanol was the only suitable solvent for the methacrylate metal salts (see table III-3). The polymerizations

were carried out under vacuum and the procedure is described in detail as follows:

Dilatometers with volumes ranging from 100 ml to 300 ml were used as polymerization vessels. They were flamed out and then washed with different solvents and dried out under vacuum.

Introduction of initiator

The recrystallised AIBN was introduced first into the reaction dilatometer as a standard solution in methanol. The solvent was removed under vacuum.

Introduction of solid monomer (salt)

The weighed crystalline powder was introduced into the dilatometer through a small funnel with the help of a one foot long copper wire and an electric vibrator which prevented the particles from sticking to the sides of the dilatometer neck.

The dilatometer containing both initiator and solid monomer was then put under partial vacuum several times before being opened fully to the vacuum pumps. These precautions are necessary because a sudden opening to the vacuum will result in filling the vacuum line with the powder sucked out of the dilatometer.

Distillation of methyl methacrylate

MMA in a graduated reservoir 1, purified as

previously described was degassed thoroughly, then distilled at ambient temperature into another graduated reservoir 2, the first and the last part of the distillate being rejected. From this vessel, a calculated amount of MMA was distilled into the main dilatometer.

Distillation of methanol

Methanol (Analar grade) previously dried for a week over calcium chloride was distilled into the dilatometer using the same technique as for MMA, except that special care had to be taken during freezing, degassing and thawing of the solvent. Freezing had to be carried out very gradually from the bottom of the reservoir up to the top, whereas the warming up after degassing had to be done instantly and thoroughly with hot water (50°C) otherwise the reservoir would crack as a result of the high cubic expansion of methanol.

Polymerization

The dilatometer was sealed off under a vacuum better than 10^{-5} mm Hg., and then warmed up to room temperature and swirled for a while in water, at ambient temperature, to accelerate the dissolution of solid monomer.

Polymerization was carried out at 60°C in a thermostat tank controlled to $\pm 0.01^\circ\text{C}$. The volume

contraction during polymerization was followed in order to restrict conversion to around 10% in homopolymers and less than 5% in copolymer systems.

The volume of MMA and methanol used for a given copolymer was worked out according to the total volume of the dilatometer, temperature of polymerization, composition of the copolymer in the monomer feed, and measured coefficients of cubic expansion of MMA and methanol which are respectively $0.000160(^{\circ}\text{C})^{-1}$ and $0.00119(^{\circ}\text{C})^{-1}$.

The total monomer/solvent ratio used was kept around 10g/100mls for NaMA/MMA and KMA/MMA copolymer systems and 20g/100mls for LiMA/MMA copolymers.

POLYMER ISOLATION AND PURIFICATION

The copolymers were precipitated (copolymers are soluble in methanol throughout the range of compositions) in absolute ethanol (Burroughs Ltd.).

However, it was observed that the copolymers having a mole fraction of salt unit in the chain between 0.12 and 0.26 approximately, did not precipitate in ethanol. Many unsuccessful attempts were made to find a suitable solvent to act selectively as a precipitant for these copolymers and not for the residual monomeric salts left. Finally, the procedure adopted to extract these copolymers consisted of the following:

The mixture of copolymer plus residual monomer left in methanol at the end of copolymerization was

precipitated in an excess of actone (Analar grade) or chloroform (Analar grade). The gel-like solid obtained was isolated by centrifugation, dried under vacuum, ground and washed in fairly large amounts of absolute ethanol with vigorous stirring for twenty four hours. The procedure often needed to be repeated at least three times in order to have a copolymer completely freed of any trace of monomer (alkali metal methacrylate salts have a very poor solubility in ethanol: less than 1%.) The copolymers thus purified were dried in a vacuum oven at 50°C overnight, then finally ground and passed through a sieve (mesh number 150) and re-dried under vacuum at 60°C for three days.

PROOF OF COPOLYMERIZATION

The major proof for the copolymerization of these systems, lies in their solubility characteristics: the materials obtained were copolymers and not physical mixtures of two homopolymers since all copolymers dissolved to some extent in methanol whereas neither poly(methyl methacrylate) nor any of the polymers of the alkali-metal methacrylate salts were soluble.

INFRA RED ANALYSIS

KBr discs of the homopolymers of LiMA, NaMA and KMA gave I R spectra which were in general agreement with

those obtained by Leyte and co-workers⁽⁹⁷⁾ who prepared the polymers by neutralising the polyacid with the required base.

I R spectra of the copolymers showed the presence of both MMA carbonyl absorption at 1725cm^{-1} and that of the carboxylate ion (1560cm^{-1}) (see fig.III-2).

No difference was observed between I R spectra of PLiMA, PNaMA and PKMA. As for the copolymers, the only differences observed in I R spectra throughout the composition range were the relative sizes of the absorptions of MMA units and salt units, due to changes in the composition of the copolymers.

ANALYSIS OF THE COPOLYMERS

The most difficult problem encountered in the elementary analysis of these copolymers was their highly hygroscopic character: the results given by microanalysis and metal content analysis never agreed. The copolymers containing a high percentage of salt units in their chains can absorb up to 30% (of their own weight) of water if left in the atmosphere for two minutes. This characteristic made their handling very difficult, so much so that it was impossible for a long time to determine reactivity ratios, because of the contradicting elementary analysis results.

The problem was finally solved when it was observed that the absorption of water from the atmosphere by

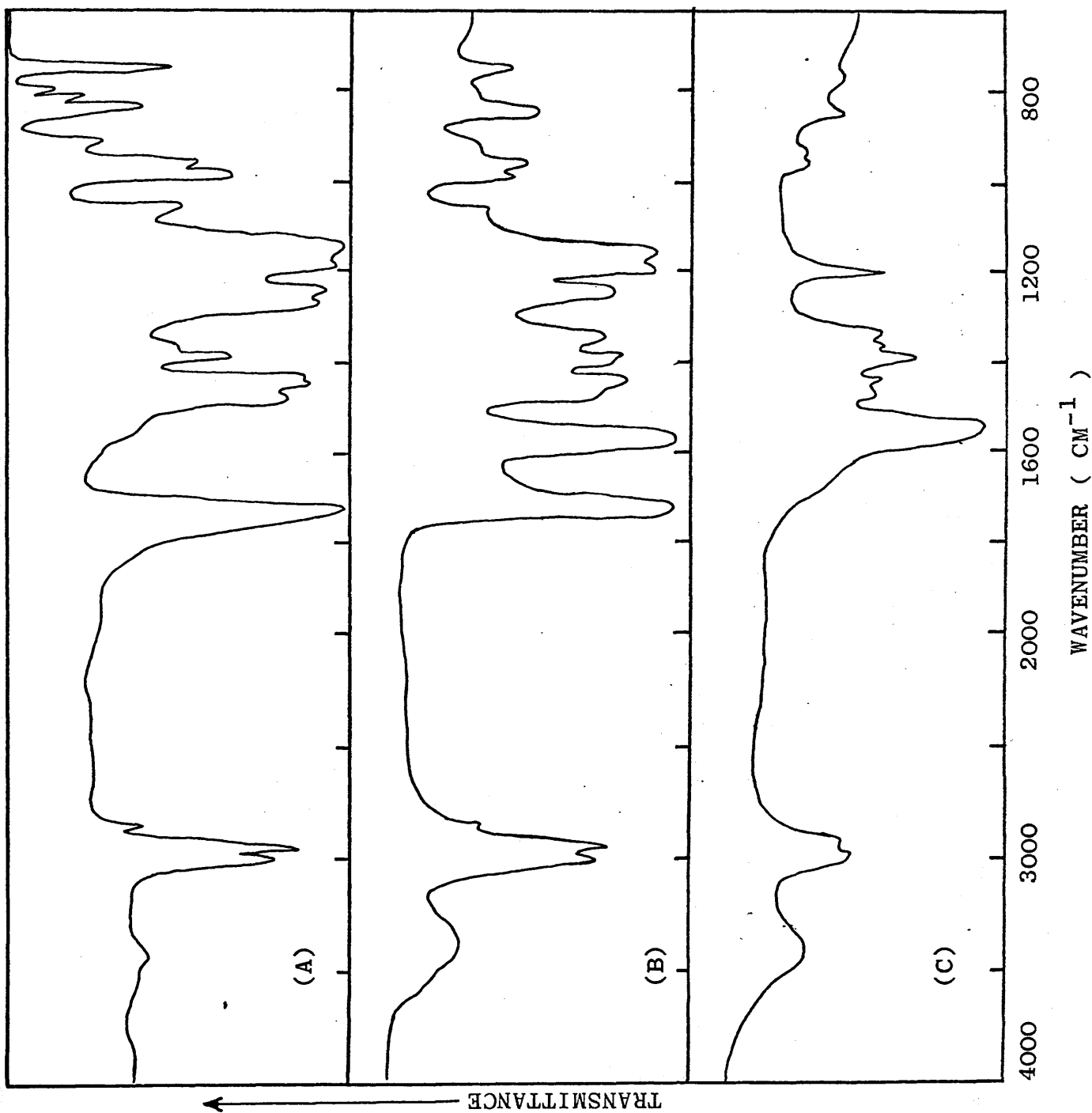
FIG. III-2
INFRA RED SPECTRA OF :

(A) POLY(METHYL
METHACRYLATE) ;

(B) 40 % KMA/MMA
COPOLYMER ;

(C) POLY(POTASSIUM
METHACRYLATE) .

(KBr DISCS)



the copolymers reached a saturation point after several days. The polymers and copolymers were left in the atmosphere for a week and then, the amount of water was determined by thermogravimetric analysis. From the results of elementary analysis of these samples, after allowance for the water content, the composition could be calculated.

The amount of water taken up by polymers or copolymers at a fixed temperature was found to increase both with the size of the metal ion involved in the polymer and also with the proportion of salt units in copolymers. The T G curves in figures III-3 and III-4 show the amount of moisture taken up by some samples in four days.

Before going any further, it is of extreme importance to consider the effect of this water taken up by polymers and copolymers.

EFFECT OF THE WATER ABSORBED ON THE CHEMICAL STRUCTURE OF THE POLYMERS

If the water taken up by the polymers and copolymers causes any significant hydrolysis of the salt units in the chains, then the extreme case of over saturation or dissolution of these polymers in water would result in the hydrolysis of the salt units to an extent at least detectable by I R analysis. To this end, a freshly prepared sample of KMA/MMA copolymer (60% MMA) was

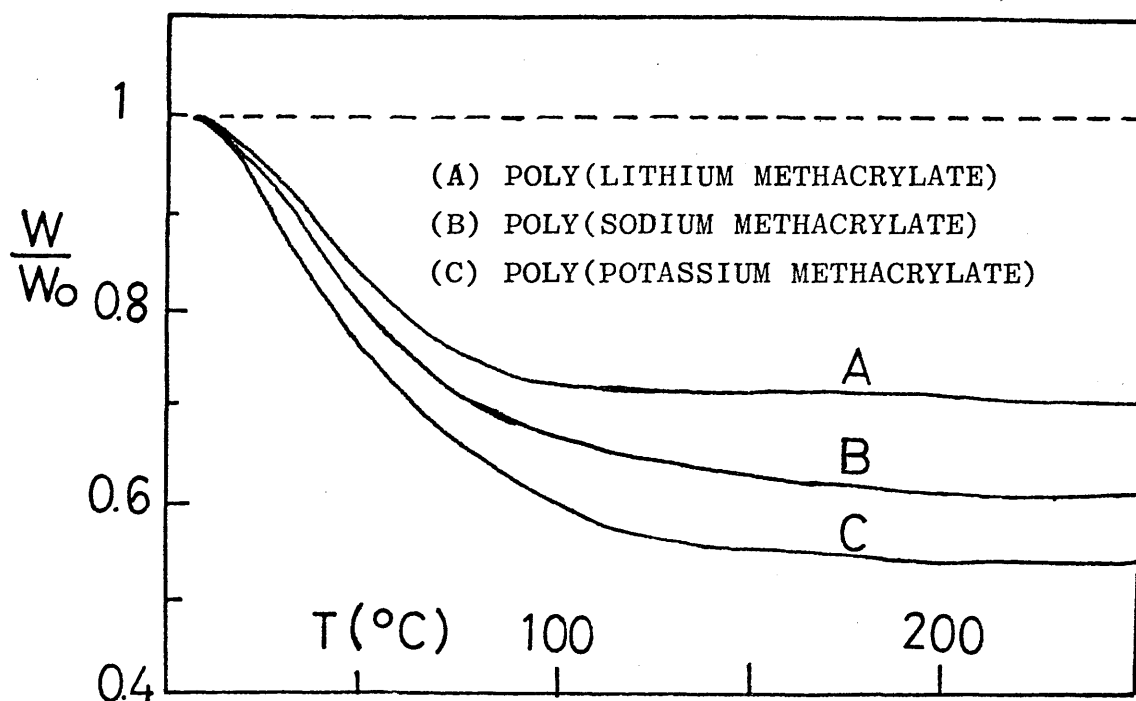


FIG. III-3: TG CURVES FOR POLY(ALKALI METAL METHACRYLATES), SHOWING THE AMOUNT OF WATER TAKEN UP FROM THE ATMOSPHERE WITHIN FOUR DAYS.

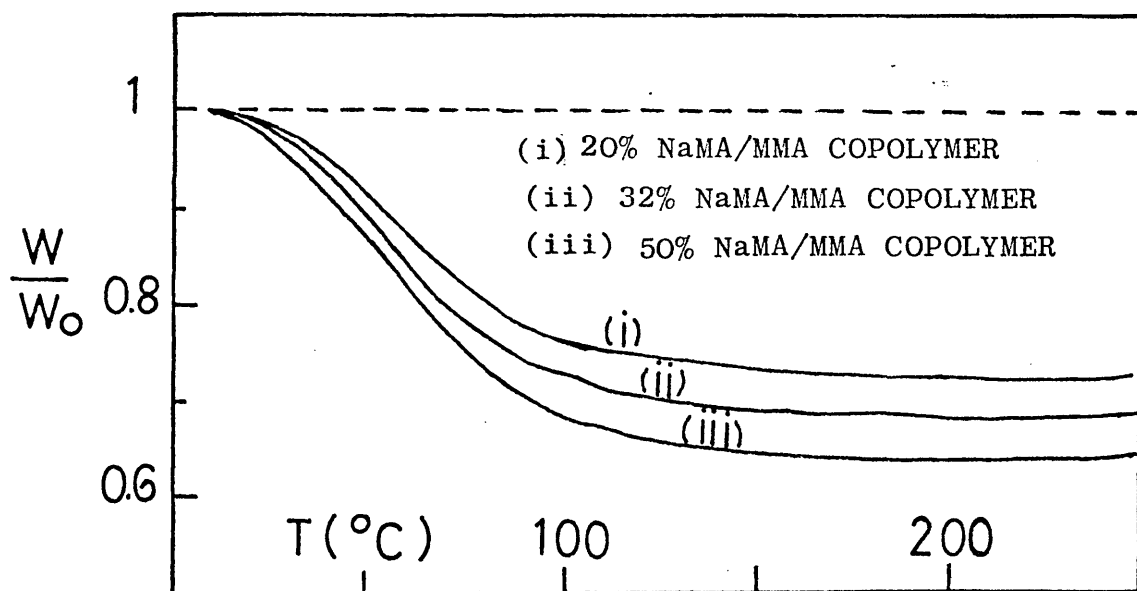


FIG. III-4: TG CURVES FOR THREE NaMA/MMA COPOLYMERS, SHOWING THE AMOUNT OF WATER TAKEN UP FROM THE ATMOSPHERE WITHIN FOUR DAYS.

"dissolved" into water and left for forty eight hours at ambient temperature; the water was then blown out and the resulting polymer film dried under vacuum. The comparison of the I R spectrum of that film with that of the solid state spectrum of the same copolymer non-treated with water showed no detectable difference in the copolymer chain structure (see fig. III-5).

This spectroscopic evidence shows that the hydrolysis of the salt units in the copolymer chains is very unlikely to take place under the influence of water absorbed.

This evidence is furthermore supported by all the published work on the counterion binding tendency of polyelectrolytes in aqueous solutions. Historically, one of the most striking characteristics of polyelectrolyte behaviour was the extremely low activity of counterions in aqueous solutions containing macroions. The measured activity coefficients of counterions in solutions of polyelectrolyte are invariably much less than one, even in the case of high dilutions, at which ionic activity coefficients of small electrolytes tend towards unity. Even in high diluted solutions of strong polyelectrolytes such as sodium poly(ethylene sulfonate), the activity coefficient of the Na^+ ions is only about 0.25⁽⁹⁸⁾.

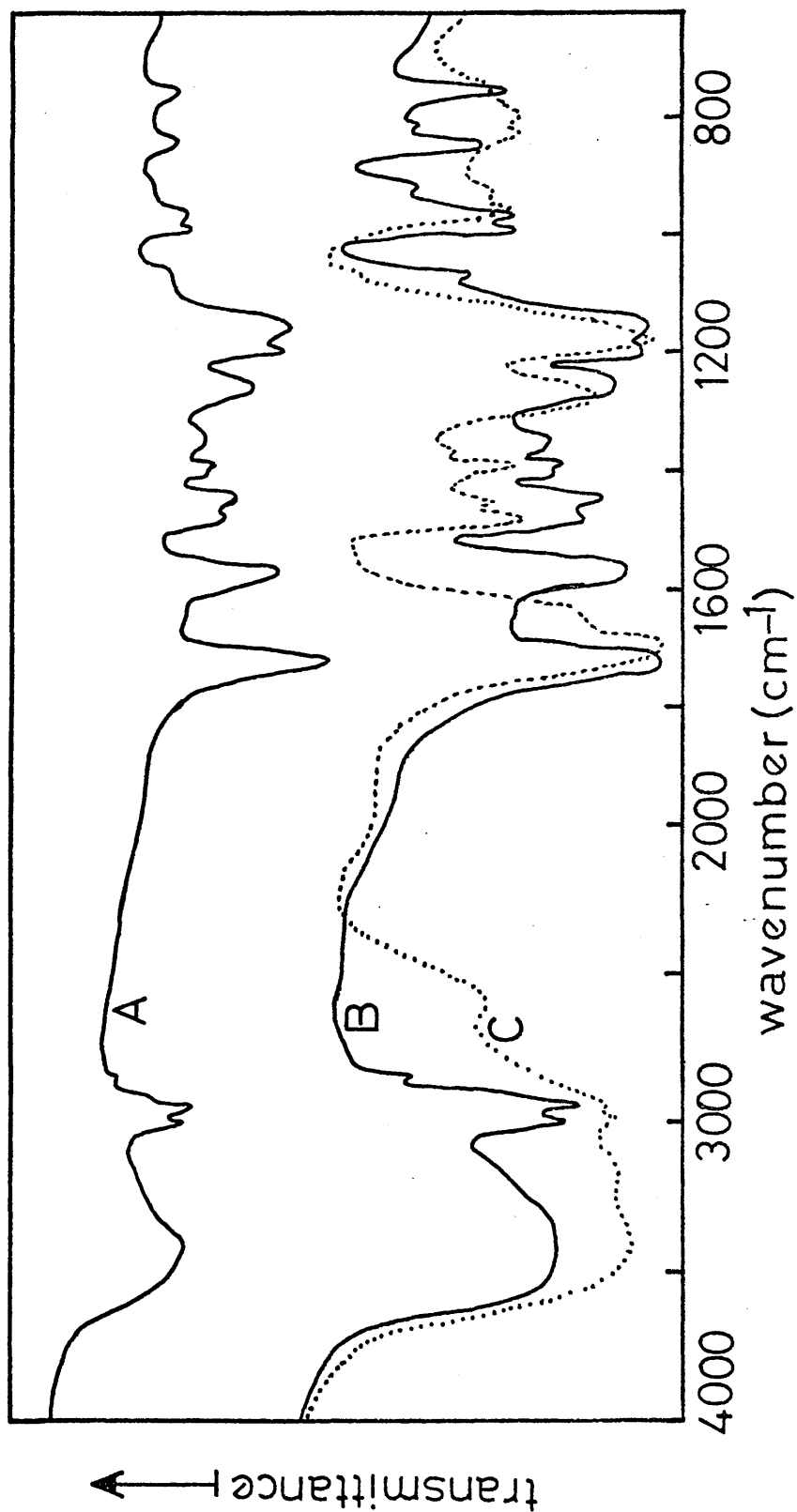


FIG. III-5 : EFFECT OF WATER ON THE CHEMICAL STRUCTURE OF THE 40 % KMA/MMA COPOLYMER ; INVESTIGATION BY INFRA RED SPECTROSCOPY IN KBr DISCS:
(A) : 40% KMA/MMA COPOLYMER, (B) : 40% KMA/MMA COPOLYMER AFTER HAVING BEEN LEFT IN DISTILLED WATER FOR TWO DAYS, (C) : POLY(METHACRYLIC ACID).

These non-idealities are a consequence of the large electrostatic potentials which exist around the polyions with multiple charges; counterions become "trapped" in these regions of high potential and as a result, lose their identity as independent mobile species. The most graphic historical evidence of the importance of this immobilization of counterions was provided by the transport studies of Wall and co-workers⁽⁹⁹⁾ in 1950 who showed that even under the influence of a potential field, 60% of the Na^+ ions in a solution of sodium salt of poly(acrylic acid) moved towards the positive electrode in opposition to the electrical field. This surprising finding can be explained only if one postulates that the Na^+ ions are an integral part of the migrating macroion.

Gregor and co-workers^(100,101) found that the degree of cation binding depends on the nature of the cation and decreases in the order of increasing cation radius: $\text{Li}^+ < \text{Na}^+ < \text{K}^+$.

But even in the case of the K^+ ion which appears to be bound least by the polyion no hydrolysis was observed as shown in fig. III-5.

This experimental evidence suggests that any hydrolysis of the polymers by the absorbed water would be completely insignificant.

SOLUBILITY OF THE COPOLYMERS

No good pure solvent was found for these copolymers. Depending on their relative compositions, the copolymers dissolved only in water or methanol, the copolymers with a high proportion of salt units dissolving better in water than methanol and vice-versa for copolymers at the other end of the composition range. In most cases, the result obtained was not a true solution. It varied from a swollen gel to a non-transparent viscous "solution". This was probably due to the affinity of only certain segments in the chain for the solvent, the others staying out of it. The methyl methacrylate units in the chain being hydrophobic account for the character of bad solubility in water and the salt units having practically no affinity for an organic solvent (because of their electrolytic nature) oppose in the same way the solubility in methanol.

The solubility was however very highly improved by mixing the two solvents (water and methanol) in various proportions depending on the relative composition of the concerned copolymer.

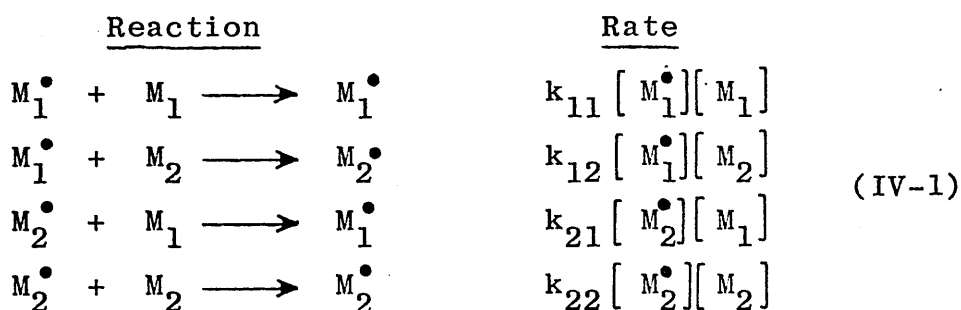
Due to the laborious difficulties in making and purifying appreciable quantities of these copolymers, no quantitative investigations on their solubility were attempted.

CHAPTER IV

MONOMER REACTIVITY RATIOS

THE COPOLYMERIZATION EQUATION

The first attempt on the mechanism of copolymerization was made by Dostal⁽¹⁰²⁾ who assumed that the rate of addition of monomer to a growing free radical depended only on the nature of the end group on the radical chain. In this way, monomers M_1 and M_2 lead to radicals of types M_1^\bullet and M_2^\bullet . Four ways of monomeric addition are possible:



Because of the four independent rate constants involved, Dostal made no attempt to test this assumption experimentally.

After several unsuccessful approaches, the kinetics of copolymerization were elucidated in 1944 by Alfrey,⁽¹⁰³⁾ Mayo,⁽¹⁰⁴⁾ Simha⁽¹⁰⁵⁾ and Wall.⁽¹⁰⁶⁾ They added to

Dostal's reaction scheme the steady state assumption applied to each radical separately, i.e., the concentrations of M_1^\bullet and M_2^\bullet must remain constant and therefore the rate of conversion of M_1^\bullet to M_2^\bullet must be equal to that of conversion of M_2^\bullet to M_1^\bullet :

$$k_{21} [M_2^\bullet] [M_1] = k_{12} [M_1^\bullet] [M_2] \quad (\text{IV-2})$$

The rates of disappearance of the two types of monomer will be:

$$\begin{aligned} -d [M_1] / dt &= k_{11} [M_1^\bullet] [M_1] + k_{21} [M_2^\bullet] [M_1] \\ -d [M_2] / dt &= k_{22} [M_2^\bullet] [M_2] + k_{12} [M_1^\bullet] [M_2] \end{aligned} \quad (\text{IV-3})$$

By defining $r_1 = k_{11}/k_{12}$ and $r_2 = k_{22}/k_{21}$, and combining equation (IV-2) and (IV-3), the copolymerization equation can be obtained:

$$\frac{d [M_1]}{d [M_2]} = \frac{[M_1] r_1 [M_1] + [M_2]}{[M_2] [M_1] + r_2 [M_2]} \quad (\text{IV-4})$$

MONOMER REACTIVITY RATIOS

In the discussion to follow, we have adopted the following notation: M_u = the mole fraction of monomer u (where $u = 1, 2$) in the reaction system, m_u = the mole fraction of monomer u in the copolymer composed entirely of the two monomers, and r_u = the monomer reactivity ratio of the unit u.

The monomer reactivity ratios r_1 and r_2 for a particular copolymer system are defined as the ratios of the rate constants for a given radical adding its own monomer to that for its adding the other monomer:

$$r_1 = k_{11}/k_{12} \quad \text{and} \quad r_2 = k_{22}/k_{21}$$

Thus $r_1 > 1$ means that the radical M_1 prefers to add M_1 and $r_1 < 1$ means that it prefers to add M_2 .

Since the rate constants for initiation and termination reactions do not appear in the copolymerization equation (IV-3), it follows that the composition of the copolymer is totally independent of overall reaction rate and initiator concentration. In most cases, the reactivity ratios are unaffected by the presence of inhibitors, chain transfer agents or solvents. However, a change from a free radical to an ionic mechanism changes r_1 and r_2 markedly.

METHODS FOR DETERMINING r_1 AND r_2 VALUES

The determination of monomer reactivity ratios in copolymerization is entirely dependent on the accuracy of analysis of the products of low conversion experiments (not higher than 5%).

Several experimental methods of analysing the data are available. A brief description of the ones mostly used will be given.

A-) THE CURVE FITTING METHOD

This method⁽¹⁰⁷⁾ is based on the assumption that if the experimental conditions are such that the monomer concentrations do not change appreciably, and if the polymer is of adequate molecular weight then equation (IV-4) can be replaced by equation (IV-5):

$$\frac{m_1}{m_2} = \frac{r_1 M_1^2 + M_1 M_2}{r_2 M_2^2 + M_1 M_2} \quad (\text{IV-5})$$

This method consists of preparing a graph of the observed mole fraction m_1 in the copolymer versus M_2 and then drawing the curve represented by equation (IV-5) on the graph for selected values of r_1 and r_2 until the curve appears to pass through or "near enough to" a sufficient number of the observed points.

This method of trial and error is poor since the composition curve is rather insensitive to small changes in r_1 and r_2 and the final choice of a "best fit" for a sigmoid curve determined by two parameters is largely a matter of individual judgement.

B-) THE INTERSECTION METHOD

Another method of "intersecting slopes" is more commonly used. Solving equation (IV-5) for r_1 gives:

$$r_1 = \left\{ \frac{m_1 M_2^2}{m_2 M_1^2} \right\} r_2 + \left[\frac{M_2}{M_1} \right] \cdot \left\{ \frac{m_1}{m_2} - 1 \right\} \quad (\text{IV-6})$$

If we consider $(m_1 M_2^2 / m_2 M_1^2)$ and $[M_2 / M_1] \cdot (m_1 / m_2 - 1)$

respectively as the slope and intercept, we can plot for each copolymerization experiment a different straight line, where r_1 represents the ordinate and r_2 the abscissa. If there is little experimental error, a series of lines for a group of copolymers covering the composition range should intersect at a common point in the r_1, r_2 plane. This, unfortunately, is not the most frequent case. However, the region within which the intersection is most likely to be, gives a good indication of the magnitude of the experimental errors on r_1 and r_2 . This method first used by Mayo and Lewis⁽¹⁰⁴⁾ has been fully discussed elsewhere.^(107,108)

C-) THE LINEARIZATION METHOD

This method is also known as the Fineman & Ross⁽¹⁰⁹⁾ method. Equation (IV-5) can be rearranged to yield:

$$\frac{M_1(m_2 - m_1)}{M_2 m_1} = \left[\frac{-m_2 M_1^2}{m_1 M_2^2} \right] r_1 + r_2 \quad (\text{IV-7})$$

Plotting $M_1(m_2 - m_1)/M_2 m_1$ against $-m_2 M_1^2/m_1 M_2^2$ will give for each experiment one point on a straight line, the slope of which is r_1 and the intercept r_2 .

This more recent method has not yet received as much attention in the literature as the preceeding two. The results of this method, like those of the

curve fitting method and to a greater extent than those of the intersection method, depends largely upon individual judgement.

The last two methods applied to the analytical data obtained from the analysis of the copolymer systems dealt with in this work, gave reactivity ratios in good agreement with each other. In order to avoid individual judgement in finding the reactivity ratios, the estimation of the reactivity ratios corresponding to the best fit possible with the analytical results was carried out using a Fortran computer program based on a new method for minimising a sum of squares.

D-) THE NEW METHOD

The process uses a recently published powerful method for minimising sums of squares without calculating gradients. (110)

Let $f_i(r_1, r_2)$ be the following form of the copolymer equation (i represents the i^{th} experimental run):

$$f_i(r_1, r_2) = r_1 M_1^i m_2^i + M_1^i M_2^i (m_2^i - m_1^i) - r_2 M_2^i m_1^i = 0$$

The planar vector $r = (r_1, r_2)$ which gives a minimum value for $F(r_1, r_2)$ is to be determined, where:

$$F(r_1, r_2) = \sum_{i=1}^n \left\{ f_i(r_1, r_2) \right\}^2$$

and m is the total number of experimental runs.

The method is essentially Gauss Newton in that the functions $f_i(r_1, r_2)$ are approximated at the point r by a linear form:

$$f_i = h_i + \sum_u g_{iu} r_u$$

or, in a matrix notation:

$$f = h + Gr$$

where h is a constant vector and G is the Jacobian matrix:

$$G_{iu} = (\partial f_i / \partial r_u)_r$$

The value of r at the minimum of the sum of squares is y given by:

$$G^T G y = - G^T h$$

From an initial estimate of the minimum point easily obtained from very approximate values of the reactivity ratios (values given by intersection method or Fineman & Ross method for instance) a set of at least three points is generated and the corresponding values of F are calculated, with the best set of r_1 and r_2 values given by the minimum value of F .

The method based on the direct use of the copolymer equation operates as the curve fitting method with

this difference that the final choice of the reactivity ratios does not depend on the subjectivity of the operator. It is thought that this method complements the other experimental methods in the sense that the values of r_1 and r_2 obtained are unique, since for a given data any person or set of persons following the outlined calculation procedure will reach the same results at the end. The method is fully discussed elsewhere^(110,111) and the documented Fortran program⁽¹¹¹⁾ used to this end is given in the Appendix.

EXPERIMENTAL ERRORS

By their magnitude and effect, experimental errors involved in determining monomer reactivity ratios are of great importance in estimating the validity of the tests of the copolymerization equation. Experience with many systems investigated throughout the literature leads to the conclusion that provided copolymerization in each case is not taken to a yield higher than 5% and that proper techniques of polymer isolation are used, the major experimental error will arise from errors in the analysis of copolymers. In the case of the present work, since microanalysis was used, the analytical error was taken as 0.3% carbon. The effect of this error can be seen in the diagrams corresponding to the Fineman & Ross method applied to

our three copolymer systems (figs. IV-2, 4 and 6).

One practical way of estimating the effect of these errors⁽¹⁰⁸⁾ upon the accuracy of the determination of the monomer reactivity ratios is based upon the size of the region in which the lines intersect in the graphical intersection method described earlier on (see figs. IV-1, 3 and 5).

ANALYSIS OF DATA

Copolymerization for the three systems LiMA/MMA, NaMA/MMA and KMA/MMA was carried out homogeneously, under vacuum, in methanol at the temperature of 60°C. AIBN was used as initiator of polymerization in the proportion of 0.1% for the NaMA/MMA and KMA/MMA systems and 0.05% for the LiMA/MMA system, the percentages being expressed in terms of weight of initiator by total weight of monomer. The analysis of the copolymers carried out as outlined in chapter III gave for each copolymer system the results shown in table IV-1, IV-2 and IV-3.

Table IV-1

Analytical results from copolymerization of MMA (1)
and LiMA (2) in methanol

Copolymer	M_1	m_1	Polymerization time (min)	Conversion %
A 1	0.800	0.786	25	5.9
A 2	0.666	0.682	45	5.2
A 3	0.600	0.645	60	5.6
A 4	0.500	0.587	70	4.3
A 5	0.400	0.566	70	4.0
A 6	0.250	0.486	75	4.9
A 7	0.200	0.479	80	5.2

Table IV-2

Analytical results from copolymerization of MMA (1)
and NaMA (2) in methanol

Copolymer	M_1	m_1	Polymerization time (min)	Conversion %
B 1	0.850	0.956	75	3.8
B 2	0.700	0.908	90	4.1
B 3	0.600	0.866	105	4.0
B 4	0.500	0.817	120	4.6
B 5	0.400	0.756	150	4.0
B 6	0.250	0.631	160	5.1
B 7	0.100	0.390	140	4.8

Table IV-3

Analytical results from copolymerization of MMA (1)
and KMA (2) in methanol

Copolymer	M_1	m_1	Polymerization time (min)	Conversion %
C 1	0.916	0.983	60	3.3
C 2	0.750	0.951	80	3.9
C 3	0.600	0.898	90	3.8
C 4	0.500	0.845	200	4.7
C 5	0.400	0.792	195	4.3
C 6	0.250	0.676	195	4.0
C 7	0.200	0.609	210	4.0
C 8	0.048	0.252	270	3.9

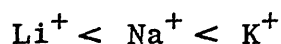
Note that in the notation r_u , M_u and m_u (where $u = 1,2$), $u = 1$ corresponds to the methyl methacrylate unit and $u = 2$ corresponds to either the lithium, sodium or potassium methacrylate unit depending upon the particular copolymer system considered.

One first and unexpected conclusion that may be drawn from the above data is that the overall rate of copolymerization in the three copolymer systems dealt with in the present work seems to increase in the order:

$$K^+ < Na^+ < Li^+$$

whereas the rate of polymerization of the alkali metal

methacrylates polymerized separately increases in the opposite order: (94,112)



REACTIVITY RATIOS

The intersection method applied to our data, gave for each copolymer system the reactivity ratios shown in table IV-4 and the corresponding diagrams are shown in figures IV-1, 3 and 5.

Table IV-4

Reactivity ratios for the three systems studied, found by the intersection method

Copolymer system	r_1 (MMA)	r_2 (MetMA)
LiMA/MMA	0.56 ± 0.30	0.06 ± 0.03
NaMA/MMA	3.94 ± 0.20	0.12 ± 0.03
KMA/MMA	5.50 ± 0.32	0.127 ± 0.025

The Fineman & Ross method was also used to verify the reactivity ratios obtained by the intersection method; the less accurate graphical results are given in table IV-5 and the corresponding diagrams are shown in figures IV-2, 4 and 6.

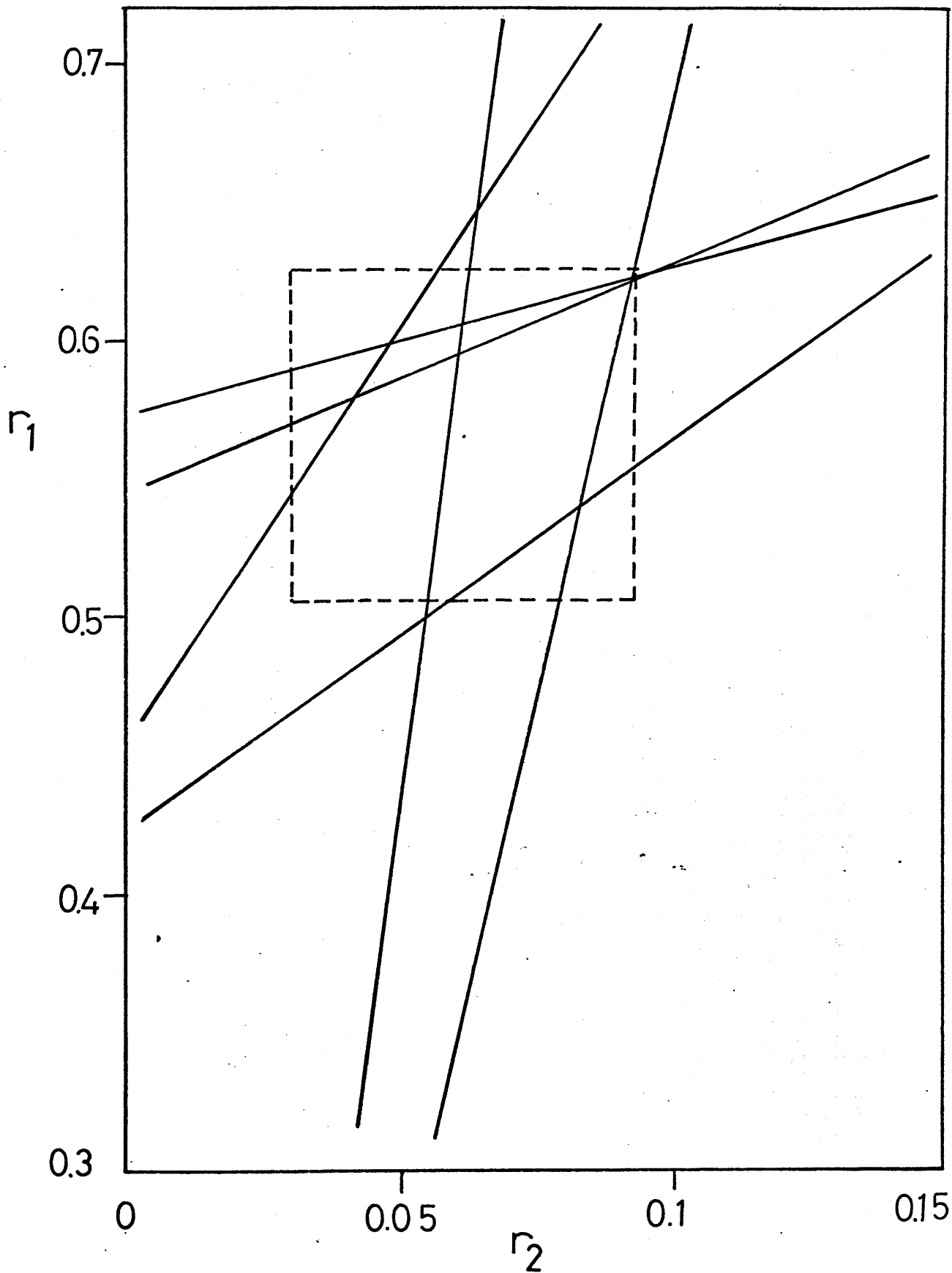


Fig. IV-1

MAYO & LEWIS DIAGRAM FOR THE COPOLYMERIZATION
OF MMA(1) AND LiMA(2)

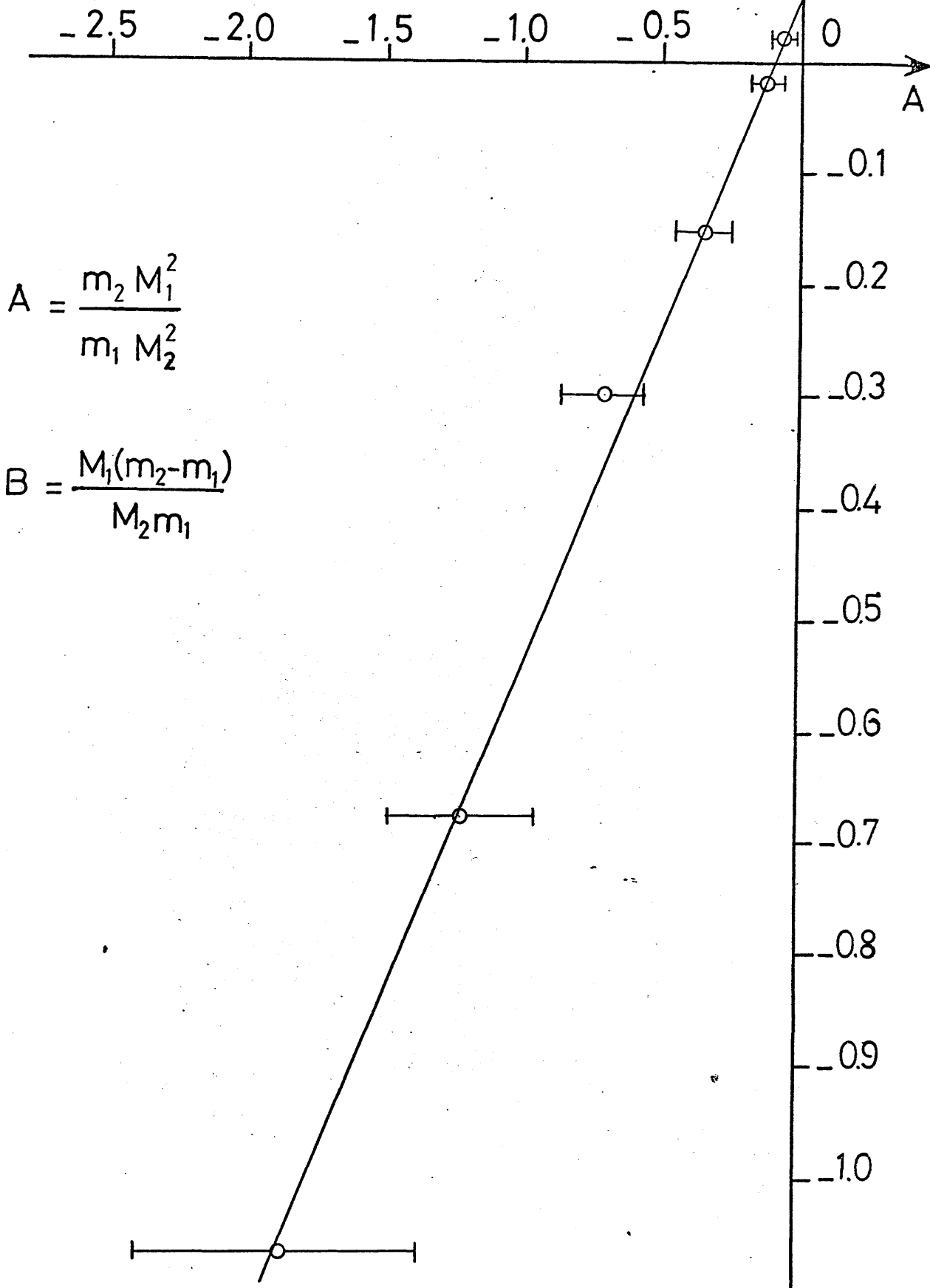


Fig. IV-2: FINEMAN & ROSS DIAGRAM FOR THE COPOLYMERIZATION OF MMA(1) AND LiMA(2)

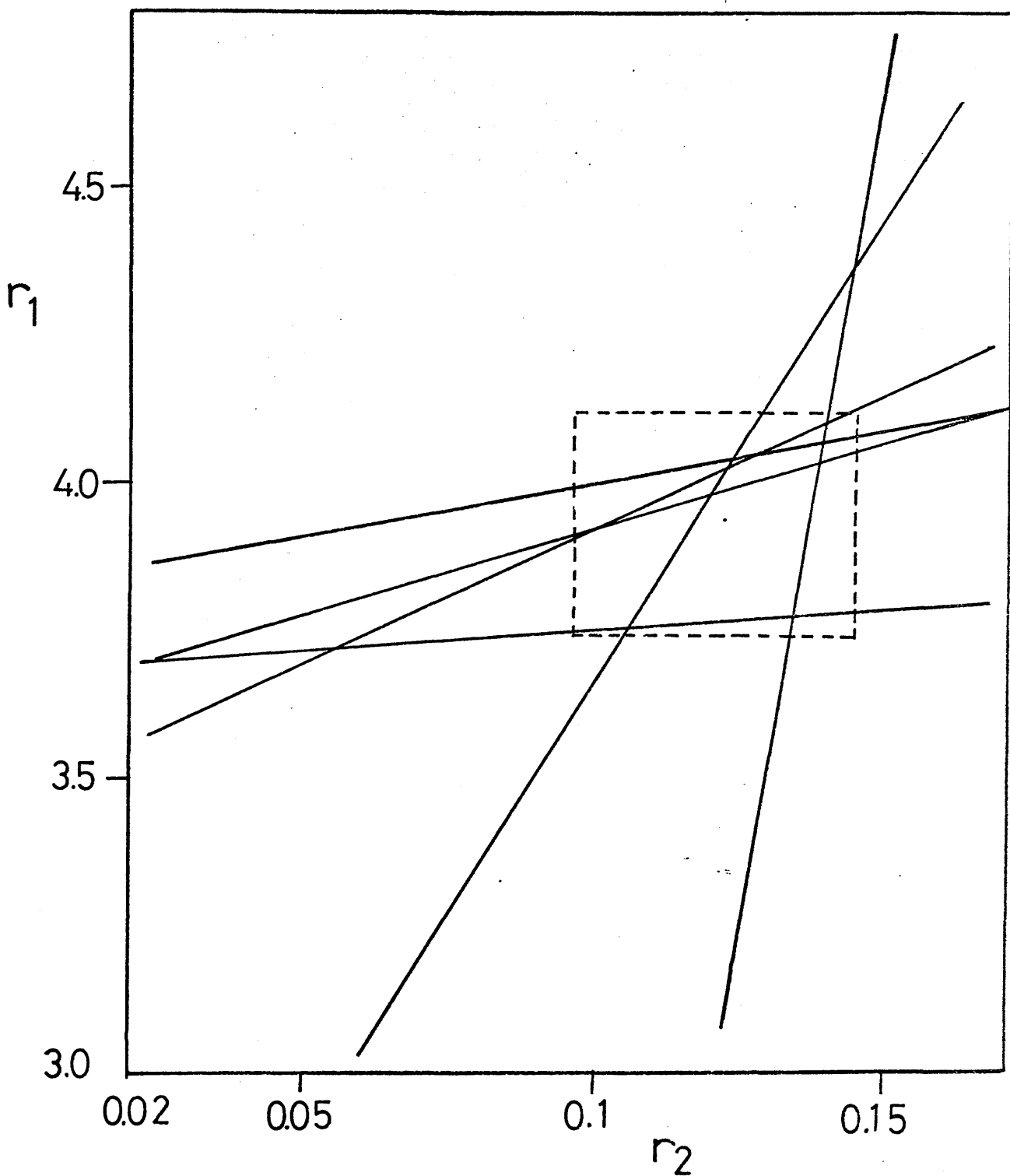
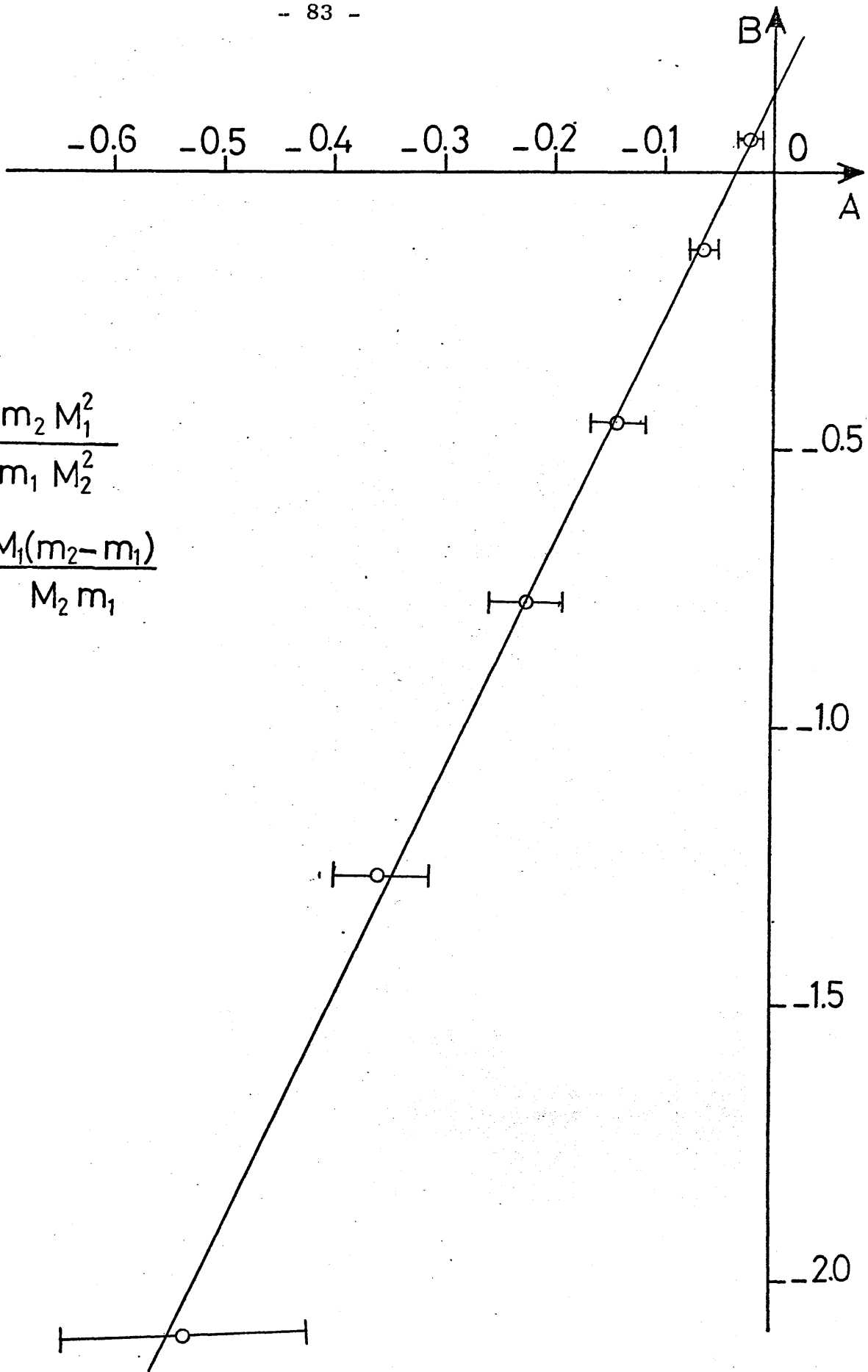


Fig. IV-3

MAYO & LEWIS DIAGRAM FOR THE COPOLYMERIZATION
OF MMA(1) AND NaMA(2)



$$A = \frac{m_2 M_1^2}{m_1 M_2^2}$$

$$B = \frac{M_1(m_2 - m_1)}{M_2 m_1}$$

Fig. IV-4: FINEMAN & ROSS DIAGRAM FOR THE COPOLYMERIZATION OF MMA(1) AND NaMA(2)

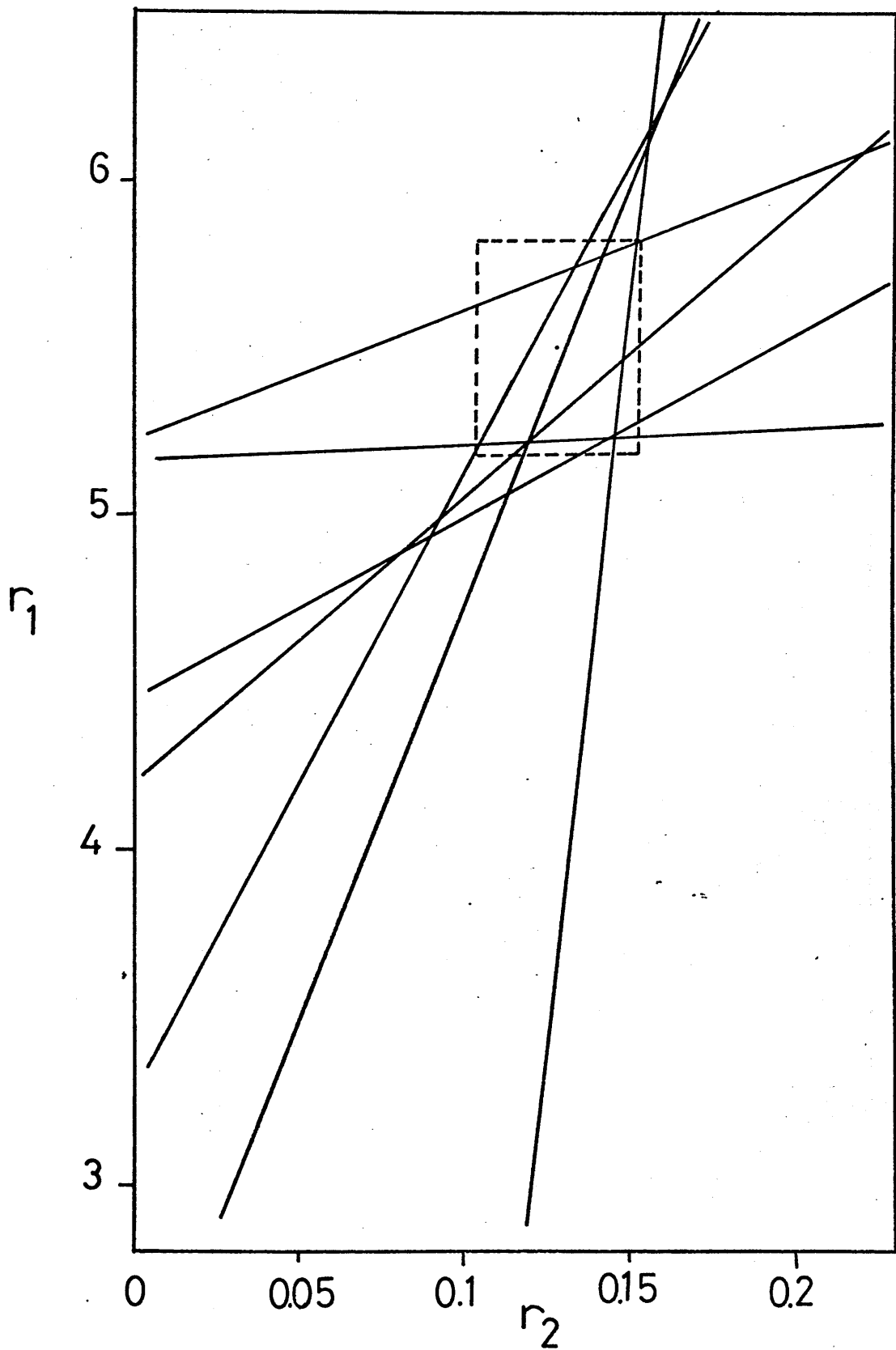


FIG IV - 5

MAYO & LEWIS DIAGRAM FOR THE
COPOLYMERIZATION OF MMA(1) AND KMA(2)

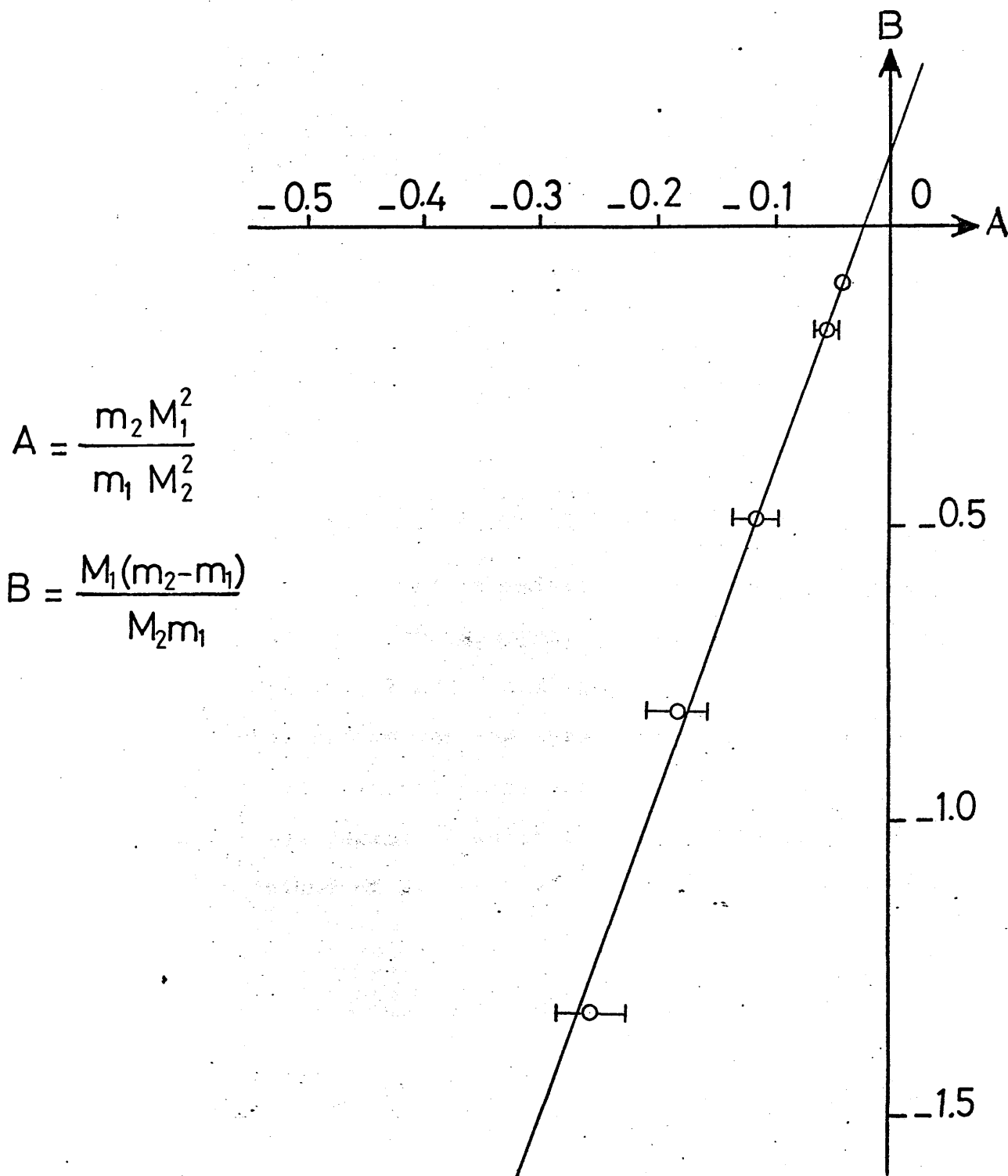


Fig. IV-6

FINEMAN & ROSS DIAGRAM FOR THE COPOLYMERIZATION
OF MMA(1) AND KMA(2)

Table IV-5

Reactivity ratios for the three systems studied,
found by the Fineman & Ross method

Copolymer system	r_1 (MMA)	r_2 (MetMA)
LiMA/MMA	0.52 ± 0.30	0.06 ± 0.02
NaMA/MMA	3.28 ± 0.60	0.12 ± 0.04
KMA/MMA	6.00 ± 1.20	0.15 ± 0.03

The new method of minimising sums of squares gave in the case of each copolymer system the results shown in tables IV-6, 7 and 8 and the final values of the reactivity ratios for the three copolymer systems, together with experimental errors estimated from the size of the region in which the lines "intersect" in the method of Mayo & Lewis⁽¹⁰⁴⁾ are given in table IV-9:

Table IV-6

Results obtained by the new method on each iteration
for the system LiMA (2) - MMA (1)

Iteration	Sum of squares	r_1	r_2
0	0.16191×10^{-3}	0.563	0.061
1	0.16143×10^{-3}	0.563	0.0671
2	0.12175×10^{-3}	0.595	0.0732
3	0.12173×10^{-3}	0.596	0.0733
4	0.12173×10^{-3}	0.596	0.0733

Table IV-7

Results obtained by the new method on each iteration
for the system NaMA (2) - MMA (1)

Iteration	Sum of squares	r_1	r_2
0	0.44185×10^{-2}	3.28	0.12
1	0.12252×10^{-2}	3.608	0.12
2	0.10303×10^{-3}	3.936	0.1251
3	0.89806×10^{-4}	3.975	0.1258
4	0.89806×10^{-4}	3.975	0.1258

Table IV-8

Results obtained by the new method on each iteration for the system KMA (2) - MMA (1)

Iteration	Sum of squares	r_1	r_2
0	0.94506×10^{-3}	5.5	0.127
1	0.88079×10^{-3}	5.617	0.1397
2	0.87761×10^{-3}	5.6495	0.1432
3	0.87761×10^{-3}	5.6495	0.1432

Table IV-9

Final reactivity ratios of monomers in copolymerization of MMA with MetMA (Met = Li, Na and K)

MetMA	r_1 (MMA)	r_2 (MetMA)	$1/r_2$	Ionic radii ⁽¹¹⁴⁾ of the metal (Å)
LiMA	0.596 ± 0.3	0.073 ± 0.03	13.64	0.68
NaMA	3.975 ± 0.2	0.126 ± 0.03	7.95	0.97
KMA	5.65 ± 0.32	0.143 ± 0.025	6.98	1.33
MAA*	0.345	0.956	1.04	—

* The results of the reactivity ratios for the system MAA/MMA given for reference are due to Smets and Van Gorp⁽¹¹³⁾

As an illustration, the curve fitting method was used to compare the experimental data with the results calculated from the final reactivity ratios (see figures IV-7, 8 and 9).

FIRST OBSERVATIONS

From the results shown in table IV-9, it follows that in the copolymerization of methyl methacrylate with the lithium, sodium and potassium methacrylates, certain observations on each system can be made:

A-) LiMA/MMA COPOLYMER

In the lithium methacrylate/methyl methacrylate copolymer system we observe that both monomer reactivity ratios are less than unity. From this we will expect a point in the composition range where there will be an azeotropic copolymerization.⁽¹⁰⁷⁾ The curve of figure IV-7 crosses the line representing $m_1 = M_1$. At that point of intersection the copolymerization proceeds without change in the composition of feed or polymer. The solution of the copolymer equation (equation IV-5) for $m_1/m_2 = M_1/M_2$ gives the critical composition of the azeotrope:

$$m_1 = \frac{1-r_2}{2-(r_1+r_2)} = 0.7$$

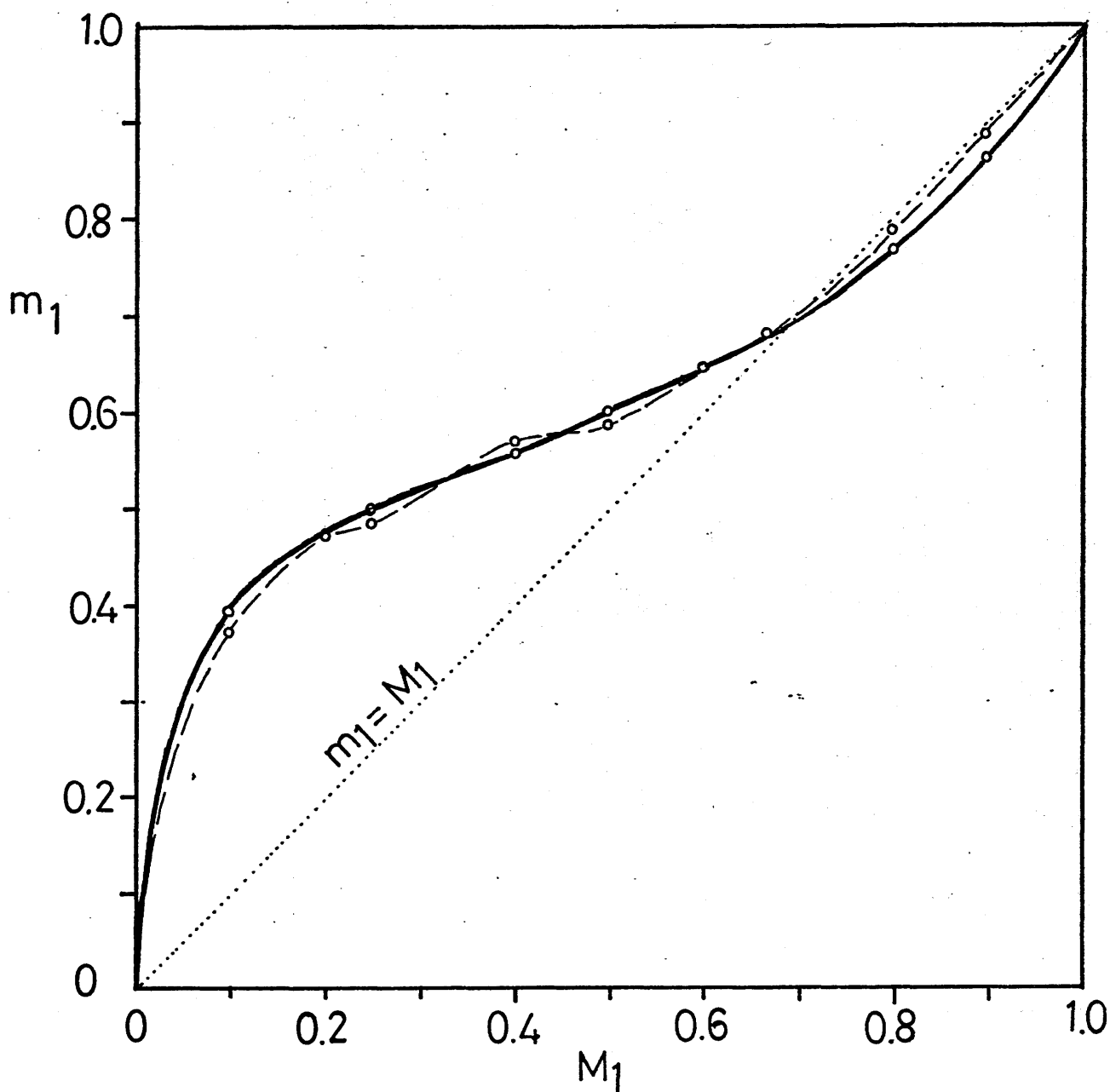


Fig. IV-7

CURVE FITTING FOR THE COPOLYMERIZATION OF LiMA AND MMA

—○— ANALYTICAL RESULTS

—○— CURVE DRAWN USING THE FINAL REACTIVITY RATIOS
AND COPOLYMER EQUATION

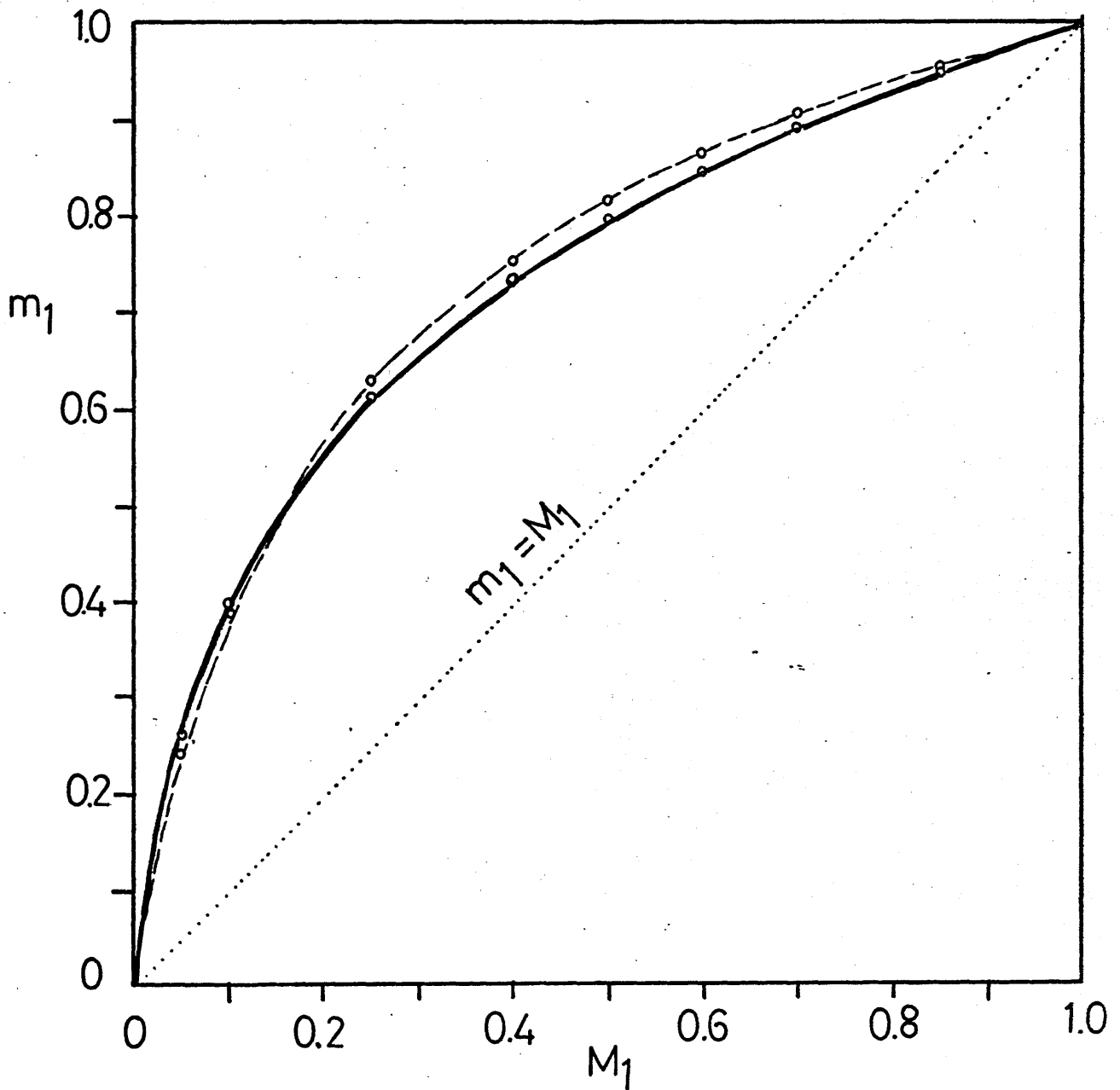


Fig. IV-8

CURVE FITTING FOR THE COPOLYMERIZATION OF NaMA AND MMA

--○-- ANALYTICAL RESULTS

—○— CURVE DRAWN USING THE FINAL REACTIVITY RATIOS
AND THE COPOLYMER EQUATION

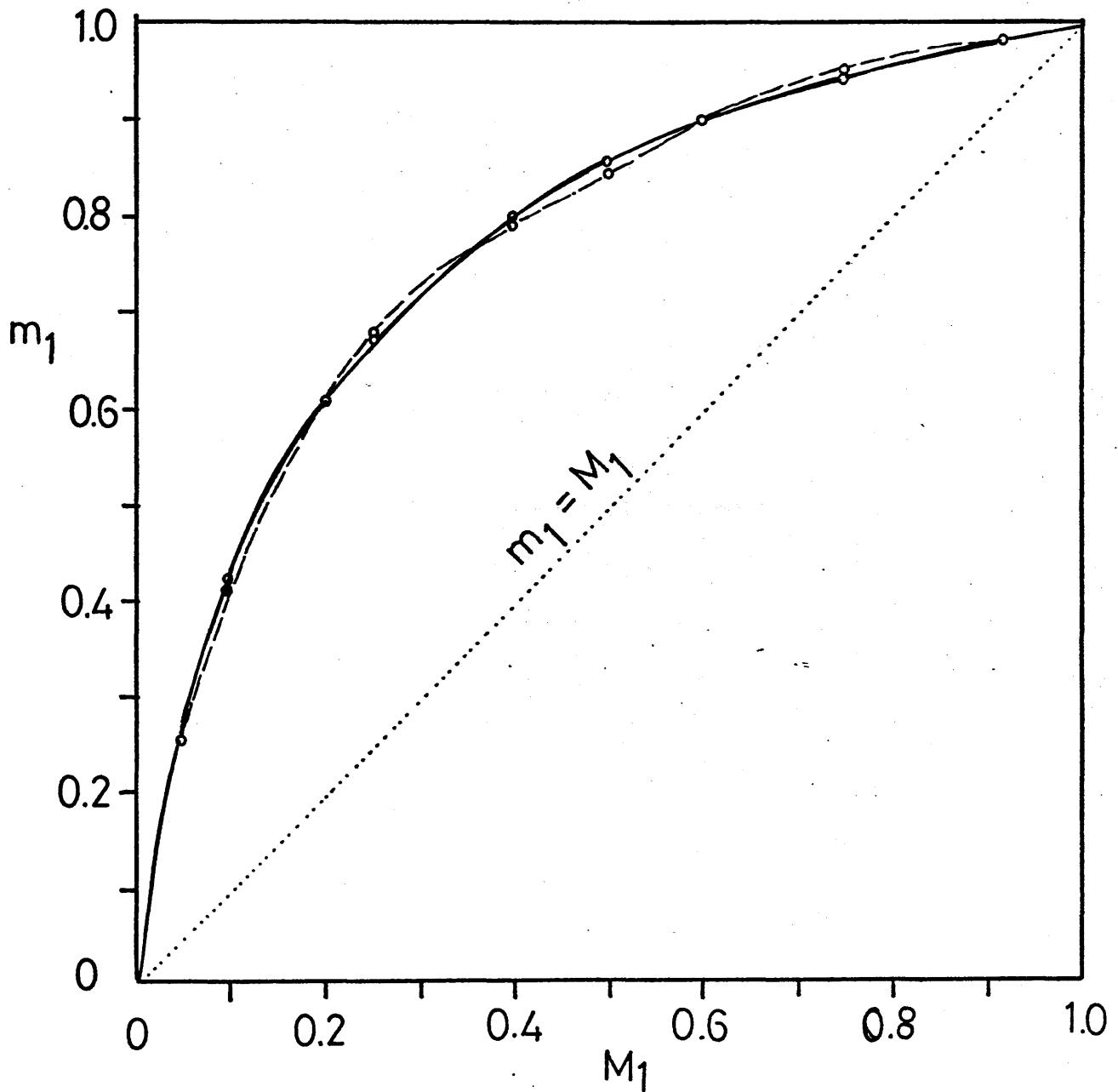


Fig. IV-9

CURVE FITTING FOR COPOLYMERIZATION OF KMA AND MMA

--○-- ANALYTICAL RESULTS

—○— CURVE DRAWN USING THE FINAL REACTIVITY RATIOS
AND THE COPOLYMER EQUATION

The reactivity ratios for this system show also that a radical terminating in an MMA unit adds the LiMA monomer about twice as fast as its own, whereas a radical terminating in a LiMA unit prefers to add the MMA monomer at a rate fourteen times faster than that of adding its own.

B-) NaMA/MMA COPOLYMER

In this system, the monomer reactivity ratio of MMA (>1) shows that the radical methyl methacrylate prefers to add to its own monomer since the rate constant for such an addition, k_{11} , is almost four times higher than k_{12} .

The reactivity ratio of NaMA monomer on the other hand ($r_2=0.126$) shows that the radical sodium methacrylate adds the MMA monomer at a rate eight times faster than that of adding its own.

C-) KMA/MMA COPOLYMER

In this system again, the monomer reactivity ratio of MMA (>1) shows that the MMA radical adds to its own monomer at a rate nearly six times higher than that of adding the other monomer, whereas the KMA reactivity ratio ($r_2=0.143$) shows that the radical terminating in a KMA unit prefers statistically to add the MMA monomer since the rate constant corresponding to this reaction (k_{21}) is about seven times higher than k_{22} .

This type of copolymerization corresponds nearly to the ideal case^(101,108) since the two radicals show almost the same preference for adding one of the monomers over the other.

From these results one can see that the radical ending in the alkali metal methacrylate prefers in each of the three copolymer systems studied, to add the MMA monomer rather than adding its own, and this affinity (expressed by $k_{21}/k_{22} = 1/r_2$) increases in the opposite order with the ionic radius of the corresponding alkali metals (see table IV-9 and figure IV-10).

PREVIOUS WORK

Many workers observed that polymerization rates of various acrylic and methacrylic salts depend significantly upon the nature of the cation.^(94,112,115) It has also been established that reactivity ratios for acrylamide with methacrylate salts of the group I and II elements, during aqueous copolymerization, depend very closely on the nature of the cation.⁽⁸⁷⁻⁹¹⁾ Wojnarowski^(87,89) interpreted the effect mainly in terms of a dependence of the reactivity of methacrylic monomer on the ionic character of the O—metal bond. The size as well as the electronegativity of the cation plays an important role. The results are interpreted by considering cation binding by polyacrylic and

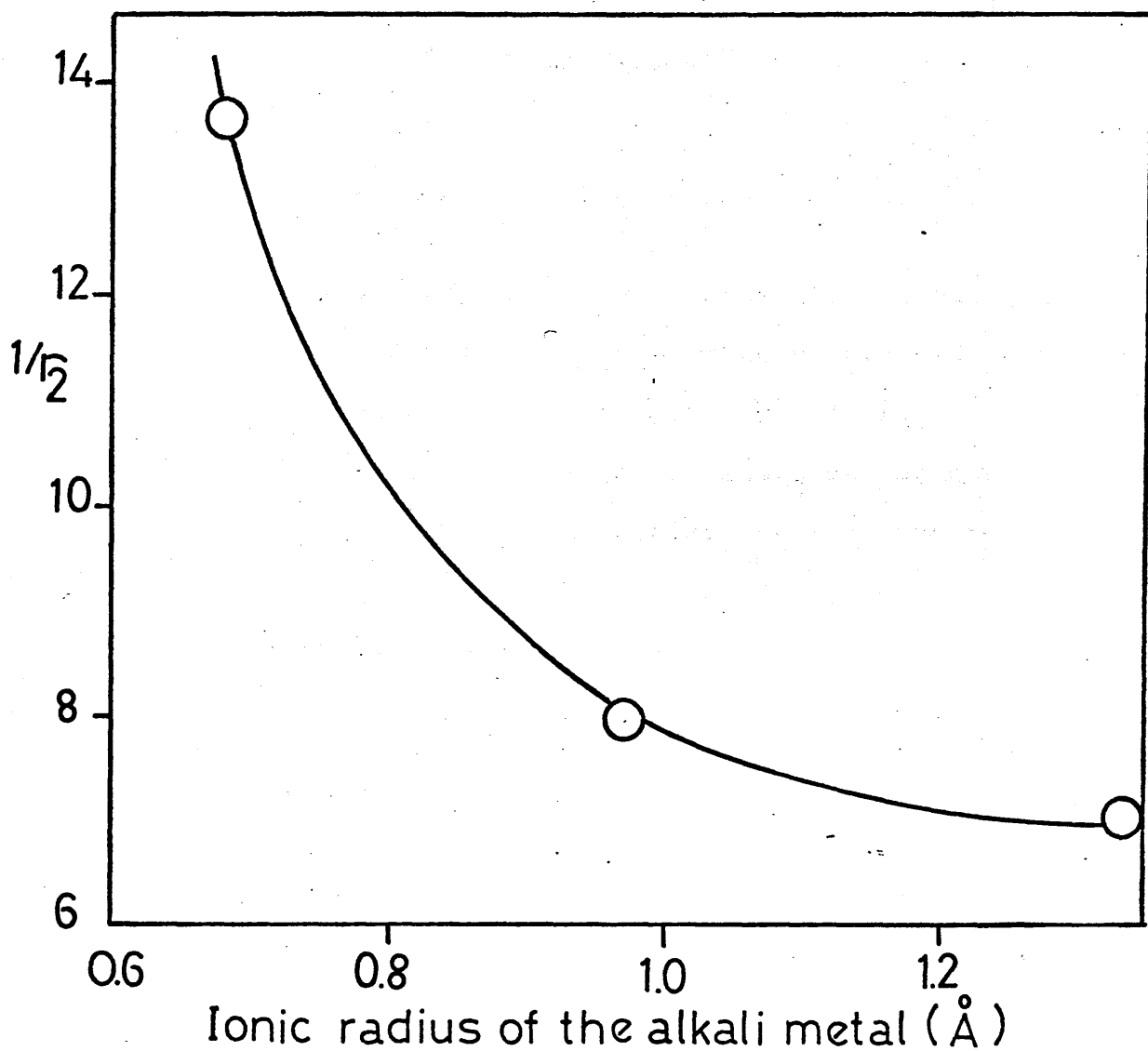


Fig. IV-10

VARIATION OF THE RECTIVITY OF THE ALKALI METAL METHACRYLATE
RADICAL(TOWARDS MMA ADDITION DURING COPOLYMERIZATION) WITH
THE SIZE OF THE METAL ION.

polymethacrylic parts of macroradicals since in aqueous polymerization the monomeric salts are almost completely dissociated and therefore react in the form of acrylic acid and methacrylic acid anion.

DISCUSSION OF THE PRESENT RESULTS

In this work, the overall copolymerization rates increased with the decrease of the ionic radius of the corresponding alkali metal in the order $K^+ < Na^+ < Li^+$ since for the same order of conversion and composition, the polymerization time required was higher for the system with the larger ion (see tables IV-1, 2 and 3) $Li^+ < Na^+ < K^+$.

At this point it is important to note that in the case of homopolymerization of the alkali metal salts of methacrylic acid, the polymerization rates increase in the same order with the size of the cation $Li^+ < Na^+ < K^+$, i.e., the opposite order than in the case of our copolymer systems.

We have also seen that the reactivities of the radicals of both types of monomers (salt and MMA) were closely dependent upon the nature of the alkali metal in methacrylate salts; in the case of the present work, values of both r_1 and r_2 increase in the order $Li^+ < Na^+ < K^+$.

Since in the case of this work, the copolymerization medium is organic, the cation binding character of the macroradicals cannot be expected to justify significantly the dependence of the reactivities of monomers upon the nature of the alkali metal. The entire molecule of the methacrylate salt will react in the system since no significant dissociation can take place in a non-aqueous medium.

The increase of the r_1 values with the size of the metal ion can essentially be attributed to a decrease of k_{12} due to a combination of electrostatic and steric effects in the monomeric salt (monomer 2):

The double bond in the monomeric salt is subject to steric effects due to both the methyl group and the metal ion, the salt being more reactive the smaller the alkali metal.

Electrostatic effect is also thought to be significant: the bigger the cation, the longer and therefore the weaker becomes the oxygen — metal bond and the stronger the repulsion forces between functional groups of the macroradical and the approaching methacrylate salt.

The increase of r_2 with the size of the metal can be attributed to an increase of k_{22} while k_{21} remains practically constant. An increase in k_{22} is consistent

with the observation that the rate of homopolymerization of the alkali metal methacrylates increases with the size^(94,112) of the metal ion in the order: $\text{Li}^+ < \text{Na}^+ < \text{K}^+$.

CONCLUSION

In conclusion, one sees that the reactivities of the two types of radicals dealt with in the copolymer systems of the present work are completely different from what might have been expected from the Q and e scheme.⁽¹⁰⁸⁾

From published⁽¹¹⁶⁾ values of Q and e for each monomer, one could predict the reactivity ratios for two monomers in copolymerization using the empirical equations:⁽¹⁰⁸⁾

$$r_1 = (Q_1/Q_2) \exp(-e_1(e_1 - e_2))$$

$$r_2 = (Q_2/Q_1) \exp(-e_2(e_2 - e_1))$$

$$\text{and } r_1 r_2 = \exp(-(e_1 - e_2)^2)$$

Table IV-10

Reactivity ratios "predicted" using the empirical
Q and e scheme. (108)

Copolymer system	Q_1	Q_2	e_1	e_2	r_1	r_2
MMA(1)/LiMA(2)	0.74	0.64	0.4	0.3	1.11	0.891
MMA(1)/NaMA(2)	0.74	1.36	0.4	-1.18	0.289	0.285
MMA(1)/KMA(2)	0.74	0.54	0.4	0.01	1.172	0.733

The predicted values of r_1 and r_2 for our three systems (table IV-10) do not agree at all with the values found experimentally (see table IV-9) and this again shows how the behaviour of a particular radical depends very closely on the nature of the units previously added, on the working conditions and environment and, cannot always be predicted from empirical and uncertain measures of resonance stabilization of radical (Q) and polarity of monomer and corresponding radical (e).

CHAPTER V

THE THERMAL DEGRADATION OF COPOLYMERS OF METHYL METHACRYLATE WITH ALKALI METAL METHACRYLATES I: PRODUCTS AND GENERAL CHARACTERISTICS OF THE REACTION

INTRODUCTION

The thermal behaviour of polyelectrolytes has not been given much attention in the past. This is largely due to their specific applications based mainly upon their electrolytic characteristics in water. Typical uses of acrylic and methacrylic types of polyelectrolytes include waste treatment, water purification and conditioning. They have also been used as processing additives in the textile and paper industries.

It is very likely however, that polyelectrolytes will be used increasingly to improve and extend the uses of some more important polymers in the form of copolymers so that prior knowledge of their thermal behaviour will be required.

THERMAL DECOMPOSITION OF PMMA

The thermal decomposition of PMMA which was briefly discussed in chapter I appears to be well understood as compared with that of other poly (alkyl methacrylates). PMMA degrades thermally to give an almost quantitative yield of monomer. A free radical mechanism of depolymerization, initiated by random chain scission, has been suggested by Grassie and Melville.⁽⁵⁰⁾ The radicals thus produced are stabilized by resonance in the ester group. As a result, these macroradicals simply "unzip" to monomer which distils out, since it is volatile at the degradation temperature.

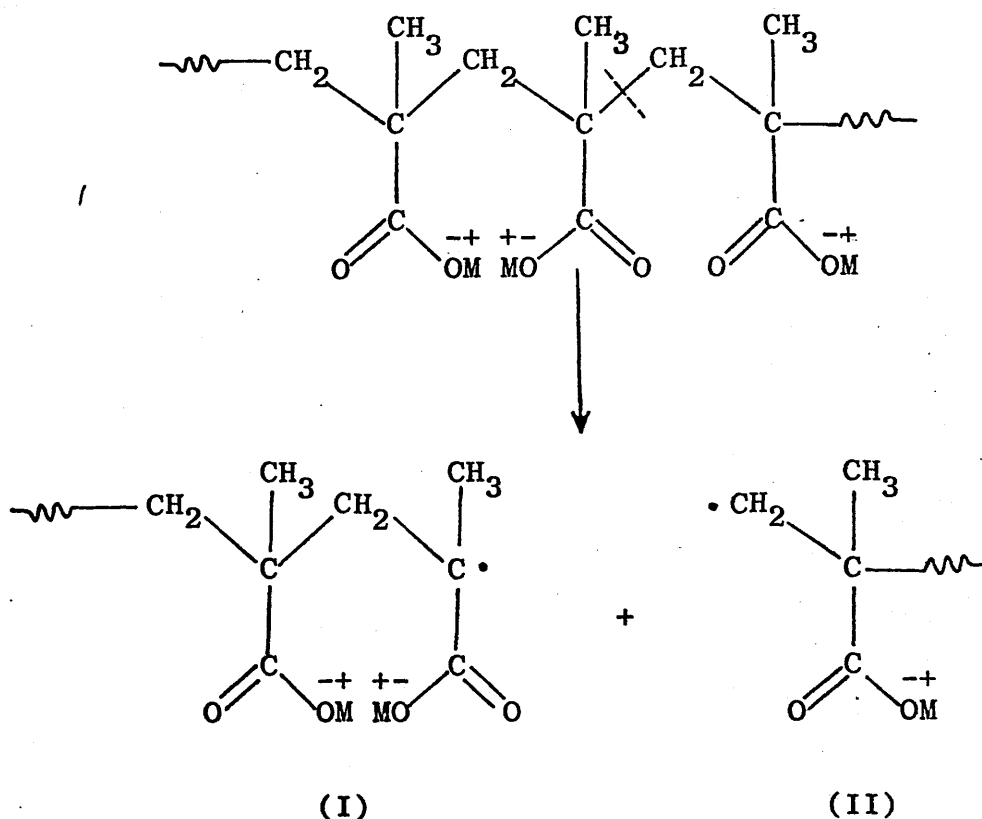
THERMAL DECOMPOSITION OF POLY(ALKALI METAL METHACRYLATES)

The thermal decomposition of the homopolymers of alkali metal salts of methacrylic acid, studied in detail by McNeill and Zulfiqar⁽⁹⁴⁾ is similar in some respects to that of PMMA: monomer and isobutyrate are among the major products and this suggests that depolymerization is taking place to an appreciable extent.

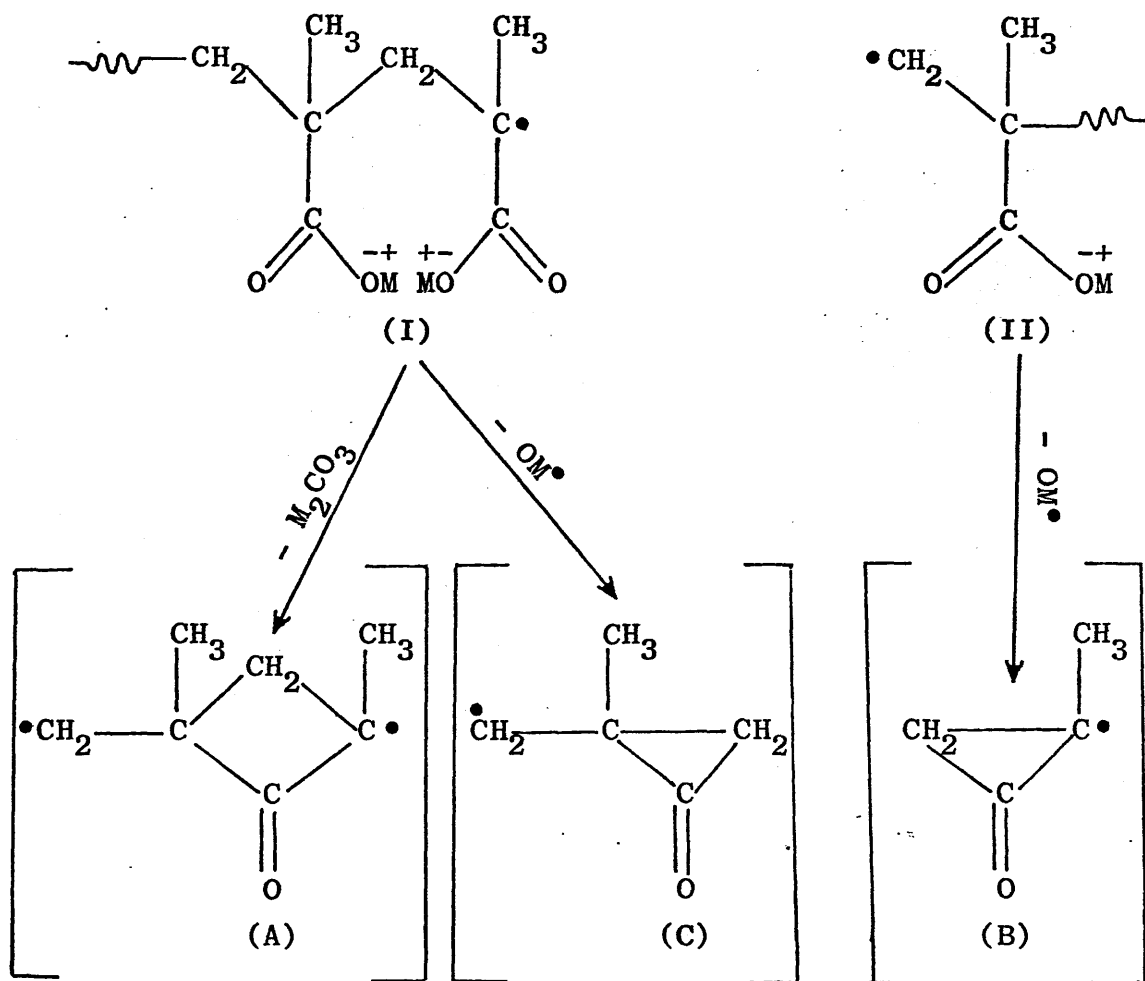
But because of the different functional groups which, in competition with depolymerization, decompose to give metal carbonate, the chain degradation becomes more complex. In the four cases (PLiMA, PNaMA, PKMA and PCsMA) the total thermal decomposition occurs in

a one stage breakdown starting at a low rate at about 350°C and reaching a maximum around 450°C. The major volatile products are monomer, metal isobutyrate, carbon dioxide, cyclic five membered ring ketones, aliphatic ketones and aldehydes, alkenes, methane and carbon monoxide; the residue consists of the metal carbonate and charcoal.

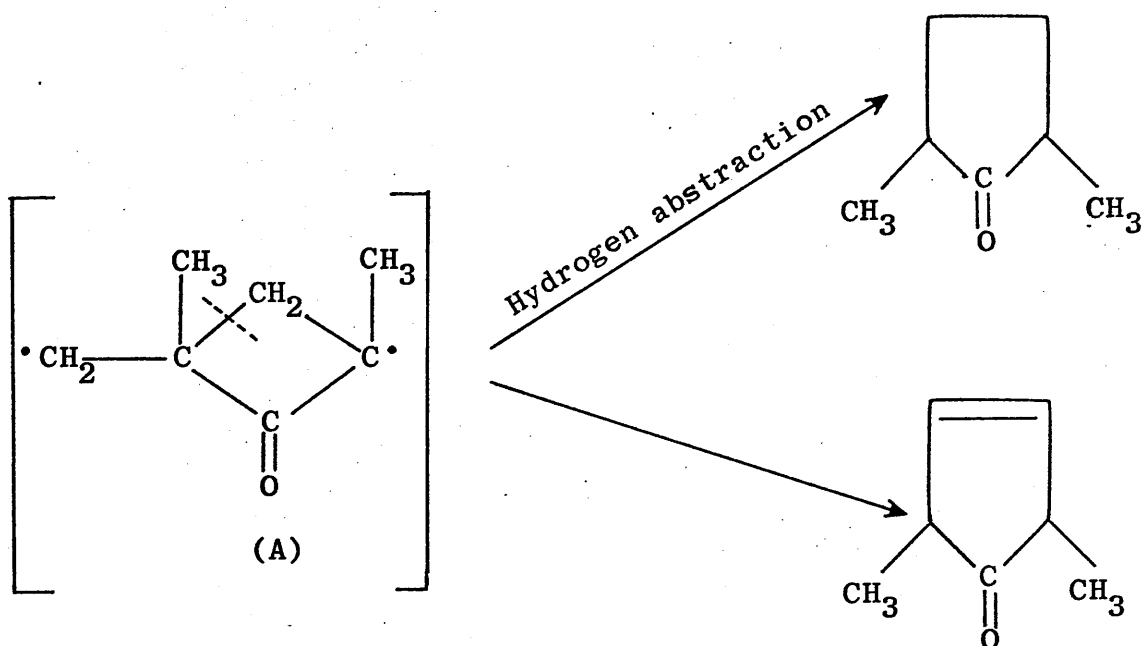
The reaction mechanism put forward by McNeill and Zulfiqar⁽⁹⁴⁾ to account for the formation of ketones, aldehydes, metal carbonate, methane and carbon monoxide is believed to involve three parallel processes depending on whether carbonate formation precedes chain scission or not:



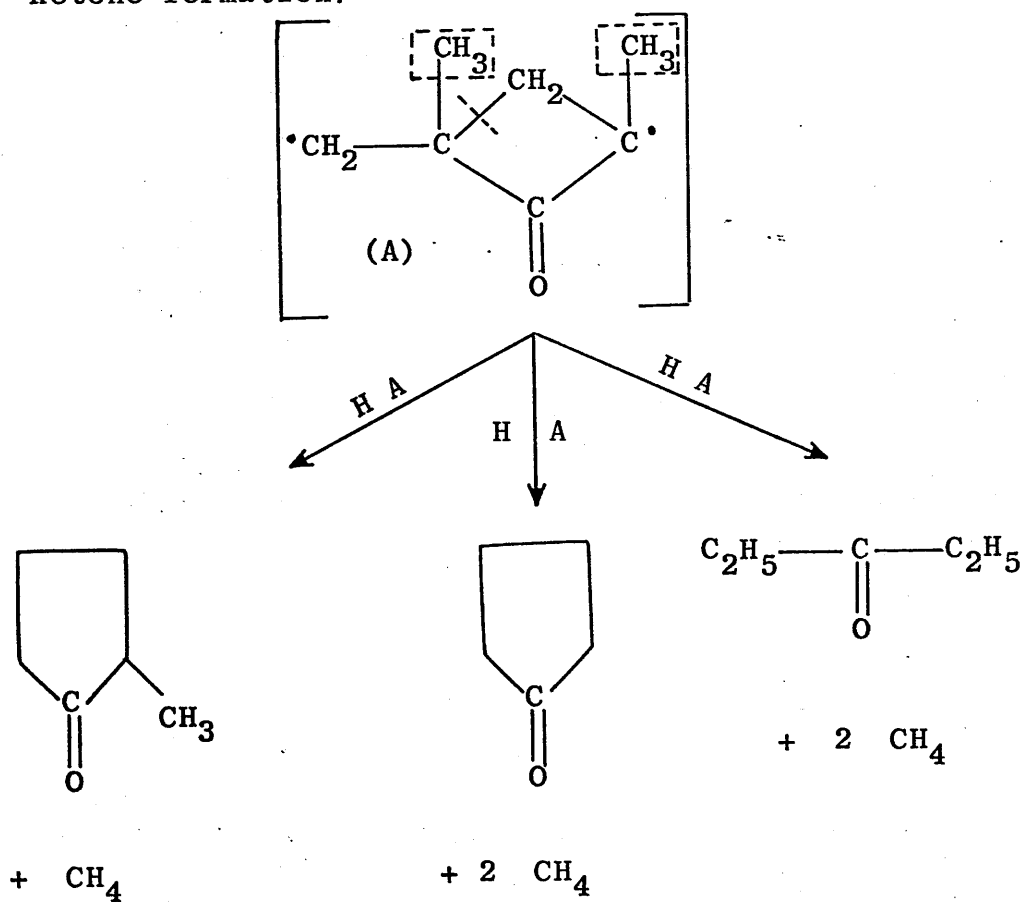
These two radicals (I and II) can lead to three other transient states A, B and C:



These three possible transient states, being formed at very high temperature, will undergo rearrangements and abstract hydrogen very rapidly to lead to different carbonyl containing compounds. Transient form A could lead to cyclic ketones:

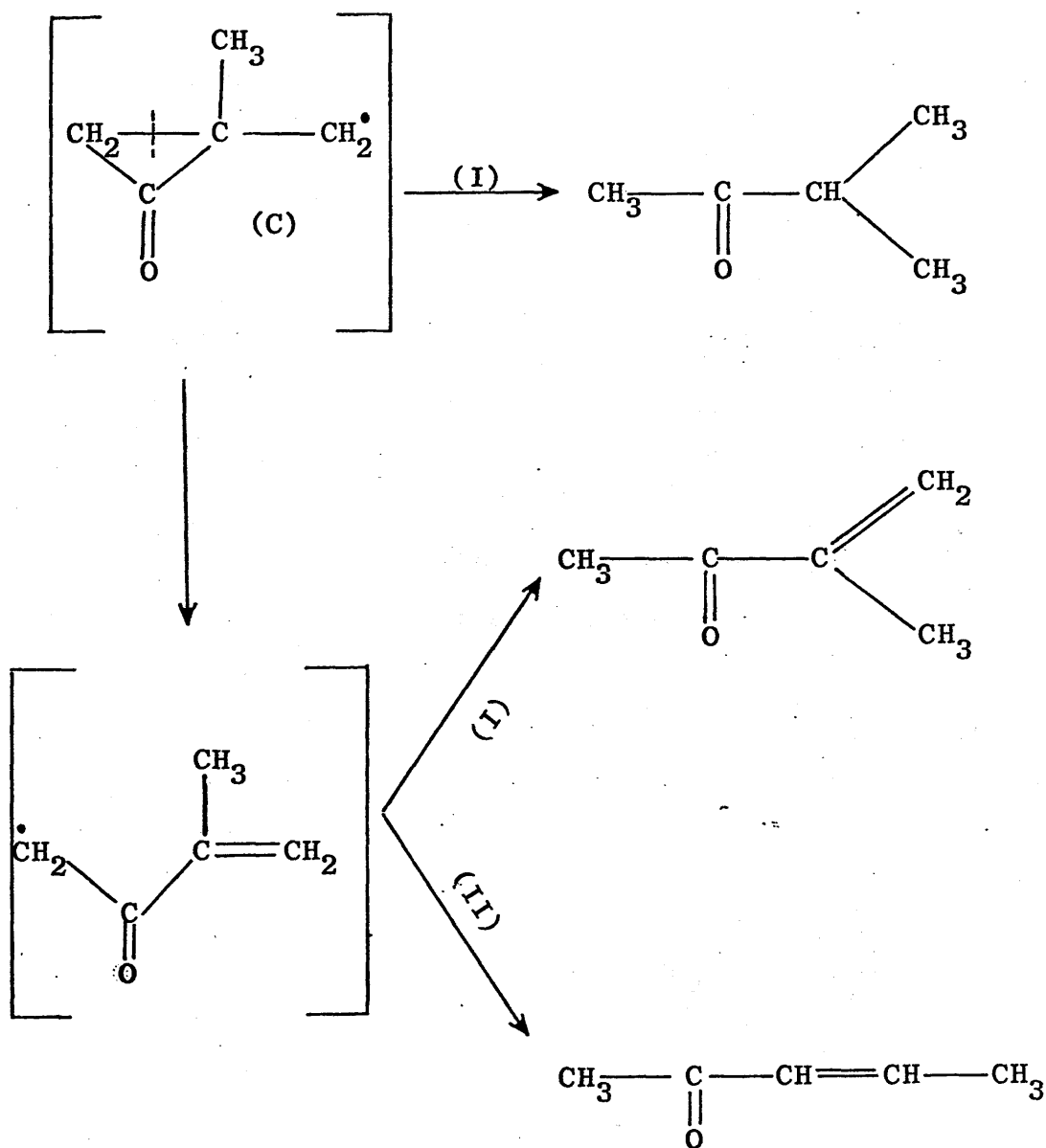


or with the loss of CH_3 as methane prior to ketone formation:



H A = Hydrogen abstraction.

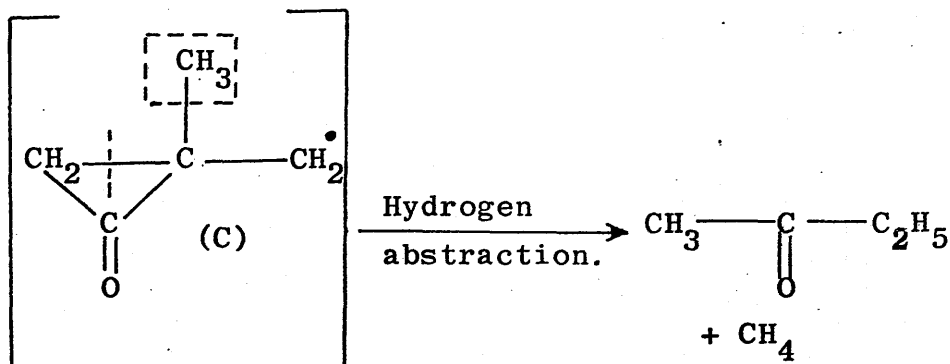
The formation of methyl isopropyl ketone, methyl prop-2-enyl ketone, methyl isopropenyl ketone and methyl ethyl ketone result from transient state C:



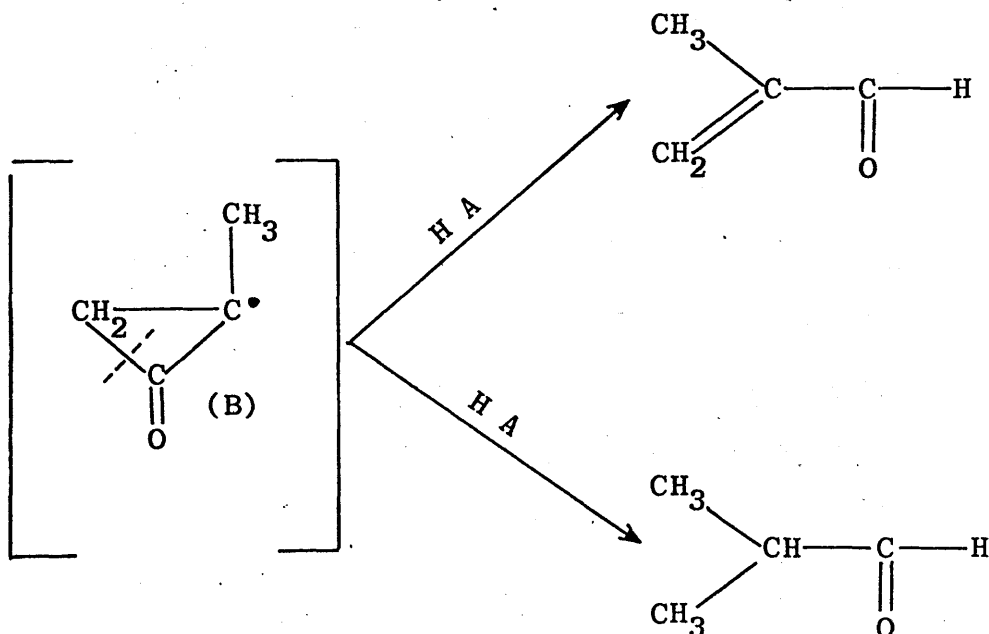
(I) : Hydrogen abstraction.

(II) : Free radical rearrangement.

also with prior loss of the methyl group as methane:

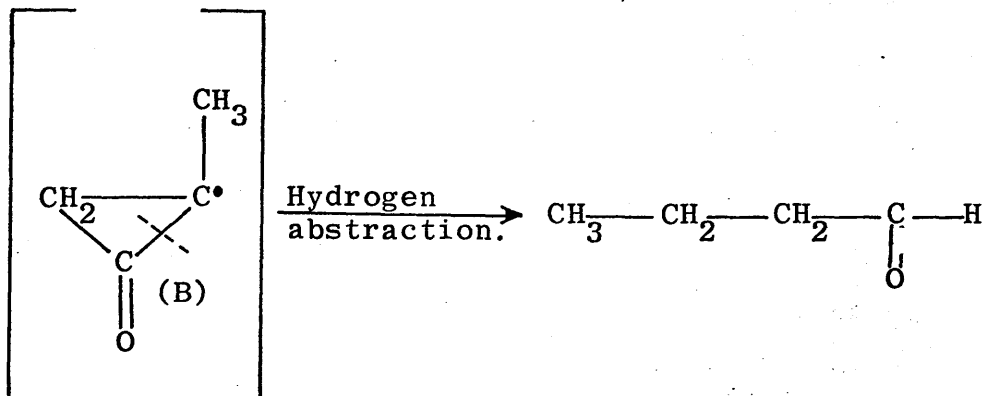


Finally the transient state B is believed to lead to the formation of aldehydes and acetone:

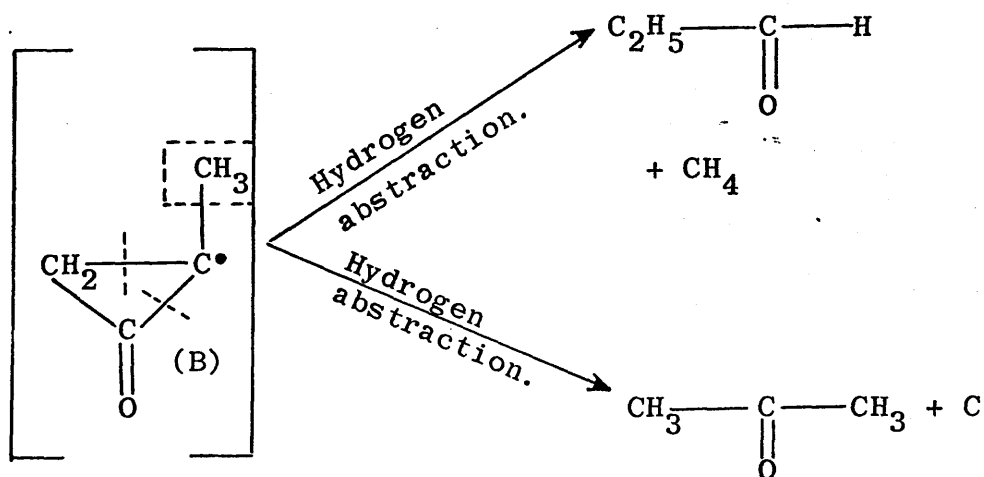


H A = Hydrogen abstraction.

or, if scission occurs where indicated:

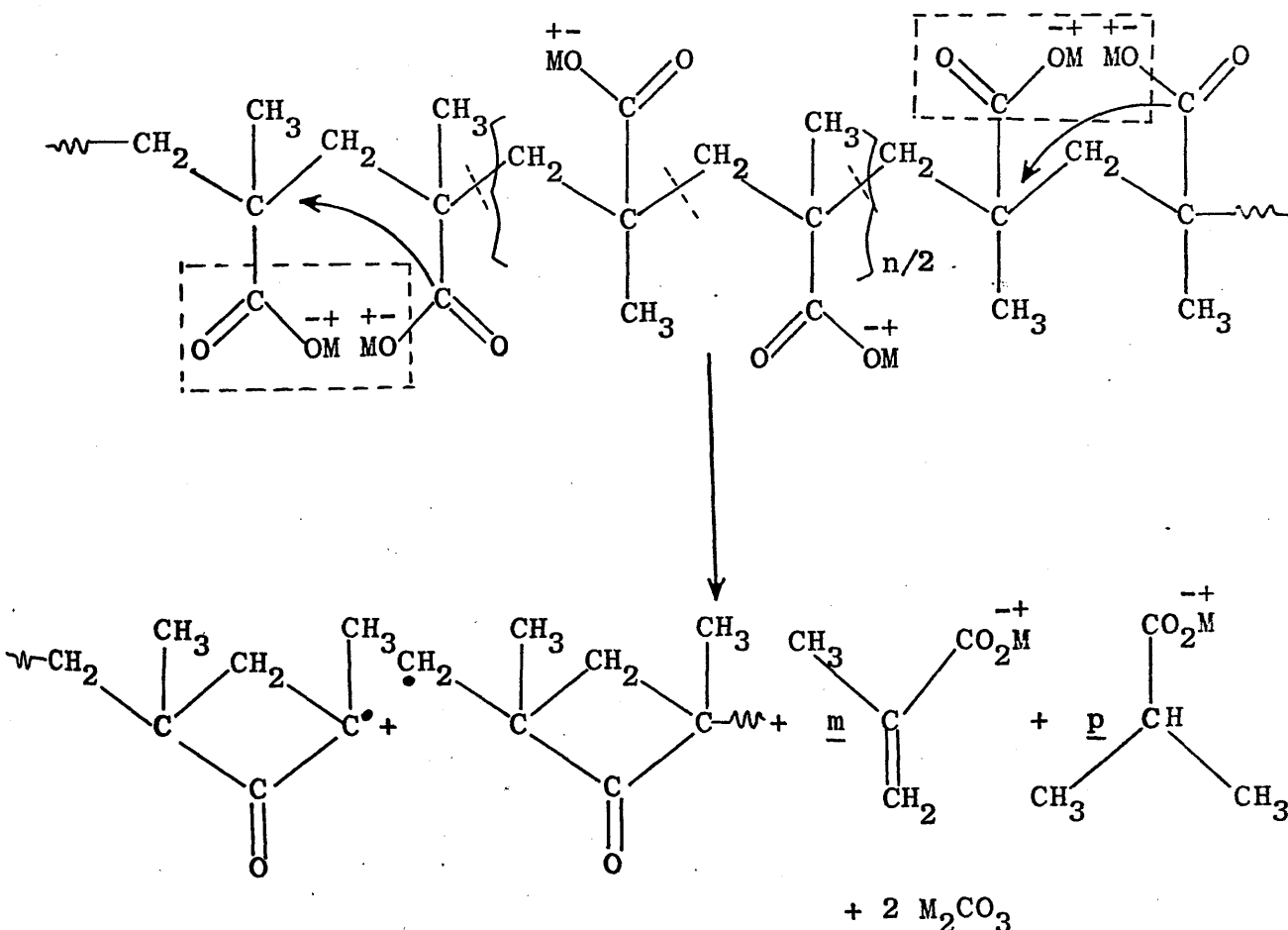


and again methane loss is possible prior to product formation:



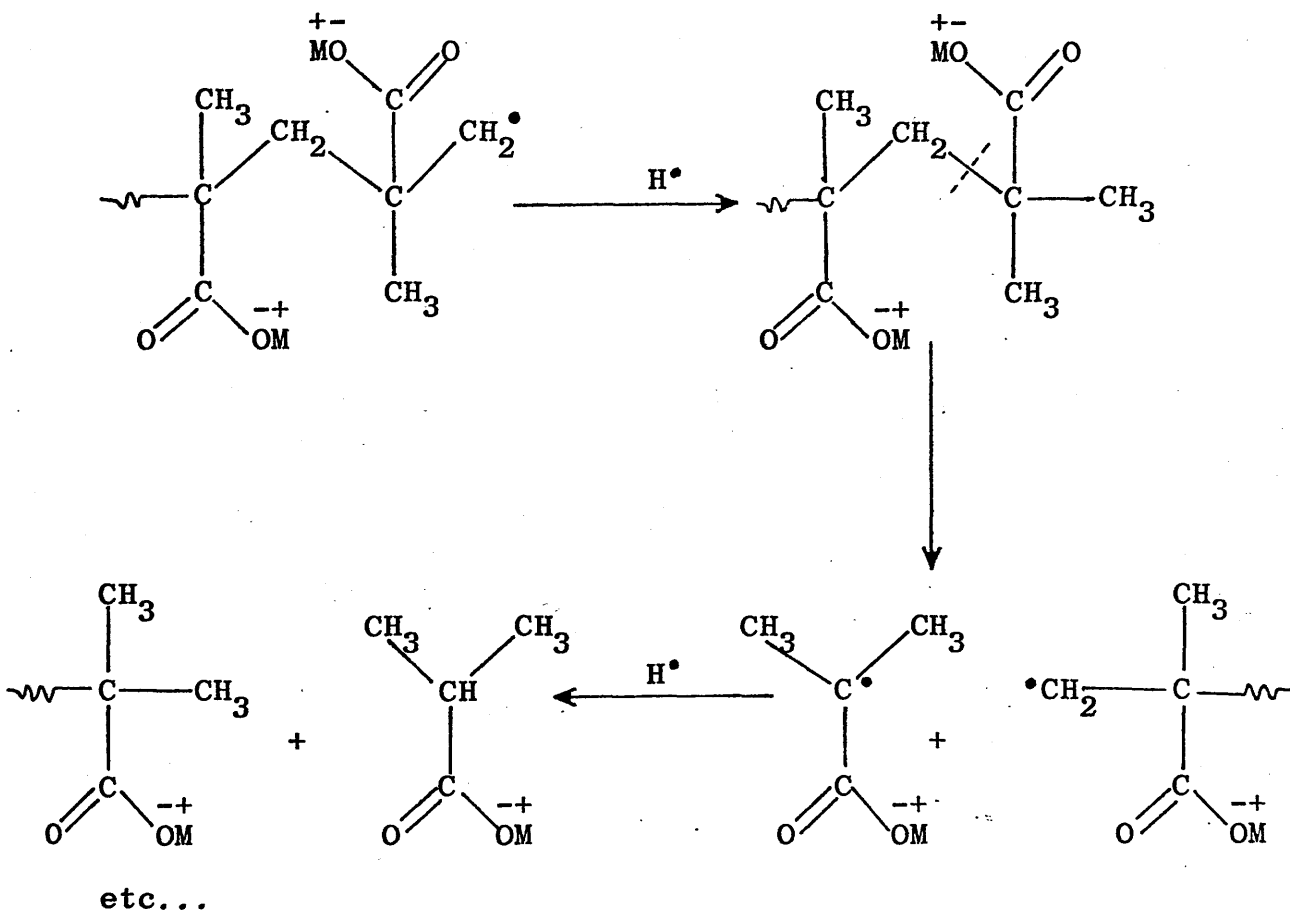
The formation of isobutene, n-butene, propylene and ethylene is believed to result after loss of the CO radical and rearrangement of the three transient states.

With regard to the presence of monomer and isobutyrate, which were found to sublime at degradation temperature onto the cold ring, their yield has been found to increase with the size of the metal ion used. This was explained in terms of tacticity of the homopolymers; syndiotacticity in the polymers increases with the size of the ion. (117,118) This explains the small amount of ketones given from PCsMA and PKMA compared with the cases of PLiMA and PNaMA, the polymers with the bigger ion giving more monomer and isobutyrate, due to the difficulty for two adjacent functional groups to eliminate M_2CO_3 :



with $\underline{m} + \underline{p} = n$

The formation of metal isobutyrate is believed to result in the same fashion as above except for the hydrogen abstraction prior to further chain scission:

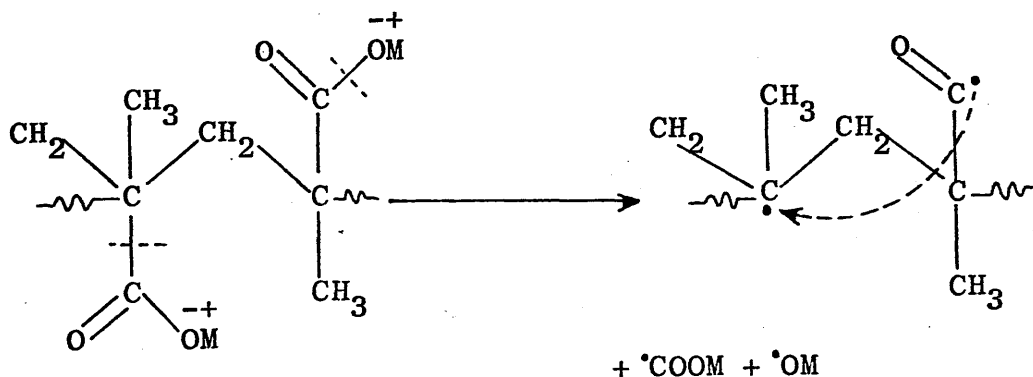


Finally the presence of carbon dioxide as a major product, the amount of which increases with the size of the metal ion, is ambiguous. McNeill and Zulfiqar suggested two possible routes:

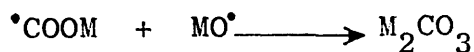
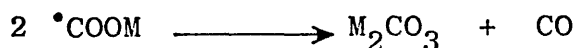
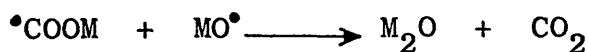
- (i) It could arise from direct decomposition of M_2CO_3 leaving M_2O but this seems unlikely since Na_2CO_3 and Li_2CO_3 are both stable up to 500°C under

vacuum. However, impurities in the residue like carbon might make the metal carbonate decompose to some extent.

(ii) It has also been suggested that carbon dioxide could have its origin in the simple radical decomposition of pendant carboxylate groups:



Reactions of OM and COOM radicals could lead to carbon dioxide and other products:



and the reason for the absence of oxides in the final residue will simply be due to the presence of CO_2 in the atmosphere which would instantly reconvert them

to carbonates (the alkali metal oxides are very reactive).

This second route for carbon dioxide formation would be favoured by greater syndiotacticity in the polymers and this is supported by the results of quantitative analysis for carbon dioxide which appears in greater yield as ion size increases.

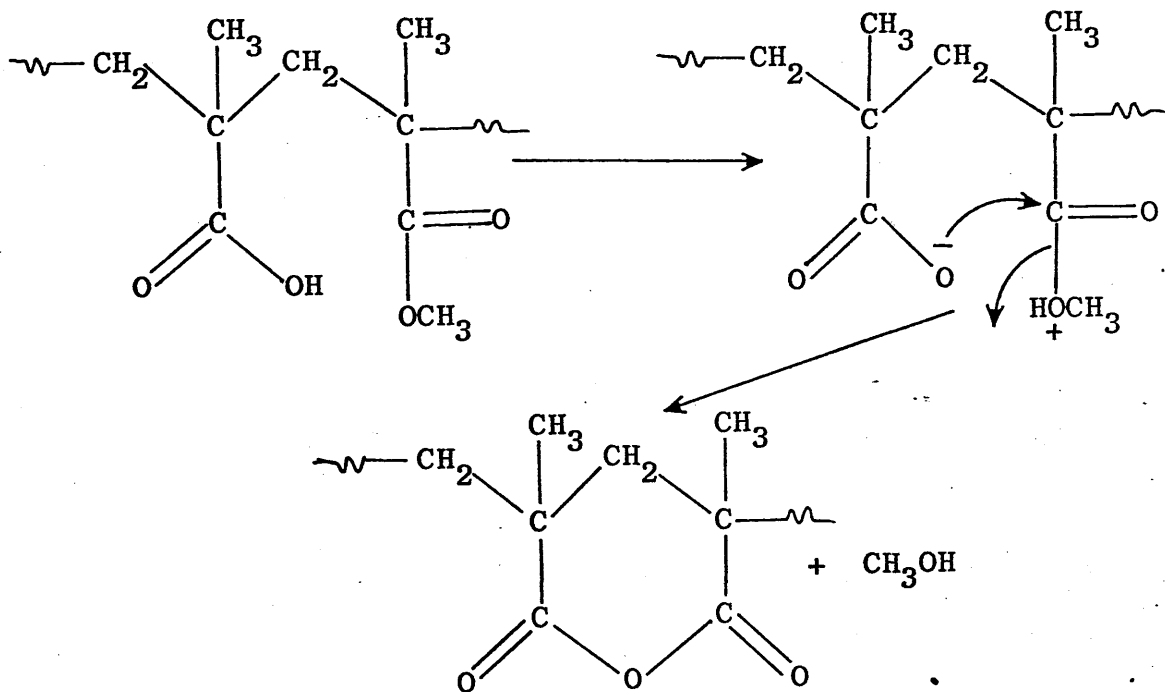
In conclusion the overall picture of the thermal decomposition of poly(alkali metal methacrylates) appears to be in good agreement with the quantitative analysis of the products: when syndiotacticity increases (i.e., when the size of the metal ion increases) the production of monomer, metal isobutyrate and carbon dioxide increases, whereas the production of cyclic ketones decreases markedly.

THERMAL DECOMPOSITION OF METHACRYLIC ACID/METHYL METHACRYLATE COPOLYMER

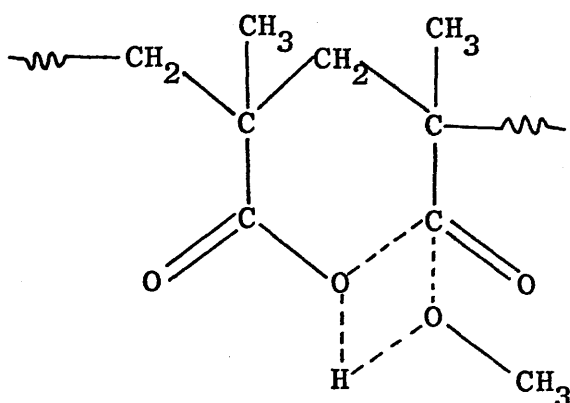
Because of the somewhat similar pattern of degradation of this copolymer when compared with those dealt with in the present work, it is appropriate to consider very briefly the main features of its degradation process, which was studied in detail by McNeill and Jamieson.⁽⁷¹⁾ They found that the copolymers were producing water and methanol below 300°C and leaving six membered ring anhydride structures in the residue. Above this temperature they also found methyl methacrylate, carbon dioxide,

carbon monoxide and methane. They compared quantitatively the experimental yields of methanol with predicted yields from sequence distribution considerations. Methanol is believed to originate from two sources:

(i) Intramolecular cyclization of MAA and MMA units at low temperature:



the overall reaction passing through the transition state:



(ii) Decomposition of ester units in competition with depolymerization at higher temperatures.

THERMAL VOLATILIZATION ANALYSIS

As all the copolymers and polymers used in this work, except PMMA, absorb moisture from the atmosphere, it was necessary to determine the amount of water taken up by thermogravimetry as explained in chapter III. All the samples sizes referred to in the forthcoming discussion correspond to the pure polymers and copolymers excluding water.

In TG/TVA experiments the samples were examined in the powder form and the sample sizes were 25-30 mg degraded up to 500°C at the heating rate of $10^{\circ}\text{C}/\text{minute}$ under normal TVA conditions (see chapter II).

Before all degradation experiments under vacuum, all samples (except PMMA) were heated up to 150°C for five minutes under high vacuum in order to expel all traces of water taken up from the atmosphere. It has been checked that the copolymers do not undergo any change in their structure after this heating.

The polymer and copolymer samples dealt with in this chapter were all prepared and purified under the same conditions as those described in chapter III.

THERMAL VOLATILIZATION ANALYSIS OF PMMA

The TG/TVA trace for a sample of PMMA prepared for reference by a free radical mechanism under the same conditions as the copolymers is illustrated in fig. V-1. The Pirani response in each curve is typical of that of a single substance passing through the trap system: methyl methacrylate. The monomer is not condensed in either the 0°C or the -45°C trap. It is partially condensed in the -75°C trap. The plateau in the -75°C curve shown as a continued response after the maximum rate of monomer evolution is typical of the behaviour of MMA monomer in the TVA system. It is due to condensed MMA distilling into the common liquid nitrogen trap at a steady rate and is referred to as a limiting rate effect.

Two distinct rate maxima are apparent in the

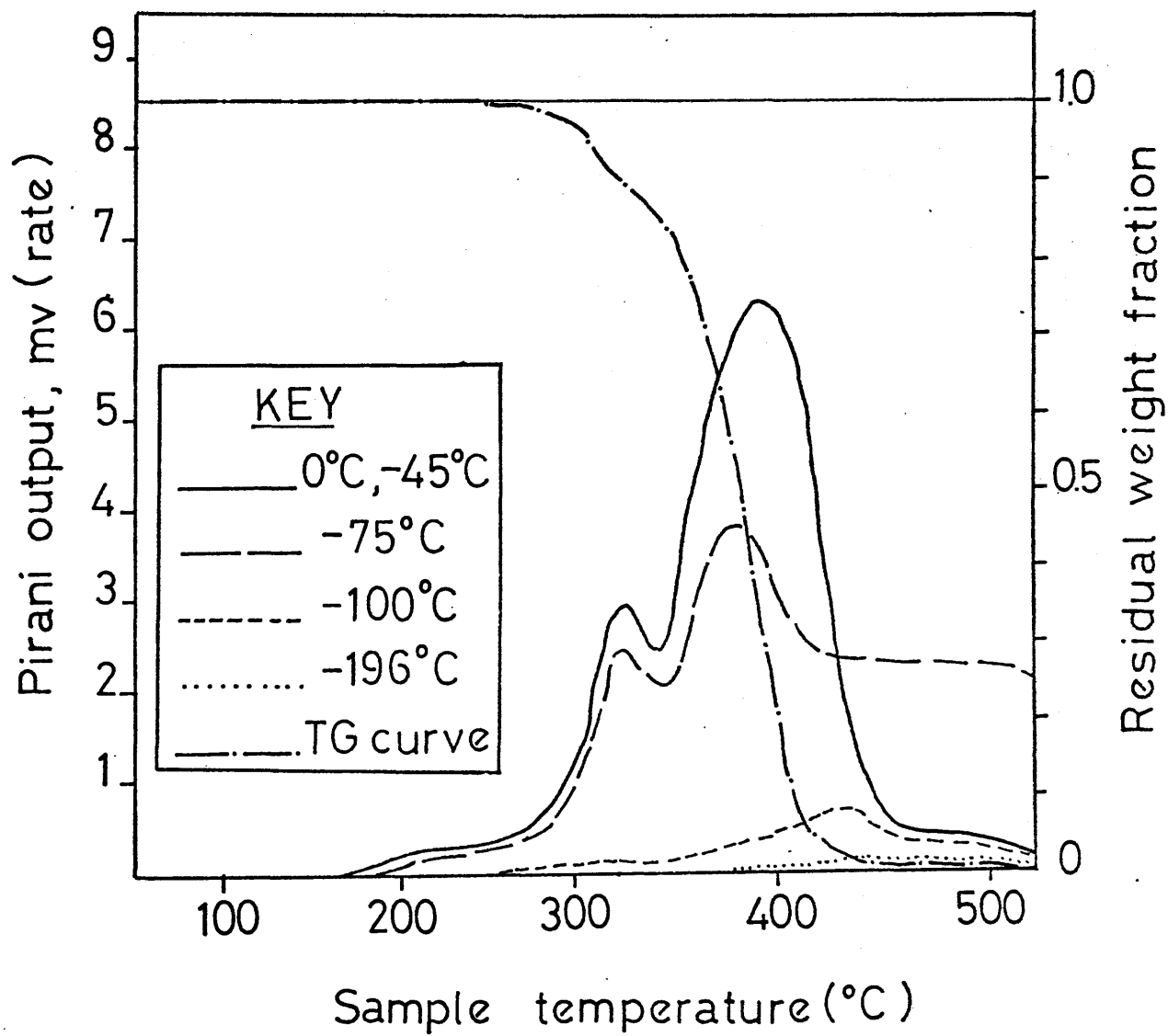


Fig. V - 1

TG/TVA FOR POLY(METHYL METHACRYLATE)

TG/TVA trace, one occurring at 320°C, the other around 380°C. The lower temperature peak results from monomer evolved by depolymerization initiated at unsaturated chain ends formed during polymerization by disproportionation reactions. The high temperature peak is then due to the "unzipping" of macroradicals formed by random chain scission. The relative amount of monomer produced by each mode of decomposition will depend upon the proportion of unsaturated chain ends present in the polymer, which is, in turn, dependent upon both the molecular weight* and the polymerization technique employed. TVA studies by McNeill have demonstrated the molecular weight dependence on the monomer evolution in PMMA.⁽¹¹⁹⁾

The TG curve in the same figure shows also the two decomposition stages and the absence of residue at the end of the degradation, indicating that all polymer has decomposed to yield monomer.

THERMAL VOLATILIZATION ANALYSIS OF POLY(ALKALI METAL METHACRYLATES)

TG/TVA traces for poly(Li, Na and K methacrylates) are shown in fig. V-2, 3 and 4 respectively. In agreement with what McNeill and Zulfiqar⁽⁹⁴⁾ found, all three traces are similar in as much as their

* The molecular weight of the PMMA sample dealt with is 90.000.

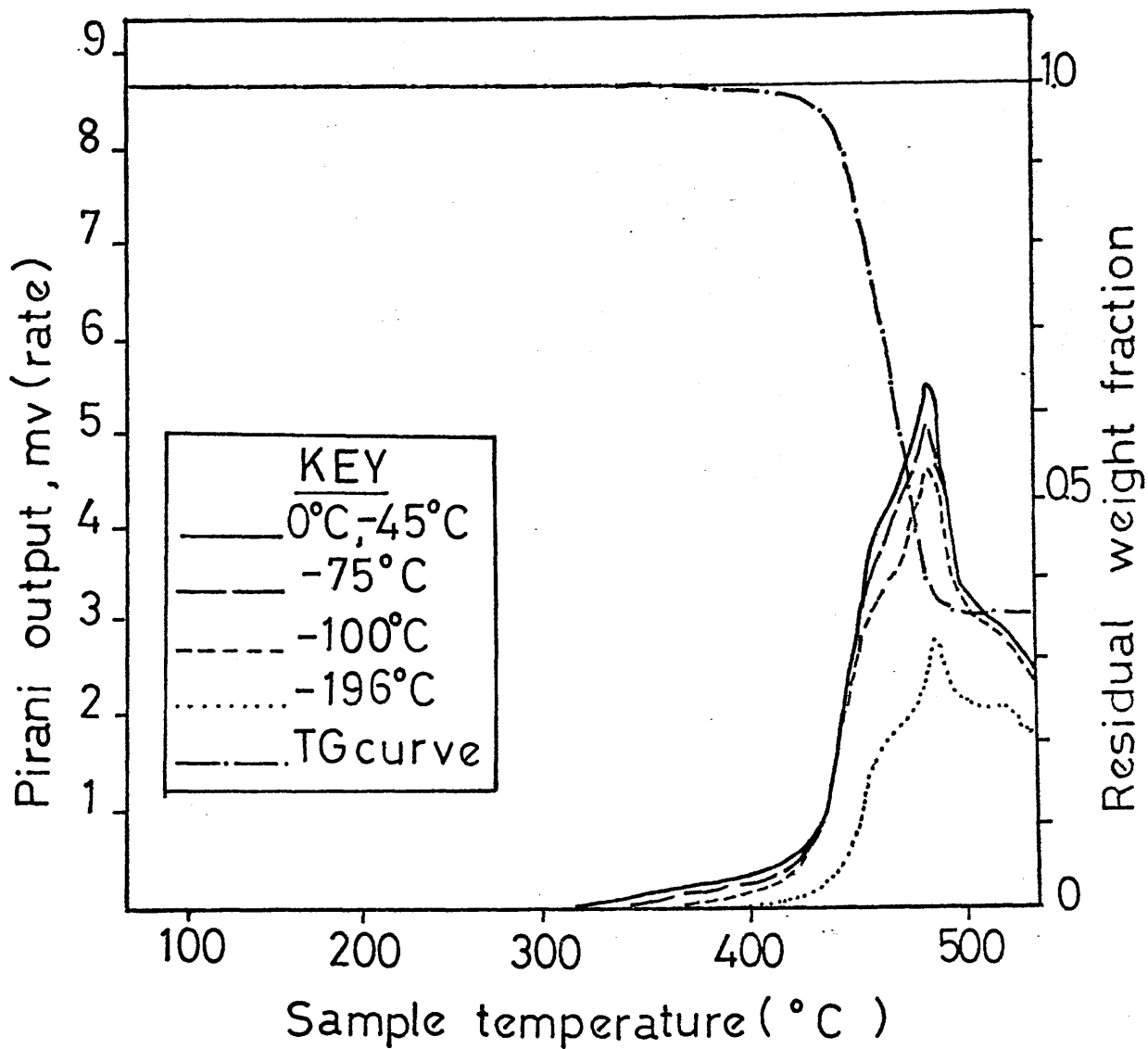


Fig. V - 2

TG/TVA FOR POLY(LITHIUM METHACRYLATE)

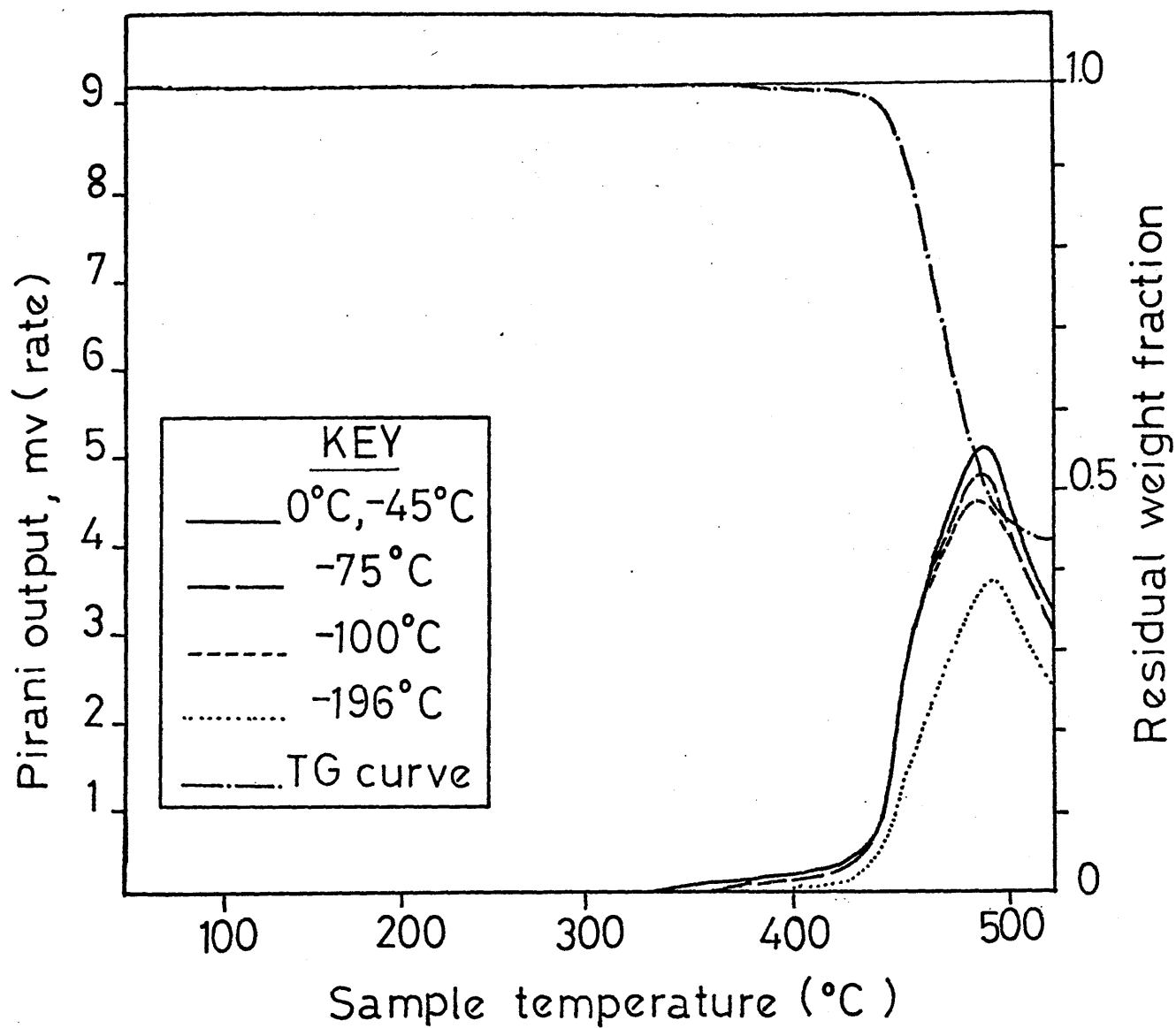


Fig. V-3

TG/TVA FOR POLY(SODIUM METHACRYLATE)

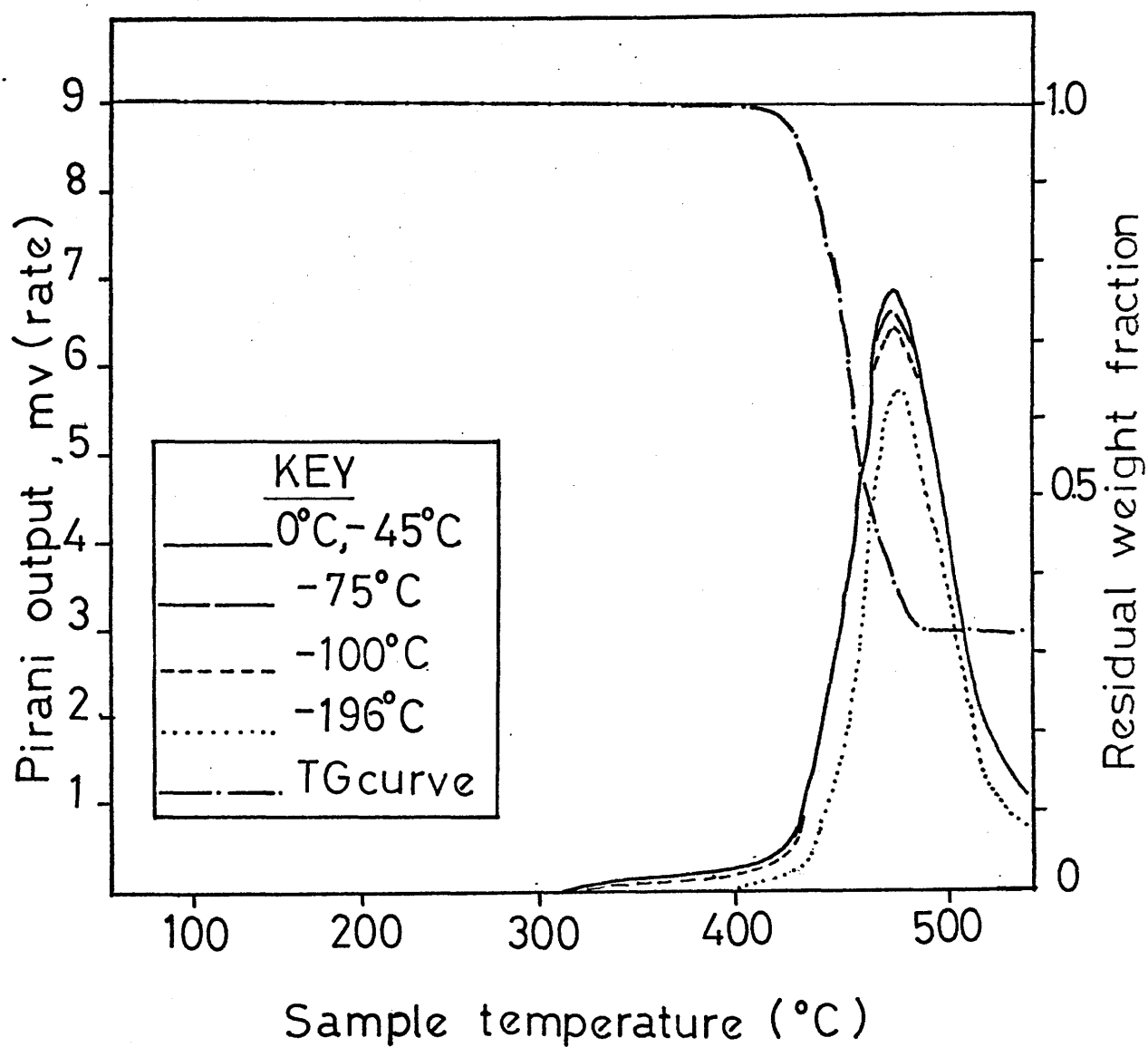


Fig. V - 4

TG/TVA FOR POLY(POTASSIUM METHACRYLATE)

thermal breakdown is a one stage reaction with a maximum rate of degradation at about 470°C . In all three cases the 0°C and -45°C traces are coincident showing no condensation at these traps. On the other hand, the -75°C and -100°C curves are apart from the common curve corresponding to the 0°C and -45°C traps, indicating the condensation in these traps of the high boiling point ketones reported by McNeill and Zulfiqar. It is also clear from the three thermograms that the separation between the 0°C , -75°C and -100°C curves increases in the order K^{+} Na^{+} Li^{+} , which confirms the fact that the ketone production increases as the size of the metal ion decreases: figure V-4 for PKMA, shows hardly any condensation in the first four traps in comparison with the cases of PLiMA and PNaMA (figs. V-2 and 3).

Also, the separation of the -196°C common back up trap curve shows an appreciable amount of low boiling point products condensing in this trap, these products being mainly carbon dioxide and small olefins presumably arising by scission of the residual backbone.

Finally the Pirani curve given by the gauge following the -196°C trap reaches a maximum well above the baseline, indicating the presence in an appreciable amount of volatile material non condensable at that temperature (i.e. methane and

carbon monoxide).

Table V-1 shows for each polymer the temperatures at which volatilization starts at a very low rate (threshold temperature) and that at which the maximum rate is reached (T_{\max}); also listed in the table is the weight percentage of the residue at 500°C recorded under vacuum.

Table V-1

TG/TVA data for poly(alkali metal methacrylates)

Homopolymer	Threshold temperature(°C)	T_{\max} (°C)	Weight % of residue
PLiMA	315	465	36
PNaMA	340	480	43
PKMA	320	475	33

The one stage decomposition reaction observed in the TVA traces is also confirmed by the shape of the TG curves in the same diagrams. Table V-1 shows an increase in the weight % of the residue at 500°C from PLiMA to PNaMA and then a drop from PNaMA to PKMA. This has been explained by the possibility that K_2CO_3 formed during the degradation decomposes to a significant extent to yield carbon dioxide and

K_2O (unlike Li_2CO_3 and Na_2CO_3); and this could reduce the weight % of the residue of PKMA at $500^{\circ}C$ in comparison with the other two polymers.

THERMAL VOLATILIZATION ANALYSIS OF THE COPOLYMERS

The TG/TVA curves for the three series of copolymers are similar in as much as they all present two distinct rate maxima corresponding to two different main reactions in the decomposition processes.

The consideration in detail of the traces corresponding to each series of copolymers separately, will provide, however, some important information about the differences in the degradation characteristics of the three copolymers.

THERMAL VOLATILIZATION ANALYSIS OF LiMA/MMA COPOLYMERS

TG/TVA traces for five LiMA/MMA copolymers having a LiMA content of 4%, 20%, 38%, 52% and 91% are shown in figures V-5, 6, 7, 8 and 9 respectively. As the LiMA content of copolymer increases, the character of the TVA traces changes progressively. In all five cases two main reactions are taking place, reactions manifested by two distinct rate maxima at about $400^{\circ}C$ and $500^{\circ}C$. In the copolymers of low LiMA content (4% and 20%), a low rate reaction with T_{max} around $330^{\circ}C$ is also evident: this corresponds

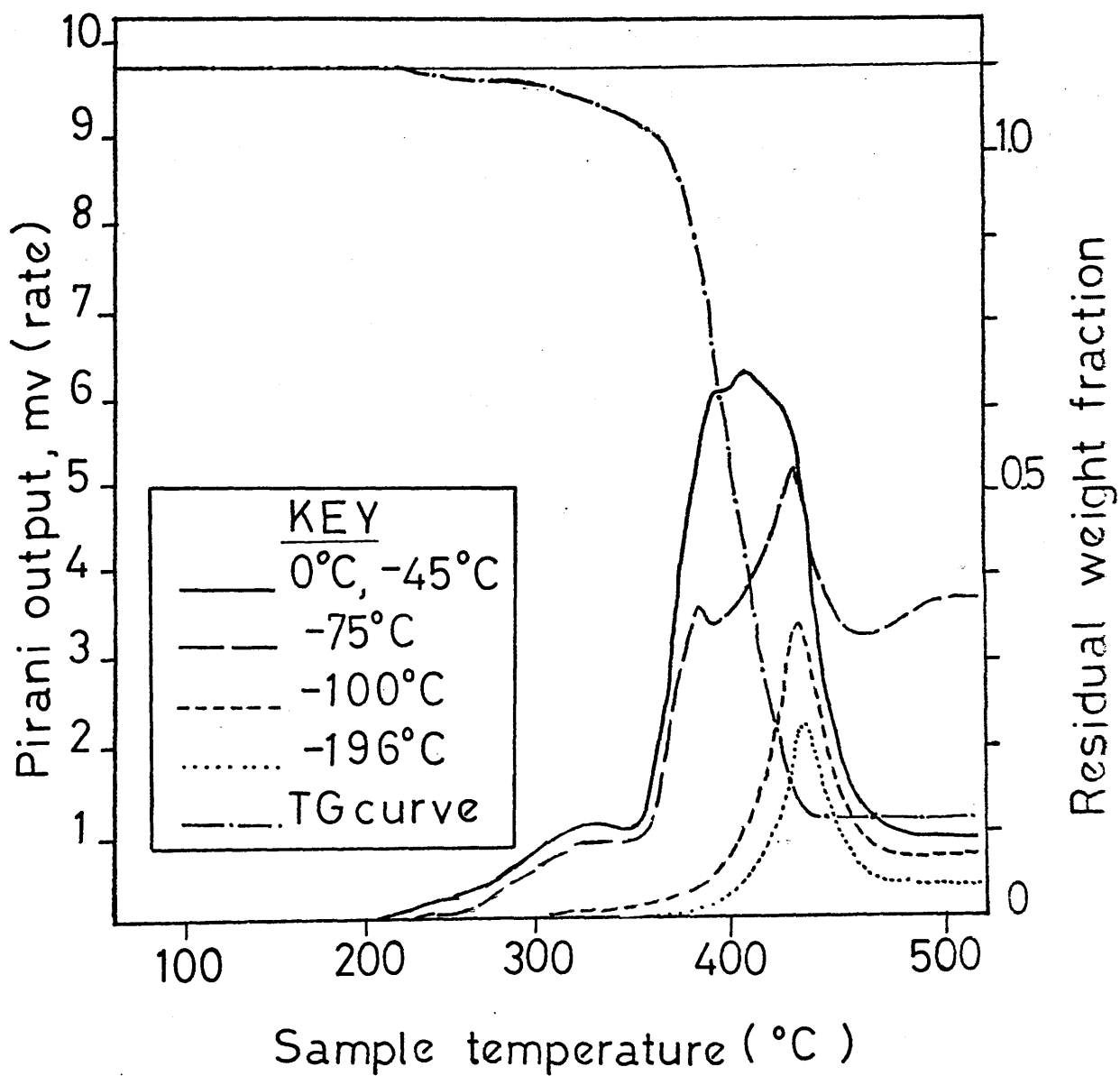


Fig. V-5

TG/TVA FOR 4% LiMA/MMA COPOLYMER

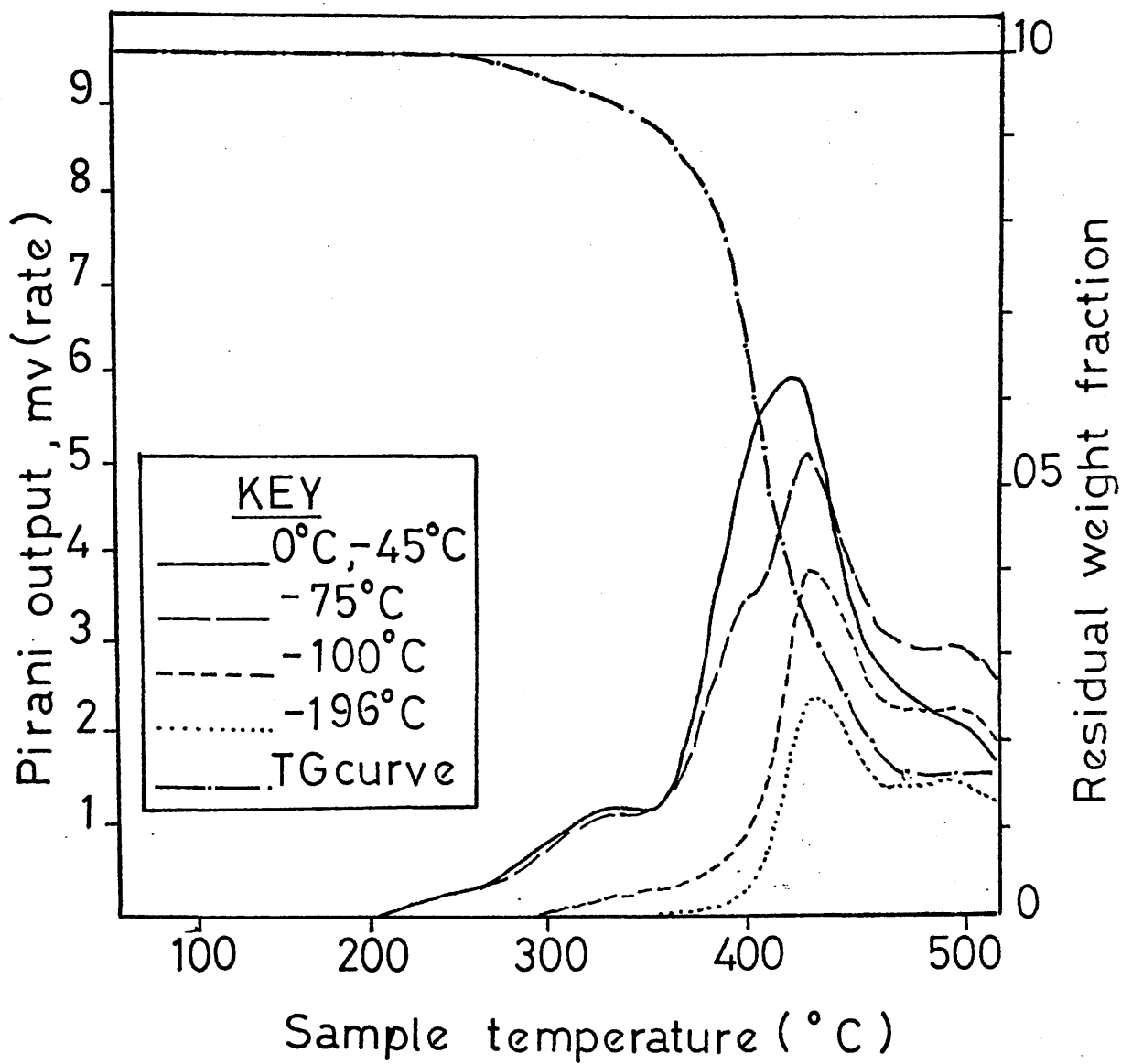


Fig. V-6

TG/TVA FOR 20%LiMA/MMA COPOLYMER

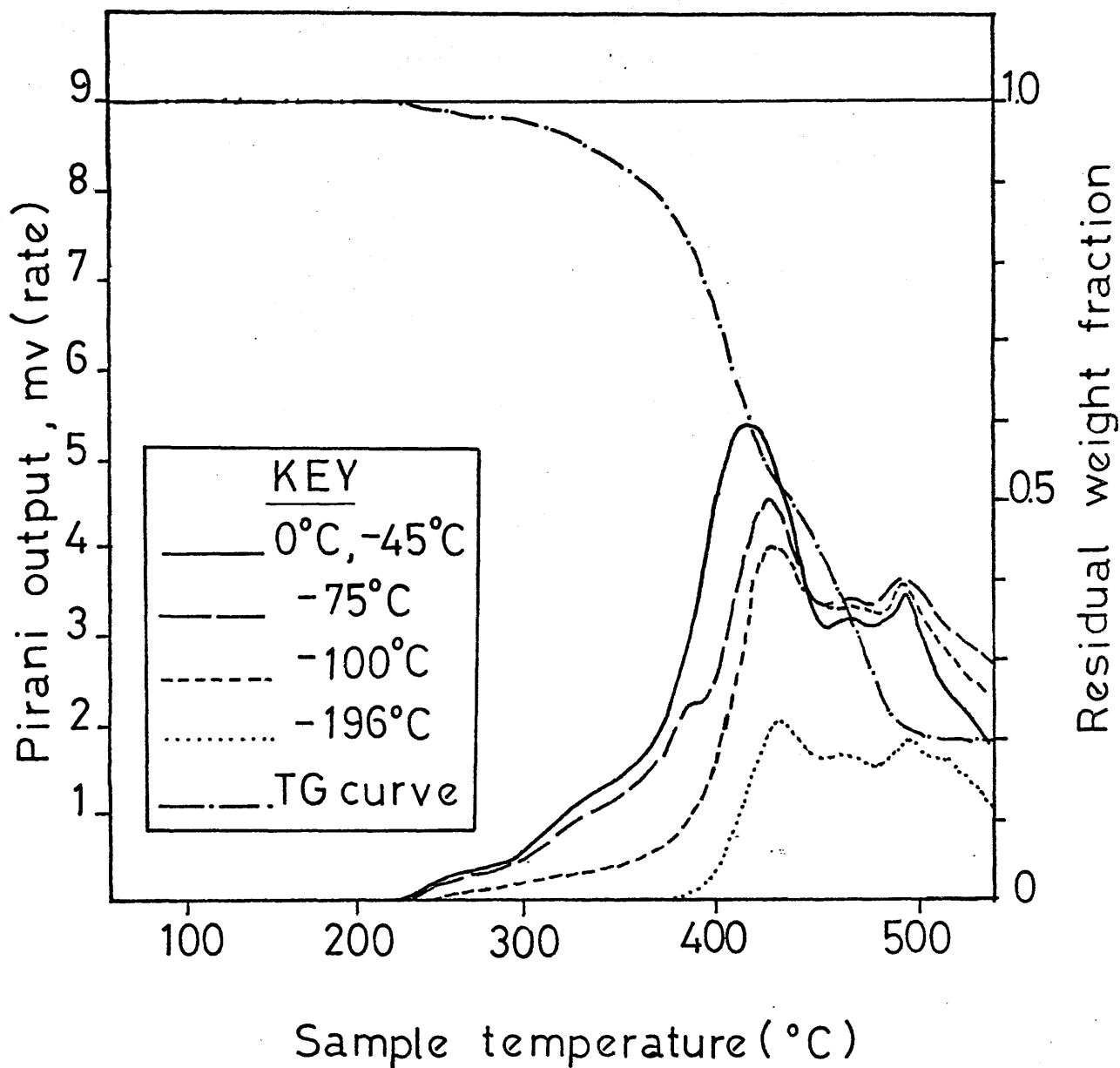


Fig. V-7

TG/TVA FOR 38% LiMA/MMA COPOLYMER

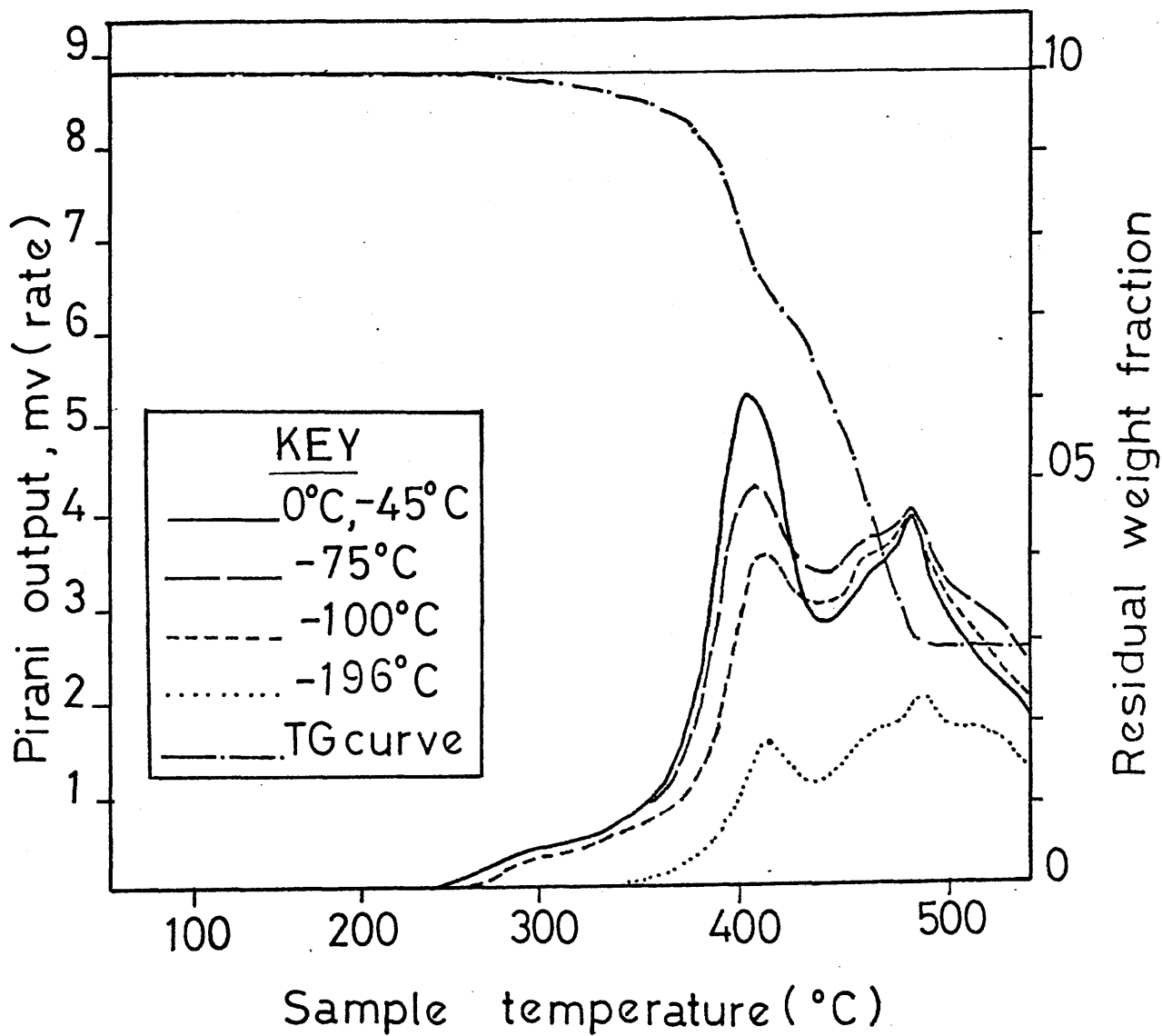


Fig. V-8

TG/TVA FOR 52%LiMA/MMA COPOLYMER

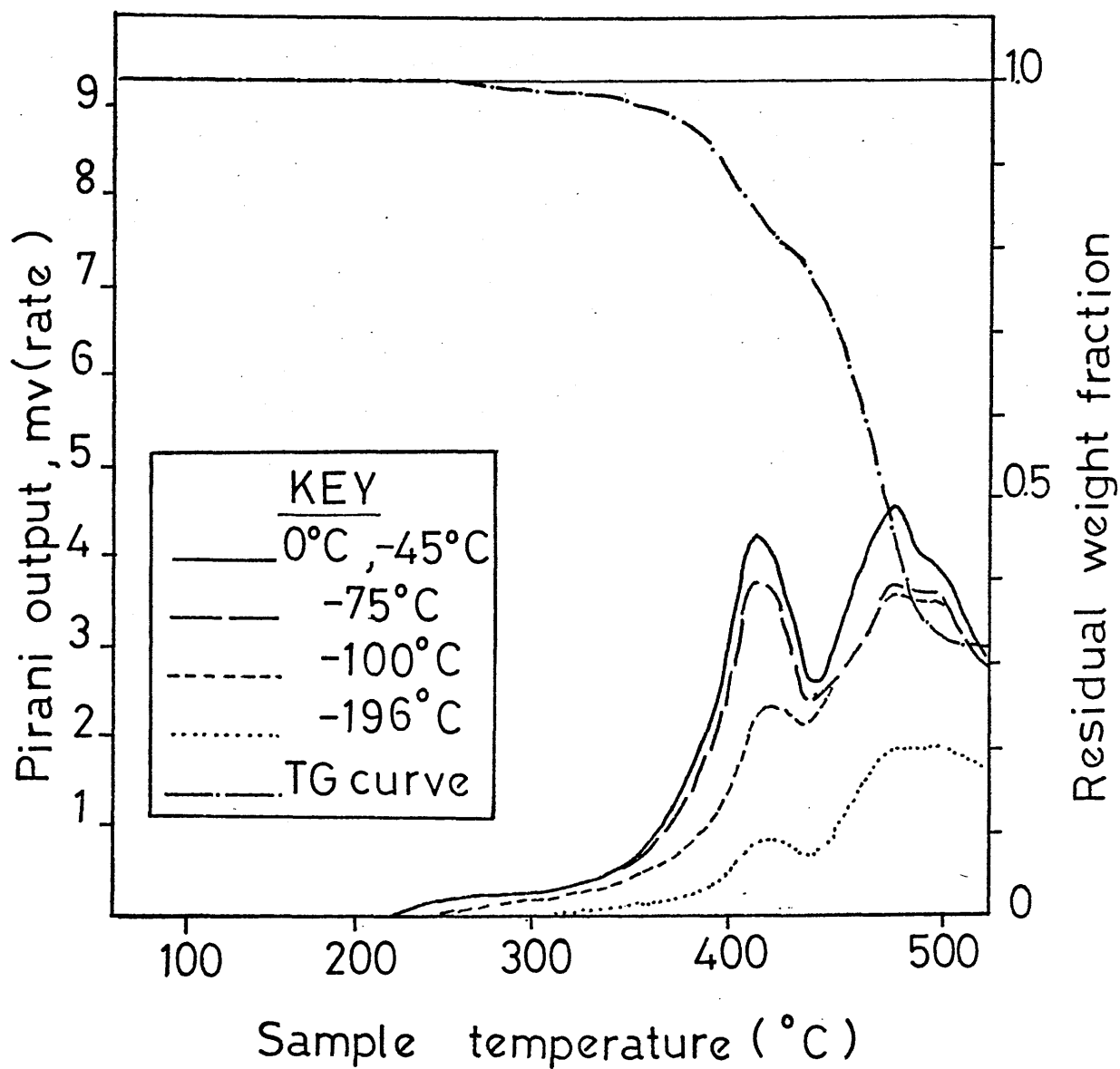


Fig. V-9

TG/TVA FOR 91%LiMA/MMA COPOLYMER

probably to MMA produced by initiation at chain end unsaturation. Then comes the main chain scission reaction producing monomer indicated by the limiting rate effect in the -75°C curve. But a new competitive reaction (distinct in the cases of the copolymers containing 4% and 20% LiMA) begins and displaces the -75°C curve due to continued limiting rate distillation of MMA monomer. This new reaction reaches a maximum rate in the -100°C curve at about 435°C (see figures V-6, 7 and 8) and thus yields products of high volatility, one of which giving a limiting rate in the -100°C curve. But this limiting rate in the -100°C curve, and the -75°C limiting rate due to MMA monomer distillation, are both again displaced by another complex reaction which, due to its increasing importance as the LiMA content increases in the copolymer series, must correspond to the independent decomposition of electrolyte units left in the chain.

A possible degradation product which could give a limiting rate in the -100°C curve is methanol, and supporting evidence for this interpretation will be given in the subsequent identification of methanol as a major product among the volatiles.

The threshold temperatures and T_{max} values for the two main decomposition reactions are given for all samples including the homopolymers in table V-2.

Table V-2TVA data for LiMA/MMA copolymers

LiMA % in copolymers	Threshold temperature($^{\circ}\text{C}$)	$T_{\text{max}}^1(^{\circ}\text{C})$	$T_{\text{max}}^2(^{\circ}\text{C})$
0	180	380	—
4	206	404	—
20	203	423	494
38	223	421	495
52	238	410	487
91	220	415	485
100	315	—	465

In all copolymers both the threshold temperatures and T_{max}^1 values, corresponding respectively to the beginning and the rate maximum of the MMA segments breakdown, are higher than the values for PMMA. Consequently LiMA must be stabilizing the MMA decomposition in the copolymers.

The production of MMA monomer, as illustrated by the limiting rate effect in the -75°C curve (displayed by the second main reaction of salt unit decomposition) is apparent in all of the copolymers. Methyl methacrylate

must therefore be the major product of the first main reaction. Next to MMA, another major product of this first main reaction proves to be methanol as illustrated by the limiting rate effect in the -100°C curve (giving a lower reading than the -75°C limiting rate) again also displaced by the second main reaction. This limiting rate (-100°C) is only apparent in the curves for the second, third and fourth copolymers. This leads to the conclusion that the production of methanol is enhanced by the incorporation of more LiMA units into the copolymer chain.

Although the small shoulder in the -75°C curve at about 380°C (4% LiMA/MMA copolymer fig. V-5) might indicate that depolymerization is taking place before the reaction producing methanol, the shape of the TVA traces as the LiMA content increases in the copolymers, rather suggests that depolymerization is happening in competition with methanol formation and chain fragmentation (presence of products non-condensable at -196°C): the overlap of the curves corresponding to the different traps increases as the LiMA content increases in the copolymer chain.

The production of methanol, which can only originate from MMA units, indicates that the depolymerization of MMA segments in the chain will not be quantitative and must be inhibited by the presence of blocking structures (the nature of which will be discussed subsequently) in the chain.

THERMAL VOLATILIZATION ANALYSIS OF NaMA/MMA COPOLYMERS

TG/TVA traces for five NaMA/MMA copolymers having a NaMA content of 5%, 9%, 37%, 61% and 90% are shown in figures V-10, 11, 12, 13 and 14 respectively. The threshold temperatures and T_{\max} values for the two main decomposition reactions are listed in table V-3.

Table V-3

TVA data for NaMA/MMA copolymers

NaMA % in copolymers	Threshold temperatures($^{\circ}\text{C}$)	$T_{\max}^1(^{\circ}\text{C})$	$T_{\max}^2(^{\circ}\text{C})$
0	180	380	—
5	200	400	—
9	202	415	—
37	230	415	470
61	240	410	474
90	242	415	480
100	340	—	480

Here again the NaMA appears to be stabilizing the decomposition of the MMA units in the copolymers (the

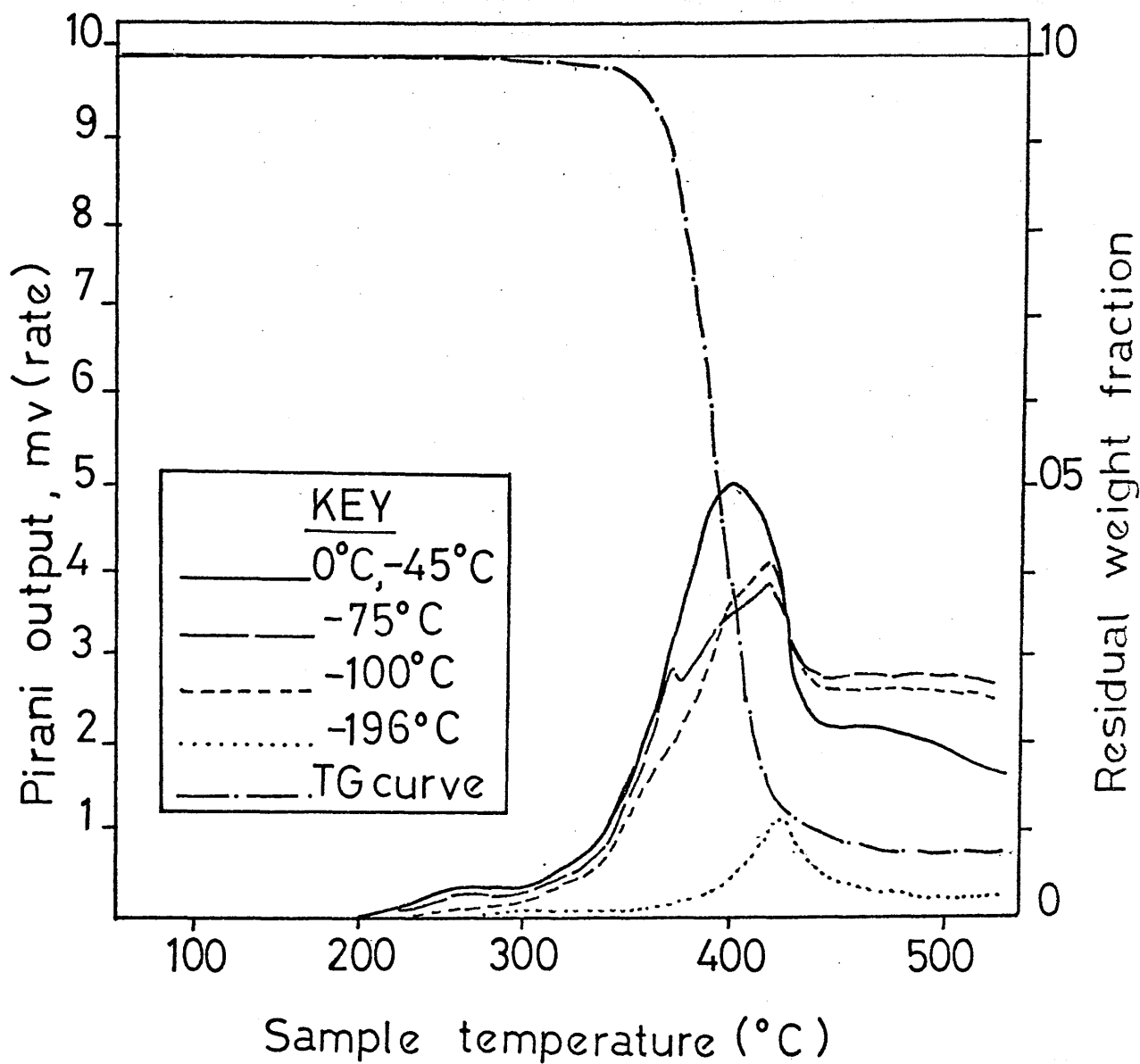


Fig. V-10

TG/ TVA FOR 5% NaMA/MMA COPOLYMER

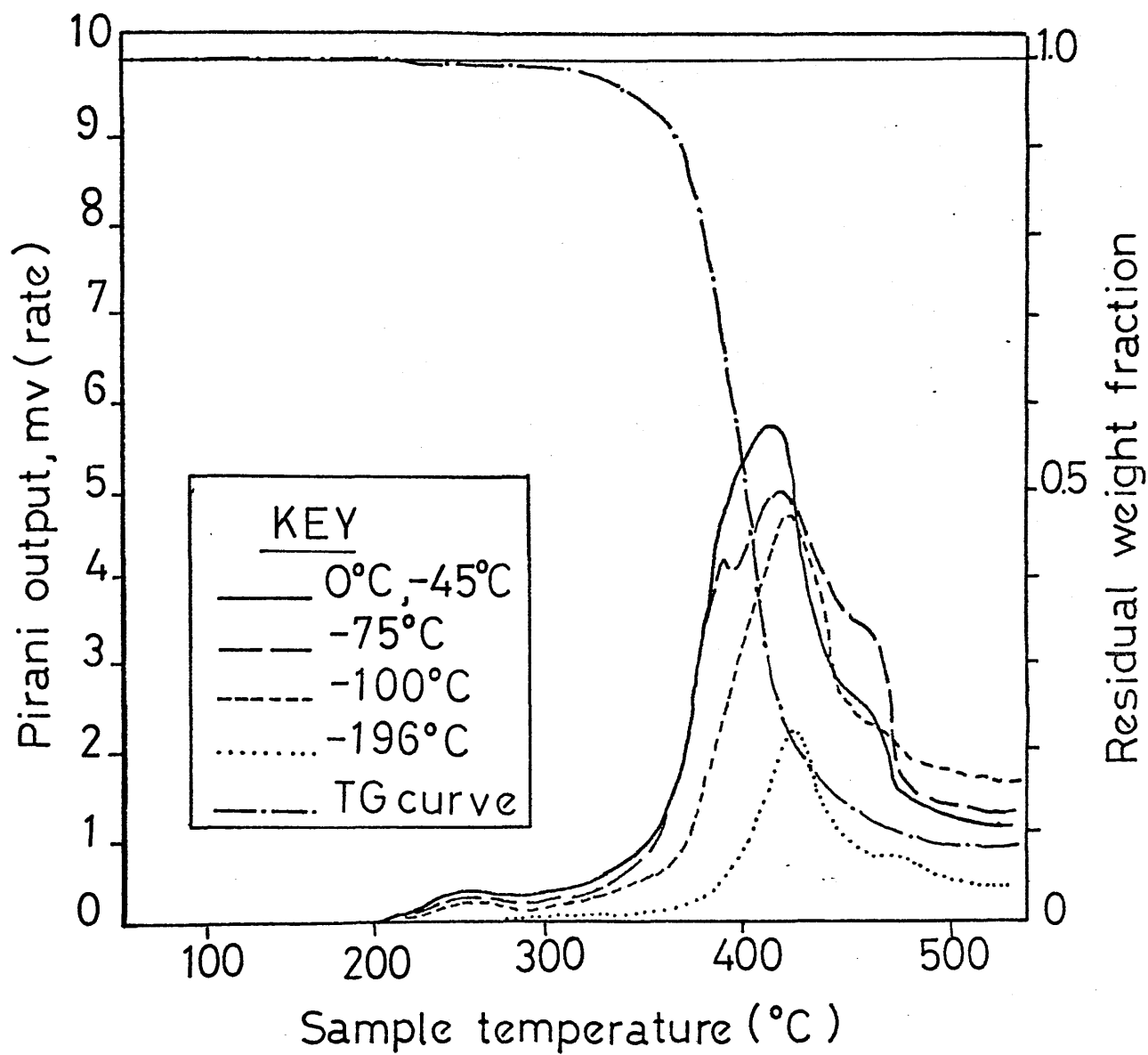


Fig. V-11

TG/TVA FOR 9%NaMA/MMA COPOLYMER

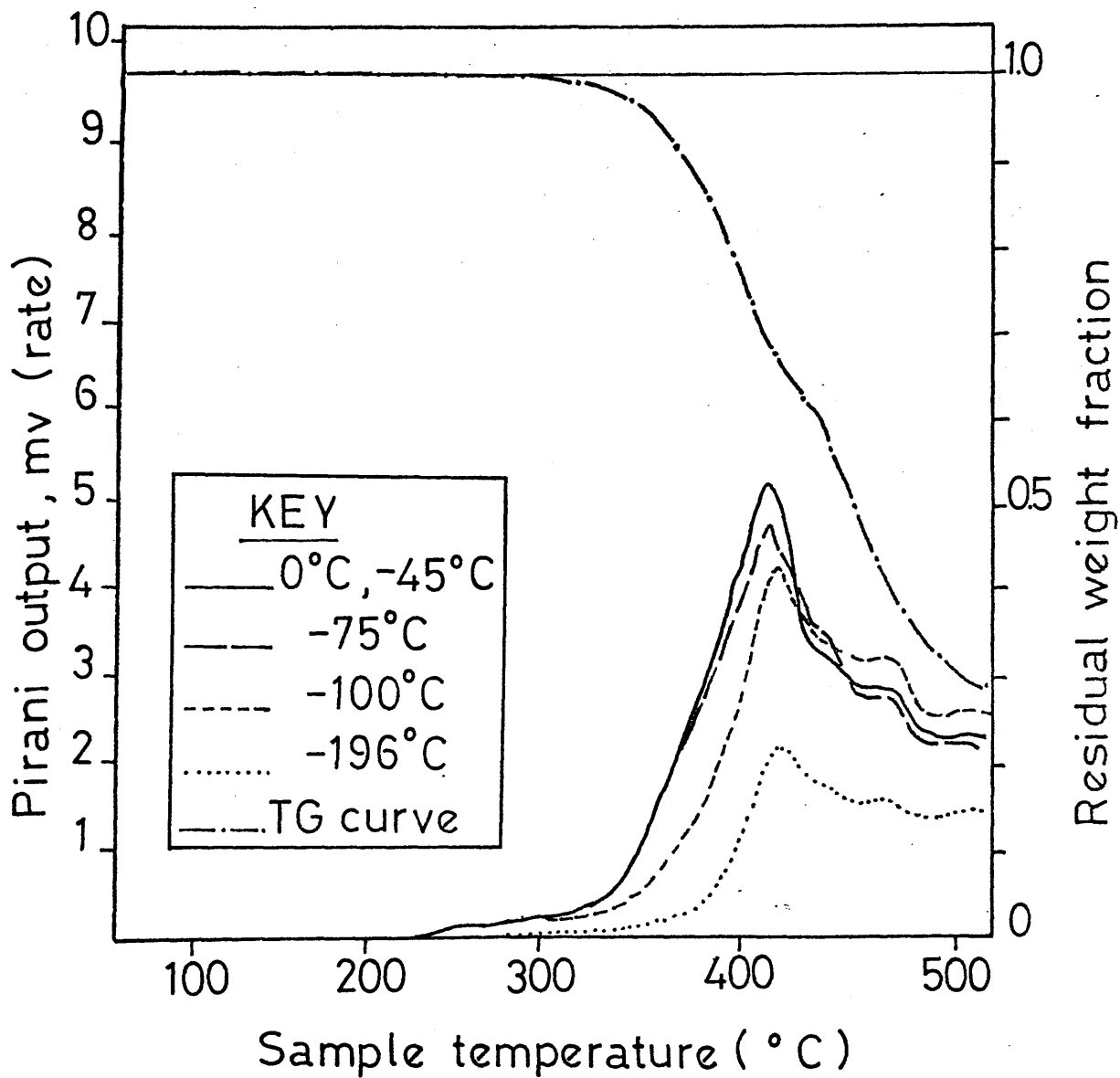


Fig. V - 12

TG/TVA FOR 37%NaMA/MMA COPOLYMER

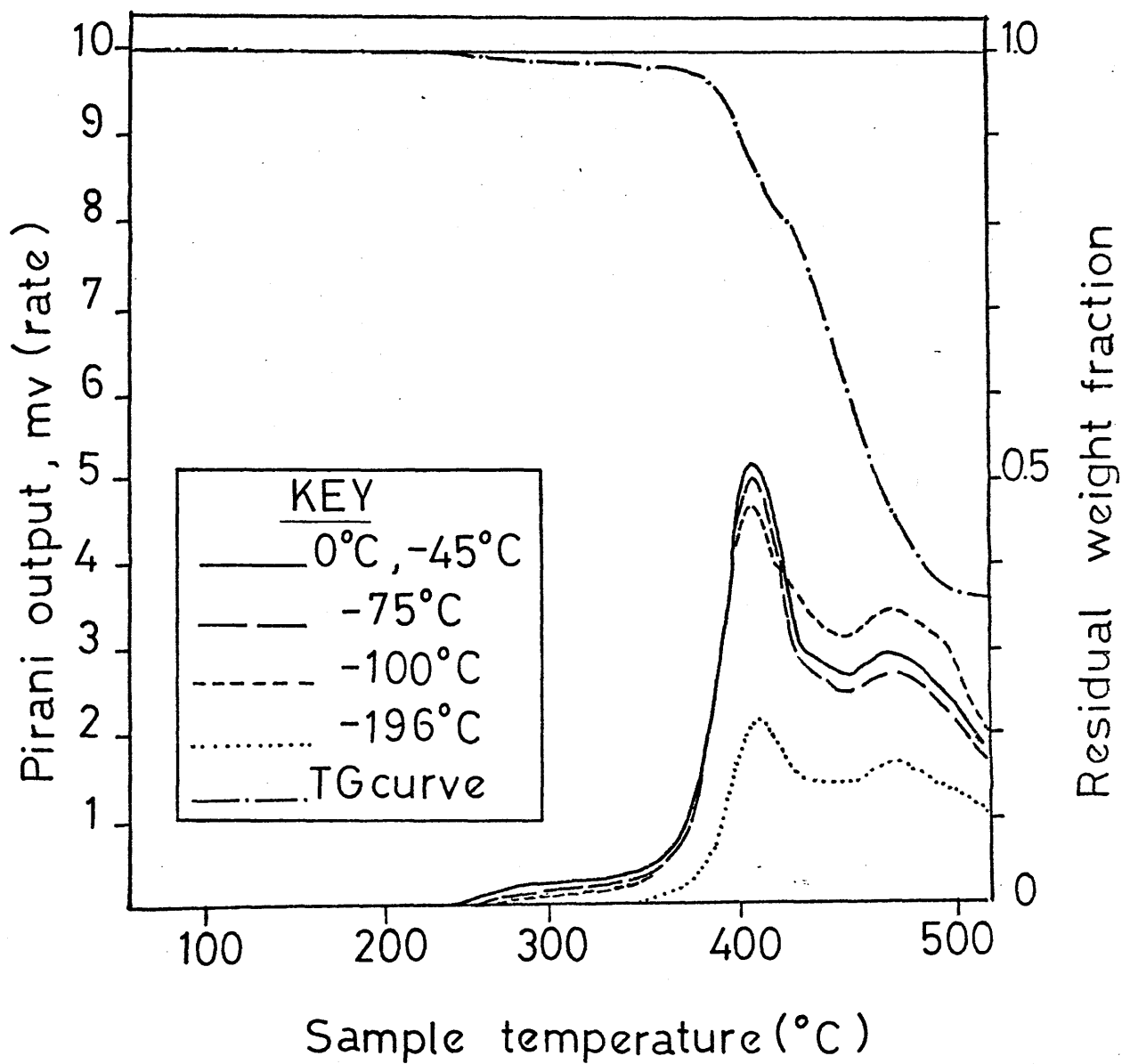


Fig. V-13

TG/TVA FOR 61%NaMA/MMA COPOLYMER

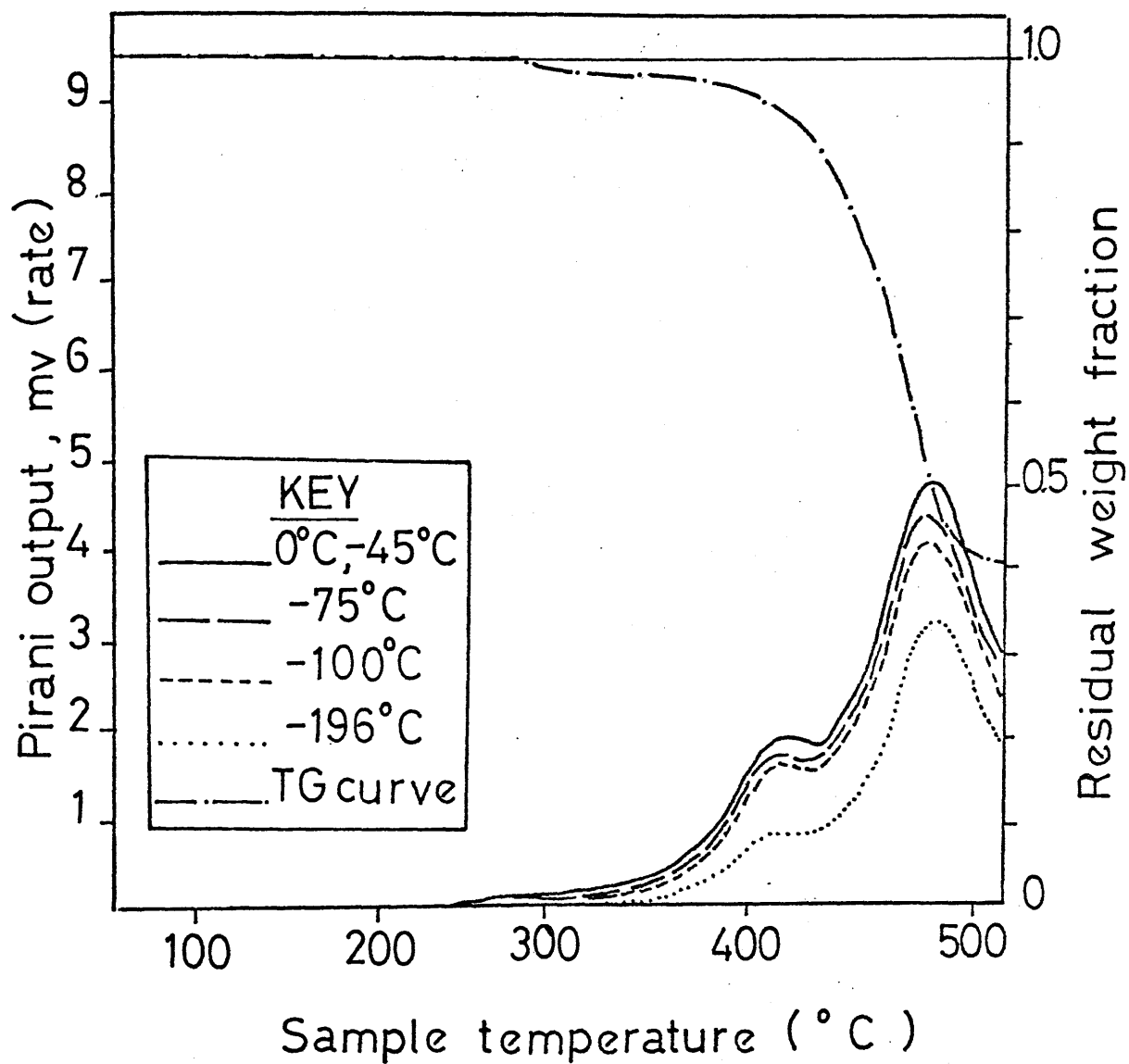


Fig. V-14

TG/TVA FOR 90% NaMA/MMA COPOLYMER

threshold temperatures and T_{\max}^1 values are all higher than for PMMA). Both MMA and methanol are produced in the first main peak as illustrated by the limiting rates in the -75°C and -100°C curves. However, two new and interesting features in the decomposition of these copolymers indicate some difference in the way in which LiMA/MMA copolymers decompose:

(i) The early low rate peak observed at about 330°C in the first two LiMA/MMA copolymers appears to be absent in the TVA curves of NaMA/MMA copolymers. This suggests that the NaMA/MMA copolymers may be of a higher molecular weight than the LiMA/MMA copolymers.

(ii) The -100°C limiting rate curve (showing the presence of methanol among the major products) again displaced by the second main reaction, is not only apparent in the 5% NaMA/MMA copolymer (which was not the case with the 4% LiMA/MMA copolymer), but also continues after the limiting rate of MMA in the -75°C curves has ceased, as observed in figures V-12 and 13. This clearly indicates that the evolution of methanol from the NaMA/MMA copolymer is more important than in the case of the LiMA/MMA copolymer; and this again leads to the conclusion that the inhibition of depolymerization of MMA units will be more pronounced in the NaMA/MMA copolymers as compared with the case of the LiMA/MMA copolymers. This inhibition will probably be the

result of a higher blocking group content in the copolymer chains during depolymerization.

THERMAL VOLATILIZATION ANALYSIS OF KMA/MMA COPOLYMERS

TG/TVA traces for five KMA/MMA copolymers containing 9%, 21%, 50%, 75% and 92% KMA in the chain are shown in figures V-15, 16, 17, 18 and 19. The main characteristics are again similar to those of the NaMA/MMA copolymers:

(i) Stabilization of the MMA breakdown (see table V-4 for threshold temperatures and T_{\max} values).

Table V-4

TVA data for KMA/MMA copolymers

KMA % in copolymers	Threshold temperature($^{\circ}\text{C}$)	$T_{\max}^1(^{\circ}\text{C})$	$T_{\max}^2(^{\circ}\text{C})$
0	180	380	—
9	200	408	493
21	232	408	498
50	218	405	495
75	210	398	497
92	200	398	484
100	320	—	475

(ii) Absence here again of MMA monomer produced by chain end initiation, indicating that KMA/MMA copolymers are of a higher molecular weight than LiMA/MMA

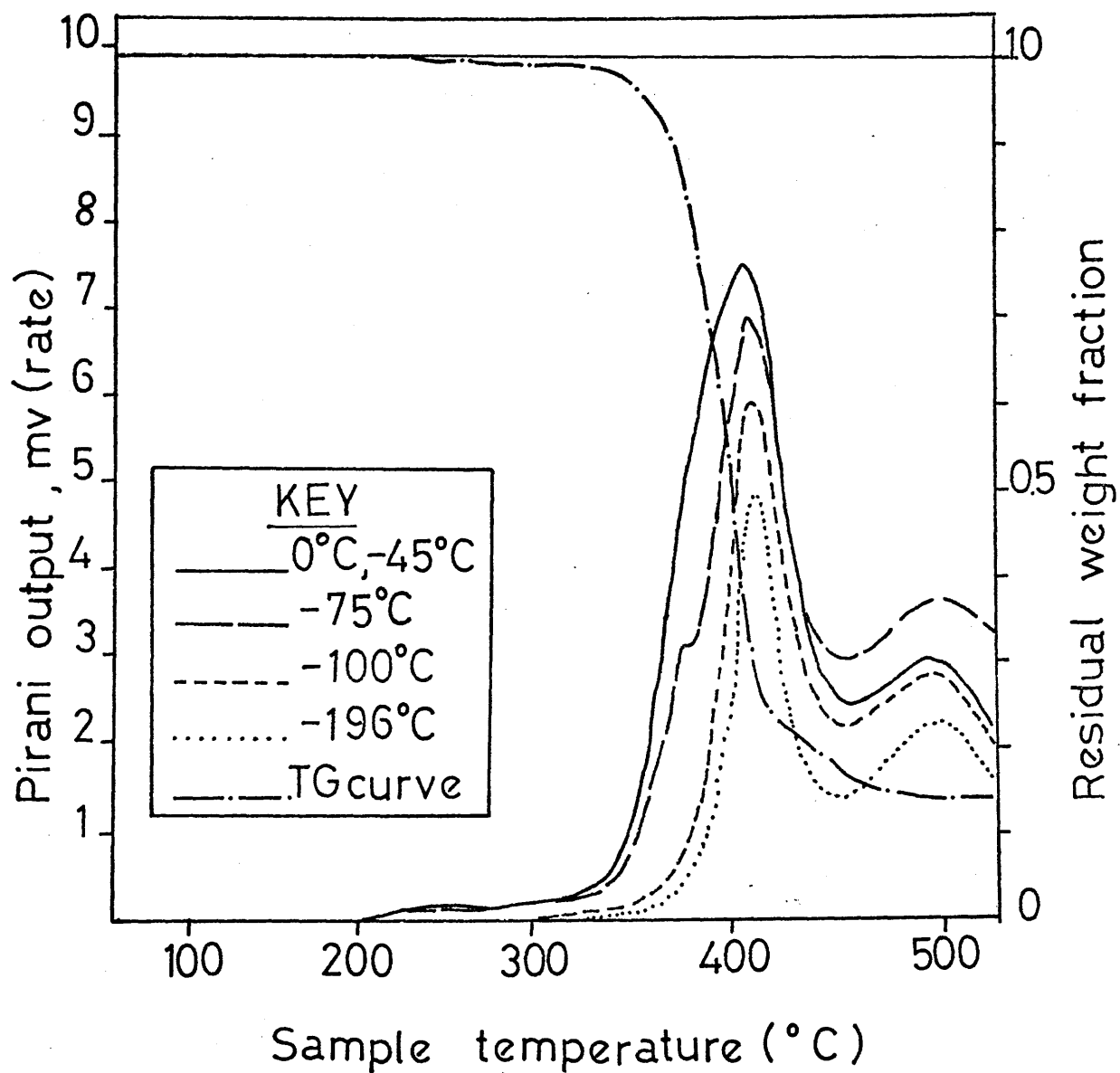


Fig. V-15

TG/ TVA FOR 9%KMA /MMA COPOLYMER

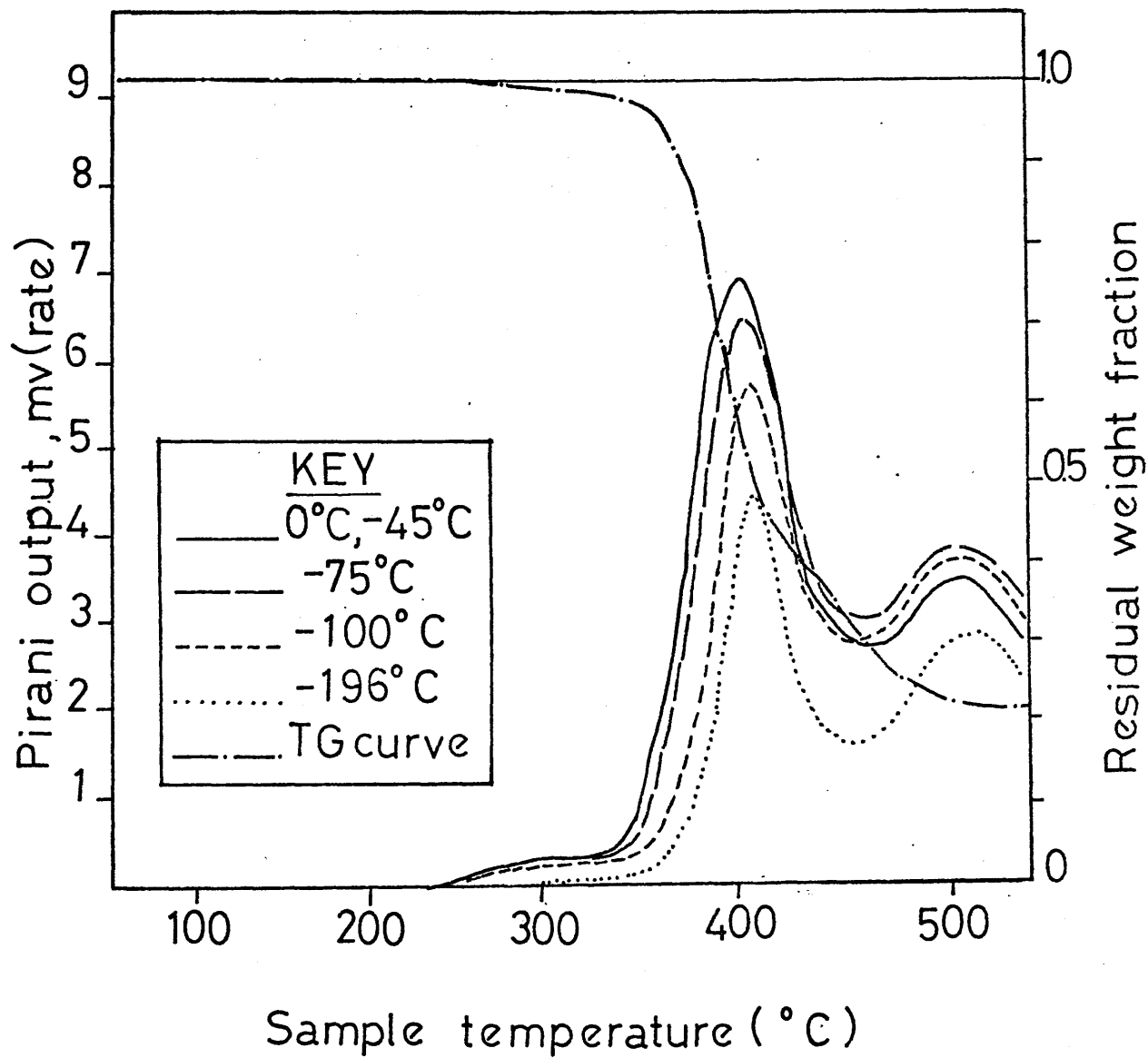


Fig. V-16

TG/ TVA FOR 21%KMA/ MMA COPOLYMER

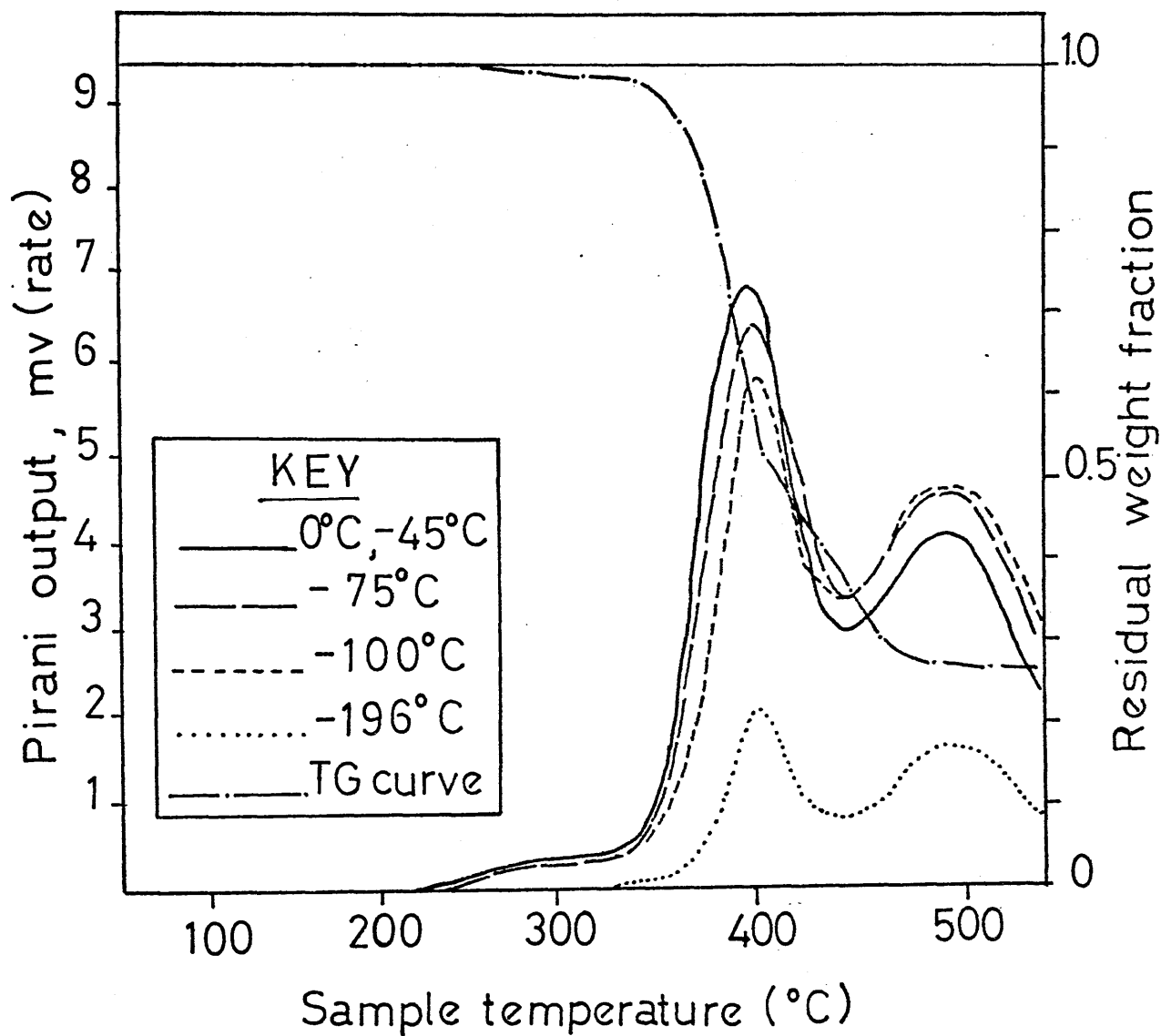


Fig. V-17

TG/TVA FOR 50% KMA/MMA COPOLYMER

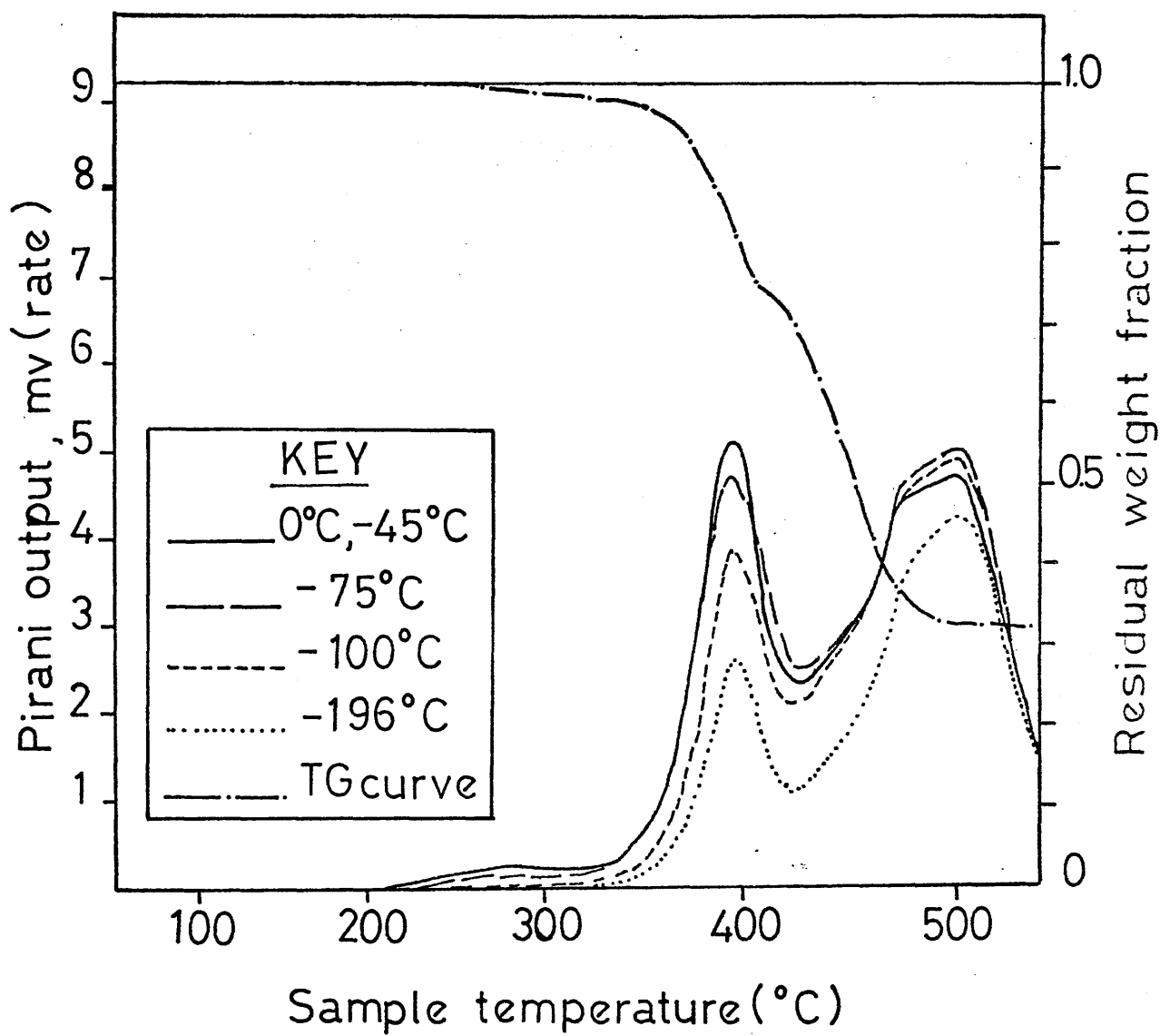


Fig. V-18

TG/TVA FOR 75% KMA/MMA COPOLYMER

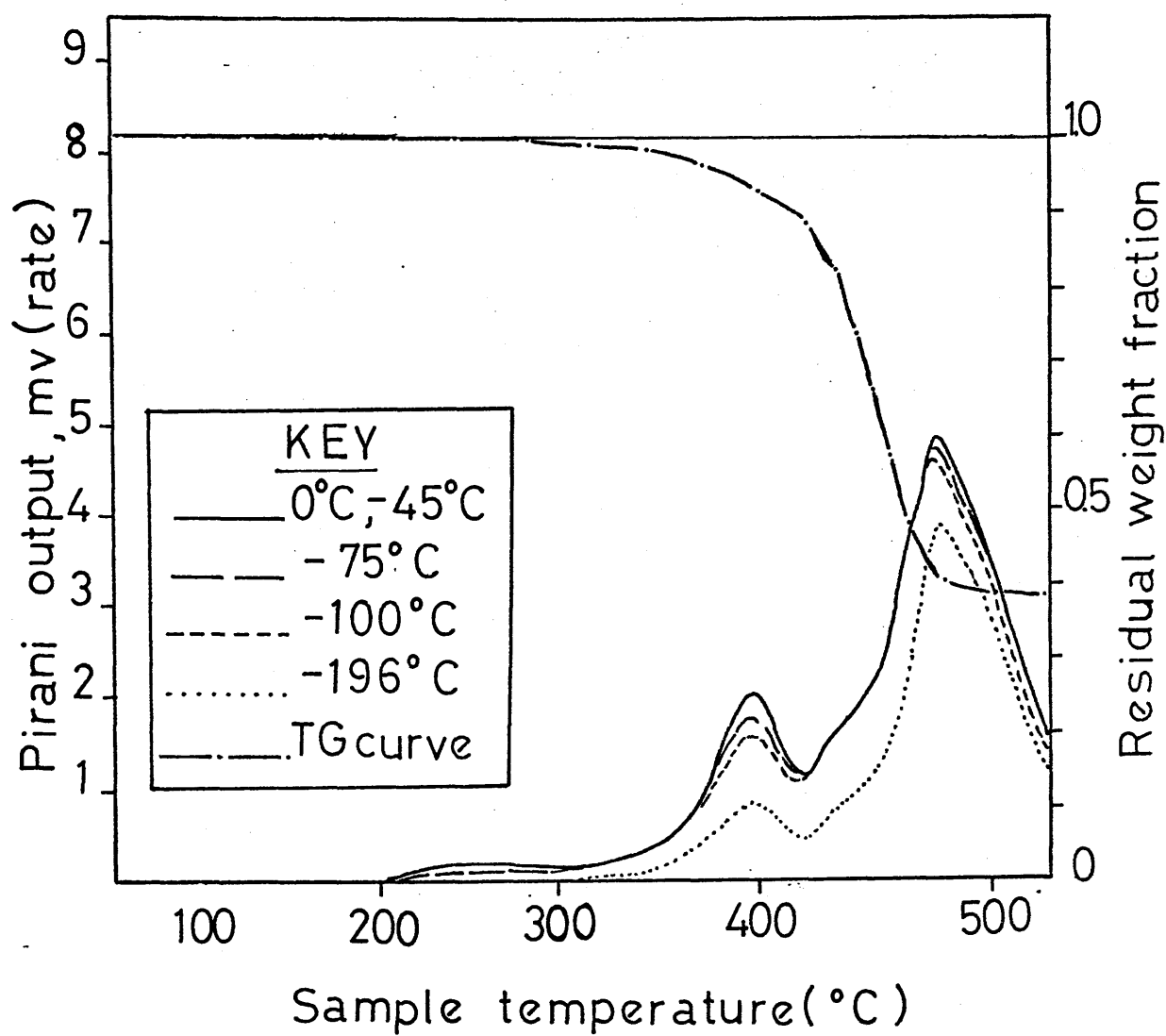


Fig. V-19

TG/TVA FOR 92%KMA/MMA COPOLYMER

copolymers.

(iii) Both -75°C and -100°C curves show limiting rate effects indicating methanol and methyl methacrylate as major degradation products.

In fig. V-17, the -100°C limiting rate is displaced by the second main reaction to a higher rate than the -75°C limiting rate curve, hence the production of methanol in KMA/MMA copolymers is more important than in the LiMA/MMA copolymers and probably more important than in the NaMA/MMA copolymers as well. And the reason to this would be the overlap of the five cold trap curves in the first peak, indicating that in the case of the KMA/MMA copolymers, methanol is produced in real competition with depolymerization, whereas in the cases of the two previous series of copolymers the maxima of the cold trap curves occurs at different temperatures, indicating that the competition of methanol production with depolymerization takes place at a later stage (i.e. higher temperature).

In the light of this difference we can predict an even higher yield of methanol from KMA/MMA copolymers as compared to both previous series of copolymers.

In the same way, as explained in the previous cases, the inhibition factor to depolymerization in KMA/MMA copolymers will play a more important role than in LiMA/MMA and NaMA/MMA copolymers.

THERMOGRAVIMETRIC ANALYSIS OF THE COPOLYMERS

The TG curves confirm distinctly the two main stages of degradation of the copolymer and the stabilization of the MMA segments decomposition.

Furthermore, all copolymers leave a black residue increasing in weight with the alkali metal salt content in the chain, a result which is expected since the degradation of PMMA gives no residue whereas that of poly(alkali metal methacrylates) leaves a residue (see table V-5).

Table V-5

Weight % of residues from degradation of copolymers of MMA with alkali metal methacrylates. Data obtained by TGA under vacuum at 500°C.

LiMA % in copolymers	Weight % of residue	NaMA % in copolymers	Weight % of residue	KMA % in copolymers	Weight % of residue
0	0	0	0	0	0
4	12	5	7	9	14
20	16	9	8	21	22
38	20	37	28.5	50	27
52	29	61	36	75	33
91	33	90	40	92	38
100	36	100	43	100	33

DIFFERENTIAL THERMAL ANALYSIS OF THE COPOLYMERS

DTA curves for all the samples are very similar, the main endotherms changing only in size with the copolymer composition. As an illustration, DTA curves (see experimental conditions: chapter II) for PMMA, PKMA and a 50% KMA/MMA copolymer are shown in fig. V-20.

PMMA has a small endotherm around 110°C which is close to the glass transition temperature of 104°C ,⁽¹²⁰⁾ and a large endotherm beginning around 305°C , preceded by a small endothermic shoulder at 280°C , both of which are due to depolymerization of PMMA to monomer.

PKMA has a large and broad endotherm around 150°C associated with the loss of water taken up from the atmosphere. At around 460°C the endothermic system becomes complex during the fragmentation of the chain concurrent with depolymerization. The complexity of the endothermic system is probably due to further decomposition of monomer and metal isobutyrate which cannot sublime out of the polymer sample except under vacuum (the experiments were run under a dynamic nitrogen atmosphere).

The 50% KMA/MMA copolymer also shows a broad endotherm around 120°C corresponding to the loss of absorbed water; the endotherm around 280°C is believed to be due to the melting of the copolymers. The endotherm starting around 330°C is associated with depolymerization of MMA segments

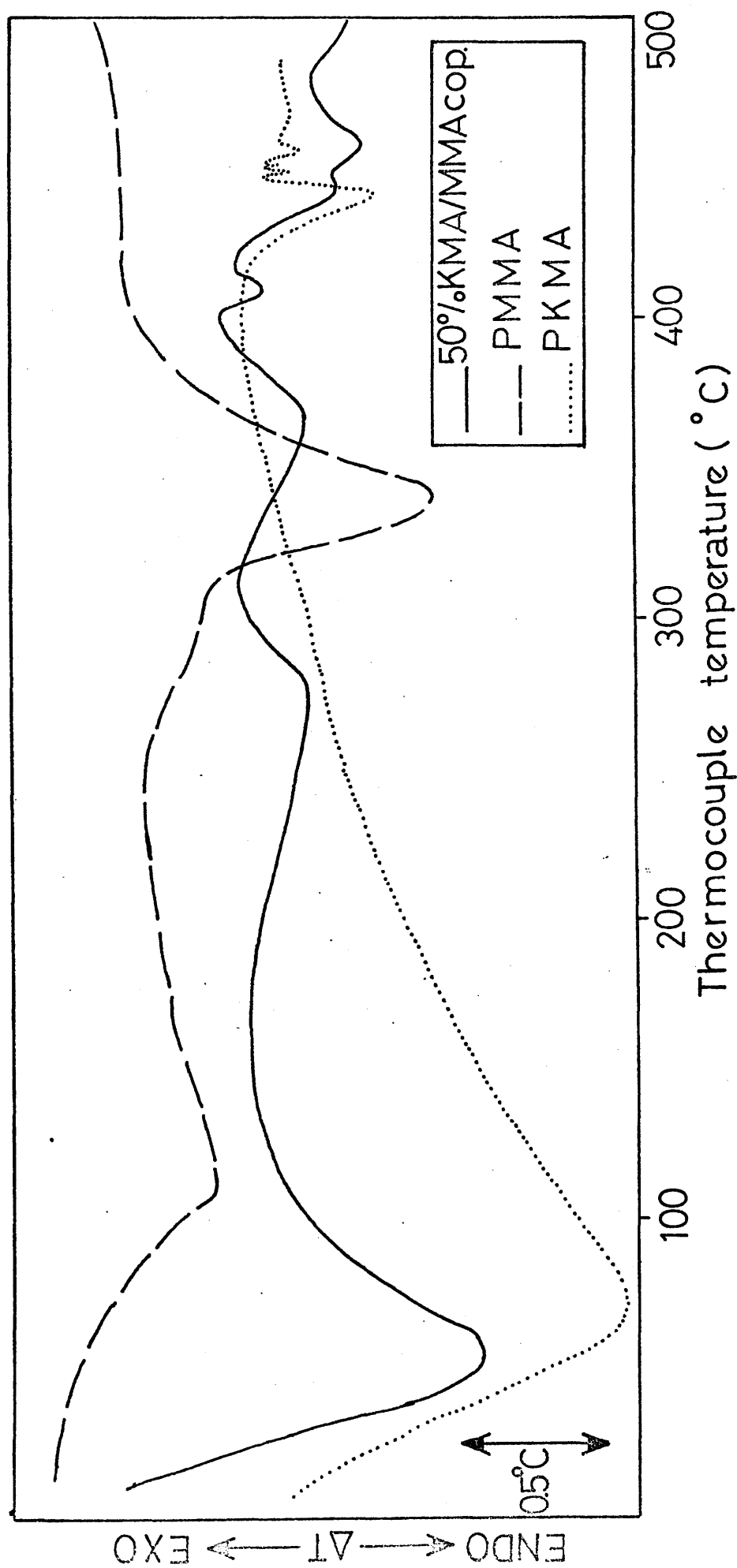


FIG. V-20

DTA CURVES FOR PMMA (— — —), 50% KMA/MMA COPOLYMER (———), AND PKMA (.....).
HEATING RATE: 10°C/MIN.; NITROGEN FLOW: 70ml/MIN.

in competition with methanol production and chain fragmentation. The small endotherm at about 420°C could be attributed to further decomposition of methyl methacrylate and methacrylic acid chain fragments which would have condensed in the cold ring fraction during normal degradation under vacuum. Finally, the complex endothermic system observed beyond 450°C is again associated with the decomposition of the remaining KMA units in the chain.

In conclusion, the DTA curve of the 50% KMA/MMA copolymer illustrates again both the stabilization of PMMA breakdown by copolymerization, and the inhibition of the depolymerization of MMA segments (compare the position and the size of the depolymerization endotherm in the copolymer relatively to that of PMMA).

VOLATILES ANALYSIS

The analysis of the volatile products was carried out using the techniques described in chapter II. Samples of 100mg in powder form were degraded in vacuo up to 500°C at the heating rate of 10°C/min.

INFRA RED ANALYSIS OF THE TOTAL VOLATILES

Infra red analysis of the total products (condensable at -196°C) from poly(alkali metal methacrylates) allows the identification of the reported ketones, ⁽⁹⁴⁾ carbon dioxide and alkenes (see fig. V-21 and table V-6 for

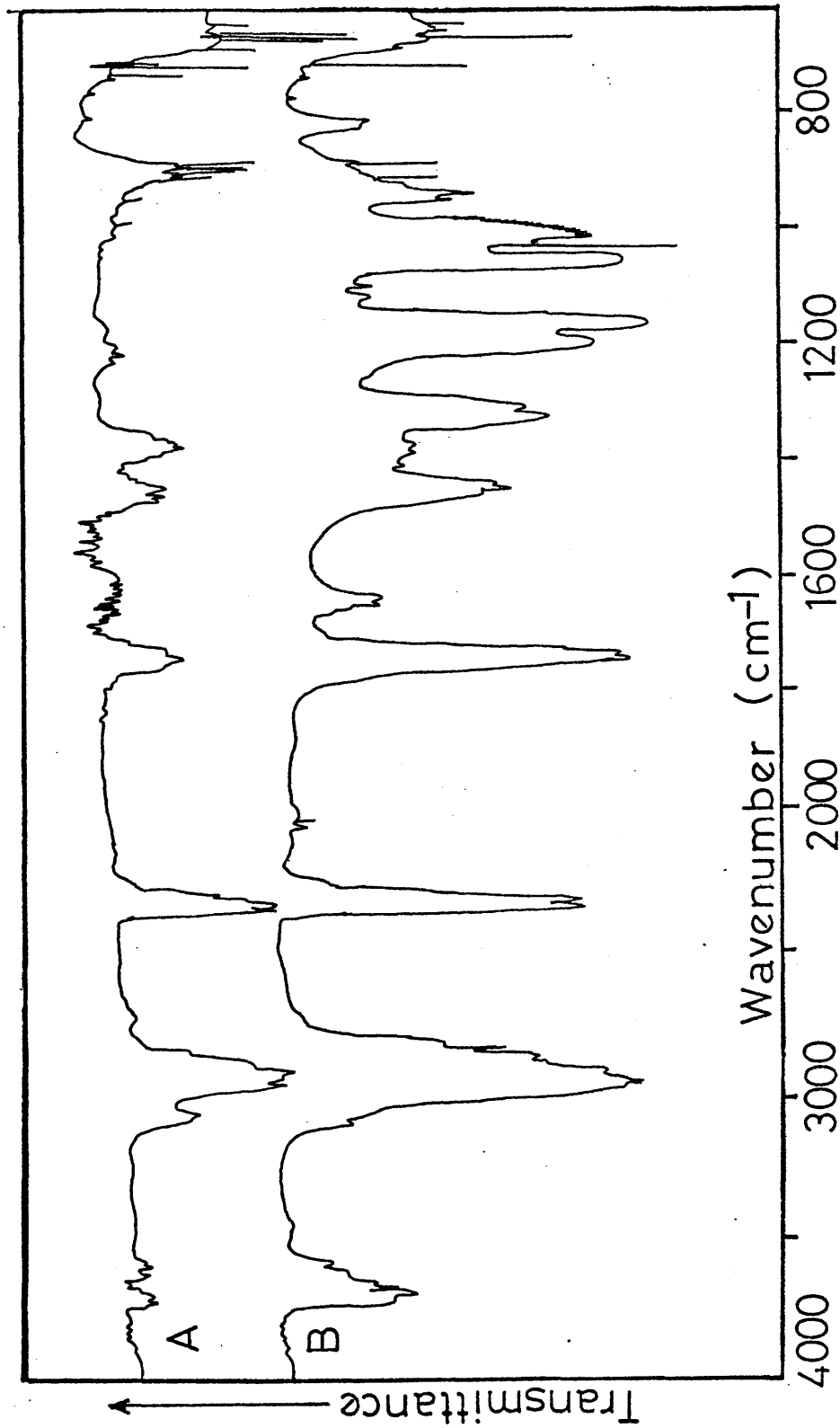


FIG. V-21: COMPARISON BETWEEN IR SPECTRA IN THE GAS PHASE OF THE TOTAL CONDENSABLE

(AT -196°C) PRODUCTS FROM PROGRAMMED DEGRADATION TO 500°C OF.: (A) PLiMA, (B) 41%

LiMA/MMA COPOLYMER.

Table V-6

Assignment of IR peaks from degradation
of PLiMA (see fig. V-21)

<u>Frequency (cm⁻¹)</u>	<u>Mode of vibration</u>	<u>Compound or functional group</u>
3600 -3720	O=C=O overtone combinations	Carbon dioxide
3080	C—H stretching (asymmetric)	>C=CH_2
2845 - 2965	C—H stretching	CH ₃ , CH ₂ , CH
2340	C=O stretching	Carbon dioxide
1745 (broad)	C=O stretching	Carbonyl
1640 - 1670	C=C stretching	Carbonyl
1445 - 1465	>C—H deformation	Carbonyl
1385 (broad)	—CH ₃ symmetrical deformation	—CH ₃
1215 - 1170	C—C—C skeletal $\begin{array}{c} \text{O} \\ \parallel \end{array}$	Ketones
993	C—H out of plane deformation	Propene
950	C—H out of plane deformation	Ethylene
912	C—H out of plane deformation	But-1-ene
900	C—H out of plane deformation	?
890	C—H out of plane deformation	Isobutene
734	C—H out of plane deformation	Acetylene
722	C—O bending	Carbon dioxide
694	C—H bending	Toluene
675	C—H bending	Benzene
669	C—O bending	Carbon dioxide

IR spectrum and assignment of peaks). Degradation in a closed system allows also the identification of methane and carbon monoxide.

The IR spectrum of the total volatiles (condensable at -196°C) from a 41% LiMA/MMA copolymer is also shown in fig. V-21. It shows not only the presence of the products expected from PLiMA but also, in great abundance, methyl methacrylate monomer and methanol, and in trace amounts some dimethyl ether (1116, 1103 and 1091 cm^{-1}). Note that due to the overlap of the carbonyl absorptions from MMA and ketones it is not possible to assess the specific presence of ketones from the IR spectrum of the copolymer degradation products.

It is also clear from fig. V-21 that the production of carbon dioxide is much greater in the copolymer than from PLiMA.

Again here, the degradation of the same copolymer in a closed system allows the identification of an appreciable amount of methane and carbon monoxide, both produced in greater abundance than from PLiMA.

These qualitative results were observed for the three series of copolymers in comparison with the corresponding polyelectrolyte homopolymers.

LIQUID PRODUCTS ANALYSIS BY GAS LIQUID CHROMATOGRAPHY

The total liquid products obtained from programmed

degradation of 100mg samples of copolymer to 500°C were separated and identified by GLC under the conditions described in chapter II, using a six foot long and $\frac{1}{8}$ inch diameter column containing 13.5% MBEA and 6.5% di-2-ethyl-hexyl sebacate on Chromosorb P, 80-100 mesh, under isothermal conditions. The GLC trace of the total liquid degradation products from a 70% LiMA/MMA copolymer is shown in fig. V-22 and the assignment of the products is given in table V-7. The early small peaks observed before peak n^o1 on the chart are believed to correspond to gaseous products dissolved in the liquid fraction and to the presence of traces of air from the injection syringe.

The products reported by McNeill and Zulfiqar⁽⁹⁴⁾ were found to be present in small amounts (see table V-7), indicating that the alkali metal methacrylate segments do decompose independently to some extent. But two other products are also present: MMA and methanol and both are by far the major products in the liquid fraction of the products. Note that most of these products were also identified by mass spectrometry.

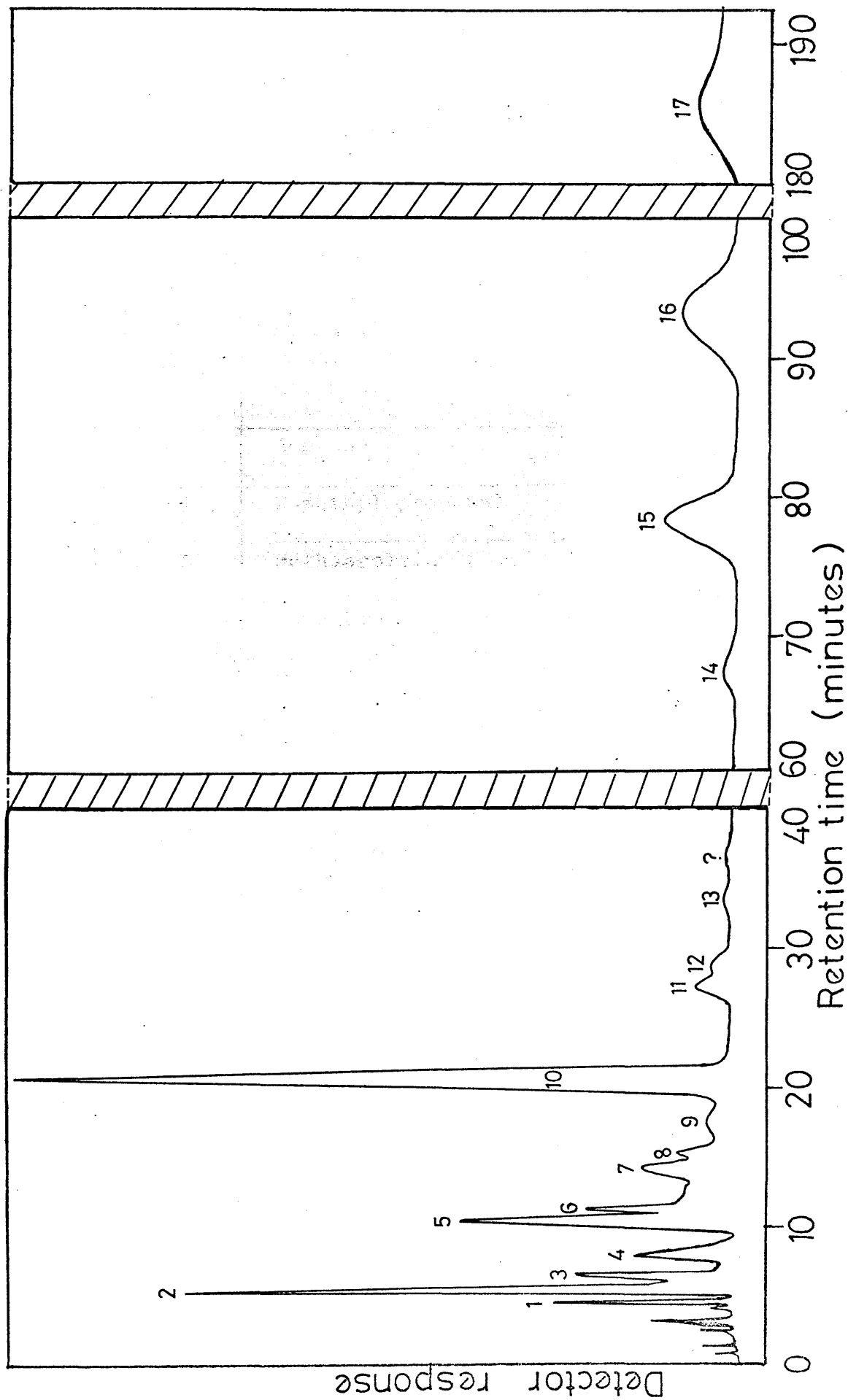


FIG. V-22 : GLC ANALYSIS OF THE LIQUID DEGRADATION PRODUCTS FROM 70% LiMA/MMA COPOLYMER. COLUMN TEMPERATURE : 70°C ; HELIUM CARRIER GAS : 35 ml/MIN.

Table V-7

Assignment of liquid products from the
GLC trace shown in fig.V-22

Peak N ^o	Name of product
1	Propanal
2	Methanol
3	Acetone
4	2-methyl propanal
5	Methacrolein
6	Butanal
7	Methyl ethyl ketone
8	Methyl isopropyl ketone
9	Methyl isopropenyl ketone
10	Methyl methacrylate
11	Methyl prop-2-enyl ketone
12	Toluene
13	Di-isopropyl ketone
14	Cyclopentanone
15	2-methyl cyclopentanone
16	2,5-dimethyl cyclopentanone
17	2,5-dimethyl cyclopent-3-enone

COLD RING FRACTION (CRF) ANALYSIS

All copolymers gave a cold ring fraction having a colour ranging from light brown (in the composition region of the copolymer where MMA predominates) to white (in the region of high alkali metal methacrylate content).

Infra red spectra in the solid state (KBr discs) of the cold ring fraction from a 25% LiMA/MMA copolymers are compared in fig. V-23 with solid state IR spectra from LiMA monomer and lithium isobutyrate. PLiMA, PNaMA and PKMA all give monomer and metal isobutyrate in the cold ring fraction, as reported by McNeill and Zulfiqar; the copolymers were also found to give a CRF containing mainly electrolyte monomer and metal isobutyrate, even from the copolymers having a low composition of metal methacrylate in the chain (see fig. V-23). But in the IR spectra of cold ring fractions from all copolymers, two shoulders at 1695 and 1725 cm^{-1} are also apparent. They both indicate the presence in the CRF of some MMA and MAA chain fragments. The evidence for these chain fragments is clearer if these are isolated from the rest of the CRF by dissolution in CCl_4 and observed by infra red analysis in the liquid form (see fig. V-24). The light brown colouration of the cold ring is believed to be due to the presence of these MMA and MAA chain

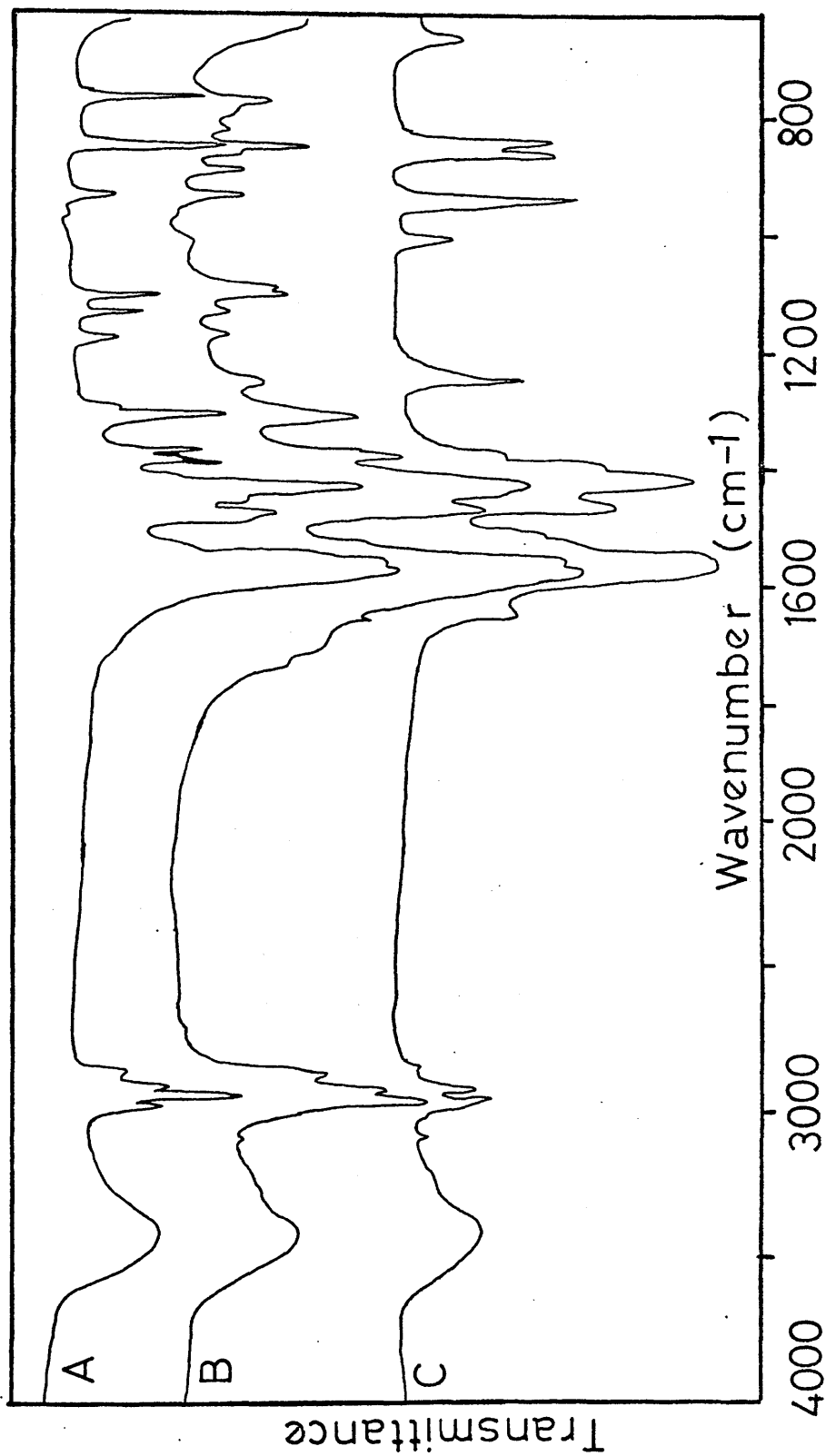


FIG. V-23

INFRARED SPECTRA IN KBr DISCS OF : (A) : LITHIUM ISOBUTYRATE, (B) : CRF FROM DEGRADATION OF 25% LiMA/MMA COPOLYMER, (C) : LITHIUM METHACRYLATE MONOMER.

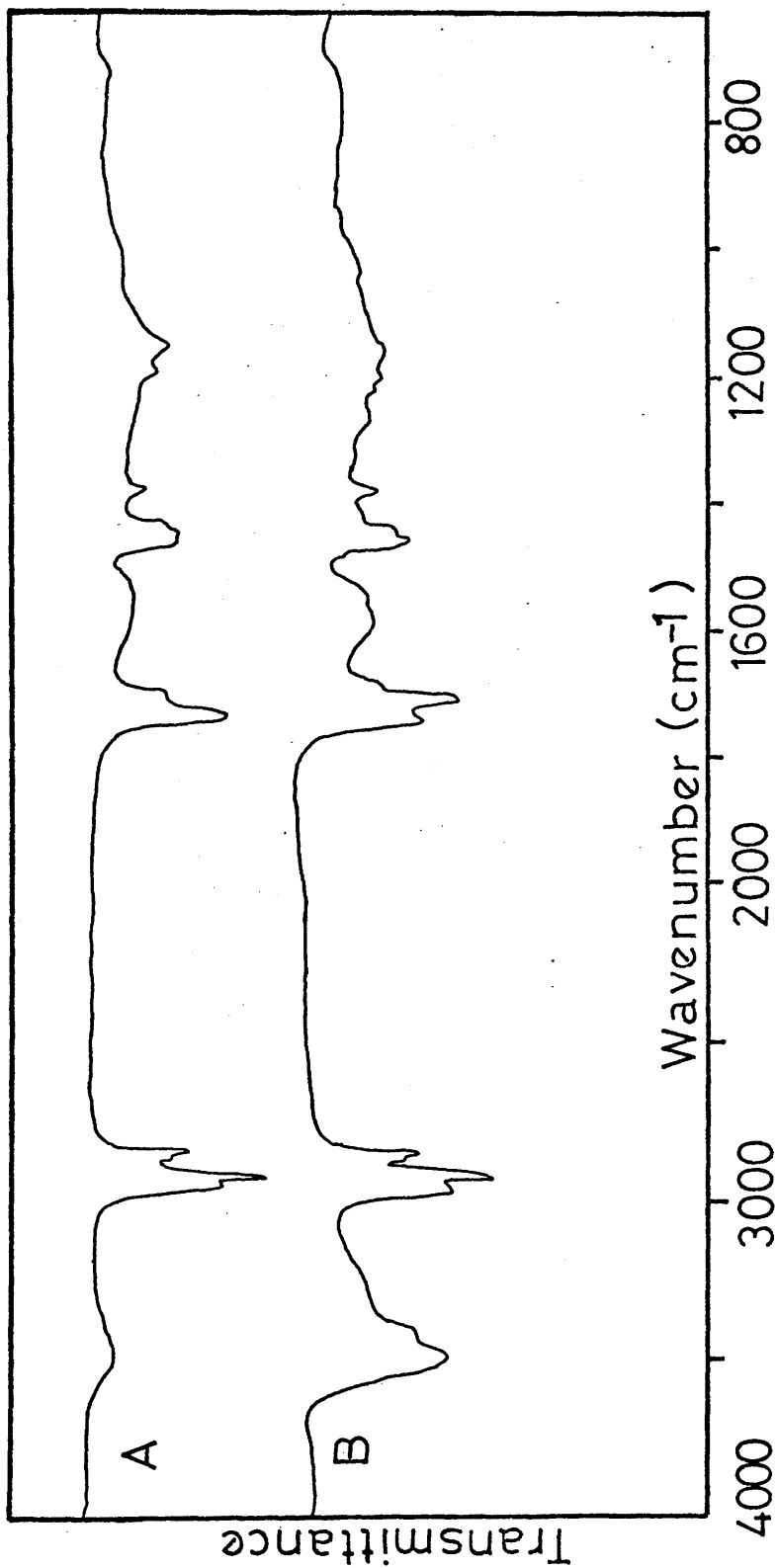


FIG. V-24

INFRARED SPECTRA FOR FRACTION OF CRF SOLUBLE IN CCl₄, FROM DEGRADATION OF :
(A) : 25% LIMA/MMA COPOLYMER, (B) : 25% KMA/MMA COPOLYMER.

fragments. It was also observed that the ratio of MAA to MMA chain fragments was increased as the size of the metal ion increased at any particular copolymer composition (see example of fig. V-24). This will be explained subsequently.

RESIDUE ANALYSIS

Infra red spectroscopy was again used to investigate the contents of the black residues obtained from programmed degradation of the copolymers at 500°C.

The spectra were all similar to those of the residues from poly(alkali metal methacrylates), showing the presence of metal carbonates and charcoal (see fig. V-25).

STRUCTURAL CHANGES DURING DEGRADATION

A 38% KMA/MMA copolymer sample was heated isothermally at 300°C in vacuo for different lengths of time and both products and residue were examined step by step. The structural changes in the copolymer chain are shown in fig. V-26.

Heating for five minutes results in the appearance of three new absorptions at 1800, 1758 and 1020 cm^{-1} in the IR spectrum of the residue. These bands are in close agreement with the peak values obtained⁽¹²¹⁾ for the six-membered ring glutaric anhydride (1802, 1765 and the C—O—C absorption at 1022 cm^{-1}). The

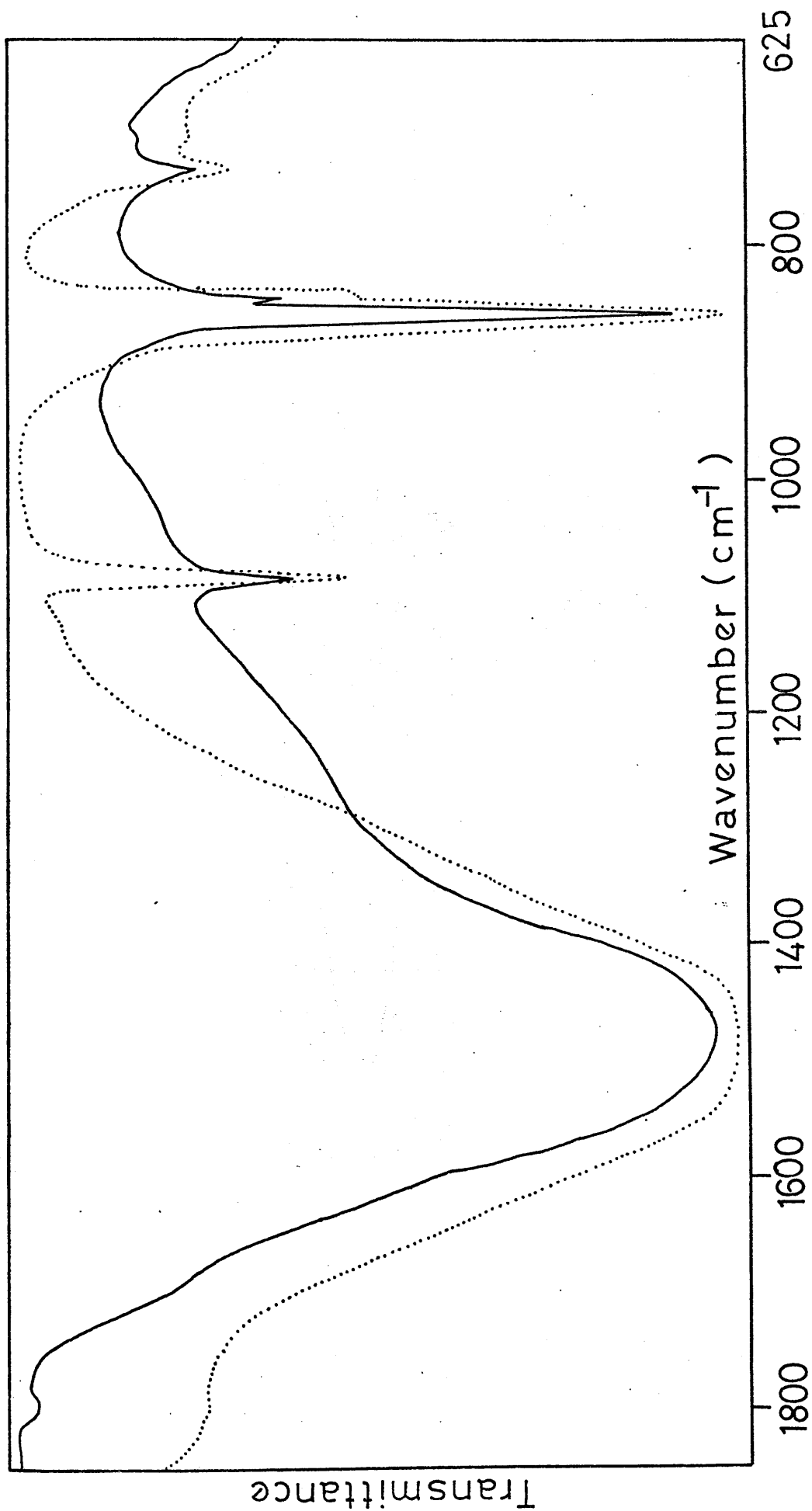


FIG. V-25

INFRA RED SPECTRA IN KBr DISCS OF : (.....) BLACK RESIDUE FROM PROGRAMMED DEGRADATION TO 500°C OF LiMA/MMA COPOLYMERS, (——) ANALARD LITHIUM CARBONATE.

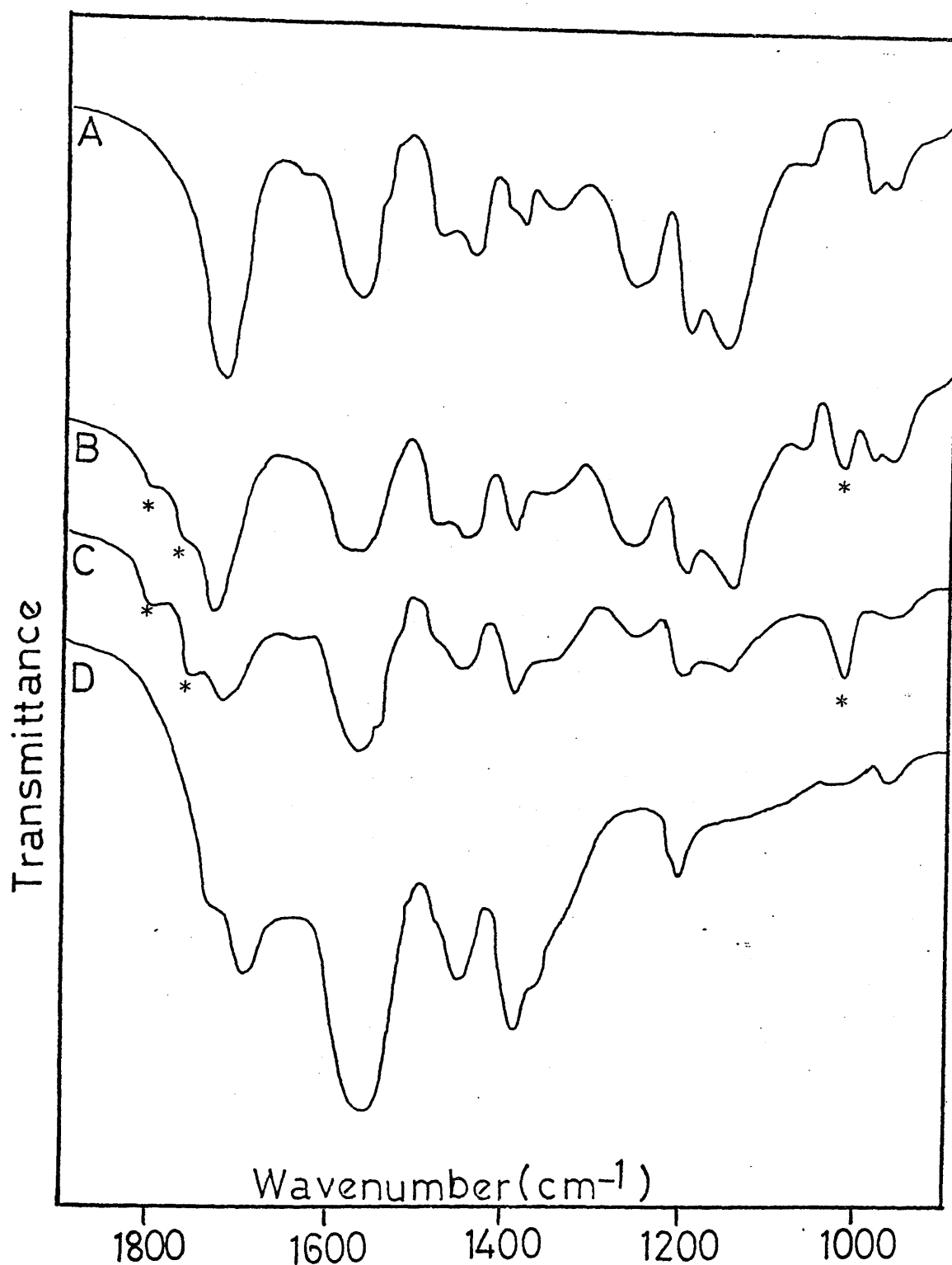


FIG. V-26

IR SOLID STATE SPECTRA FOR 38% KMA/MMA COPOLYMER : (A) :
NORMAL, (B) : HEATED ISOTHERMALLY AT 300°C FOR 5 MINUTES,
(C) : HEATED ISOTHERMALLY AT 300°C FOR 30 MINUTES, (D) :
HEATED ISOTHERMALLY AT 300°C FOR 7 HOURS.

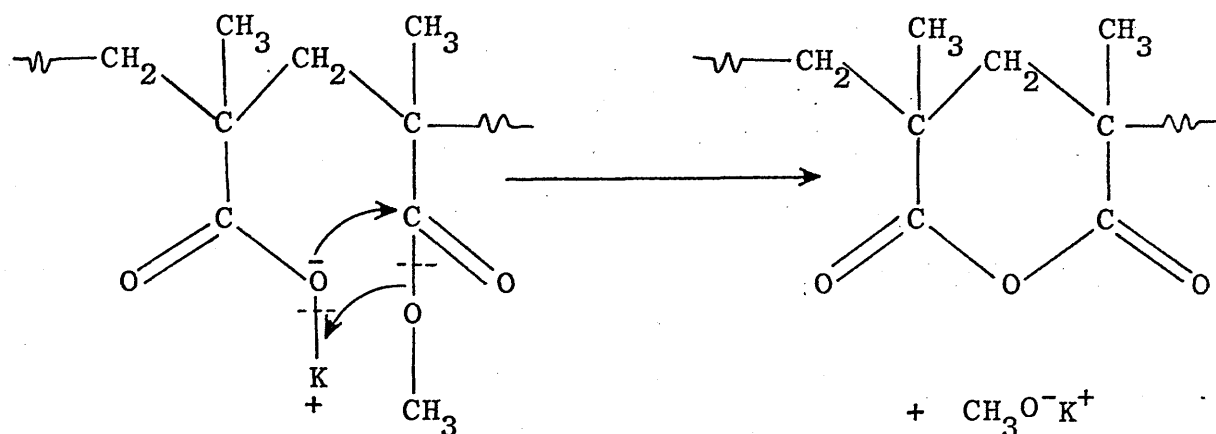
products are methyl methacrylate from depolymerization and methanol.

Further heating for thirty minutes results in the formation of more anhydride in the residue (see fig. V-26) which becomes yellowish, and more MMA and methanol is observed in the volatile fraction.

Analogous observations were made by McNeill and Jamieson⁽⁷¹⁾ during the degradation of MMA/MAA copolymers (methanol elimination in these copolymers takes place between two adjacent MAA and MMA units, leaving a six membered ring anhydride structure in the chain). In the KMA/MMA copolymers, however, the production of methanol can only be explained if:

(i) The copolymers contain an appreciable amount of methacrylic acid units in the chain, which is highly unlikely (see chapter III):

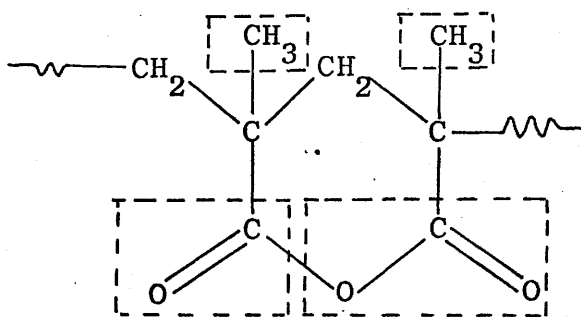
(ii) An intermediate product like potassium methoxide (possibly eliminated between two adjacent MMA and KMA units in the chain and leaving the anhydride structure), is at the origin of the methanol formation perhaps by a further reaction with MMA units, a reaction which still needs to be clarified;



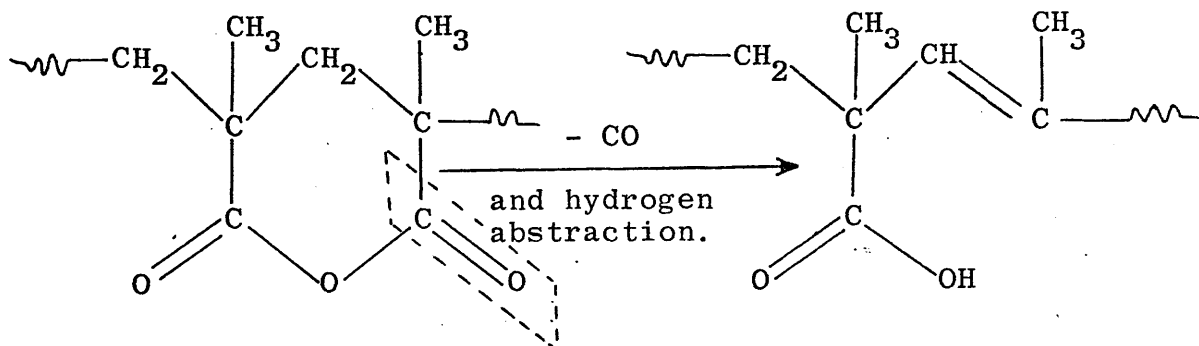
(iii) If methanol is produced from the decomposition of pendant ester groups.

The origin of methanol will be given more detailed attention subsequently (chapter VI).

Further heating at 300°C of the 38% KMA/MMA copolymer for a longer time results in the formation of MMA monomer and methanol plus carbon dioxide, carbon monoxide, methane and alkenes, these last products probably originating from the decomposition of anhydride structures and the start of the chain fragmentation:



After seven hours of isothermal heating at 300°C, no more volatiles are observed in the products fraction and the IR trace of the residue shows a spectrum of PKMA plus a shoulder at 1127 cm^{-1} corresponding to some isolated MMA units in the chain, plus a new band at 1690 cm^{-1} . This band is associated with the presence of some isolated methacrylic acids units in the chain, believed to result from the anhydride structures after release of carbon monoxide and hydrogen abstraction:



The colouration of the residue is believed to be due to the formation of conjugated unsaturation along the chain subsequent to hydrogen abstractions.

These MMA and MAA isolated units will escape to the cold ring after further heating of this residue (curve 4, fig. V-26) at a higher temperature (350°C for fifteen minutes) leaving a residue consisting

of PKMA and charcoal.

Note at this point that when all anhydride has been formed and decomposed, KMA units in the chain (1560 cm^{-1} , fig. V-26) are still present in an appreciable amount. This is surprising if we consider that most of them should have been converted to something else after interaction with MMA units to give anhydride structures. This anomaly will be explained in chapter VI.

Similar results were obtained for the three series of copolymers except for the amounts of methanol and anhydride units which were found to decrease substantially with decreasing size of the metal ion, and this confirms the fact already mentioned that the MAA chain fragments are the result of partial decomposition of anhydrides since the proportion of MAA chain fragments in the CRF was found to increase with the size of the metal ion (see fig. V-24).

QUANTITATIVE ANALYSIS FOR METHANOL AND MMA

This was carried out by GLC as outlined in chapter II. The calibration plots for methanol and MMA using n-butyl alcohol as internal standard are shown in figure V-27 and from these curves the sensitivity factors (see chapter II) for methanol and MMA are determined:

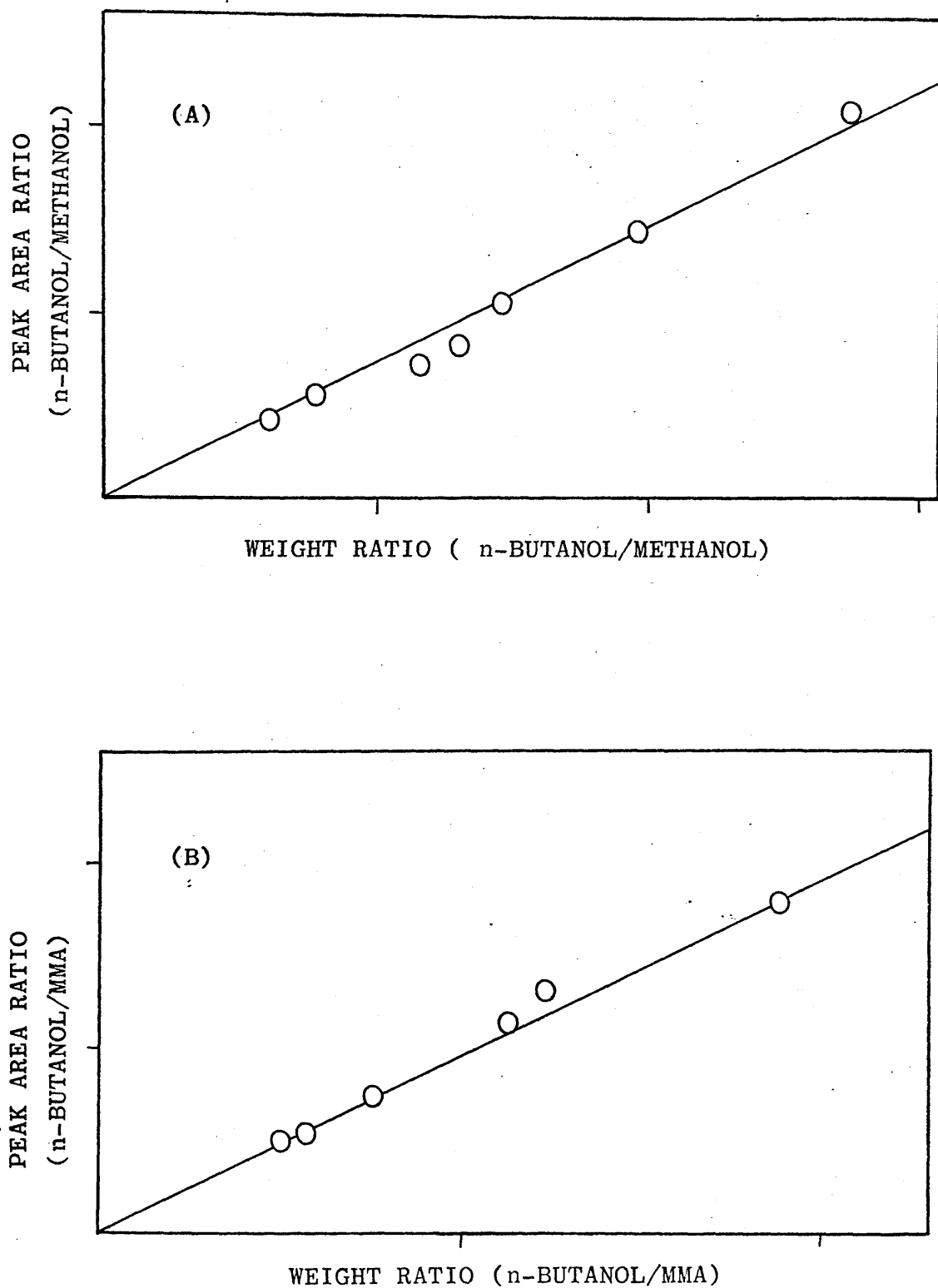


FIG.V-27 : GLC CALIBRATION PLOTS FOR : (A) : METHANOL,
(B) : MMA, USING n-BUTANOL AS INTERNAL STANDARD ;
COLUMNS : 13 $\frac{1}{2}$ % MBEA + 6 $\frac{1}{2}$ % DI-2-ETHYL HEXYL SEBACATE ON
CHROMOSORB P, 80-100 MESH ; 50°C ; HELIUM CARRIER GAS :
35 ml/MINUTE.

$$K_{(\text{methanol})} = 0.492$$

$$K_{(\text{MMA})} = 0.483.$$

Using these values of K and the expressions given in chapter II, the number of moles of methanol and MMA produced by 100 mg of copolymer sample (water excluded) is calculated, then the mole percentage is worked out. The results for the three series of copolymers are shown in figures V-28 and 29 and tabulated in tables V-8, 9 and 10.

Table V-8

Methanol and MMA production from LiMA/MMA copolymer on programmed degradation (10°C/min.) to 500°C

LiMA % in copolymers	Mole % of methanol produced	Mole % of MMA produced
0	0	100
0.10	5.64	45.12
0.25	12.58	30.47
0.32	14.87	23.13
0.41	12.80	19.31
0.52	11.2	14.38
0.70	3.07	8.18
0.95	1.11	2.49
1.0	0	0

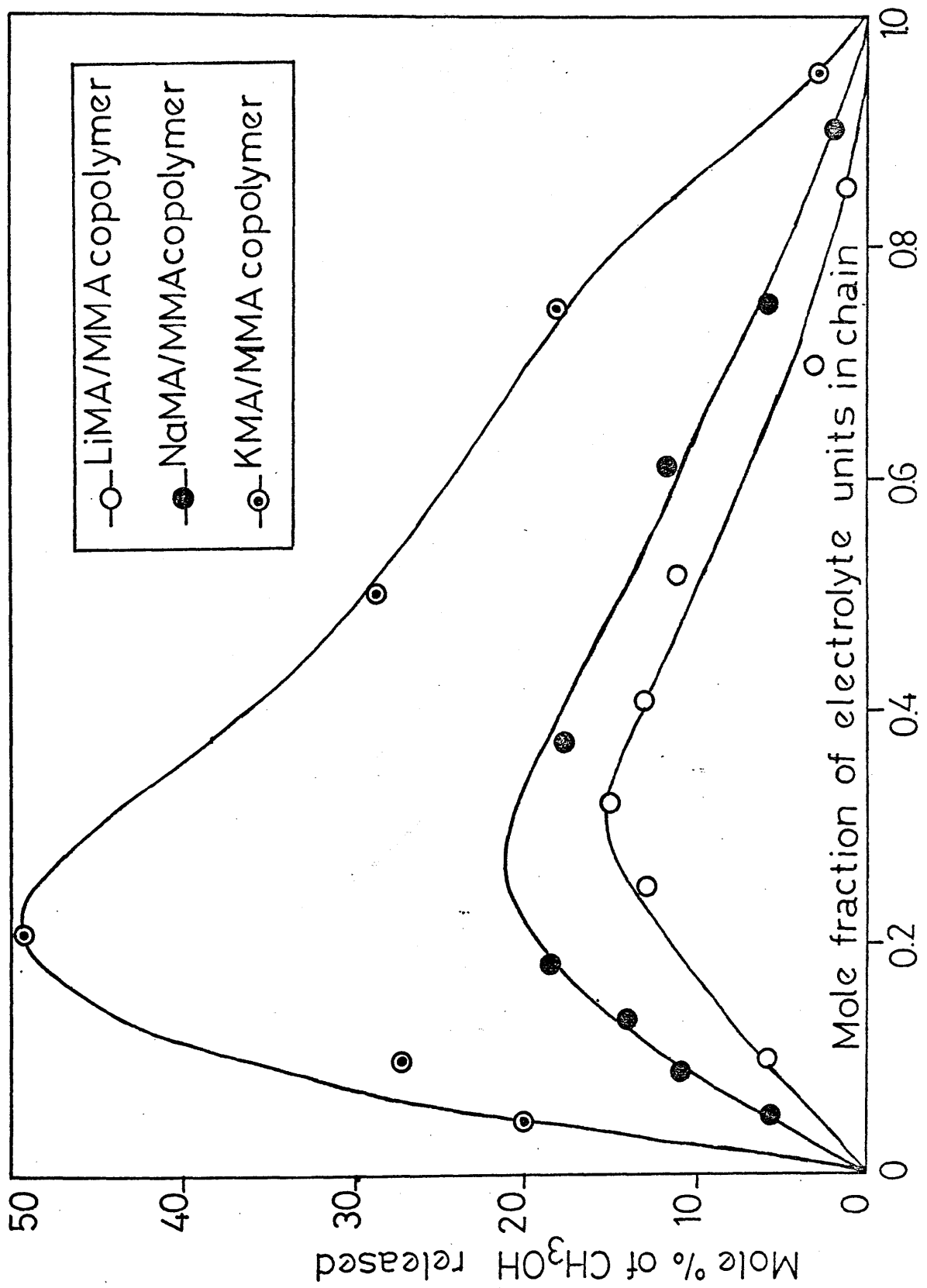


FIG. V-28 : METHANOL PRODUCTION FOR THE THREE SERIES OF COPOLYMERS.

FIG. V-29

METHYL METHACRYLATE PRODUCTION FROM THE
THREE SERIES OF COPOLYMERS.

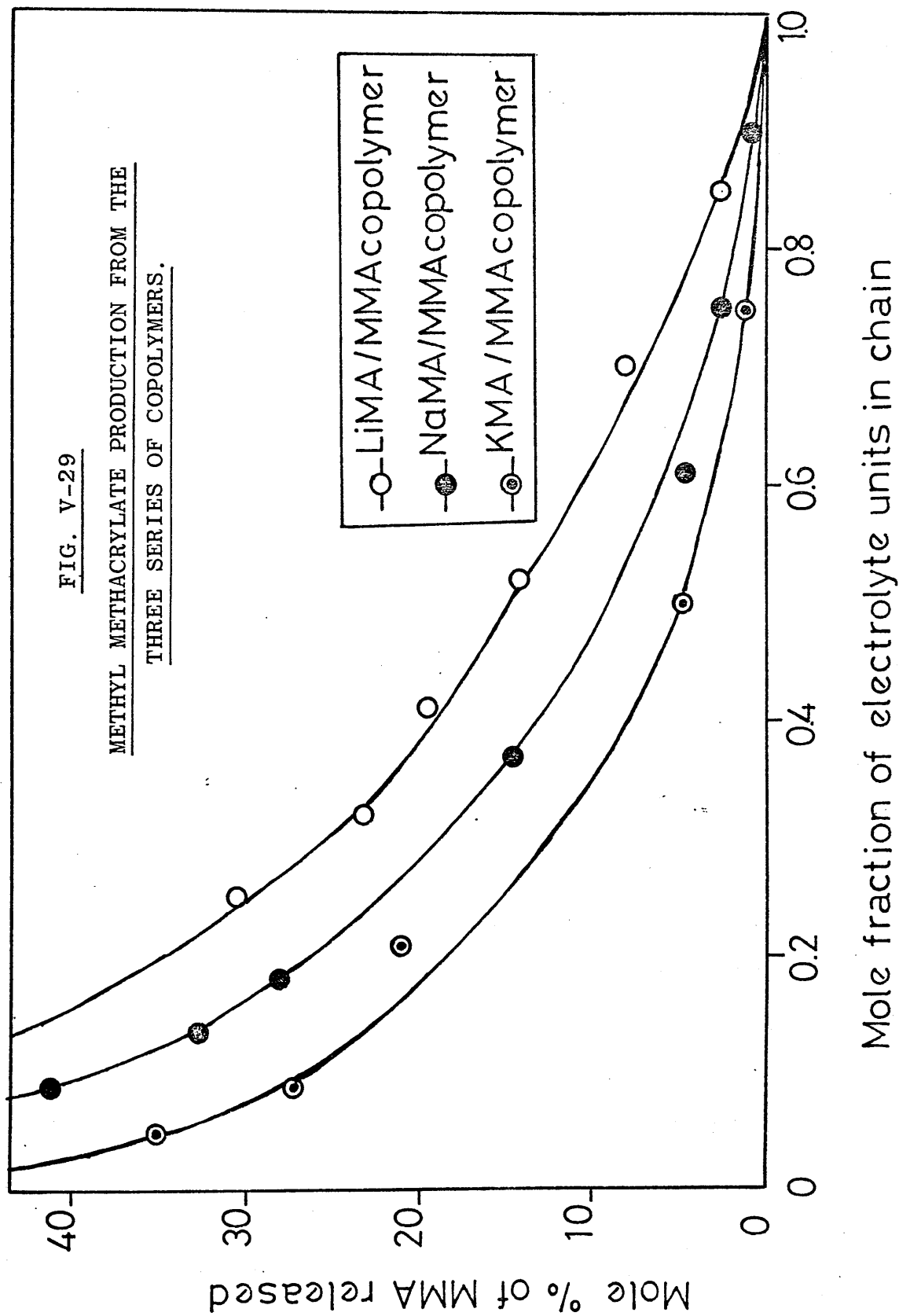


Table V-9

Methanol and MMA production from NaMA/MMA copolymer
on programmed degradation (10°C/min.) to 500°C

NaMA % in copolymers	Mole % of methanol produced	Mole % of MMA produced
0	0	100
0.05	5.35	47.3
0.09	10.74	41.23
0.134	13.58	32.48
0.18	18.51	28.13
0.37	17.51	14.56
0.61	11.6	4.49
0.75	5.57	2.24
0.90	1.5	0.95
1.0	0	0

Table V-10

Methanol and MMA production from KMA/MMA copolymer
on programmed degradation (10°C/min.) to 500°C

KMA % in copolymers	Mole % of methanol produced	Mole % of MMA produced
0	0	100
0.05	19.86	34.87
0.1	27.15	27.28
0.21	49.26	21.00
0.50	28.75	4.85
0.75	18.62	1.34
0.95	2.73	0.08
0.10	0	0

Figures V-28 and V-29 confirm the two points already deduced qualitatively from the observation of the differential condensation TVA traces, i.e.;

(i) For any particular composition of copolymer the methanol production increases with the size of the metal ion, reaching a maximum in the composition region of higher MMA content;

(ii) The inhibition to depolymerization of MMA segments increases in the same way with the size of the metal ion (fig. V-29) probably through direct blockage by anhydride units the concentration of which was found to increase with the size of the metal ion.

QUANTITATIVE ANALYSIS FOR CARBON DIOXIDE

This was carried out by isolation of carbon dioxide from the total volatiles by differential distillation (see chapter II) and then expansion of the gas into a closed system of known volume V; the pressure P is measured and the number of moles of carbon dioxide will simply be given by the expression:

$$n = PV/RT$$

The technique is explained in detail in chapter II. The results obtained for the three series of copolymers are shown in fig. V-30 and tabulated in table V-11.

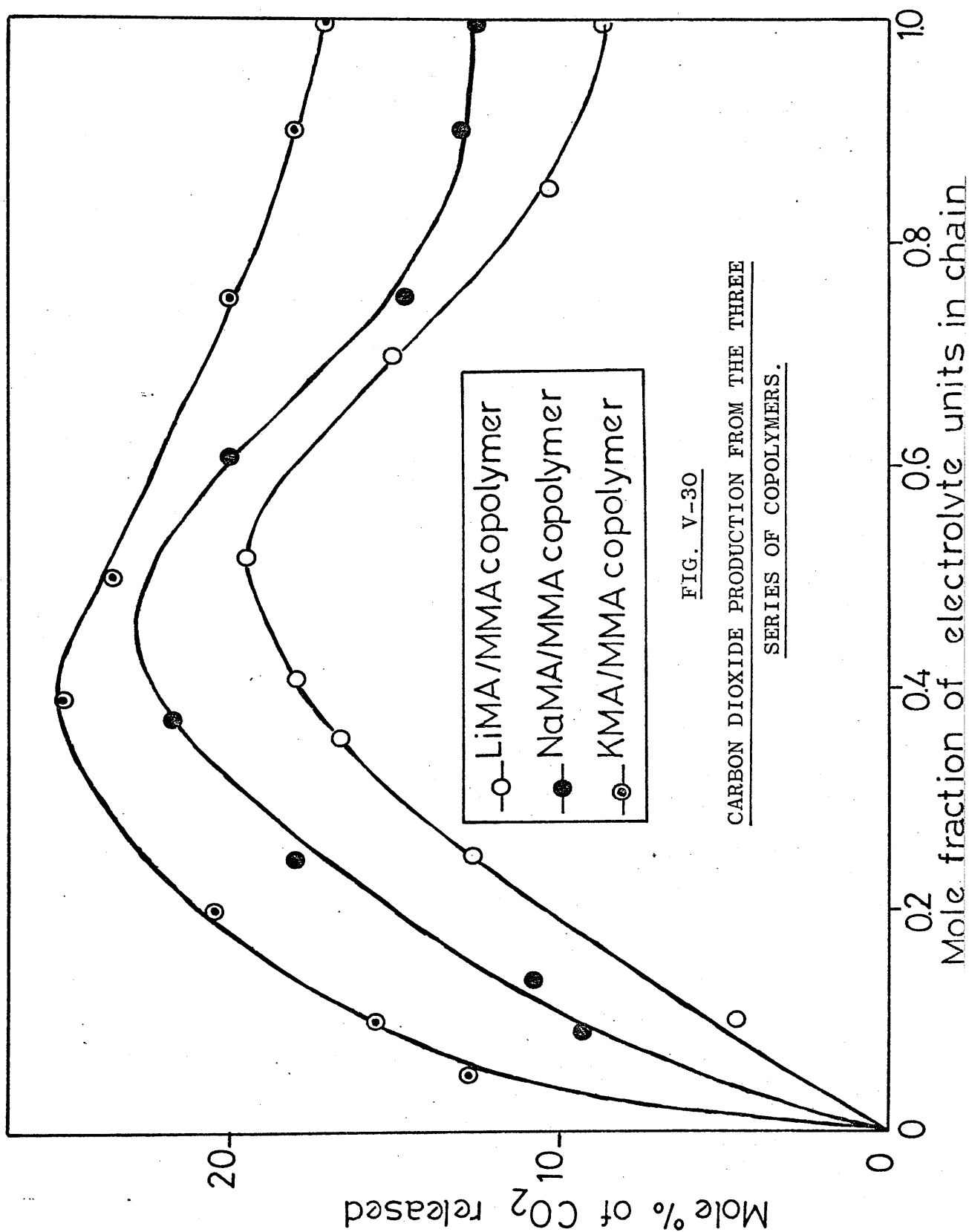


FIG. V-30
CARBON DIOXIDE PRODUCTION FROM THE THREE
SERIES OF COPOLYMERS.

Table V-11

Carbon dioxide production from copolymers of MMA with
alkali metal methacrylates. Results obtained on
programmed degradation ($10^{\circ}\text{C}/\text{min.}$) to 500°C

LiMA % in copolymers	Mole % of CO_2	NaMA % in copolymers	Mole % of CO_2	KMA % in copolymers	Mole % of CO_2
10	4.67	9	9.28	5	12.84
25	12.81	13.3	10.75	10	15.5
35.5	16.75	24.4	17.99	20	20.58
41	18.01	37	21.89	39	25.05
52	19.6	61	19.95	50	23.52
70	15.06	75	14.76	75	19.96
85	10.28	90	13.15	90	17.89
100	8.77	100	12.48	100	16.91

Again here the carbon dioxide evolution increases for any particular composition with the size of the alkali metal ion, a result already observed by McNeill and Zulfiqar in the extreme case of the poly(alkali metal methacrylates). Figure V-30 shows that the carbon dioxide production reaches a maximum around the 50% composition which indicates that an appreciable part of the total carbon dioxide evolved is the result of decomposition of anhydride structures; and the fact that carbon dioxide evolution increases with the size of the metal ion fits again with the conclusion that anhydride formation increases in the same way.

QUANTITATIVE ESTIMATION OF METAL CARBONATE IN THE
RESIDUE

Since the infra red spectra of the residues (at 500°C) in KBr discs show the presence of the alkali metal carbonate, M_2CO_3 , the neutralization of this residue with standard acid solution enables us to determine the amount of metal carbonate present in the products. The determination was carried out as follows: an excess of 0.01N hydrochloric acid was added to the black residues at 500°C from the degradation of 100 mg samples of homopolymers and copolymers, respectively. The hydrochloric acid converts all carbonate into metal chloride and carbon dioxide. The excess hydrochloric acid was back titrated with 0.01N sodium hydroxide. The amount of hydrochloric acid which reacted, will give us the weight % (weight of carbonate per 100 mg of copolymer sample used) of metal carbonate in the residue. This weight % is compared for all three series of copolymers with the weight % of the total residue recorded under vacuum at 500°C (see tables V-12, 13 and 14 and figures V-31, 32 and 33).

Table V-12

Data of residue analysis for
LiMA/MMA copolymer at 500°C

LiMA % in copolymers	Weight % of metal carbonate in residue	Weight % of total residue given by TGA
10	1.49	9
25	3.33	19
32	4.21	21
41	7.95	24
52	11.56	29
70	18.6	31
85	23.7	33
100	30.21	36

Table V-13

Data of residue analysis for
NaMA/MMA copolymer at 500°C

NaMA % in copolymers	Weight % of Na_2CO_3 in residue	Weight % of total residue given by TGA
5	1.32	7
9	2.63	8
13.4	3.18	14
18	4.20	17.5
37	9.57	28.5
61	16.34	36
75	22.46	38
90	27.87	40
100	31.96	43

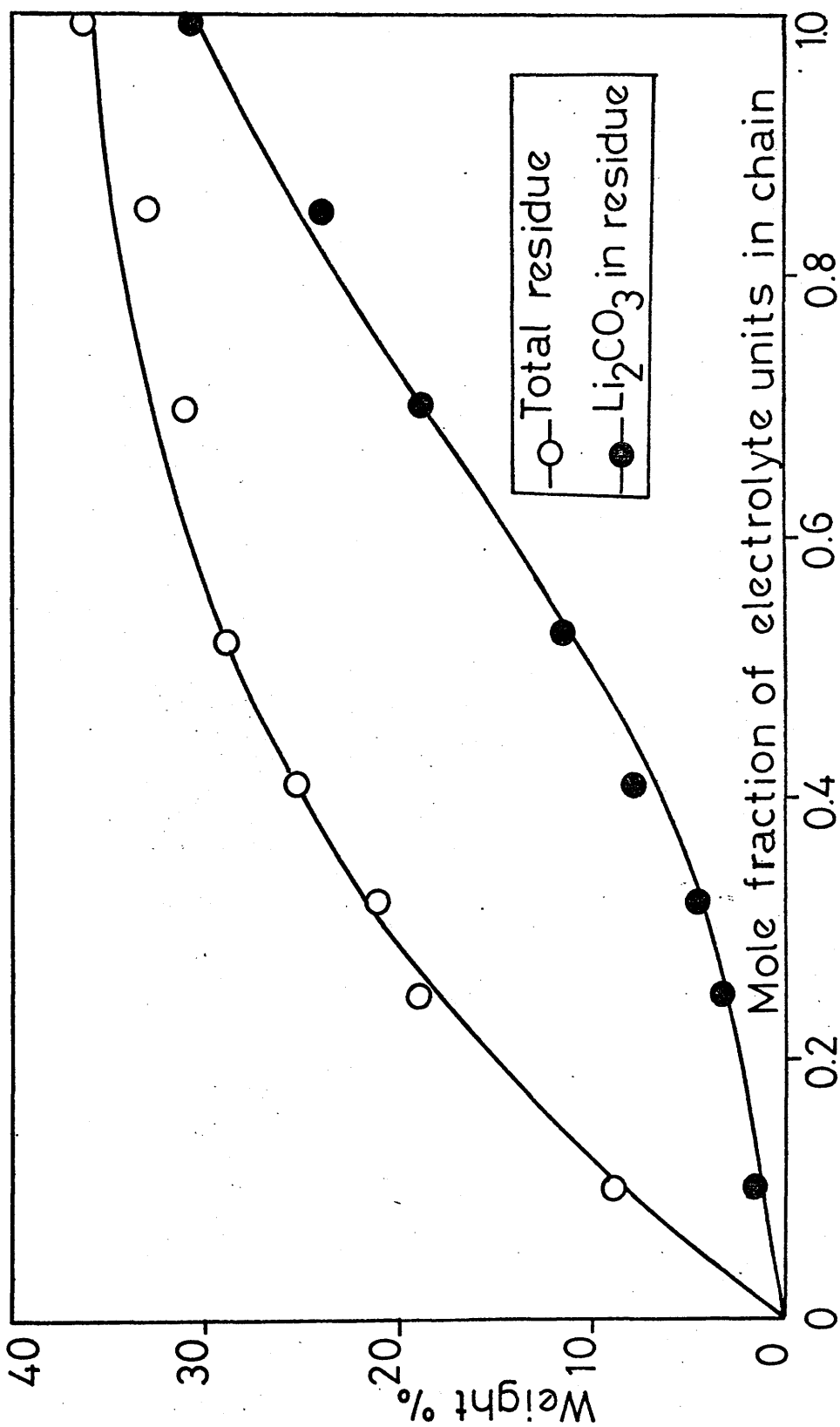


FIG. V-31

RESIDUE DATA FOR LiMA/MMA COPOLYMERS.

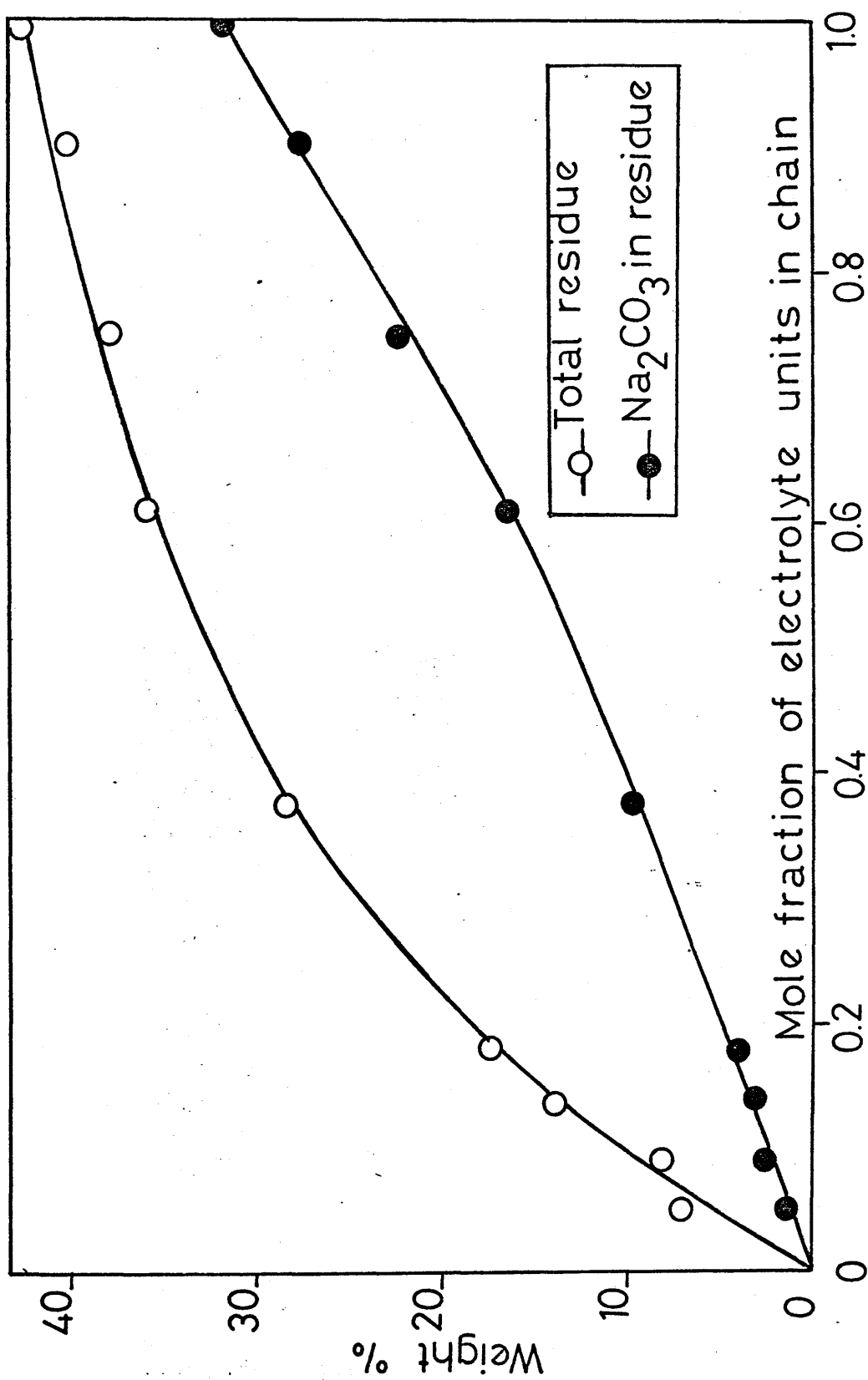


FIG. V-32
RESIDUE DATA FOR NaMA/MMA COPOLYMERS.

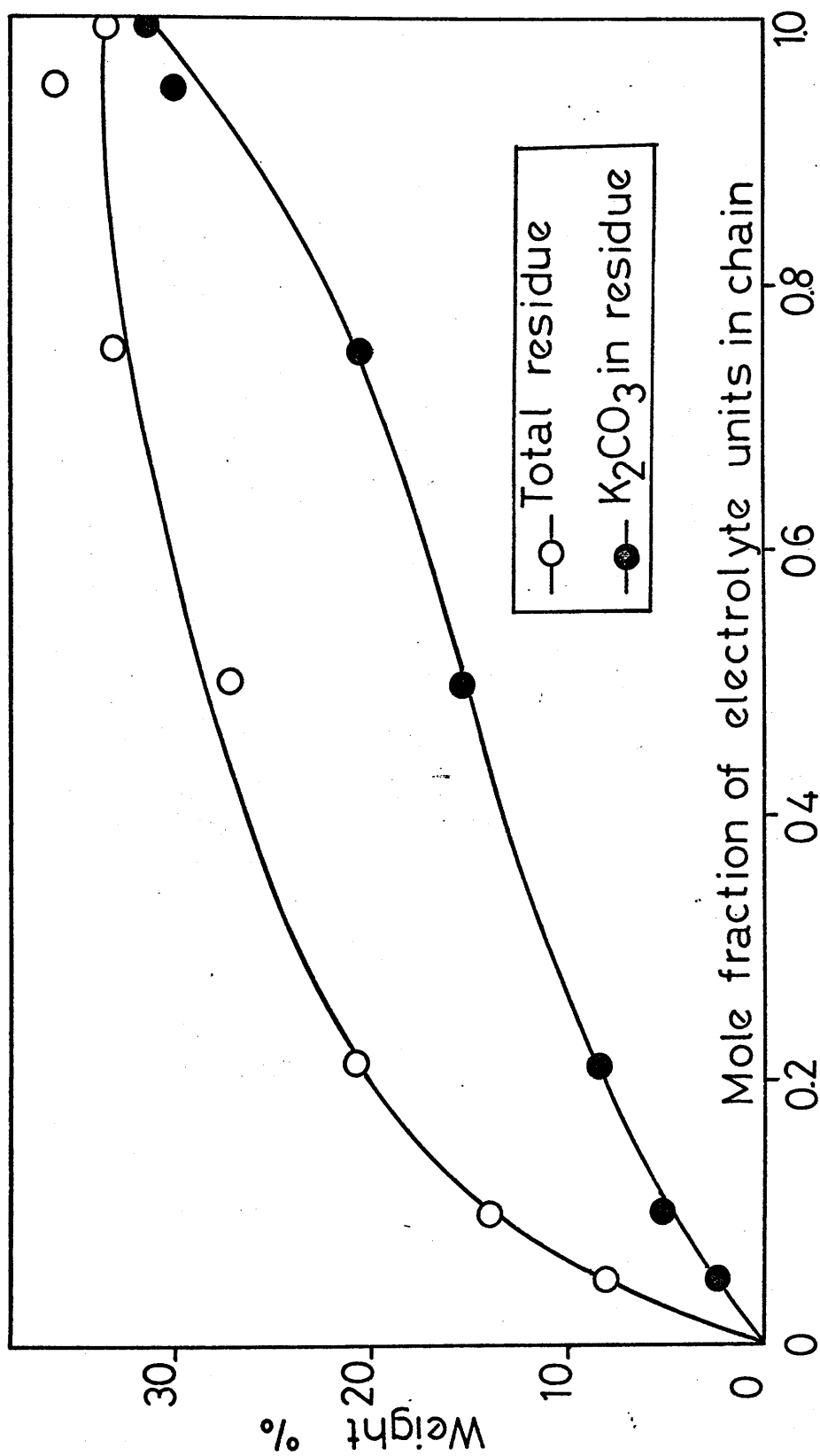


FIG. V-33

RESIDUE DATA FOR KMA/MMA COPOLYMERS.

Table V-14

Data of residue analysis for
KMA/MMA copolymer at 500°C

KMA % in copolymers	Weight % of K_2CO_3 in residue	Weight % of total residue given by TGA
5	2.57	8
10	5.1	14
21	7.93	22
50	14.8	27
75	20.4	33
95	30.36	37
100	31.5	33

From the results of these three tables and the observation of figures V-31, 32 and 33, one sees that the weight of M_2CO_3 in the residue is always lower than the total weight of that residue recorded under vacuum at 500°C, the difference being due to the amount of charcoal which is always present. It is also interesting to note, in the three diagrams that this difference appears to decrease towards the region of the composition range where the alkali metal methacrylate content predominates in the copolymers. This difference is almost negligible in the extreme case of the PKMA homopolymer (see fig. V-33). This is surprising since chain fragmentation and hydrogen abstraction processes

are expected to play a significant role in the thermal decomposition of the alkali metal methacrylate parts of the copolymers. This can only be explained if one assumes that the metal carbonate M_2CO_3 , formed during the decomposition of the salt units in the copolymer chains, is, as postulated by McNeill and Zulfiqar, ⁽⁹⁴⁾ decomposing to some extent, giving carbon dioxide and leaving the metal oxide, M_2O , in the residue. Under these considerations, the total weight of the residue recorded under vacuum at 500°C (upper curves in figures V-31, 32 and 33) would not only contain metal carbonate and charcoal, but also some metal oxide, M_2O ; and this would result in lowering the upper curves of figures V-31, 32 and 33 towards the composition region where the alkali metal methacrylate content predominates in the copolymers. The reason for the absence (IR evidence) of metal oxide in the final residue could be due to the fact that the oxides, whose instability increases with the size of the metal ion, are converted back to carbonates in presence of carbon dioxide from the atmosphere after the degradation tube is removed for residue analysis.

QUANTITATIVE ESTIMATION OF METAL METHACRYLATE MONOMER AND METAL ISOBUTYRATE IN THE CRF

Two of the major products from the degradation of salts units segments in the copolymers are the result

of the depolymerization of these electrolyte unit sequences: monomer and metal isobutyrate; since it was impossible to separate them from each other and from the rest of the products in the CRF, they were estimated in terms of mole percentage of methacrylate units (in the form of monomer or isobutyrate) in the CRF: this was done in consideration of the fact that no alkali metal compound was volatile beyond the CRF. Hence, the evaluation of the quantity of alkali metal in the residue, subtracted from the known quantity of metal in the polymer sample before degradation, will give us the amount of metal in the CRF, and therefore the mole percentage of electrolyte units in either of the two forms in the cold ring fraction.

The amount of metal in the residue can easily be worked out from the results of the estimation of the residue content (see tables V-12, 13 and 14).

This led to the quantitative estimation of the electrolyte units which escaped to the cold ring fraction during degradation and the results for the three series of copolymers and the respective homopolymers are shown in figure V-34 and tabulated in table V-15.

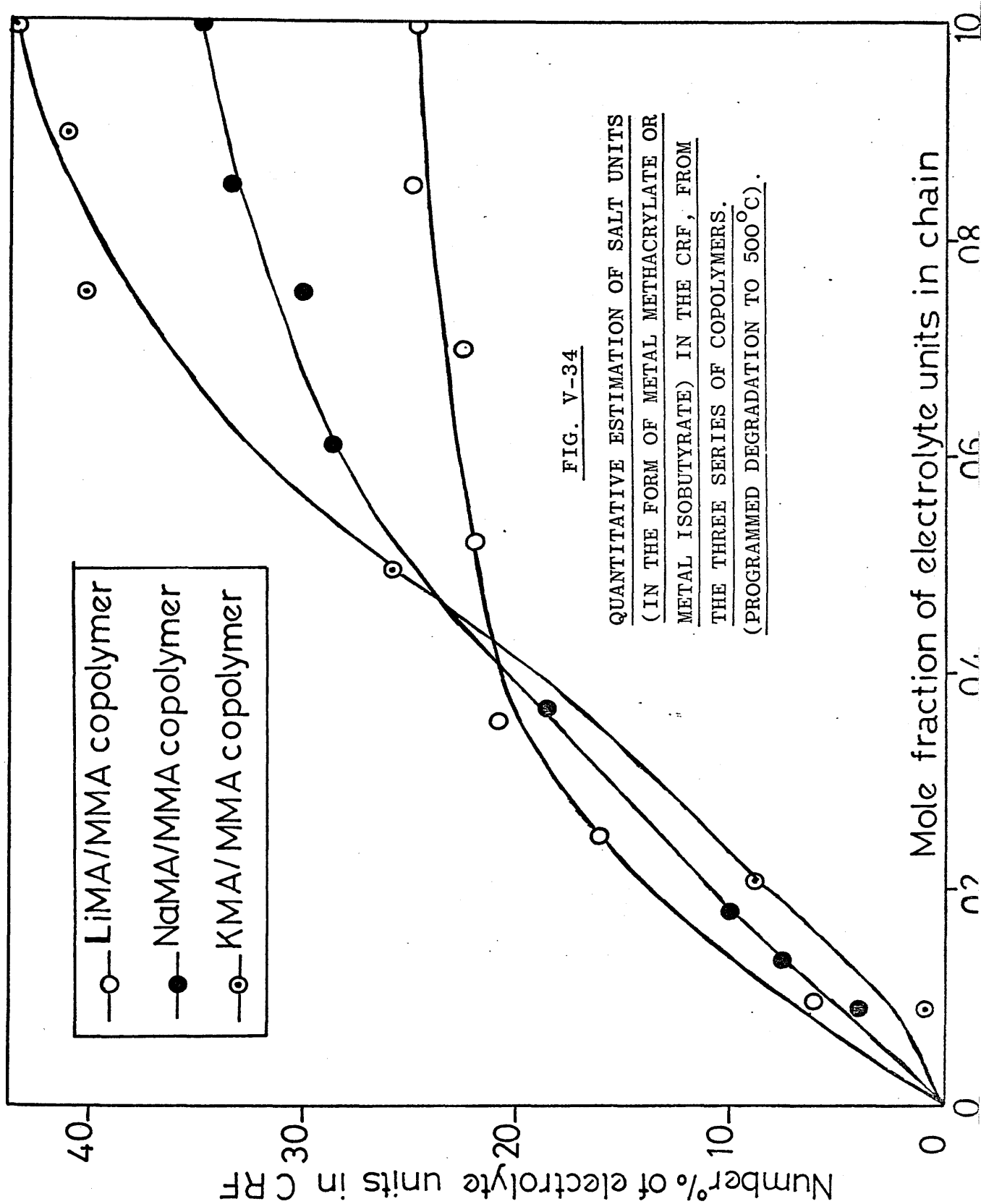


FIG. V-34

QUANTITATIVE ESTIMATION OF SALT UNITS
(IN THE FORM OF METAL METHACRYLATE OR
METAL ISOBUTYRATE) IN THE CRF, FROM
THE THREE SERIES OF COPOLYMERS.
(PROGRAMMED DEGRADATION TO 500°C).

Table V-15

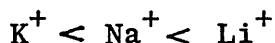
Estimation of salt content (in the form of metal methacrylate or metal isobutyrate) in the CRF from programmed degradation of copolymers of MMA with alkali metal methacrylates

LiMA % in copolymers	Mole % of salt units in CRF	NaMA % in copolymers	Mole % of salt units in CRF	KMA % in copolymers	Mole % of salt units in CRF
10	6.03	5	2.5	5	1.3
25	16.17	9	4.0	10	2.5
32	20.91	13.3	7.33	21	8.93
41	20.19	18	9.97	50	26.01
52	22.00	37	18.41	75	40.11
70	22.49	61	28.65	95	40.97
85	25.11	75	33.03	100	43.45
100	24.8	90	33.617	—	—
—	—	100	34.764	—	—

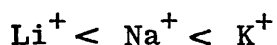
Figure V-34 shows that the sublimation of metal methacrylate and metal isobutyrate into the cold ring increases as the electrolyte content increases in the copolymer chains, which is expected.

But an interesting observation arises from the relative contribution to this sublimation between the three series of copolymers. Two distinct and opposite features are apparent in figure V-34:

(i) In the composition region ranging between 0 and 50% of metal methacrylate content in the copolymers, the sublimation of the salt units to the CRF seems to increase as the size of the metal ion decreases:



(ii) In the other region of the copolymer composition range, this sublimation increases with the size of the metal ion:



This ambiguity can be explained in view of the fact that in the first copolymer composition region (high MMA content), the formation of anhydride structures by intramolecular cyclization between the two types of monomer units in the chain is favoured as the size of the metal ion increases; this explains the decrease (in that composition region) of the sublimation of salt units to the CRF as the size of the metal ion increases,

since at the same time the contribution of salt units to produce anhydride structures increases.

As for the second region of copolymer composition (high salt unit content in chain), the increasing abundance of electrolyte units in the CRF with the size of the metal ion is normal, since, as reported by McNeill and Zulfiqar,⁽⁹⁴⁾ the syndiotacticity in the alkali metal methacrylate sequences is also increasing in the same order,^(117,118) thus preventing interaction between adjacent electrolyte units and favouring depolymerization and production of metal isobutyrate.

QUANTITATIVE ANALYSIS FOR SOME CARBONYL CONTAINING PRODUCTS BY GLC

The production of ketones and aldehydes which is very low in the cases of alkali metal methacrylates homopolymers,⁽⁹⁴⁾ is understandably even lower in the cases of the copolymers.

It was found that ketone formation from KMA/MMA copolymers was hardly detectable even in the composition region of high KMA content. For this reason only LiMA/MMA and NaMA/MMA copolymers were investigated at two high salt contents in each case for the quantitative estimation by GLC (see chapter II) of methacrolein, methyl ethyl ketone, 2-methyl cyclopentanone, 2,5-dimethyl cyclopentanone

and 2,5-dimethyl cyclopent-3-enone, n-butanol was again used as internal standard. The sensitivity factors used were obtained by McNeill and Zulfiqar⁽⁹⁴⁾;

Methacrolein (MAC) --- $K_1 = 1.3$

Methyl ethyl ketone (MEK) --- $K_2 = 1.1$

2-methyl cyclopentanone (MCP) --- $K_3 = 1.11$

2,5-dimethyl cyclopentanone (DMCP) --- $K_4 = 1.28$

2,5-dimethyl cyclopent-3-enone (DMCP=) -- $K_5 = 1.4$

The results are shown in tables V-16 and 17.

Table V-16

Ketone formation from two LiMA/MMA copolymers

Product (mole %)	75% LiMA/MMA copolymer	85% LiMA/MMA copolymer	PLiMA*
MAC	0.8	1.1	3.0
MEK	0.44	0.73	1.4
MCP	1.42	1.70	2.2
DMCP	1.40	1.72	2.6
DMCP=	1.33	1.2	2.8

* Data of McNeill and Zulfiqar. (94)

Table V-17

Ketone formation from two NaMA/MMA copolymers

Product (mole %)	75% NaMA/MMA copolymer	90% NaMA/MMA copolymer	PNaMA*
MAC	0.63	0.7	2.16
MEK	0.72	0.91	1.9
MCP	1.12	1.23	1.0
DMCP	0.81	0.80	0.8
DMCP=	trace	0.32	1.0

* Data of McNeill and Zulfiqar. (94)

From these results two facts are evident:

(i) Ketone formation is much lower in the copolymers than in the corresponding homopolymer, a result which is expected since some of the salt units in the copolymers are interacting with MMA units to give anhydride structures.

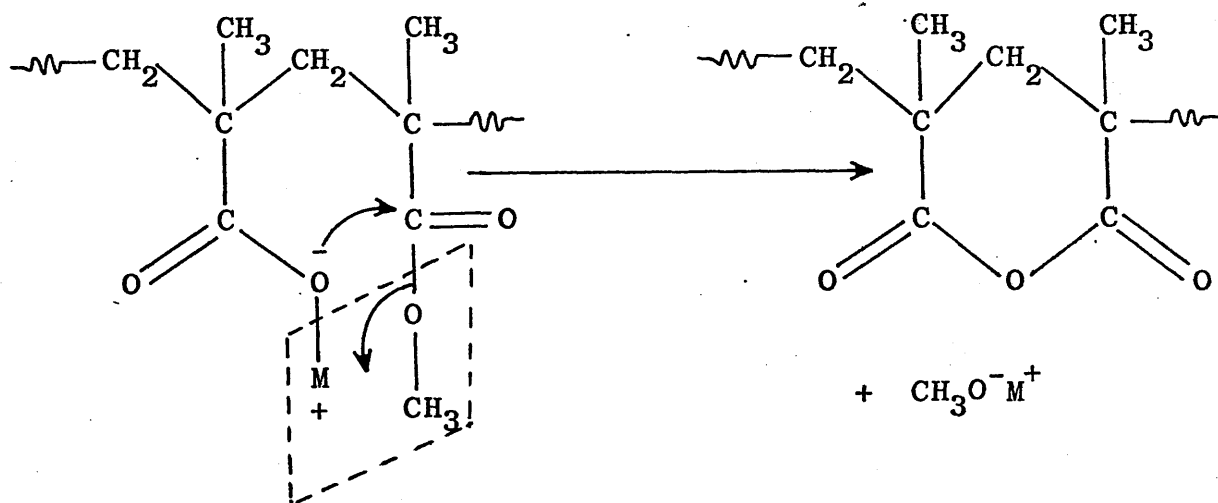
(ii) Ketone formation increases as the size of the metal ion decreases, as already observed by McNeill and Zulfiqar, (94) who explained it in terms of syndiotacticity increasing in the order:



CONCLUSIONS

In the light of these degradation results, it becomes clear that the thermal degradation of copolymers of MMA with alkali metal methacrylates displays two main decomposition reactions: firstly, depolymerization, in competition with anhydride decomposition and methanol production, and secondly, the breakdown of the alkali metal methacrylate units remaining in the chain in a similar manner to that which occurs in the corresponding homopolymers.

Anhydride formation between the two adjacent types of monomer is believed to result from a nucleophilic attack by the oxygen atom of the O—M bond towards the ester carbonyl with formation of metal methoxide:



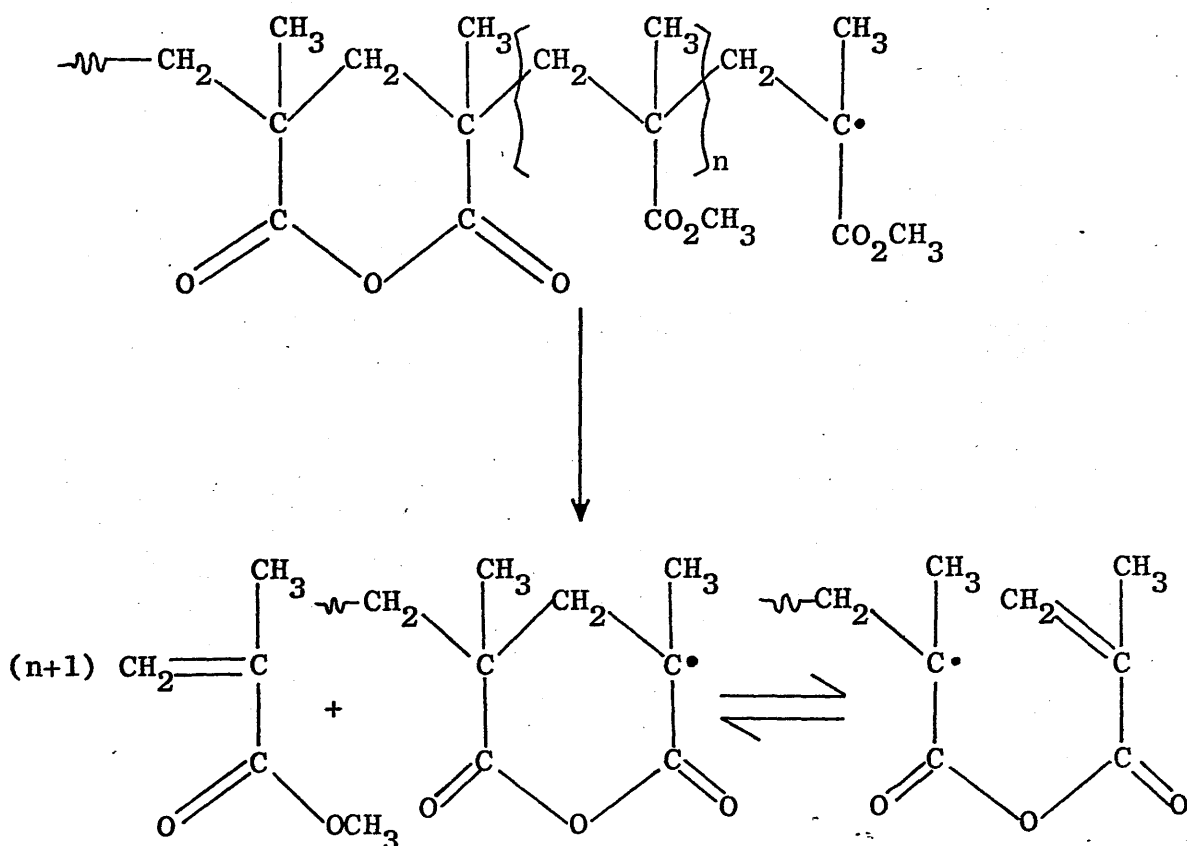
The presence of methoxide has not been established

at any stage, since this product decomposes readily in the atmosphere to give methanol and metal hydroxide. This product could also be degrading or reacting to give another product as soon as it is formed.

The observation of the fact that formation of anhydride structures is favoured as the size of the metal ion increases in the copolymer series, can also be explained in the following manner: as the size of the metal ion increases, the oxygen-metal bond of the metal carboxylate group becomes longer, therefore weaker, and the negative character of the oxygen atom from which nucleophilic attack takes place increases, thus favouring the formation of the six-membered ring anhydride structure in the chains.

The inhibition to depolymerization of MMA segments was found to be more effective as the size of the metal ion increases in the three series of copolymers, i.e., less PMMA depolymerization where there is more anhydride present in the chains. This suggests that the depolymerization is directly blocked by anhydride structures in the copolymer chain. This inhibition or blockage will probably be the result of an equilibrium between the anhydride radical resulting from chain scission adjacent to the anhydride ring, and the radical which is the product of the liberation

of one further ethylemic unit from the chain end^(71,122) as illustrated below:



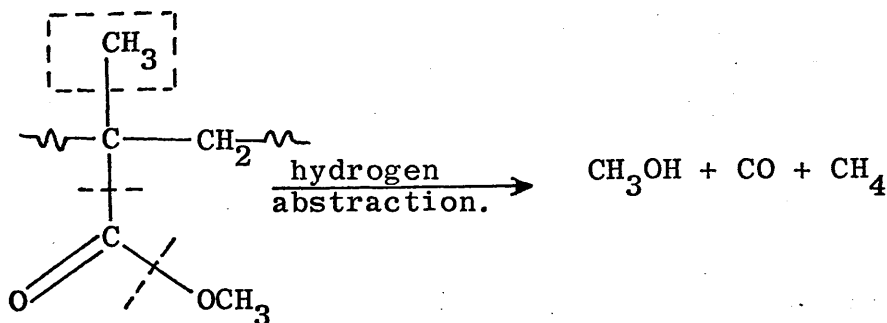
The production of anhydride rings and the depolymerization characteristics for the three series of copolymers appear to fit closely with the other quantitative results (i.e., production of carbon dioxide and electrolyte units sublimation to the cold ring).

At this point, however, the origin of the methanol

evolution (as a major product) from the copolymers, is still not clearly established.

At any particular copolymer composition, the methanol formation increases with the size of the metal ion and seems to originate from anhydride formation.

The most plausible explanation for the methanol formation on the basis of the experimental results so far presented would appear to be decomposition of MMA segments trapped between anhydride structures:



But could the alkali metal methoxide, "produced" during the degradation, react in a further step with MMA units in the chain to produce methanol?

To clarify this point, further investigations were needed. In the next chapter the yields of methanol will be compared to those predicted from sequence distribution calculations based on the hypothesis that one molecule of methanol is released each time one anhydride structure is formed.

CHAPTER VI

THE THERMAL DEGRADATION OF COPOLYMERS OF METHYL METHACRYLATE WITH ALKALI METAL METHACRYLATES II: ORIGIN OF METHANOL AND DISCUSSION

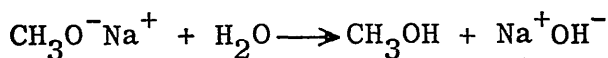
If the alkali metal methoxide produced by the interaction of the two types of monomer units in the chain (leaving an anhydride structure) does react with MMA units to give methanol, then the thermal degradation of PMMA blended with alkali metal methoxide should also give methanol.

THERMAL DEGRADATION OF PMMA/SODIUM METHOXIDE BLEND

Freshly prepared sodium methoxide (see preparation in Appendix) degraded to 500°C under normal TVA conditions gave methane, carbon monoxide, hydrogen and a small amount of methanol solvent. The residue at 500°C observed by IR spectroscopy revealed the presence of sodium carbonate which was probably formed by contact between atmospheric carbon dioxide and sodium oxide.

The same amount of $\text{CH}_3\text{O}^-\text{Na}^+$ was also degraded under the same conditions in presence of PMMA in the proportion 1/2 by weight (methoxide to PMMA). The major products

were MMA monomer, dimethyl ether and methanol. Thus methanol is a product from the degradation of the blend. At 350°C the IR spectrum of the yellowish residue showed also the presence of sodium methacrylate units in the chain. Can sodium methoxide react with MMA ester to give methanol and sodium methacrylate units in the chain? $\text{CH}_3\text{O}^-\text{Na}^+$ could probably convert MMA units to give NaMA units and produce dimethyl ether, but the production of methanol from the blend is highly unlikely, unless the sodium methoxide contains appreciable amounts of sodium hydroxide which can react with MMA units and give methanol (this was checked by investigating the thermal degradation of a PMMA/ Na^+OH^- blend). The presence of Na^+OH^- with $\text{CH}_3\text{O}^-\text{Na}^+$ is possible, resulting from the high affinity of the metal methoxides for water, which can be taken up from the atmosphere:



Consequently, the methanol production from the PMMA/ $\text{CH}_3\text{O}^-\text{Na}^+$ blend degradation does not give a clear indication as to its origin (from the degradation of the copolymers), since it was found impossible to prepare a sample of metal methoxide and blend it with PMMA without putting it in contact with the atmosphere for a short time.

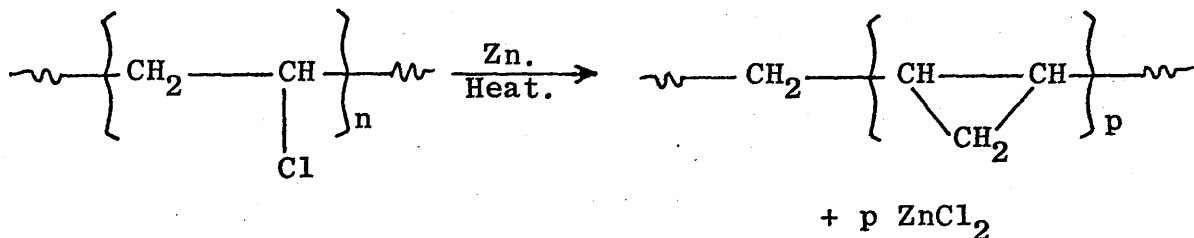
To clarify this point a comparison had to be made

between the experimental yields of methanol from the copolymers and those predicted from sequence distribution calculations. The extent of the cyclization reaction between adjacent MMA (A) and electrolyte (B) units in the copolymer chains can be predicted for the three series of copolymers, from their reactivity ratios. This involves the calculation of the fraction of total electrolyte units which are likely to cyclize in each copolymer.

Before discussing these theoretical fractions, it is appropriate to consider briefly the statistics of random interunit cyclization reaction.

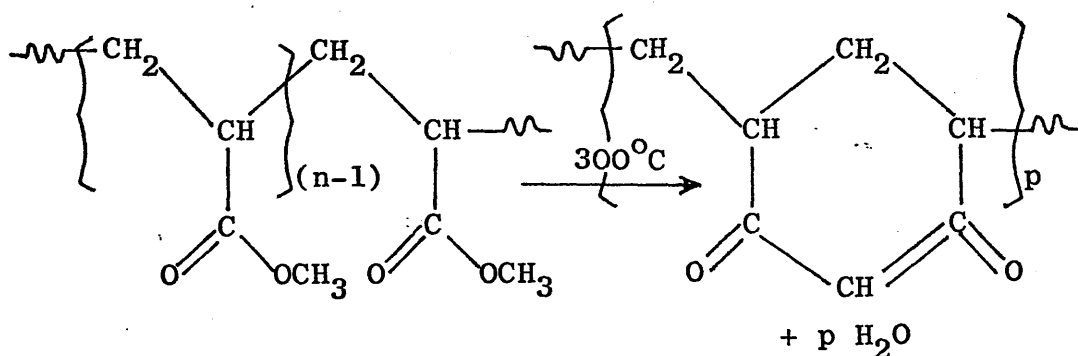
THE STATISTICS OF CYCLIZATION REACTIONS IN VINYL HOMOPOLYMERS

It has been observed in several cases that cyclization between adjacent monomer units along a polymer chain (if cyclization is known to occur) is not quantitative. Marvel and Sample⁽¹²³⁾ found for instance, that the 1,3-cyclization which occurs when head to tail PVC is heated in presence of metallic zinc was non-stoichiometric:



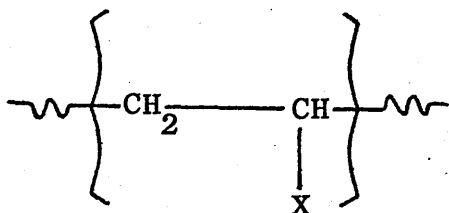
with $p < 2n$.

Marvel and Levesque⁽¹²⁴⁾ showed also that the cyclization which occurs when poly(methyl vinyl ketone) is pyrolysed at 300°C was likewise non-quantitative, producing only 85% of the total amount of water theoretically expected:



with again $p < 2n$

This anomaly was clarified by Flory⁽¹²⁵⁾ in terms of random 1,3-cyclization, in which some of the monomer units will remain isolated between neighbours which would have already reacted. For homopolymers of the general structure:



Flory showed that the number of X groups which will remain unreacted is given by:

$$S_n = \sum_{i=0}^{(n-1)} (n-i) (-2)^i / i! \quad (\text{VI-1})$$

where n is the total number of monomer units in the polymer chain. This proved to be in good accord with the experimental results.

THE STATISTICS OF CYCLIZATION REACTIONS IN VINYL COPOLYMERS

This treatment (see above) has been extended to random copolymers of the type dealt with in the present work by Alfrey, Lewis and Magel.⁽¹²⁶⁾ To describe these cyclizations in a random AB copolymer, they worked out an expression for the calculation of the total number of B units which cannot undergo cyclization (if cyclization can occur) by summation of the two possible types of B units present in the chain:

(i) those which occur within alternating sequences of the type $\sim\sim\sim\text{ABABAB}\sim\sim\sim$ and are left

isolated and unreacted by virtue of the random nature of the A-B interaction. The situation in this case falls under the category of random cyclization in a homopolymer and a modified form of Flory's equation (VI-1) can be applied;

(ii) those B units in the chain which cannot react because they are within sequences of the type $\sim\text{ABBB}---\text{BBA}\sim$. The first and last B units belong to the alternating sequences and thus fall under the above category (i); the remaining B units are given by the summation:

$$\sum_{n=3}^{\infty} (n-2) \times (\text{total number of } \underline{B} \text{ sequences of length } n)$$

The total number of sequences of a given type, (i) or (ii), is expressed as a function of the propagation probabilities of the copolymer system. If, for instance, we define P_{AB} as being the probability for a polymer radical terminated by a unit A ($\sim\text{A}\cdot$) to add a monomer molecule of the type B, during the copolymerization process, then the total number of alternating sequences of the type $\text{A} \left| \begin{array}{c} (AB)_n \\ \hline \end{array} \right| \text{A}$, for instance, will be given as:

$$(\text{Total number of } \underline{A} \text{ units in copolymer}) P_{AA}^2 \cdot P_{AB}^n \cdot P_{BA}^n$$

In a similar manner, the total number of "homopolymer" sequences of the type $\text{A} \left| \begin{array}{c} (B)_n \\ \hline \end{array} \right| \text{A}$ will be

given as:

(Total number of A units in copolymer) $P_{AB} \cdot P_{BB}^{n-1} \cdot P_{BA}$.

In all cases, P_{AA} and P_{BB} can be eliminated in view of the fact that $P_{AA} + P_{AB} = 1$ and $P_{BB} + P_{BA} = 1$, giving finally:

$$f_u(B) = \left\{ \cosh \sqrt{P_{AB} \cdot P_{BA}} - \sqrt{P_{BA}/P_{AB}} \cdot \sinh \sqrt{P_{AB} \cdot P_{BA}} \right\}^2 \quad (VI-2)$$

where $f_u(B)$ is the fraction of the total B units which cannot undergo cyclization.

All these probabilities can be calculated⁽¹²⁷⁾ for low conversion copolymers, provided the monomer reactivity ratios (r_A, r_B) and the percentage molar concentrations (A_f, B_f) of monomers in the polymerization mixture are known:

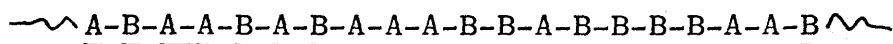
$$P_{AB} = 1/(1 + r_A A_f/B_f) \quad \& \quad P_{BA} = 1/(1 + r_B B_f/A_f)$$

Alternatively, these probabilities can be calculated from the percentage molar concentrations (A, B) of A and B in the copolymer chain and the run number, R ,⁽¹²⁸⁾ by use of the following expression:

$$P_{AB} = R/2A \quad \& \quad P_{BA} = R/2B$$

The run number is defined⁽¹²⁸⁾ as "the average

number of monomer sequences (runs) occurring in a copolymer per 100 monomer units." Let us consider, for instance, the portion of polymer chain shown below:



The chain contains twenty monomer units arranged in twelve alternating sequences (underlined) or runs. The run number for this structure will therefore be, sixty. The run number is a convenient parameter for characterizing sequence distribution in copolymers. It provides a useful mental picture of the sequence distribution and its use simplifies considerably the complex calculations involved. One useful parameter which can easily be determined from R is the number average length of a given type sequence, denoted by $\langle A \rangle$ or $\langle B \rangle$. This is simply the total number of the given type monomer units divided by the total number of runs of that type present:

$$\langle A \rangle = A/(R/2) = 2A/R$$

$$\langle B \rangle = B/(R/2) = 2B/R$$

The fraction of A units centred in BAAAB type pentads can also be given as an expression of R and the percentage molar concentrations (A,B) of the two monomers A and B in the copolymer chain:

$$P_{\text{B-A-A-A-B}} = P_{AA} \cdot P_{AB} \cdot P_{AA} \cdot P_{AB} = \frac{R^2 (A-R/2)^2}{4A^4}$$

Run numbers themselves can be predicted for low conversion copolymers from monomer reactivity ratios and monomer feed compositions (A_f, B_f) using expression (VI-3):

$$R = 200 / (2 + r_A A_f / B_f + r_B B_f / A_f) \quad (\text{VI-3})$$

Johnston and Harwood⁽¹²⁹⁾ have expressed the Alfrey-Lewis-Magel equation (VI-2) as a function of R and the percentage molar concentration (A, B) of the two monomer units in the copolymer chain:

$$f_u(B) = \left\{ \cosh \sqrt{(R^2/4AB)} - \sqrt{(A/B)} \sinh \sqrt{(R^2/4AB)} \right\}^2 \quad (\text{VI-4})$$

This final equation, very instructive to work with, indicates that $f_u(B)$ is very sensitive to R and that copolymer cyclization reactions can be used very effectively to characterize polymer structure.

THEORETICAL RESULTS FOR THE FRACTION OF CYCLIZABLE ELECTROLYTE UNITS IN COPOLYMERS

If we use the final reactivity ratios (r_A and r_B) computed for the three copolymer systems studied

(see table IV-9, chapter IV), and let MMA be unit A and the metal methacrylate be unit B, then the theoretical values for the fraction $f_c(B)$, of cyclizable electrolyte units can be calculated for each particular copolymer by first calculating the run number R and $f_u(B)$, and then using the expression:

$$f_c(B) = 1 - f_u(B)$$

The results obtained for each series of copolymers are tabulated in tables VI-1,2 and 3.

RESULTS COMPARED WITH METHANOL PRODUCTION

If one molecule of methanol is produced each time one anhydride structure is built in the copolymer chain, then the total theoretical mole % of methanol which should be expected from each copolymer will be given by simply multiplying $f_c(B)$ with the percentage molar composition of unit B in the copolymer chain, and these theoretical results are compared for the three series of copolymers in tables VI-4, 5 and 6 and in figures VI-1, 2 and 3.

Table VI-1

Theoretical determination of $f_c(B)$ for LiMA/MMA copolymers

Copolymer	A_f	B_f	R	A	B	$f_u(B) \times 100$	$f_c(B) \times 100$
A 1	93.2	6.8	19.76	90.0	10.0	0.24	99.76
A 2	77.73	23.27	48.76	75.0	25.0	1.82	98.18
A 3	66.7	33.3	61.95	68.0	32.0	3.23	96.71
A 4	50.0	50.0	74.93	59.0	41.0	9.35	90.65
A 5	25.0	75.0	82.72	49.0	51.0	21.46	78.54
A 6	4.75	95.25	57.25	30.0	70.0	58.59	41.41
A 7	1.46	98.54	28.83	15.0	85.0	82.51	17.49

Key to symbols:

A_f , B_f are the respective (%) molar concentrations of MMA and LiMA in the monomer feed.
 A , B are the respective (%) molar concentrations of MMA and LiMA in the copolymers.
 R is the run number; $f_u(B)$, $f_c(B)$ are the respective fractions of uncyclizable and cyclizable LiMA units in the copolymer chain.

Table VI-2

Theoretical determination of $f_c(B)$ for NaMA/MMA copolymers

Copolymer	A_f	B_f	R	A	B	$f_u(B) \times 100$	$f_c(B) \times 100$
B 1	85.0	15.0	8.15	95.0	5.0	0.66	99.34
B 2	70.0	30.0	17.65	90.0	10.0	0.47	99.53
B 3	60.0	40.0	24.85	86.6	13.4	1.45	98.55
B 4	50.0	50.0	32.78	82.0	18.0	2.79	97.21
B 5	25.0	75.0	54.01	63.0	37.0	15.18	84.82
B 6	10.0	90.0	55.93	39.0	61.0	46.85	53.15
B 7	4.65	95.35	41.86	25.0	75.0	68.73	31.27
B 8	1.45	98.55	18.83	10.0	90.0	88.98	11.02

Key to symbols:

A_f , B_f are the respective (%) molar concentrations of MMA and NaMA in the monomer feed.
 A , B are the respective (%) molar concentrations of MMA and NaMA in the copolymers.
 R is the run number; $f_u(B)$, $f_c(B)$ are the respective fractions of uncyclizable and cyclizable NaMA units in the copolymer chain.

Table VI-3

Theoretical determination of $f_c(B)$ for KMA/MMA copolymers

Copolymer	A_f	B_f	R	A	B	$f_u(B) \times 100$	$f_c(B) \times 100$
C 1	75.0	25.0	10.53	95.0	5.0	0.2	99.8
C 2	60.0	40.0	18.92	90.0	10.0	1.07	98.93
C 3	40.0	60.0	33.44	79.0	21.0	6.73	93.27
C 4	13.2	86.8	52.64	50.0	50.0	34.67	65.33
C 5	4.8	95.2	38.89	25.0	75.0	69.36	30.63
C 6	0.7	99.3	8.86	5.0	95.0	95.11	4.89

Key to symbols:

A_f , B_f are the respective (%) molar concentrations of MMA and KMA in the monomer feed.
 A , B are the respective (%) molar concentrations of MMA and KMA in the copolymers.
 R is the run number; $f_u(B)$, $f_c(B)$ are the respective fractions of uncyclizable and cyclizable KMA units in the copolymer chain.

Table VI-4

Methanol production in LiMA/MMA copolymers.
Comparison between experimental and theoretical yields
(predicted from sequence distribution data).

Mole % of LiMA units in copolymer chain	Methanol yield, mole %	
	Experimental	Calculated
10	5.64	9.98
25	12.58	24.54
32	14.86	30.95
41	12.80	37.17
52	11.20	40.84
70	3.07	28.98
85	1.11	14.86

Table VI-5

Methanol production in NaMA/MMA copolymers.
Comparison between experimental and theoretical yields
(predicted from sequence distribution data).

Mole % of NaMA units in copolymer chain	Methanol yield, mole %	
	Experimental	Calculated
5	5.35	4.97
10	10.74	9.95
13.4	13.58	13.40
18	18.51	17.50
37	17.51	31.38
61	11.60	32.42
75	5.56	23.45
90	1.50	9.91

Fig. VI-1

METHANOL PRODUCTION IN LiMA/MMA COPOLYMER

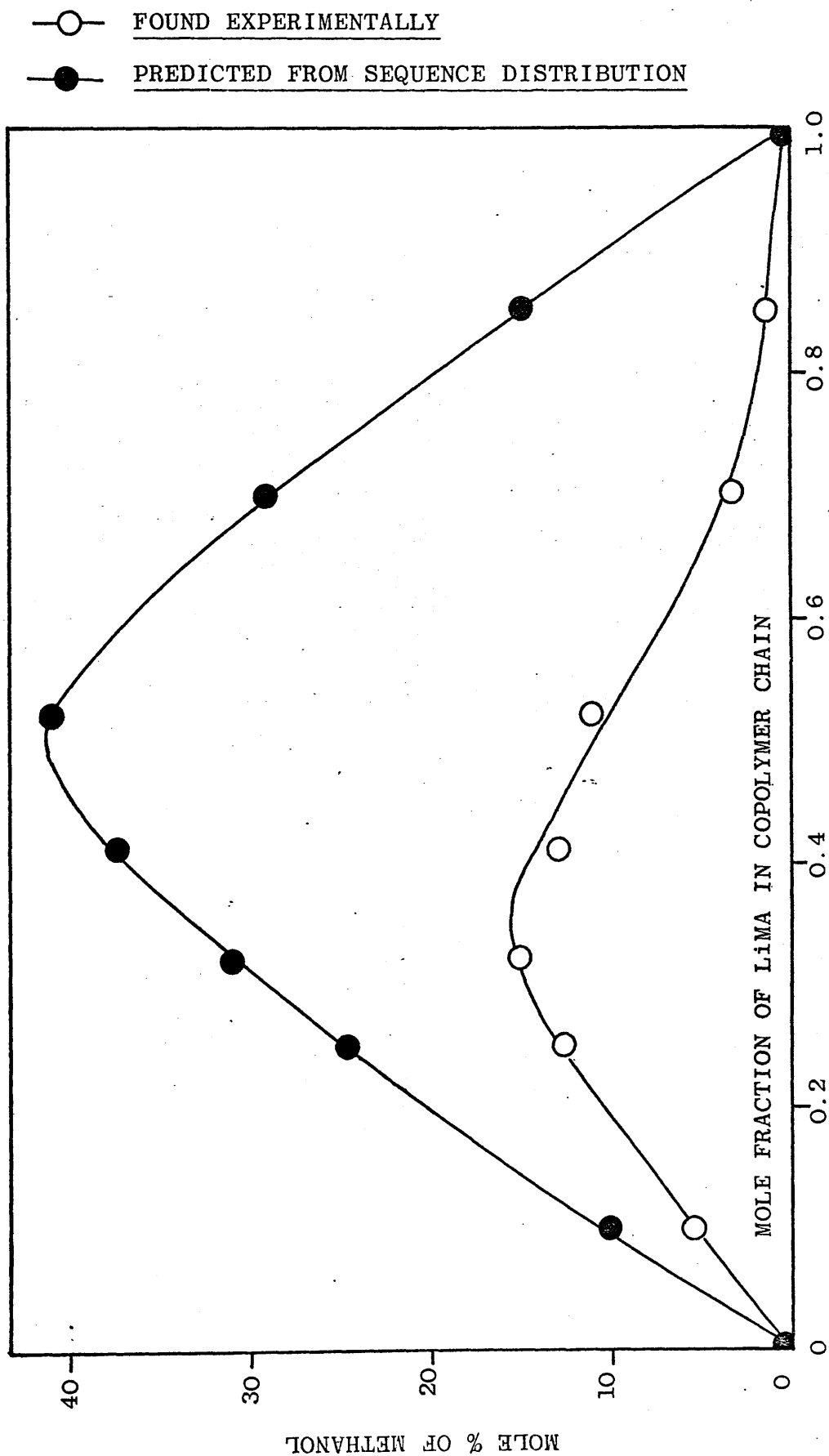


Fig. VI-2

METHANOL PRODUCTION IN NaMA/MMA COPOLYMER

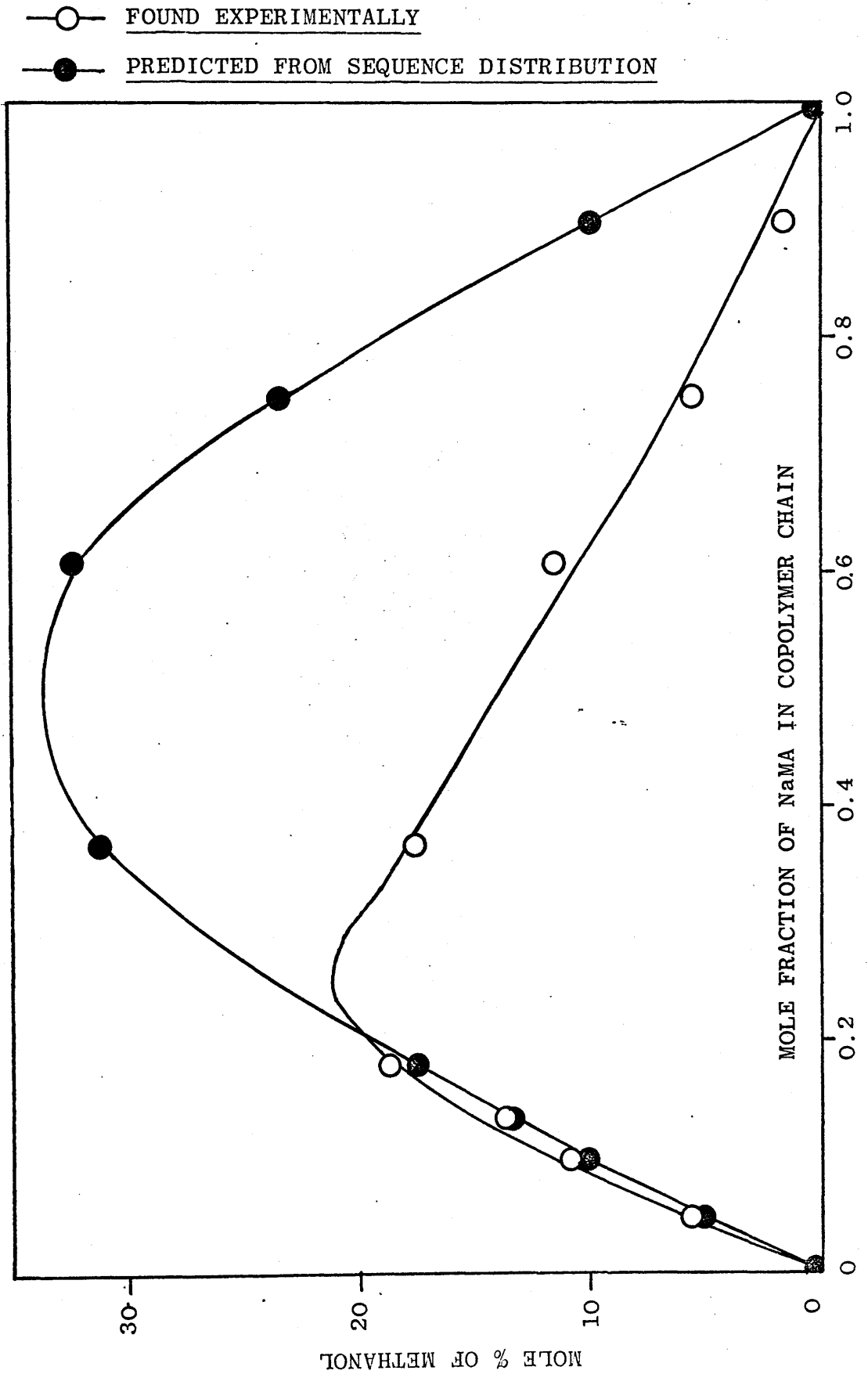
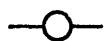


Fig. VI-3

METHANOL PRODUCTION IN KMA/MMA COPOLYMER



FOUND EXPERIMENTALLY



PREDICTED FROM SEQUENCE DISTRIBUTION

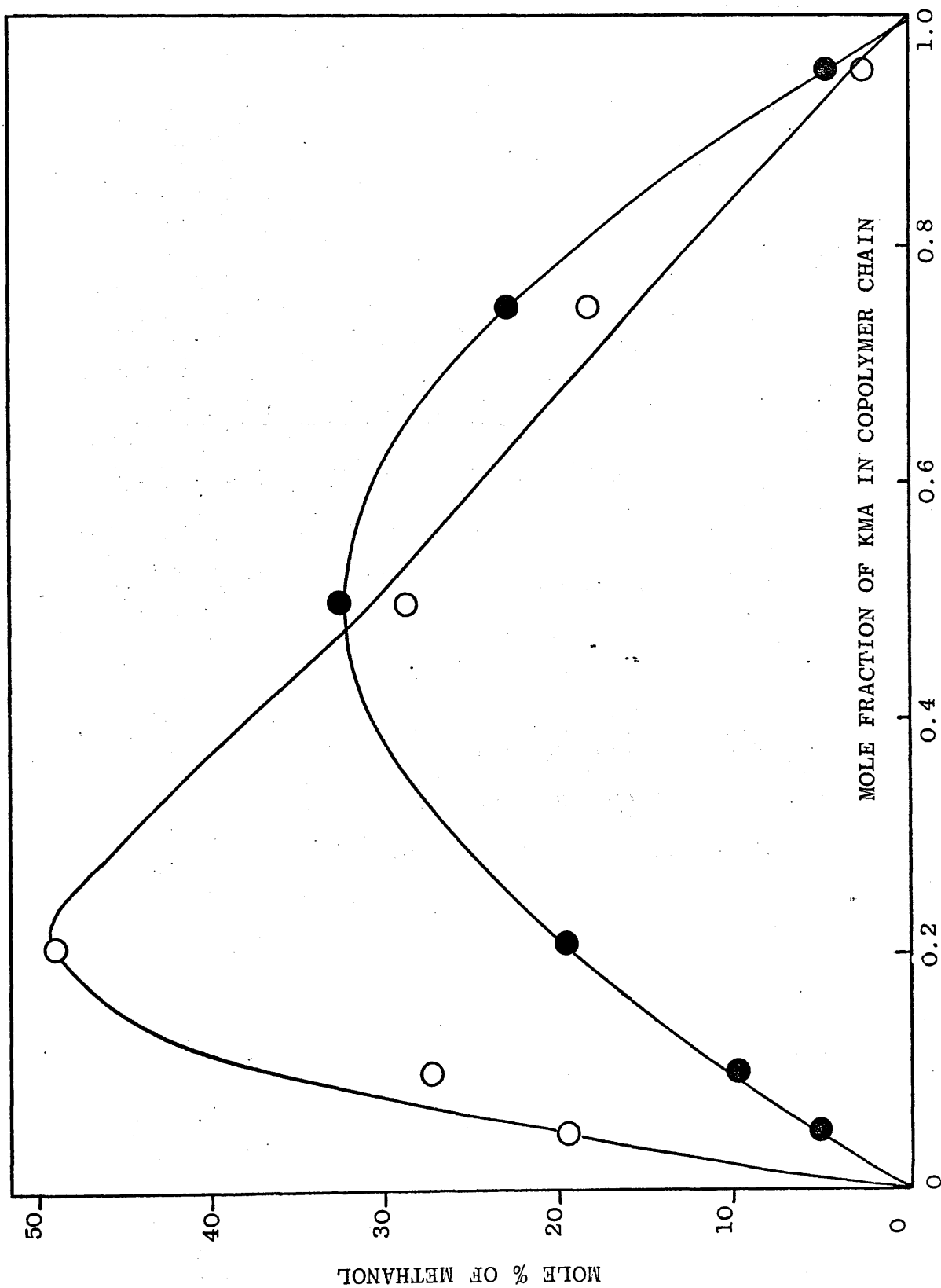


Table VI-6

Methanol production in KMA/MMA copolymers
Comparison between experimental and theoretical yields
(predicted from sequence distribution data).

Mole % of KMA units in copolymer chain	Methanol yield, mole %	
	Experimental	Calculated
5	19.86	5.00
10	27.15	9.89
21	49.26	19.58
50	28.75	32.66
75	18.62	22.97
95	2.73	4.64

The observation of figure VI-1, for the case of LiMA/MMA copolymers reveals that;

(i) the production of methanol is much lower than expected, a result which could be explained by at least two possible reasons:

- the cyclization reaction in LiMA/MMA copolymers is probably not a quantitative reaction (we have seen in chapter V that anhydride formation is less favoured as the size of the metal ion decreases);

- methanol production requires also the availability of enough MMA units in the chains at the moment when metal methoxide is formed (if the reaction between methoxide and MMA does give methanol), and the

presence of enough MMA units is not certain since depolymerization is taking place competitively.

(ii) the maximum production of methanol, which on the basis of cyclization, should have been around the 1:1 composition in the copolymer chain, is in fact observed around the 35% LiMA/MMA composition. This anomaly suggests that methanol is not produced through the expected route only.

This point is also supported by the observation of fig. VI-2 and 3 for the respective cases of NaMA/MMA and KMA/MMA copolymers. In these two diagrams, the maxima of methanol production are far away from the expected 1:1 copolymer composition, occurring in fact at 25% LiMA/MMA and 20% KMA/MMA respectively. Note also in the case of KMA/MMA copolymer system, that the methanol evolution, in the composition region which is richer in MMA content, is significantly higher than expected (see fig. VI-3).

It follows from these observations that methanol formation is:

(a) either resulting from two different routes as in the case of MAA/MMA copolymers: (71)

- intramolecular cyclization followed by reaction of metal methoxide with MMA units (if such a reaction is possible).

- decomposition of ester groups from MMA units, a

reaction which is favoured by the observed stabilization of PMMA depolymerization by copolymerization;

(b) or occurring by only one single route, i.e., decomposition of ester groups from MMA units as mentioned above.

ISOTHERMAL DEGRADATION OF KMA/MMA COPOLYMERS

To provide further information to assist in determining the origin of the produced methanol, further investigations were carried out under isothermal conditions.

Four KMA/MMA copolymers were degraded isothermally at four different temperatures (around 300°C), in turn, and the methanol (and MMA) formation as a function of time were followed using an appropriate collection assembly, and GLC (see chapter II).

The reason for the choice of the particular KMA/MMA copolymer system is based on the two following facts:

(a) From the three series of copolymers, the KMA/MMA system is the one which produces the maximum methanol.

(b) The KMA/MMA system being the one in which anhydride formation is most favoured, it follows that methanol formation from cyclization in this system (if such a process is possible), should be at a maximum as compared to other routes and to the cases of the two other systems.

(A) METHANOL PRODUCTION UNDER ISOTHERMAL CONDITIONS

KMA/MMA copolymers having KMA compositions of 5%, 20%, 50% and 75% respectively, were degraded isothermally at four different temperatures (283°C, 295°C, 305°C and 315°C) and the results for methanol production are shown in figures VI-4, 5, 6 and 7.

All curves in the first three diagrams appear to be S shaped, suggesting that there are two methanol producing reactions. But a closer observation shows also that methanol from the first process is produced in a very low quantity (less than 2% of the initial weight of copolymer sample in all cases), and therefore cannot be associated with methanol originated from intramolecular cyclization. A more likely explanation as to the origin of this early methanol is that it could be solvent from the polymerization, trapped into the samples. And this affinity of the copolymers to retain methanol solvent has been observed to increase with MMA content in the copolymer and was not detected at all in the poly(alkali metal methacrylates) homopolymers, provided the same drying procedure was used. This explains the absence of this early methanol (solvent) from the 75% KMA/MMA copolymer (see fig. VI-7).

The reason to the release of methanol solvent at such high temperatures could be associated with the particularly high melting range of the copolymers.

Fig. VI-4
METHANOL EVOLUTION

UNDER ISOTHERMAL CONDITIONS

FOR 5% KMA/MMA COPOLYMER

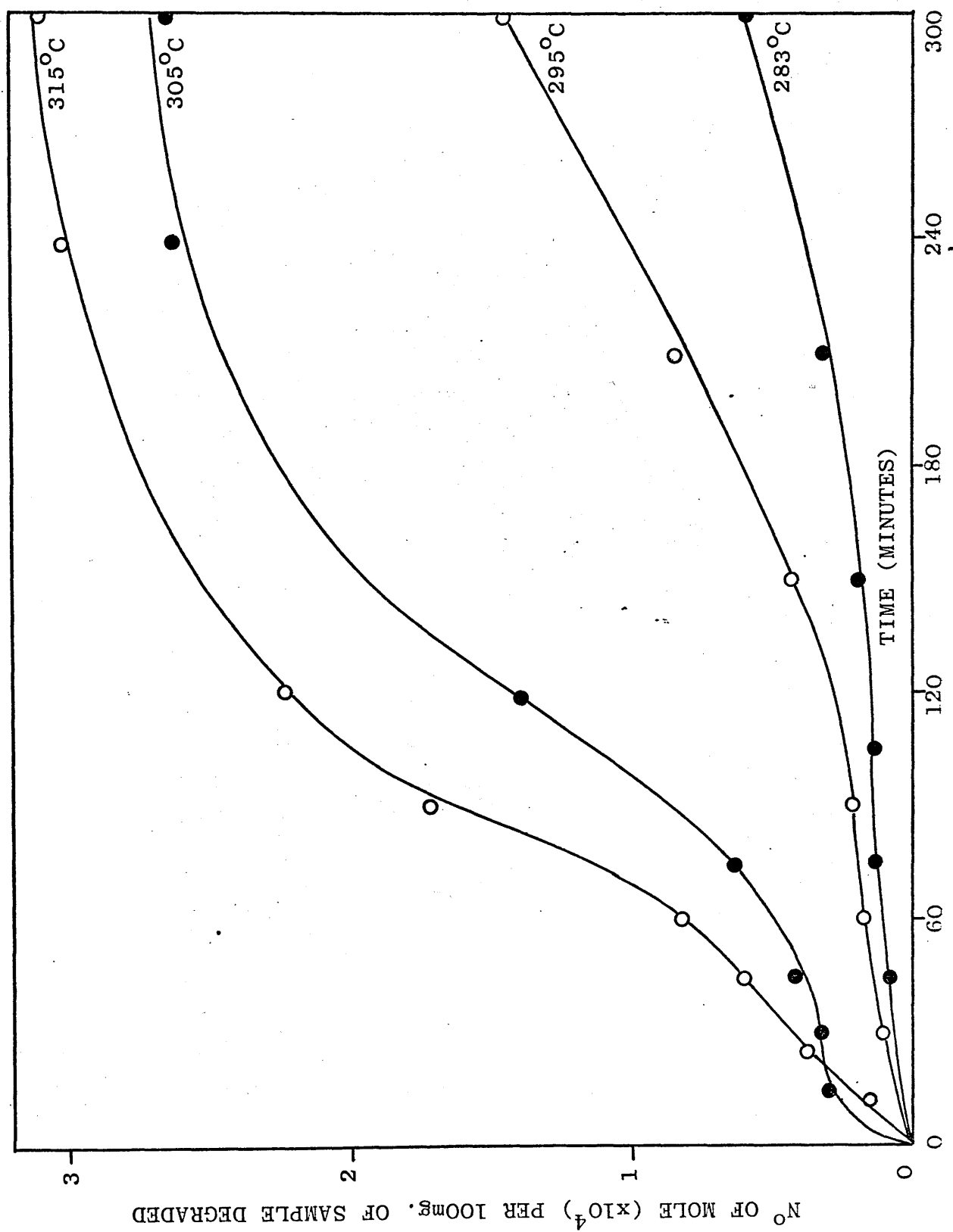


Fig. VI-5

METHANOL EVOLUTION

UNDER ISOTHERMAL CONDITIONS

FOR 20% KMA/MMA COPOLYMER

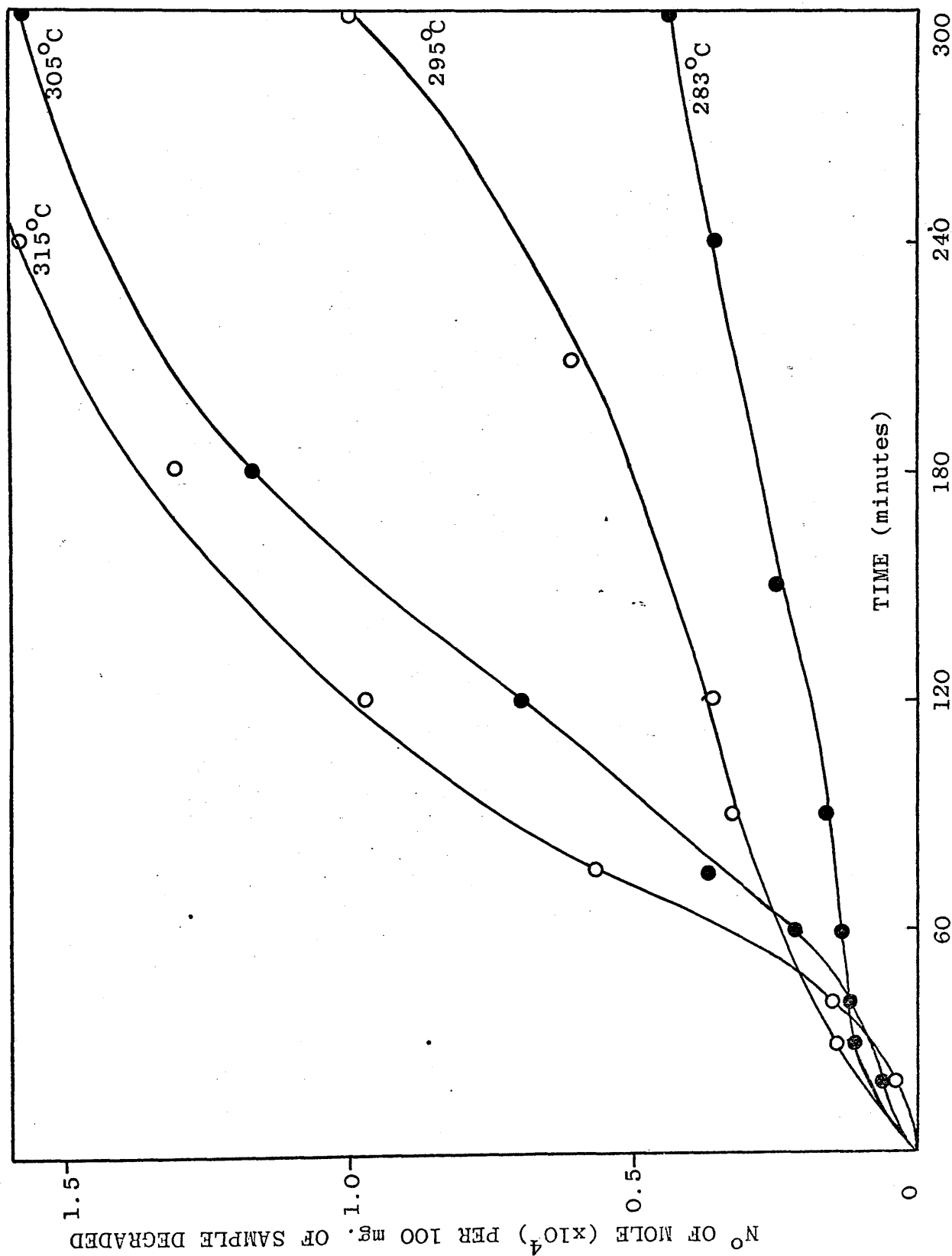


Fig. VI-6

METHANOL EVOLUTION

UNDER ISOTHERMAL CONDITIONS

FOR 50% KMA/MMA COPOLYMER

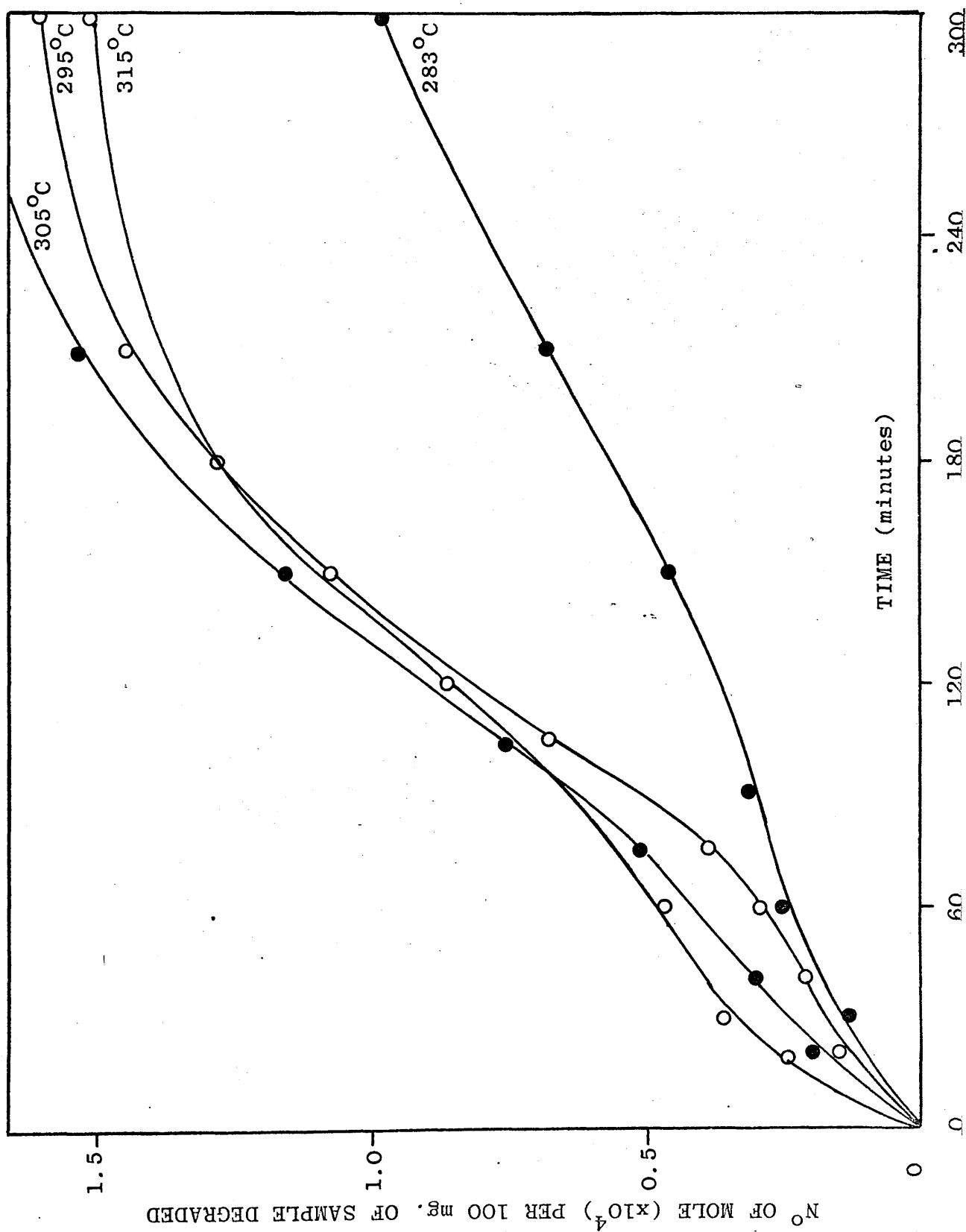
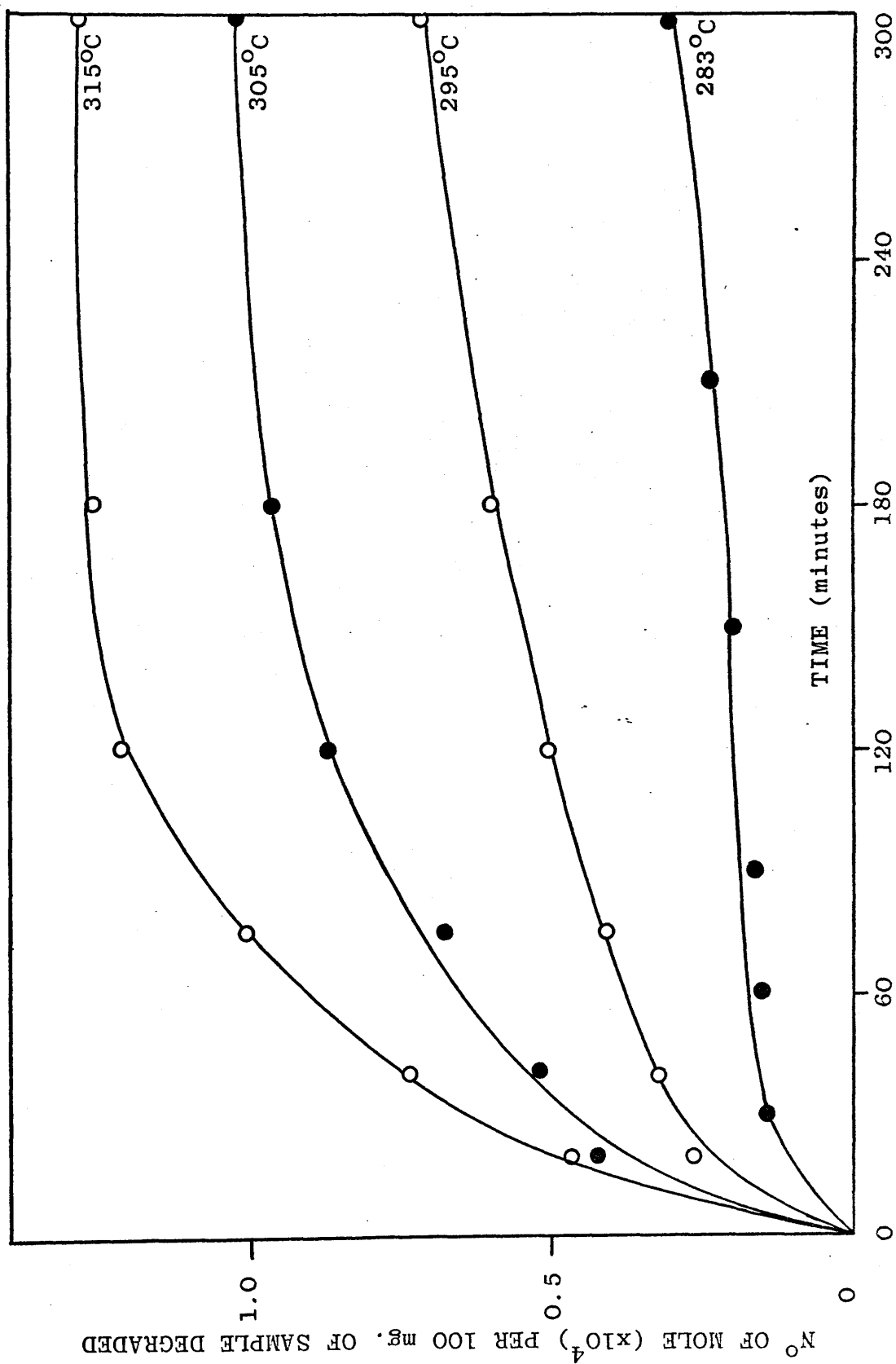


Fig. VI-7

METHANOL EVOLUTION

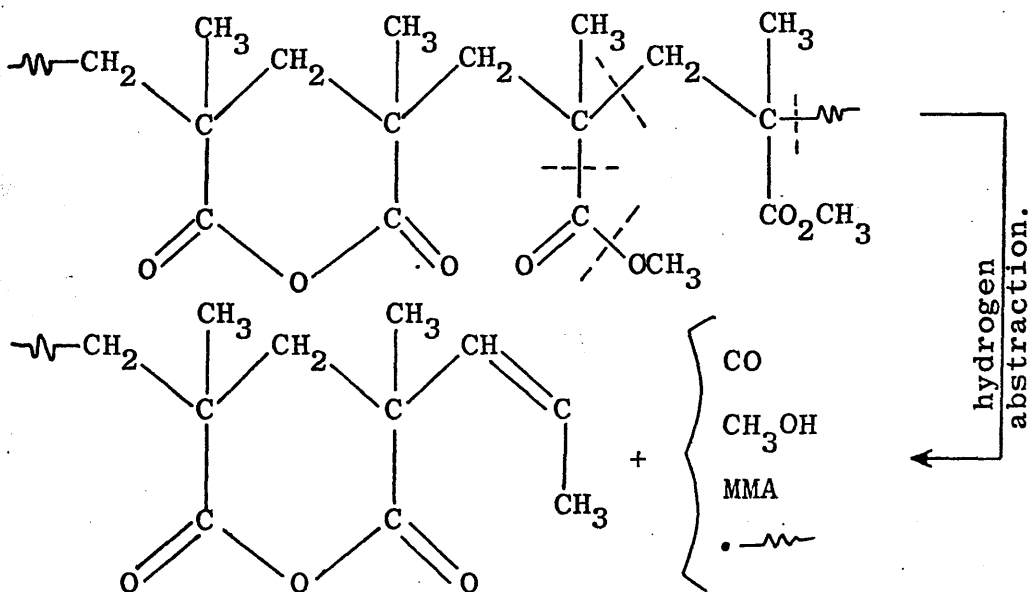
UNDER ISOTHERMAL CONDITIONS

FOR 75% KMA/MMA COPOLYMER

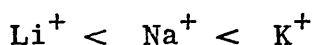


(B) ORIGIN OF METHANOL

In the light of these results it is logical to argue that the total methanol production results exclusively from the decomposition of pendant ester groups in the MMA units. This reaction will be competitive with MMA depolymerization and favoured by the observed stabilization of PMMA breakdown (i.e. by the introduction of anhydride structures in the chain). Because of the anhydride structures blocking the depolymerization, chain scission needs to be re-initiated more often than in PMMA. This way, because of the higher energy needed to produce MMA monomer, scission may take place on pendant ester groups (to produce methanol and carbon monoxide) concurrently with MMA production.



Methanol production occurring through this process will be at a maximum in the region of high MMA copolymer content and will increase (in accord with our results) with the size of the alkali metal ion:



(C) MMA PRODUCTION UNDER ISOTHERMAL CONDITIONS

The products collected from the four KMA/MMA copolymers, degraded under isothermal conditions, have also allowed the quantitative estimation, by GLC, of MMA among the products.

The comparison of MMA production from the four copolymers with that of its evolution from PMMA, during the initial stages of decomposition may provide some useful information about the way in which depolymerization occurs. Fig. VI-8 illustrates the rates of MMA evolution (determined by TGA under a dynamic nitrogen atmosphere) from a PMMA* sample. Measurements of the initial rates allows the determination of the activation energy corresponding to the depolymerization of PMMA* from the Arrhenius plot (Fig. VI-9) associated with it (see Appendix). This was found to be:

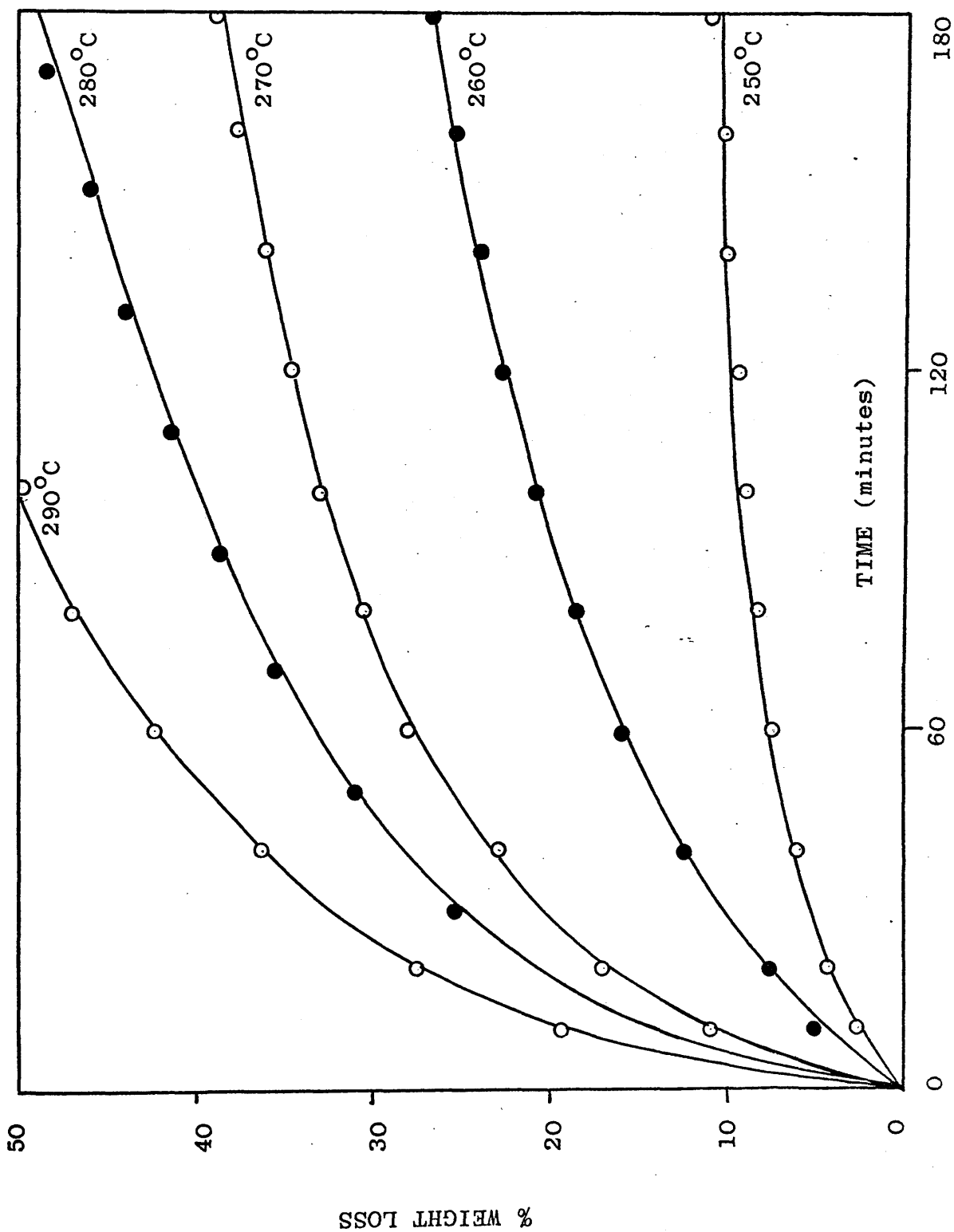
$$E_A = 35 \text{ Kcal/mole} \pm 5 \text{ Kcal/mole},$$

a relatively large error being incurred in measurements of initial rates.

*Sample prepared in the same conditions as the KMA/MMA copolymers; conversion: 10% and molecular weight: 90.000.

Fig. VI-8

WEIGHT LOSS FOR PMMA
UNDER ISOTHERMAL CONDITIONS



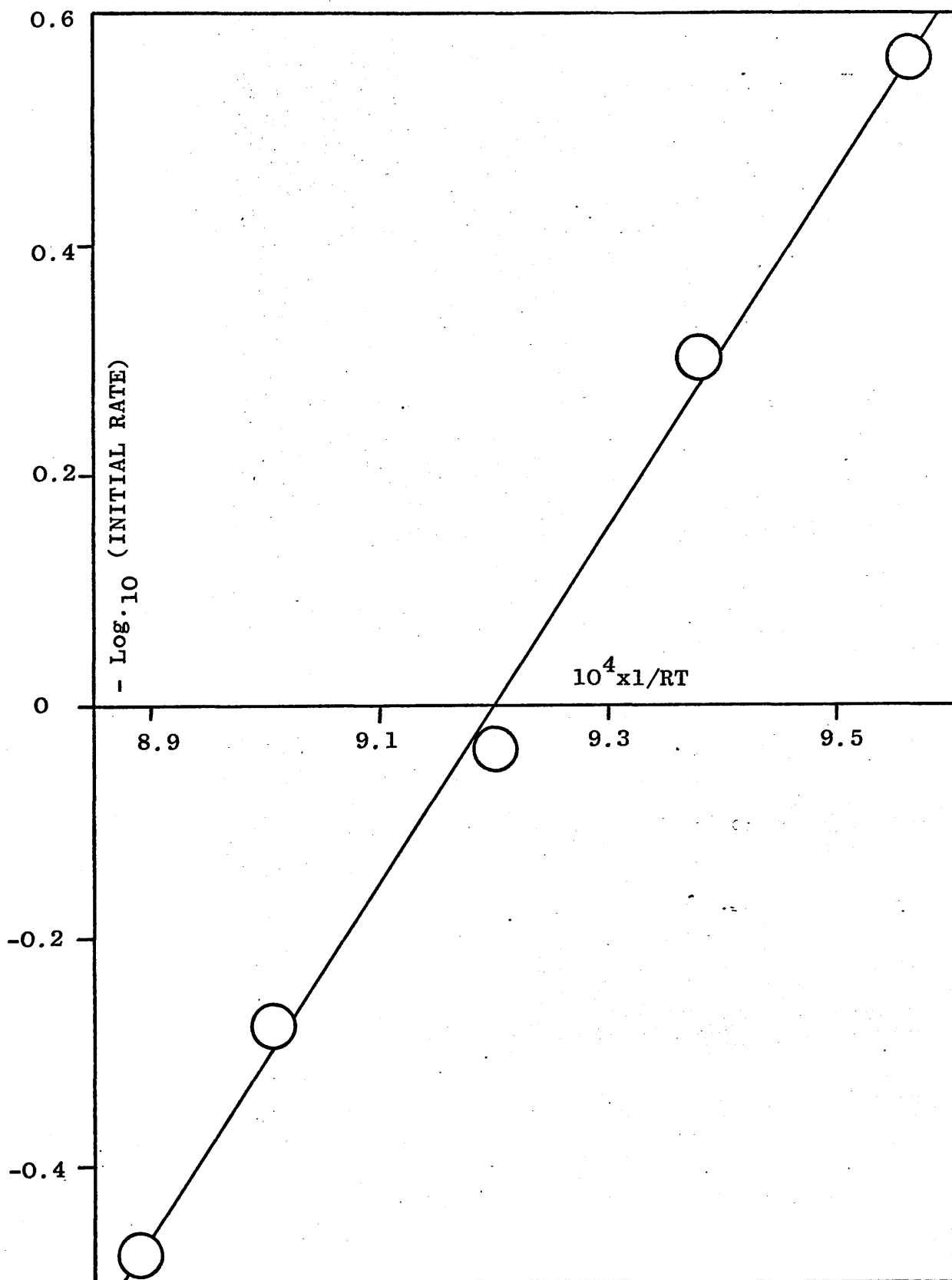


Fig. VI-9

ARRHENIUS PLOT FOR MMA EVOLUTION

IN PMMA (see fig. VI-8)

Figures VI-10, 11, 12 and 13 illustrate the rates of evolution of MMA (at 283°C, 295°C, 305°C and 315°C) for 5%, 20%, 50% and 75% KMA/MMA copolymers respectively. The Arrhenius plots associated with these four copolymers (illustrated in figure VI-14) allowed the determination of the activation energies corresponding to the depolymerization of MMA segments from these systems. The results are shown in table VI-7.

Table VI-7

Activation energies (E_A 's) associated with MMA
production from four KMA/MMA copolymers
and from PMMA homopolymer

Mole % of KMA in copolymer chain	E_A (MMA), Kcal/mole
5	45 ± 5
20	43 ± 5
50	46 ± 5
75	52 ± 5
0	35 ± 5

From these results and fig. VI-14, one sees that the activation energy for MMA production increases with the KMA content in the copolymer chain (i.e. with the

Fig. VI-10

MMA EVOLUTION UNDER ISOTHERMAL
CONDITIONS FOR 5% KMA/MMA COPOLYMER

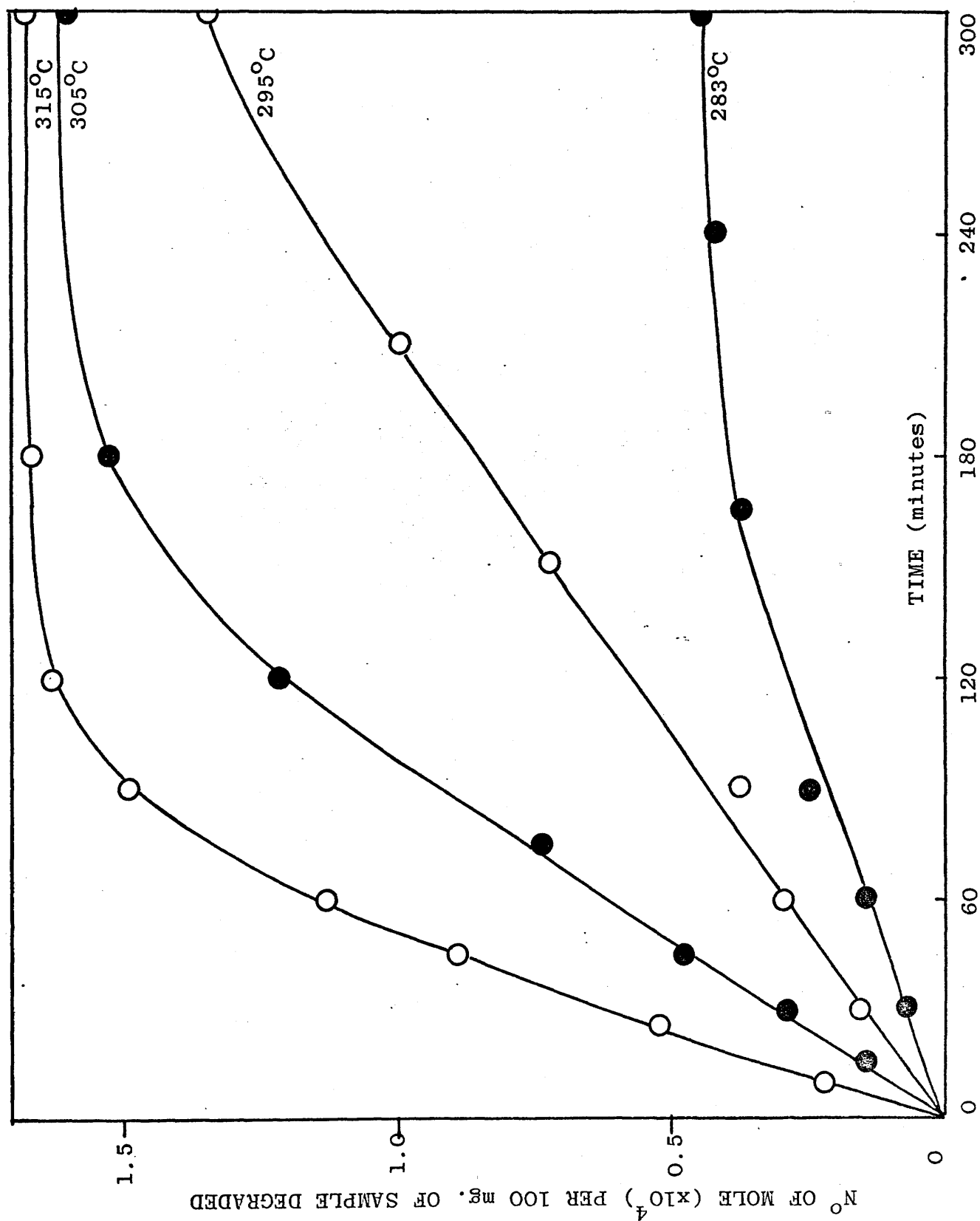


Fig. VI-11

MMA EVOLUTION UNDER ISOTHERMAL
CONDITIONS FOR 20% KMA/MMA COPOLYMER

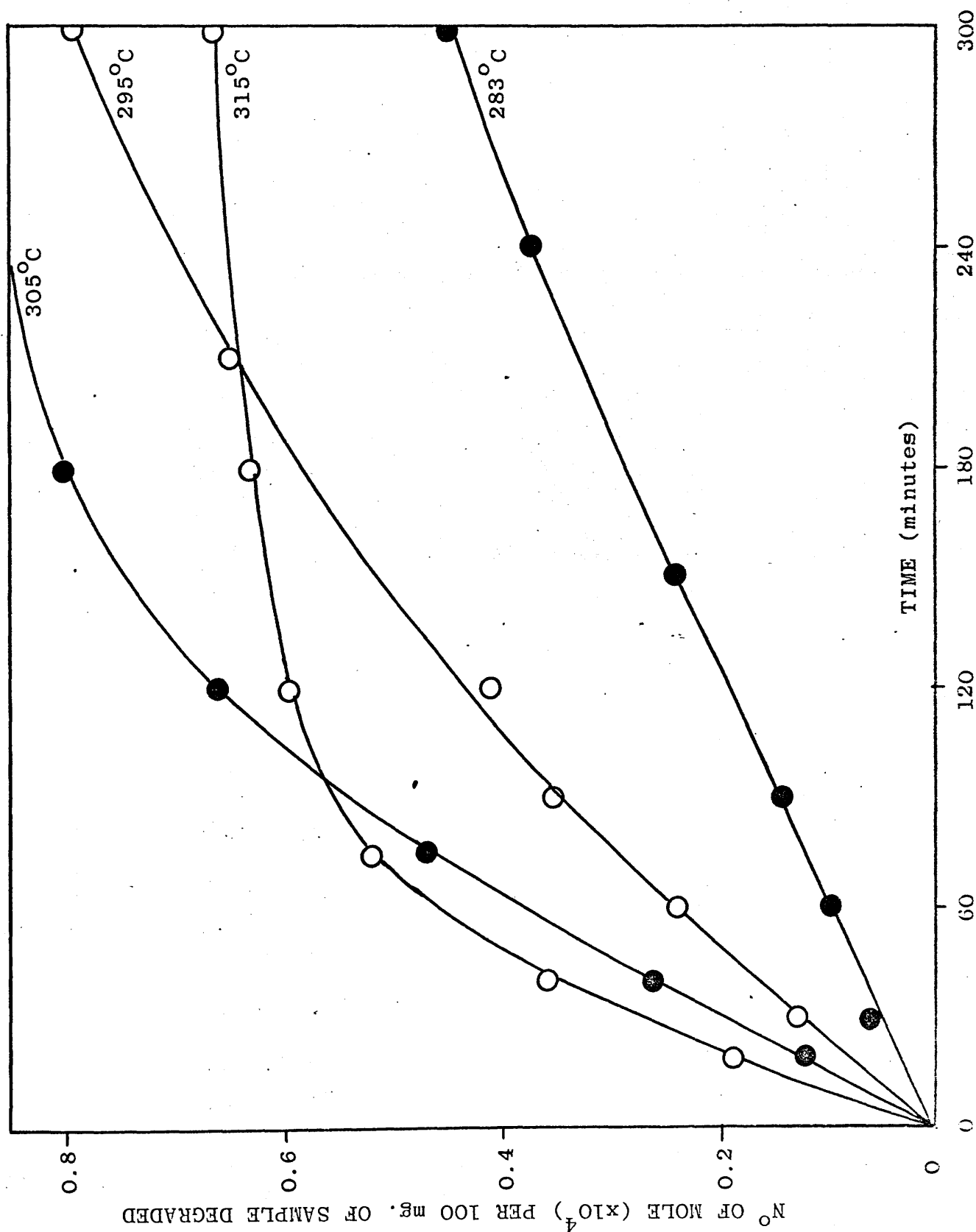


Fig. VI-12

MMA EVOLUTION UNDER ISOTHERMAL

CONDITIONS FOR 50% KMA/MMA COPOLYMER

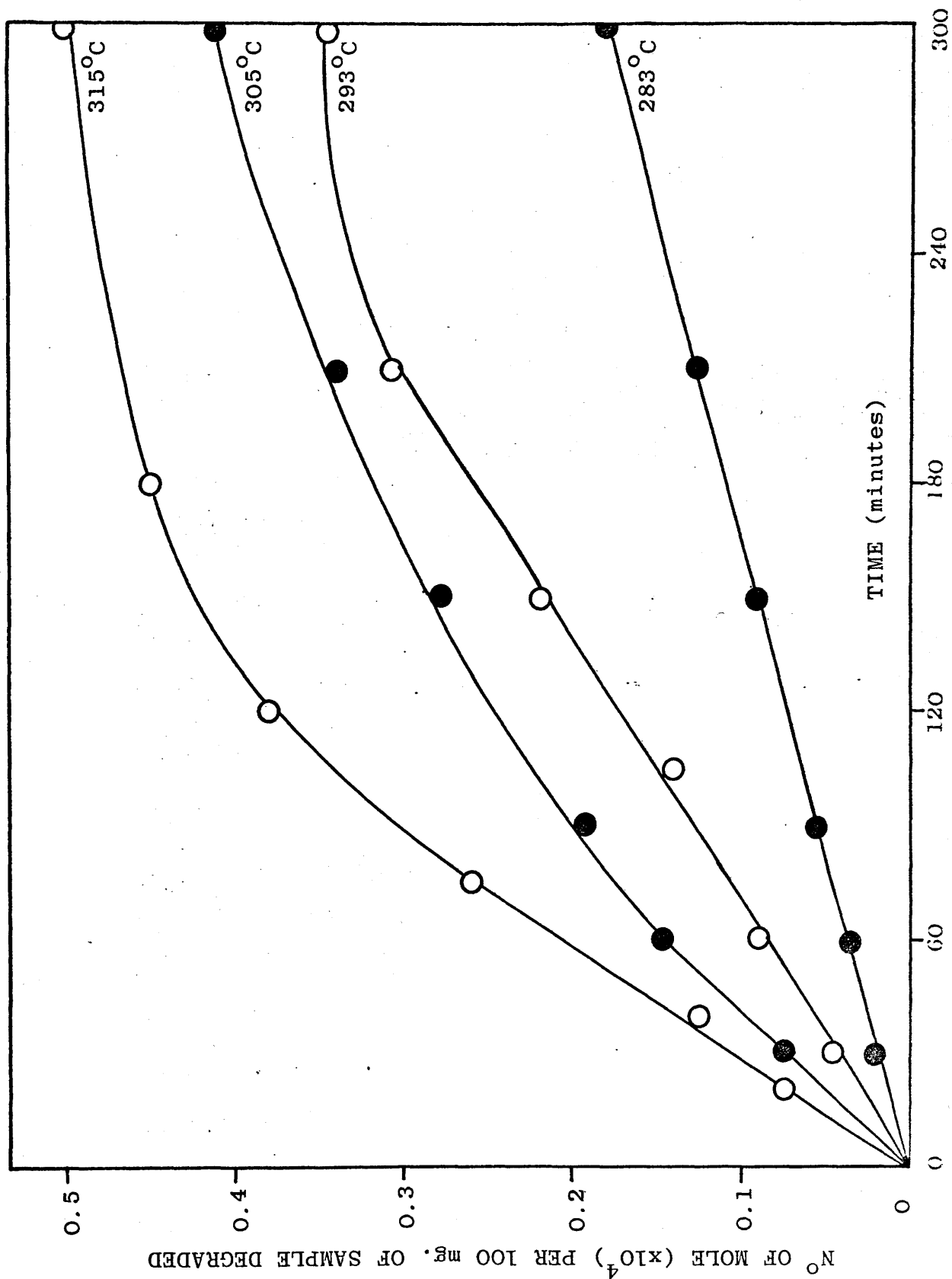
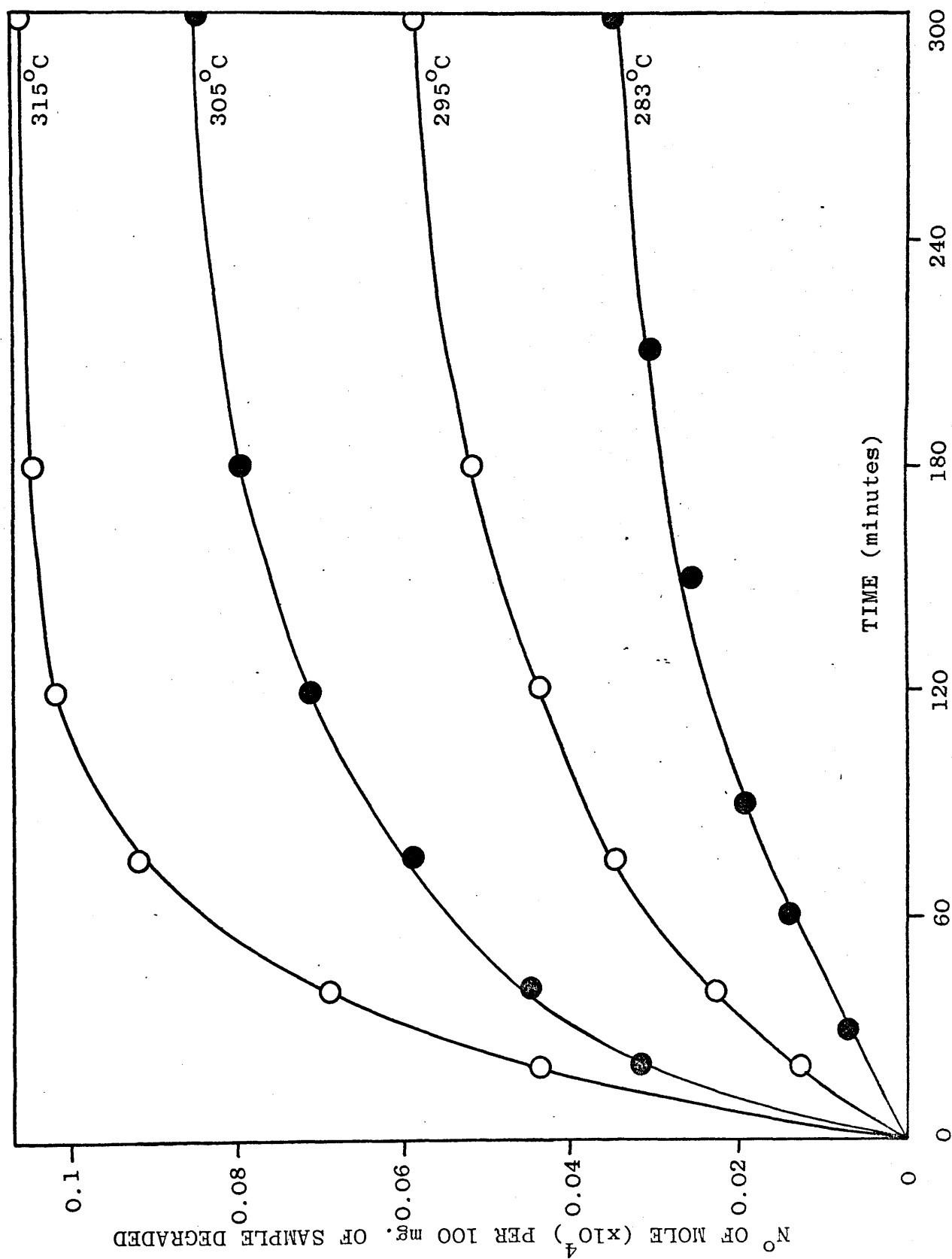


Fig. VI-13

MMA EVOLUTION UNDER ISOTHERMAL

CONDITIONS FOR 75% KMA/MMA COPOLYMER



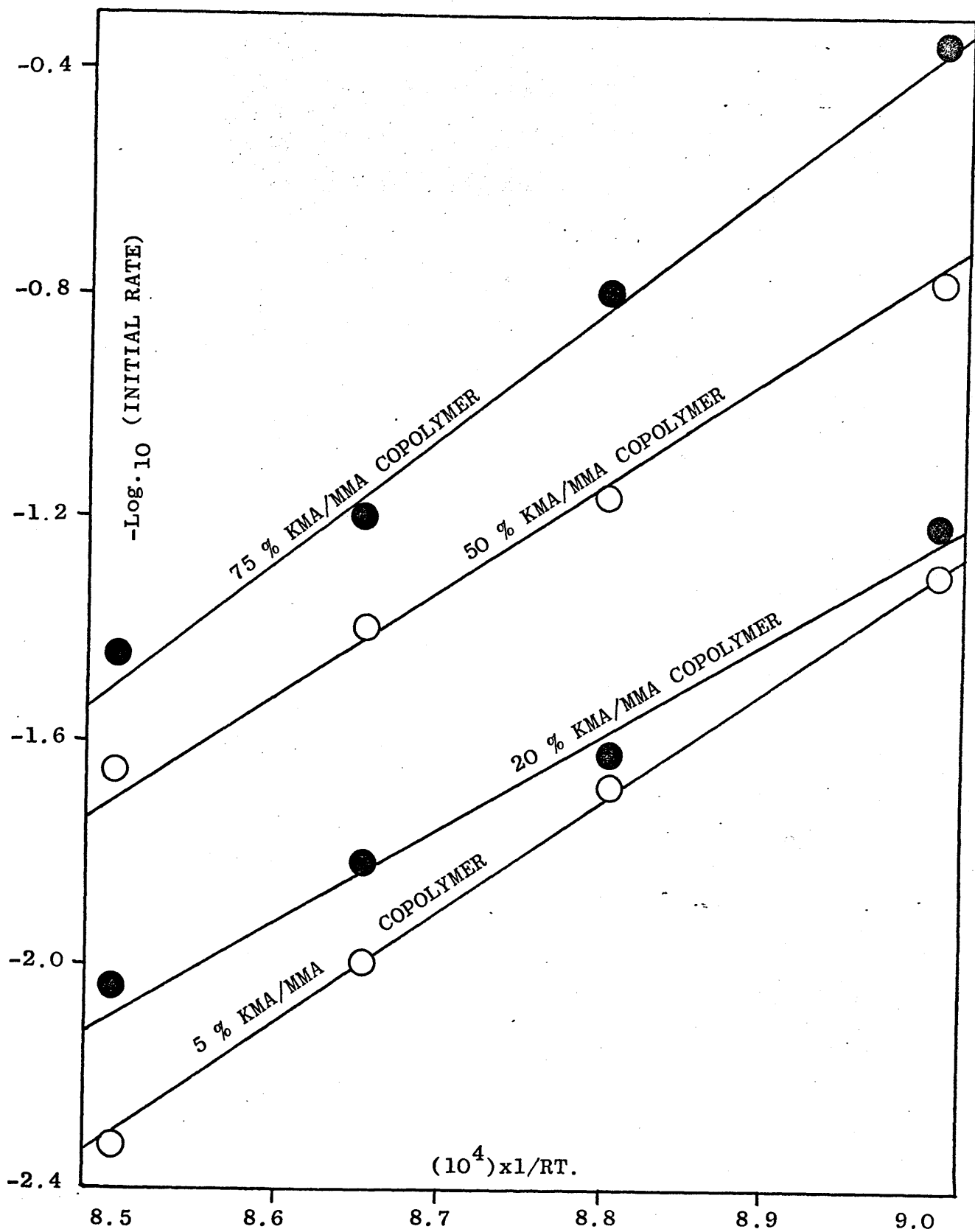


Fig. VI-14

ARRHENIUS PLOTS FOR MMA EVOLUTION IN 4 KMA/MMA COPOLYMERS

(see fig.VI-10,11,12 and 13)

anhydride content relatively to MMA units). This reveals that MMA units, as they are found in smaller and smaller segments trapped between anhydride units, need more and more energy for their release since depolymerization has consequently to be re-initiated more often along these sequences. In the extreme case of the 75% KMA/MMA copolymer, the particularly high activation energy observed suggests that each MMA monomer unit is released in a separate process requiring activation energy and that depolymerization is not feasible since these units will be mostly isolated alone, trapped between anhydride structures.

Note that this increase in the activation energy of MMA production with KMA content in the copolymers is also consistent with the results showing the fate of MMA units in the copolymer chain as the composition changes (tables VI-8, 9 and 10). These decompose more to methanol units as the KMA content in the chain increases (i.e. as the activation energy for MMA production increases). The higher energy needed for monomer production also allows the scission to occur on pendant ester groups (to produce methanol) in competition with chain scission.

Table VI-8

Mode of breakdown of the MMA parts of the
LiMA/MMA copolymer chains (mole %)

Mole % of MMA in copolymer chain	Methanol	MMA	Other
90	6.27	50.13	43.6
75	16.78	40.62	42.6
68	21.86	43.01	44.13
59	21.70	32.73	45.57
48	23.34	29.95	46.71
30	10.23	27.25	62.52
15	7.42	16.6	75.98

Table VI-9

Mode of breakdown of the MMA parts of the
NaMA/MMA copolymer chains (mole %)

Mole % of MMA in copolymer chain	Methanol	MMA	Other
95	5.63	49.80	44.57
91	11.80	45.31	42.89
86.6	15.68	37.51	46.81
82	22.58	34.31	43.11
63	27.80	23.11	49.09
39	29.74	11.51	58.75
25	22.26	8.96	68.78
10	14.98	9.53	75.49

Table VI-10

Mode of breakdown of the MMA parts of the
KMA/MMA copolymer chains (mole %)

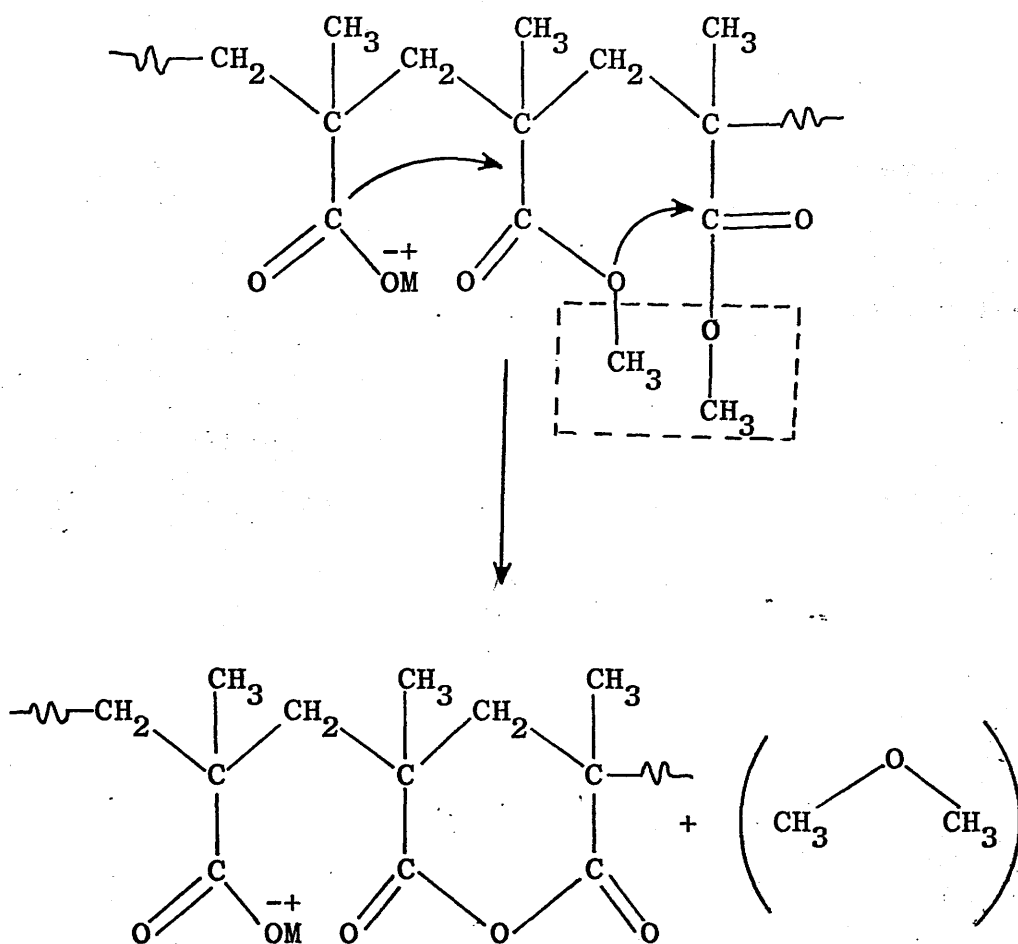
Mole % of MMA in copolymer chain	Methanol	MMA	Other
95	20.90	36.70	42.40
90	30.16	30.33	39.51
79	62.36	26.57	11.07
50	57.50	9.70	32.80
25	74.50	5.34	20.61
5	54.70	1.68	43.62

It is also interesting to note, in the three copolymer systems, the particularly high percentage of MMA units which decompose in a different way apart from producing methanol or monomer. MMA units may also decompose to give mostly MMA chain fragments in the cold ring fraction and alkali metal methoxide (by interaction between adjacent salt units), the fate of which will be discussed subsequently.

JUSTIFICATION FOR ALKALI METAL METHOXIDE FORMATION

The major reason we have to believe that alkali metal methoxide is formed at some stage of the decomposition, is that this product is the only possible one that could be

eliminated between two adjacent dissimilar monomer units (MMA and electrolyte) to produce an anhydride structure. It may be argued, however, that anhydride formation could occur between two adjacent MMA units (producing dimethyl ether) under a possible influence from a vicinal alkali metal methacrylate unit:

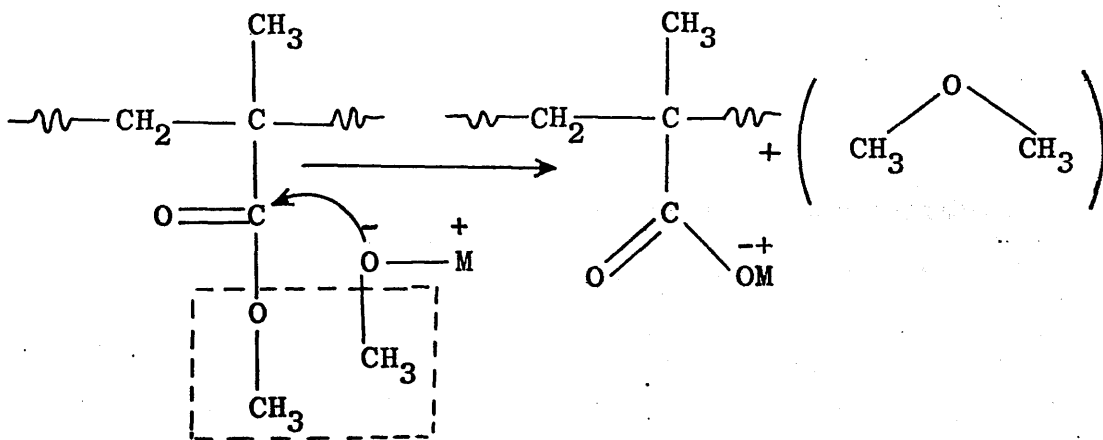


Such a process, however, for the formation of anhydride structures, is believed to be highly improbable since it would involve dimethyl ether formation in appreciable quantities, and analysis of the products only indicated very minute quantities of this product, possibly originated from a different route (see below).

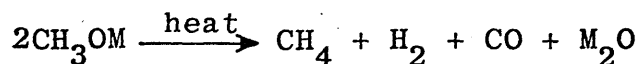
FATE OF ALKALI METAL METHOXIDE

It is believed that the alkali metal methoxide produced from intramolecular cyclization between MMA and salt units, behaves in two possible ways:

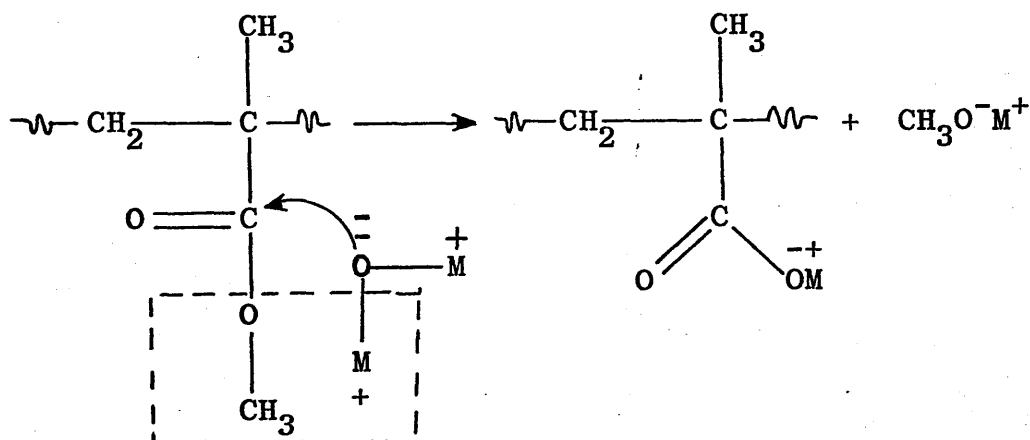
(i) If produced in the vicinity of MMA units in the chains, it may convert them to metal methacrylate units with production of dimethyl ether (and this product has been detected in small amounts from some copolymers):



(ii) It may also decompose independently to produce methane, carbon monoxide and hydrogen leaving metal oxide:



This metal oxide may, in turn, convert MMA units in the chain to metal methacrylate units with formation again of metal methoxide in the following manner:



Such conversions of MMA units to metal methacrylate account for the unexpected presence of appreciable amounts of salt units in the chain after all MMA and anhydride units have decomposed, even in the case of low metal methacrylate content copolymers (see TVA traces and IR spectra of the structural changes during degradation, chapter V).

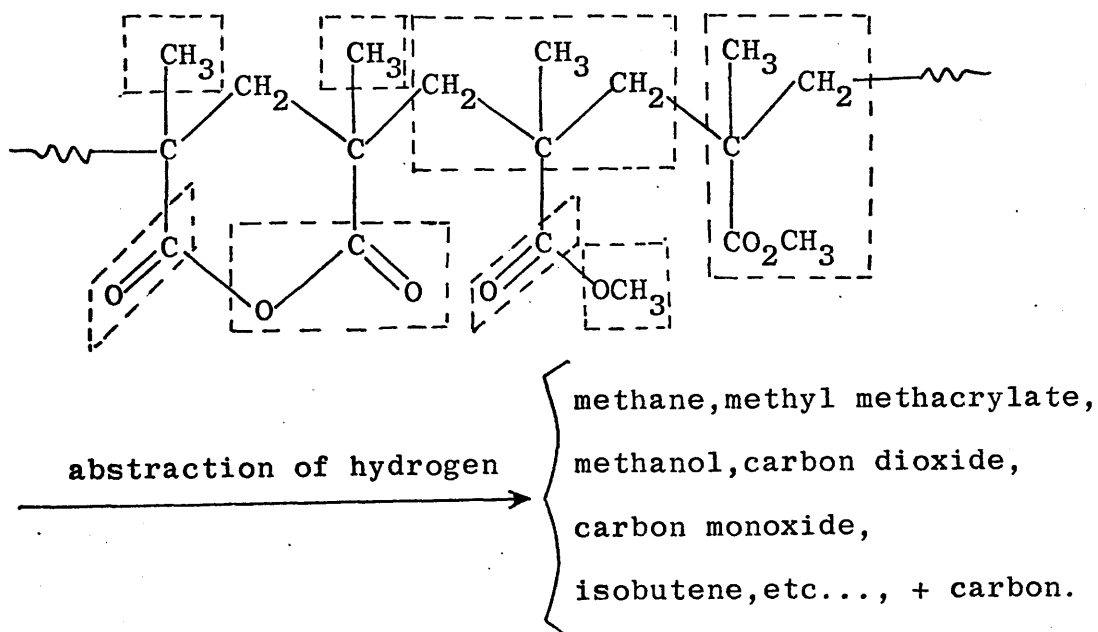
CHAPTER VII

GENERAL CONCLUSIONS

Three distinct processes may be discerned in the thermal decomposition of the copolymers of methyl methacrylate with alkali metal methacrylates, namely:-

(a) intramolecular cyclization between adjacent dissimilar monomer units, resulting in the elimination of alkali metal methoxide;

(b) depolymerization of MMA units, in competition with methanol production and decomposition of anhydride structures, the latter processes resulting also in the production of carbon dioxide, carbon monoxide, methane and alkenes from fragmentation of the backbone:



At that stage of the reaction, (b), the alkali metal methoxide is also either decomposing or converting MMA units to alkali metal methacrylates with production of dimethyl ether. Isolated MMA units in the chain and MAA (presumably formed from decomposition of anhydride) units, will also escape ultimately to the cold ring in the form of short chain fragments;

(c) and finally at higher temperatures the remaining alkali metal methacrylate units, which are much more stable, will decompose in a more or less similar manner to that of their parent homopolymers, i.e., by production of monomer and metal isobutyrate, carbon dioxide, carbon monoxide, ketones and alkenes, leaving a residue consisting of alkali metal carbonate and charcoal.

DISCUSSION

Anhydride formation in the copolymers is favoured as the size of the metal ion increases and this is believed to be due to the ionic character of the oxygen — metal bond, increasing in the order $\text{Li}^+ < \text{Na}^+ < \text{K}^+$.

As a result of this, stabilization of PMMA depolymerization occurs, and MMA monomer production is inhibited because of a direct blockage of the "unzipping" process by the anhydride rings in the chain.

Because of this blockage phenomenon in the copolymers, more energy (than in PMMA homopolymer) is needed to re-initiate repeatedly chain scission preceding MMA release.

This increase in the activation energy of MMA production is believed to result in the further disturbance of the normal "unzipping" process of depolymerization by allowing scission to take place not only along the chain but also between C—C bonds on the pendant ester groups, and resulting in the production of methanol competitively with MMA.

Consequently, at any particular copolymer composition the evolution of MMA monomer decreases as the size of the metal ion increases (i.e., as the formation of anhydride rings increases), thus allowing more methanol formation from the decomposition of the pendant ester groups.

Carbon dioxide formation increases, at any particular composition, with the size of the metal ion and this is consistent with:

(i) the fact that anhydride formation in the chain increases in the same way, and (ii) with the results observed by McNeill and Zulfiqar⁽⁹⁴⁾ for the poly(alkali metal methacrylates) homopolymers.

The production of metal methacrylate monomer and metal isobutyrate in the cold ring fraction shows the following features:

(a) it decreases as the size of the metal ion increases, in the composition region of rich MMA content, as a result

of the higher contribution of alkali metal methacrylates to the formation of anhydride structures;

(b) it increases with the size of the metal ion, in the composition region of high electrolyte content, and this, again, is consistent with the results obtained for the poly(alkali metal methacrylates).⁽⁹⁴⁾

In a final point, it is useful to examine the summation of the experimental yields for the products accounted for quantitatively, in each copolymer, in comparison with the theoretical yield of 100%. The results for the three copolymer systems are summarized in tables VII-1, 2 and 3 (see next three pages).

Considering: (a) the experimental errors involved in the estimation of these results; (b) the fact that, all gaseous products at ambient temperature (except CO_2), plus MMA and MAA chain fragments in the cold ring, have not been accounted for, the results shown in tables VII-1, 2 and 3 can be considered as acceptable.

Table VII-1

Quantitative summation of the products from programmed degradation (to 500°C) of LiMA/MMA copolymers; weight %.

LiMA % in copolymer	Liquid products	Carbon dioxide	Salt units in CRF	Residue at 500°C	Total
10	62.2 ± 2	2.1 ± 0.1	5.6 ± 0.3	9 ± 1	78.9 ± 3.4
25	46.1 ± 2	5.75 ± 0.3	15.17 ± 0.75	19 ± 1	86.02 ± 4.05
32	41.7 ± 2	7.56 ± 0.4	19.7 ± 1.0	21 ± 1	89.96 ± 4.4
41	33.8 ± 2	8.2 ± 0.4	19.2 ± 0.95	24 ± 1	85.2 ± 4.4
52	30.1 ± 2	9.0 ± 0.45	21.11 ± 1.05	29 ± 2	89.2 ± 5.5
70	25.7 ± 2	7.02 ± 0.35	21.9 ± 1.1	31 ± 2	85.62 ± 5.5
85	21.2 ± 2	4.85 ± 0.95	24.8 ± 1.2	33 ± 2	83.85 ± 6.0

Table VII-2

Quantitative summation of the products from programmed degradation (to 500°C) of NaMA/MMA copolymers; weight %.

NaMA % in copolymer	Liquid products	Carbon dioxide	Salt units in CRF	Residue at 500°C	Total
5	64.2 ± 2	2.4 ± 0.12	2.7 ± 0.13	7.0 ± 1	76.3 ± 3.3
9	62.0 ± 2	4.05 ± 0.2	4.3 ± 0.2	8.0 ± 1	78.35 ± 3.4
13.4	53.1 ± 2	4.67 ± 0.23	7.8 ± 0.4	14.0 ± 1	79.57 ± 3.63
18	47.6 ± 2	6.1 ± 0.3	10.62 ± 0.53	17.5 ± 1	81.82 ± 3.83
37	28.4 ± 2	9.35 ± 0.45	19.32 ± 0.95	28.5 ± 2	85.57 ± 5.4
61	15.9 ± 2	8.38 ± 0.4	29.5 ± 1.5	36 ± 2	89.8 ± 5.9
75	12.4 ± 2	6.14 ± 0.3	30.6 ± 1.5	38 ± 2	86.6 ± 5.8
90	15.0 ± 2	5.4 ± 0.3	33.9 ± 1.7	40 ± 2	94.3 ± 6.0

Table VII-3

Quantitative summation of the products from programmed degradation (to 500°C) of KMA/MMA copolymers ; weight %.

KMA % in copolymer	Liquid products	Carbon dioxide	Salt units in CRF	Residue at 500°C	Total
5	56.9 ± 2	5.6 ± 0.3	1.6 ± 0.1	8 ± 1	72.1 ± 3.4
10	49.3 ± 2	6.7 ± 0.3	3.03 ± 0.15	14 ± 1	73.03 ± 3.45
21	40.7 ± 2	8.6 ± 0.4	10.55 ± 0.52	22 ± 1	81.85 ± 4.0
50	18.5 ± 2	9.23 ± 0.45	28.8 ± 1.5	27 ± 2	83.53 ± 6.0
75	13.2 ± 2	7.4 ± 0.4	42.1 ± 2.1	33 ± 2	95.7 ± 6.5
95	10.0 ± 2	6.4 ± 0.3	41.3 ± 2.1	36 ± 2	93.7 ± 6.4

SUGGESTIONS FOR FUTURE WORK

Although molecular weight measurements on these copolymers have not been attempted because of their lack of solubility in particular solvents and the lengthy processes involved, it is believed that the use of mixed systems of solvents (methanol/water) could be adapted to the light scattering method (which was not available in this laboratory) to determine these molecular weights. The study of the molecular weight changes during degradation can indeed provide very valuable information towards a clearer understanding of the mechanism of the decomposition of these copolymers.

Useful information on crystallinity can be provided by X-ray diffraction studies on the copolymers as well as the related homopolymers.

Also, because of the striking contrasts in the viscometric behaviour of solutions of polyelectrolytes as compared to those of neutral polymers (see chapter I), the investigation of the viscosity changes for the solutions of these copolymers upon dilution and for different compositions, will be of high interest. This study could also be extended to the investigation, in general, of the physico-chemical (for example electrical) properties of these copolymers in water or water/methanol solutions. Such studies could lead to improved and useful applications in various fields such as paints, glues, drilling mud additives and cements.

APPENDIX 1

THE FORTRAN PROGRAMME USED FOR CALCULATING THE
REACTIVITY RATIOS OF A COPOLYMER SYSTEM, BEING
GIVEN AN INITIAL ESTIMATE OF r_1 AND r_2 AND THE
COMPOSITION ANALYSIS DATA (SEE CHAPTER IV).

// EXEC FORTRAN

//C.SYSIN DD *

```

      IMPLICIT REAL*8 (A-H,O-Z)
      DIMENSION PARA(10),V(10),F(50),W(200)
      COMMON CAPM1(50),WEEM1(50)
      EXTERNAL FUNCT,MONIT
      READ(5,49) N,(PARA(I),I=1,N)
49    FORMAT(I5,/, (8F10.0))
      WRITE(6,59) (PARA(I),I=1,N)
59    FORMAT(' PARAMETERS HAVE INITIAL VALUES',/, (1P7G16.6))
      READ(5,50) M,(CAPM1(I),WEEM1(I),I=1,M)
50    FORMAT(I5,/, (2F10.0))
      WRITE(6,60) (CAPM1(I),WEEM1(I),I=1,M)
60    FORMAT(//' CAPITAL M1                SMALL M1',/, (1P2G16.6))
      DO 12 I=1,N
12    V(I)=DMAX1(1.D-5,DABS(PARA(I))*0.1)
      MAXIT=30
      IPRINT=1
      EPS=1.E-8
      ALF=1.E-4
      IFAIL=0
      CALL E04FAF(M,N,PARA,F,S,EPS,ALF,V,W,M+M+4*N+M*N+(N*N+N)/2
1    +(N+3+N/3)*(M+2+N+N),FUNCT,MONIT,IPRINT,MAXIT,IFAIL)
      STOP
      END

```

```
SUBROUTINE FUNCT(M,N,PARA,F)
  IMPLICIT REAL*8 (A-H,O-Z)
  DIMENSION PARA(N),F(M)
  COMMON CAPM1(50),WEEM1(50)
  DO 10 I=1,M
    CAP1=CAPM1(I)
    CAP2=1.DO-CAP1
    WEE1=WEEM1(I)
    WEE2=1.DO-WEE1
10   F(I)=PARA(1)*CAP1*CAP1*WEE2+CAP1*CAP2*(WEE2-WEE1)
1   -PARA(2)*CAP2*CAP2*WEE1
  RETURN
  END
```

```
SUBROUTINE MONIT(M,N,X,S,ITERC,SING,LIM)
  IMPLICIT REAL*8 (A-H,O-Z)
  LOGICAL SING,LIM
  DIMENSION X(N)
  WRITE(6,100) ITERC
  WRITE(6,200) S
  WRITE(6,300) (X(I),I=1,N)
  IF(SING) WRITE(6,400)
  IF(LIM) WRITE(6,500)
  RETURN
100  FORMAT(11H0ITRATION ,I2)
200  FORMAT(16H SUM OF SQUARES ,E14.6)
300  FORMAT(22H VALUES OF PARAMS ARE ,3E14.6 $\frac{1}{4}$ )
400  FORMAT(9H SINGULAR)
500  FORMAT(8H LIMITED)
  END
```

//L.SYSLIB DD

//DD

//DD DSN=PLULIB.NAGLIB,DISP=SHR

//G.SYSIN DD *

C DATA CARDS

Note: CAPITAL M1 and SMALL M1 refer to the mole fractions of monomer 1 in the copolymerization feed and in the copolymer chains respectively. The parameters (reactivity ratios) are given in the order r_1 , r_2 . (See details in chapter IV).

APPENDIX 2

PREPARATION OF SODIUM METHOXIDE

1-2 grams, approximately, were put in the bottom of a three-necked flask continuously swept with dry nitrogen. The reaction was carried out under reflux in a -45°C bath. Dry methanol (previously distilled twice) was added dropwise very carefully (the addition of methanol to sodium metal being dangerously exothermic) until all of the sodium had dissolved. At the end of the reaction an extra five ml of methanol were added. The excess methanol was eliminated under vacuum. The white crystalline powder thus obtained was dried in a vacuum oven at 40°C for forty eight hours and then stored in a dessicator over sulphuric acid, until used.

APPENDIX 3

ACTIVATION ENERGY ESTIMATION FOR MMA PRODUCTION FROM COPOLYMERS

The rate constant of a chemical reaction, k , is given by the Arrhenius equation:

$$k = A \exp(-E/RT) ,$$

where A is a constant, R and T are the gas constant and the absolute temperature respectively, and E is the activation energy of the reaction expressed in Kcal.mol^{-1} if R is expressed in $\text{Kcal.mol}^{-1}(\text{°K})^{-1}$. Since

$$\log_{10} k = \log_{10} A - 2.303 E/RT ,$$

E will be easily obtained from the slope of the $\log_{10} k$ versus $1/T$ plot. The rate of a reaction is given quite generally by,

$$k C_A^a \cdot C_B^b \cdot C_C^c \dots\dots$$

in which $C_A, C_B, C_C, \dots\dots$ are the concentrations of the reactants and $a, b, c, \dots\dots$ are constants. Therefore provided rate measurements at different temperatures are carried out under the same concentration conditions, the activation energy for a particular reaction may be obtained simply from the slope of the plot \log_{10} (initial rate) versus $1/T$.

In this work, the initial rates have been obtained from the slopes of the tangents to the curves for MMA production versus time, at the origin.

REFERENCES

1. S.A. Rice and M. Nagasawa, "Polyelectrolyte Solutions", Academic Press, New York, (1961).
2. C.S. Scanley, World Oil, July, 1959.
3. N.T. Woodberry, Tappi, 44(9), 156A (1961).
4. W.F. Reynolds, Jr., et al., Tappi, 40, 839 (1957).
5. Compare, J. Thiele, Ann., 319, 220 (1910); S.V. Lebedev, J. Russ. Phys. Chem. Soc., 42, 949 (1910); C. Harries, Ann., 383, 206 (1911).
6. British Patent 27, 361 (1917).
7. I. Kondakov, Rev. Gén. Chem. Russ., 15, 408 (1912).
8. O. Aschan, Finska Vetenskapsen Soc., Helsingfors, Oversigt, 58, 122 (1915).
9. F. Hofmann, U.S. Patent 1, 068, 770 (1913).
10. F. Klatte, Austrian Patent 70, 348 (1914).
11. I. Kondakov, J. Prakt. Chem., 64, 109 (1915).
12. I. Ostromisslensky, J. Russ. Phys. Chem. Soc., 48, 1071-1114, (1916).
13. H. Plauston, British Patent 156, 118 (1918).
14. A. Voss, et al., German Patents 579, 648, 679, 943. Also E.W. Reid, U.S. Patent 1, 935, 577.
15. H. Lecher, U.S. Patent 1, 780, 873 (1931).
16. H. Staudinger and J. Schneider, Ann., 541, 151 (1939).
17. R.G.W. Norrish and E.F. Brookman, Proc. Roy. Soc., London, A163, 205 (1937).
18. R.G.W. Norrish and E.F. Brookman, Proc. Roy. Soc., London, A171, 147 (1939).
19. F.T. Wall, J. Am. Chem. Soc., 63, 1862 (1941).
20. Compare, C.S. Marvel, et al., J. Am. Chem. Soc., 64, 2356 (1942); 65, 2054 (1943); 66, 2135 (1944).

21. B.E. Conway and A. Dobry-Duclaux, "Viscosity of suspensions of electrically charged particles and solutions of polyelectrolytes", Chap. 3 in F.R. Eirich, Ed., Rheology, Vol. 3, Academic Press, New York (1960).
22. P.J. Flory, "Principles of Polymer Chemistry", Cornell University Press, Ithaca, New York, 1967, Chap. XIV-5.
23. R.M. Fuoss, Disc. Faraday Soc., 11, 125 (1951).
24. S.A. Rice, "Polyelectrolytes", Chap. 7 in J.L. Oncley et al., Eds., Biophysical Science, John Wiley & Sons, New York (1959). Revs. Modern. Phys. 31, 69 (1959).
25. C. Tanford, "Physical Chemistry of Macromolecules", John Wiley & Sons, New York (1961), Secs. 24, 26-28.
26. "Encyclopaedia of Polymer Science and Technology". Vol. 10, page 781, Interscience Publishers, Wiley, New York (1969).
27. R.M. Fuoss and U.P. Strauss, J. Polym. Sci., 3, 602-603 (1948).
28. R.M. Fuoss and U.P. Strauss, Ann. New York Acad. Sci, 12, 48 (1949).
29. H.P. Gregor, D.H. Gold and M. Frederick, J. Polym. Sci., 23, 467 (1957).
30. "Thermal Stability of Polymers", R.T. Conley (Ed.), Marcel Dekker, New York (1970).
31. R.B. Fox, "Progress in Polymer Science", Vol. 1, A.D. Jenkins (Ed.), PERGAMON, London (1967), pp.45-89.
32. N. Grassie, "Encyclopaedia of Polymer Science and Technology", Vol. 4, Wiley, New York (1966), pp.647-716.
33. L. Reich and S.S. Stivala, "Autooxidation of Hydrocarbons and Polyolefins", Marcel Dekker, New York (1969).
34. "Newer Methods of Polymer Characterization", B. Ke (Ed.), Interscience, New York (1964).
35. "Physical Methods in Macromolecular Chemistry", Vol. 1, B. Carroll (Ed.), Marcel Dekker, New York (1969).
36. "Techniques and Methods of Polymer Evaluation", Vol. 1, "Thermal Analysis", P.E. Slade and L.T. Jenkins, (Eds.), ARNOLD, London (1966).

37. "Techniques and Methods of Polymer Evaluation", Vol. 3, "Characterization and Analysis of Polymers by Gas Chromatography", M.T. Stevens (Ed.), Marcel Dekker, New York (1969).
38. "High Temperature Polymers", G.L. Segal (Ed.), Marcel Dekker, New York (1967).
39. A.H. Frazer, "High Temperature Resistent Polymers", Wiley, New York (1968).
40. V.V. Korshak and S.V. Vinogradova, "Dependence of Thermal Stability of Polymers on their Chemical Structure", *Uspekhi Khimii*, 11, 2024 (1968).
41. V. Chytry, B. Obereigner and D. Lim, *Europ. Polym. J.*, Supplement 379 (1969).
42. J.R. MacCallum, *Makromolek. Chem.*, 83, 137 (1965).
43. W.J. Oakes and R.B. Richards, *J. Chem. Soc.*, 2929 (1949).
44. T.E. Davis, R.L. Tobias and E.B. Peterli, *J. Polym. Sci.*, 56, 485 (1962).
45. S. Strauss, S.L. Madorsky, D. Thomson and L. Williamson, *J. Res. Natl. Bur. Std.*, 42, 499 (1949); *J. Polym. Sci.*, 4, 639 (1949).
46. R. Simha and L.A. Wall and P.J. Blatz, *J. Polym. Sci.*, 5, 615 (1950).
47. R. Simha and L.A. Wall, *J. Phys. Chem.*, 56, 707 (1952).
48. R. Simha and L.A. Wall, *J. Polym. Sci.*, 6, 39 (1951).
49. R. Simha, *Trans. New York Acad. Sci.*, 14, 151 (1952).
50. N. Grassie and H.W. Melville, *Proc. Roy. Soc. (London)*, Ser. A199, 1, 14, 24, 39 (1949).
51. L.A. Wall, S.L. Madorsky, D.W. Brown, S. Strauss and R. Simha, *J. Am. Chem. Soc.*, 76, 3430 (1954).
52. L.A. Wall and S. Strauss, *J. Polym. Sci.*, 44, 313 (1960).
53. J.C. Bevington, M.W. Melville and R.P. Taylor, *J. Polym. Sci.*, 14, 463 (1954).
54. W.C. Geddes, *Rubber. Chem. Technol.*, 40, 177 (1967).
55. N. Grassie, *Trans. Faraday Soc.*, 48, 379 (1952); 49, 835 (1953).

56. D. Braun, Pure and Applied Chem., 26, 173 (1971).
57. G. Palma and M. Carenza, J. Appl. Polym. Sci., 16, 2485 (1972).
58. W.J. Burlant and J.L. Parsons, J. Polym. Sci., 22, 249 (1956).
59. N. Grassie and J.N. Hay, J. Polym. Sci., 56, 189 (1962).
60. N. Grassie and D.M. Grant, Polymer., 1, 125 (1960).
61. N. Grassie and J.N. Hay, Die Makromol. Chem., 64, 82 (1963).
62. N. Grassie and J.R. MacCallum, J. Polym. Sci., A2, 983 (1964).
63. N. Grassie, "Cleavage Reactions, Thermal Degradation", in "Chemical Reactions of Polymers", E.M. Fettes (Ed.), Interscience, New York.
64. I.C. McNeill, J. Polym. Sci., A4, 2479 (1966).
65. I.C. McNeill, Europ. Polym. J., 3, 409 (1967).
66. I.C. McNeill and D. Neil, "Thermal Analysis", 353, R.F. Schwenker and P.D. Garn (Eds.), Academic Press, New York (1969).
67. I.C. McNeill, "Thermal Analysis", 417, R.F. Schwenker and P.D. Garn (Eds.), Academic Press, New York (1969).
68. I.C. McNeill, Europ. Polym. J., 6, 373 (1970).
69. I.C. McNeill, Therm. Anal., Proc. Int. Conf., 3rd., 1971 (Pub. 1972) 3, 229-44, Edited by Wiedermann, Hans G. Birkhaeuser; Basel, Switz.
70. I.C. McNeill and M.A.J. Mohamed, Europ. Polym. J., 8(8), 975 (1953).
71. I.C. McNeill and A. Jamieson, Europ. Polym. J., 10, 217 (1974).
72. N. Grassie and R.H. Jenkins, Europ. Polym J., 9(8), 697 (1973).
73. I.C. McNeill and D. Neil, J. Therm. Anal., 1, 389 (1969).
74. L. Ackerman and W.J. McGill, J. South Afr. Chem. Inst., 26(3), 82-93 (1973).
75. I.C. McNeill and L. Ackerman, unpublished.

76. H. Morawetz and I.D. Rubin, J. Polym. Sci., 57, 669-686 (1962).
77. J.B. Lando and H. Morawetz, J. Polym. Sci., Part C, 4, 789-803 (1964).
78. J.H. O'Donnel and R.D. Sothman, J. Polym. Sci., Part A-1, 6, 1073-1086 (1968).
79. B.M.J. Bowden, J.H. O'Donnel and R.D. Sothman, Makromol. Chem., 122, 186-195 (1969), (No 2950).
80. A. Katchalsky and P. Spitnik, J. Polym. Sci., 2, 432 (1947).
81. A. Katchalsky and J. Gilus, Rec. Trav. Chim., 68, 879 (1949).
82. A. Katchalsky, O. Künzle and W. Kuhn, J. Polym. Sci., 5, 283 (1950).
83. A. Katchalsky and H. Eisenberg, J. Polym. Sci., 6, 145 (1951).
84. A. Katchalsky and G. Blauer, Trans. Faraday Soc., 47, 1360 (1951).
85. G. Blauer, Trans. Faraday Soc., 56, 606-612 (1960).
86. Y. Kikuchi and K. Yamaoka, J. Science of The Hiroshima Univ., Ser. A, Vol. 21, No 2 (1957).
87. T.J. Wojnarowski and J. Tadeusz, Polimery, 14(4), 155-158 (1969).
88. T.J. Wojnarowski and J. Tadeusz, Polimery, 18(3), 128-130 (1973).
89. K. Plochoka and T.J. Wojnarowski, Europ. Polym. J., 7, 797-804 (1971).
90. K. Plochoka and T.J. Wojnarowski, Europ. Polym. J., 8, 921-926 (1972).
91. T.J. Wojnarowski and J. Tadeusz, Polimery, 13(5), 188-191 (1968).
92. R.J. Parsons and H. Warsons, J. Polym. Sci., 34, 251-269 (1959).
93. Kazanskaya, et al., Plast. Massy., 11, 16-18 (1970) (USSR).
94. I.C. McNeill and M. Zulfiqar, unpublished.

95. "Encyclopaedia of Polymer Science and Technology", Vol. 1, 198-199, Interscience Publishers, Wiley, New York (1964).
96. D.M. Grant and N. Grassie, J. Poly., Sci., 42, 587 (1960).
97. J.C. Leyte, L.H. Zuiderweg and J.H. Vledder, Spectrochimica Acta., 23A, 1397-1407 (1967).
98. J.W. Lyons and L. Kotin, J. Am. Chem. Soc., 87, 1670 (1965).
99. J.R. Huizenga, R.F. Grieger and F.T. Wall, J. Am. Chem. Soc., 72, 2636, 4228 (1950).
100. H.P. Gregor and M. Frederick, J. Polym. Sci., 23, 451 (1957).
101. H.P. Gregor, J. Am. Chem. Soc., 70, 1293 (1948).
102. H. Dostal, Monatsh., 69, 424 (1936).
103. T. Alfrey and G. Goldfinger, J. Chem. Phys., 12, 205 (1944).
104. F.R. Mayo and F.M. Lewis, J. Am. Chem. Soc., 66, 1594 (1944).
105. R. Simha and H. Branson, J. Chem. Phys., 12, 253 (1944).
106. F.T. Wall, J. Am. Chem. Soc., 66, 2050 (1944).
107. T. Alfrey, J.J. Bohrer and H. Mark, "Copolymerization", Interscience, New York (1952), p. 8-23.
108. F.R. Mayo and C. Walling, Chem. Rev., 46, 191 (1950).
109. M. Fineman and S.D. Ross, J. Polym. Sci., 5, 259 (1950).
110. G. Peckham, Computer J., Vol. 13, 418-420 (1970).
111. EO4FAF, Nottingham Algorithms Group, NAG, Library Manual, Document N° 328 (1st May, 1972).
112. H. Morawetz and I.D. Rubin, J. Polym. Sci., 57, 669 (1962).
113. G. Smets and R. Van Gorp, Europ. Polym. J., 5, 15 (1969).
114. M.J. Sienko and R.A. Plane, "Chemistry: Principles and Properties", International Student Edition, Tokyo (1966), p. 559.

115. R.P. Hopkins, Ind. Eng. Chem., 47, 2258 (1955).
116. L.J. Houng, II-387, Polymer Handbook, J. Brandrup and E.H. Immergut (Eds.), Interscience, New York (1975).
117. F.A. Bovey, J. Polym. Sci., A1, 843 (1963).
118. G. Schroeder, Makromol. Chem., 97, 232-240 (1966).
119. I.C. McNeill, Europ. Polym. J., 4, 21 (1968).
120. J.J. Keavney and E.C. Eberlin, J. Appl. Polym. Sci., 3, 47 (1960).
121. W.H. Wassermann and H.E. Zimmermann, J. Am. Chem. Soc., 72, 5787 (1950).
122. D.M. Grant and N. Grassie, Polymer, 1, 445 (1960).
123. C.S. Marvel and J.H. Sample, J. Am. Chem. Soc., 61, 3241 (1939).
124. C.S. Marvel and C.L. Levesque, J. Am. Chem. Soc., 60, 280 (1938).
125. P.J. Flory, J. Am. Chem. Soc., 61, 1518 (1939).
126. T. Alfrey, C. Lewis and B. Magel, J. Am. Chem. Soc., 71, 3793 (1949).
127. E. Merz, T. Alfrey and G. Goldfinger, J. Polym. Sci., 1, 75 (1946).
128. H.J. Harwood and W.M. Ritchey, J. Polym. Sci., Part B, 2, 601 (1964).
129. N.W. Johnston and H.J. Harwood, J. Polym. Sci., Part C, 22, 591 (1969).

